Improvement of the *Capripoxvirus*, Lumpy skin disease virus for use as a vaccine vector.

Henry Munyaradzi Munyanduki

A dissertation submitted in fulfilment of the requirements for the degree of Doctor of Philosophy (PhD) in the Division of Medical Virology, Department of Pathology, Faculty of Health Sciences, University of Cape Town

September 2018

Supervisor: Professor Anna-Lise Williamson

Co-supervisor: Dr Nicola Douglass

GENERAL TABLE OF CONTENTS

Contents	Page
ABSTRACT	iii
DECLARATION	v
ACKNOWLEDGEMENTS	vi
LIST OF ACRONYMS AND ABBREVIATIONS	vii
TABLE OF CONTENTS FOR LITERATURE REVIEW	1
LIST OF FIGURES	2
LIST OF TABLES	3
CHAPTER1: LITERATURE REVIEW	4
CHAPTER 2: COMPARISON OF THE INNATE HOST TRANSCRIPTOME INDUCED IN MICE AFTER INFECTION WITH nLSDV AND HERBIVAC	49
CHAPTER 3: CHARACTERISATION OF THE IMPACT OF THE LSDV SOD HOMOLOG ON VIRAL GROWTH, SOD ACTIVITY AND CELL DEATH	81
CHAPTER 4: CONCLUSIONS AND FUTURE STUDIES	136
REFERENCES	140
APPENDICES	179

Abstract

Lumpy skin disease (LSD) is a notifiable viral infection due both to its morbidity in cattle and its severe economic burden. The disease was confined to Sub-Saharan Africa but has in recent years spread to the Middle East and Europe. Vaccination is the only way of preventing LSD. Live attenuated lumpy skin disease virus (LSDV) has been used as a vaccine against LSD. The most successful LSD vaccine is the Neethling vaccine strain (nLSDV) from South Africa. There are however, reports of nLSDV being too attenuated or too virulent in different breeds of cattle.

A South African produced vaccine strain of LSDV, Herbivac, was said to be more immunogenic than nLSDV (personal communication, Deltamune). Whole genomic sequence comparison of Herbivac with nLSDV revealed a single potentially significant change in open reading frame (ORF) 131. This ORF encodes a superoxide dismutase (SOD) homologue. The mutation identified in Herbivac is a 2bp deletion which causes a frameshift mutation that restores the SOD homologue to resemble the full-length SOD homolog encoded by the virulent field strain. This SOD homologue gene is truncated in nLSDV.

Protein structural alignment of SOD homologues from LSDV and other characterised SOD homologues was done. Both the truncated and full-length SOD homologues lacked the catalytic arginine at position 142 which is involved in SOD activity. Some similarities with known SOD homologues which act as SOD decoys, such as the *Leporipoxviruses* myxoma and Shope Fibroma virus, were observed. Like *Leporipoxvirus'* SOD homologues, the full-length Herbivac SOD homologue contained regions of homology with the copper chaperone for SOD (CCS). The putative SOD protein from Herbivac, and not nLSDV, contained 6 out of 8 metal binding residues. Unlike the SOD decoy from myxoma virus, the full-length SOD homolog from Herbivac did not include a cysteine molecule at position 56 that stabilizes the SOD-CCS heterodimer. The alignment suggests that all SOD homologs from LSDV are inactive as enzymes.

Transcriptome analysis of messenger RNA from spleens of mice infected with nLSDV or Herbivac for 24hrs was carried out to determine the effect of Herbivac or nLSDV infection on host gene expression. Compared to the PBS control, nLSDV and Herbivac induced the differential expression of 98 genes in common, largely related to response to viral infection. nLSDV differed in the unique expression of 6 genes and Herbivac differed in the unique

expression of 36 genes, including granzyme A and Poly (ADP-ribose) polymerase (Parp 9). Herbivac upregulated genes associated with pathogen pattern recognition, interferon response, immune response and cell death. More Gene ontology (GO) processes were enriched after Herbivac infection than nLSDV infection. Amongst these processes were immune response processes, the interferon and cell death related responses.

To characterise the SOD homolog with respect to SOD activity, cell death and whether it plays a role in growth of viruses expressing it, recombinant viruses were constructed. The first set of recombinants included a SOD knock-out virus where the SOD gene from nLSDV was replaced with reporter gene GFP. A SOD knock-in virus was constructed with the SOD homologue gene altered to improve the stability of the gene. A reporter gene mCherry was also inserted.

Histological examination of CAMs infected with nLSDVdSOD-M showed vacuolation and oedema to a greater degree than nLSDV, Herbivac and nLSDVSODis-M. Herbivac showed greater immune cell infiltration. SOD knock-in, nLSDVSODis-M showed increased epithelial hyperplasia and fibroplasia.

Another set of recombinants without marker genes was made, nLSDVdSOD-UCT (SOD knock-out), and nLSDVSODis-UCT (SOD knock-in). Deleting the SOD homolog reduced virus yield by approximately ten-fold in MDBK cells. Histologically, the presence of the SOD homolog in nLSDVSODis-UCT caused greater inflammatory changes in the mesoderm after 5 days of infection compared to nLSDVdSOD-UCT.

In vitro functional studies were done in MDBK cells which are permissible to LSDV infection. No difference in SOD activity could be detected amongst the different viruses. Differences could, however, be detected in induction and inhibition of apoptosis. There was increased induction of apoptosis following infection by all viruses containing full-length SOD compared to infection with truncated or SOD knock-out virus. Viruses expressing a full-length SOD showed greater inhibition of camptothecin induced apoptosis than nLSDV or the SOD knock-out. Similarly, full-length SOD induced cell death by necrosis to a greater extent than the SOD knock-out or nLSDV; and all viruses inhibited camptothecin induced necrosis.

These results suggest that the presence of a SOD homolog in a vaccine could be advantageous with respect to growth of the vaccine to higher titres and to improved immunogenicity of the vaccine. Further work is required to test this hypothesis in a bovine animal model.

Declaration

The work described in this thesis was done at the Division of Medical Virology, Department of Pathology and Institute of Infectious Diseases and Molecular Medicine (IDM), University of Cape Town, under the supervision and guidance of Professor Anna-Lise Williamson and Dr Nicola Douglas. This is my own work, and where use has been made of others, their contribution has been acknowledged.

…Signed by candidate..

Henry Munyaradzi Munyanduki

07 September 2018

Acknowledgements

I am hugely indebted to my family for its unwavering financial and moral support. Their commitment to this work goes beyond words. To my wife, confidante and best friend, the many sleepless nights and the huge sacrifices have paid off! Thank you. To my PhD mentors and supervisors, Prof. A-LWilliamson and Dr. N Douglass, I acknowledge your input and great training. If I have indeed seen further, it is because I have stood on the shoulders of these two giants. Thank you. I acknowledge the input of my colleague Ruzaiq Omar and his help in the final parts of my PhD. I also am very grateful to Dr Offerman for her assistance in most of the bioinformatic analysis in this work. My acknowledgements go to Olivia Carulei for her support in her editorial efforts in this manuscript. I also acknowledge all the colleagues past and present of the Anna-Lise Williamson research group for their technical and moral support during these past years. A special mention goes to Dr Dzhvivhuo, Dr Jongwe, Fatima Abrahams and Harris Onywera. Indeed, a man sharpens the countenance of another man! I acknowledge Associate Professors Denver Hendricks, Collet Dandara and the faculty manager Mrs Adri Winkler for their moral support and guidance. I acknowledge Mrs Susan Cooper of the light microscopy/confocal unit for their assistance. I also thank Mr Rodney Lucas for assistance with the mice work. I also want to extend my heartfelt gratitude to the Gospel Ramah Church for their spiritual support in this journey. I acknowledge the many prayers and grooming that has culminated to this day. Special mention to my sister Flora, brothers Lycias, Victor and Senzo for being a shoulder to lean on. I also want to acknowledge the University of Cape Town for the International Scholarship, the National Research Foundation for funding and the Poliomyelitis Research Foundation for the financial support. Most importantly, I acknowledge God for the gift of life and this magnanimous opportunity. Indeed, if it had not been for the Lord, who was ALWAYS by my side, where would I be?

List of abbreviations

ANOVA -analysis of variance

bp – base pair

CAM – camptothecin

CAM – chorioallantoic membrane

CCS – copper chaperone for SOD

DNA - deoxyribonucleic acid

ecoGPT – E coli xanthine (guanine) phosphoribosyltransferase

GFP- green fluorescent protein

H&E – haematoxylin and eosin

HF – Holstein Friesian

HIV – human immunodeficiency virus

HPI – hours post infection

IFAT - Indirect Fluorescent Antibody Test

IL - interleukin

IMS - intermembrane space

IRF - Interferon

LSD – Lumpy skin disease

LSDV – Lumpy skin disease virus

MAPK - Mitogen-Activated Protein Kinase

MDBK – Madin-Darby Bovine Kidney Cells

MEK - MAPK/ERK kinase

MMP - membrane permeabilization

MOI – multiplicity of infection

MPA – mycophenolic acid

MYX – myxoma virus

NHE – Sodium (Na) hydrogen (H) exchanger

NLR – NOD like receptor

nLSDV – Neethling lumpy skin disease virus

OBP – Ondesteepoort Biological Products

OIE - World Organisation for Animal Health,

ORF – open reading frame

ORI – origin of replication

PBS – phosphate buffered saline

PCR - Polymerase chain reaction

RIG - retinoic acid inducible gene

ROS – reactive oxygen species

SEM – standard error of the mean

SFV – Shope Fibroma Virus

SNP – single nucleotide polymorphism

SOD – superoxide dismutase

TCID50 – Tissue culture Infective Dose

Tlr – Toll like receptor

UCT – University of Cape Town

VNT - Virus Neutralisation Test

VV – Vaccinia virus

WT – wild type

Chapter 1 Literature Review

1.1 Lumpy skin disease 4
1.1.1 Aetiology 4
1.1.2 Historical background 5
1.1.3 Economic Impact 7
1.1.4 Clinical Signs of LSD 7
1.1.5 Histopathology 8
1.1.6 Diagnosis 9
1.1.7 Transmission 11
1.2 Vaccination against LSDV 11
1.2.1 Vaccines against LSD 11
1.2.2 Vaccine efficacy 13
1.2.3 Adverse reactions after vaccination 15
1.3 Use of lumpy skin disease virus as a vaccine and recombinant vaccine vector 15
1.4 Virus structure and genomic organisation 18
1.4.1 Virus structure 18
1.4.2 Life cycle of poxviruses 19
1.4.3 Genome organisation of LSDV 21
1.5 Virus host interaction: Innate immunity against viral infections 26
1.5.1 The interferon stimulated genes (ISG) 30
1.5.2 Apoptosis as an antiviral mechanism 30
1.5.3 The different mechanisms of cell death 32
1.5.4 Inhibition of apoptosis 33
1.5.5 Cell death and immunogenicity 35
1.5.6 Modulation of host factors as a mechanism for immune evasion and host range 35
1.6 Generation of the superoxide anion in response to viral infection 36
1.6.1 Function of the superoxide anion 40
1.6.2 The role of the superoxide anion in apoptosis 40
1.6.3 Role of antioxidants 41
1.7 SOD homologues 44
1.8 Project motivation 47

List of Figues

Figure 1.1. Phylogenetic tree of poxviruses based on an amino acid sequence alignment of 20 genes. 4

Figure 1.2. Geographical distribution of LSDV.. 6

Figure 1.3. Symptoms of lumpy skin disease. 8

Figure 1.4. Electron micrograph of LSDV..... 18

Figure 1.5. The life cycle of a poxvirus. 20

Figure 1.6. A linear representation of the virulent LSDV genome. 22

Figure 1.7. Nucleotide alignment of ORF 131 of LSDV Nl 2490, nLSDV, and Herbivac. 26

Figure 1.8. Alignment of putative amino acid sequences of SOD homologue genes. 26

Figure 1.9. Innate immune system recognition of different antigens including poxviruses.. 29

Figure 1.10. Pathways of apoptosis.. 31

Figure 1.11. Different forms of cell death elicit either an anti- or pro- inflammatory response.. 33

Figure 1.12. Outline of both the extrinsic and intrinsic apoptotic pathways showing sites at which viral proteins inhibit these pathways.. 34

Figure 1.13. Functional domains in Cu, ZnSOD are shown and the preservation of structure between different SOD 1 proteins. 43

Figure 1.14. Putative mechanism for docking of copper onto SOD 1 by the chaperone, CCS.. 44

Figure 1.15. Amino acid alignment of viral SOD-like proteins..... 46

List of Tables

Table 1.1. Year(s) of first and subsequent lumpy skin disease incidences. 5

Table 1.2. Diagnostic methods used to detect capripoxviruses for different purposes. 9

Table 1.3. List of vaccines used against LSD, efficacy data and adverse reactions reported to date. .. 14

Table 1.4. List of ORFs found to be different between a virulent LSDV (Warmbaths strain) and an attenuated strain (Neethling vaccine strain). 24

Table 1.5. Interferon Stimulated Genes that are activated by Type 1 interferons. 30

Table 1.6. List of Poxvirus host range gene families and how they mediate their function 37

Table 1.7. Viral genes in LSDV that could be involved in modulating the immune response, host function and apoptosis.. 39

Table 1.8. A summary of reports supporting the notion that the superoxide anion is anti-apoptotic and hydrogen peroxide is pro-apoptotic. 41

Table 1.9. Summary of all the tests done on poxvirus SOD homologues to determine whether they act as functional SOD enzymes or decoy proteins. 47

Chapter 1 Literature Review

1.1 Lumpy skin disease

1.1.1 Aetiology

Lumpy skin disease (LSD) is a notifiable disease caused by the poxvirus lumpy skin disease virus (LSDV). The virus belongs to the family *Poxviridae*, which is divided into two subfamilies – *Chordopoxviridae* (vertebrate infecting) and *Entomopoxviridae* (invertebrate infecting) (Figure 1.1). The Chordopoxvirus subfamily is subdivided into ten genera namely *Parapoxvirus, Yatapoxvirus, Capripoxvirus, Suipoxvirus, Orthopoxvirus, Molluscipoxvirus, Avipoxvirus, Leporipoxvirus, Cervidpoxvirus and Crocodylidpoxvirus. LSDV belongs to the genus Capripoxvirus* (Mercer et al., 2007a), International Committee on Taxonomy of Viruses (ICTV, 2018).

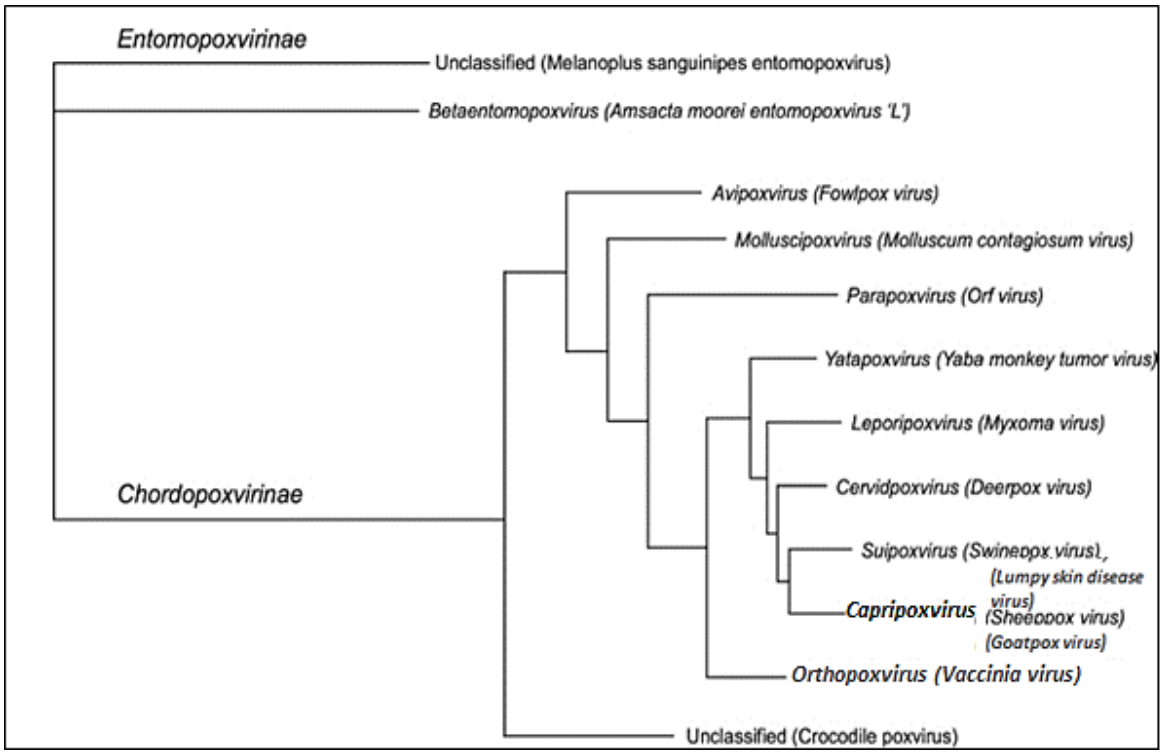

Figure 1.1. Phylogenetic tree of poxviruses based on an amino acid sequence alignment of 20 genes. A node represents a genus and the species is shown in brackets. The capripoxvirus subfamily contains 3 species, namely lumpy skin disease virus, sheeppox virus and goatpox virus. Modified from Hendrickson et al. (2010).

LSD mainly affects cattle (Bos indicus, Bos Taurus) and Asian water buffalo (Balus bubalais) and carries a significant economic burden due to the clinical presentation of the disease (reviewed in section 1.1.4) (OIE, 2017, Abera et al., 2015, Hunter and Wallace, 2001). There

has been an instance where LSDV has been isolated from sheep where it causes mild disease (Tuppurainen et al., 2014).

1.1.2 Historical background

LSD was first identified clinically in Northern Rhodesia, modern day Zambia in 1929 (reviewed by Hunter and Wallace (2001)). In the first part of the last century LSD was localised to Southern Africa but was later found in Kenya, Sudan and Ethiopia (Weiss, 1968, Davies, 1982, Abera et al., 2015, Davies, 1981). It has now spread to most of the African continent except for a few countries that include Libya, Tunisia, Algeria and Morocco. In 2007 LSD spread to the Middle East (Sihvonen and Depner, 2016, OIE, 2017, Tuppurainen and Oura, 2012, Beard, 2016). There has been a spread of the disease to Europe in the past few years including Russia (2015), Greece (2015) and Bulgaria (2016) (Beard, 2016). Table 1.1 gives the time-line for the spread of LSD.

Table 1.1. Year(s) of first and subsequent lumpy skin disease incidences.

Country	Year incidence reported	Reference
Zambia	1929	Reviewed in (Hunter and Wallace, 2001)
Botswana, Zimbabwe, Republic of South Africa	1943-1945	(Von Backstrom, 1945), reviewed by Hunter and Wallace (2001)
Kenya	1957	(Davies, 1981, Davies, 1982, Burdin and Prydie, 1959)
Sudan	1970, 1979	(Davies, 1981)
Nigeria	1974	(Nawathe et al., 1982)
Mauritania, Mali, Ghana, Liberia	1977	(OIE, 2017)
Tanzania, Kenya, Zimbabwe	1981-1986	(Davies, 1982), (Brenner et al., 2009)
Somalia	1983	(Davies, 1991)
Ethiopia	1984	(Mebratu et al., 1984)
Israel	1989, 2006/2007	(Yeruham et al., 1995), (Brenner et al., 2009)
Egypt	1988/1989, 2006	(House et al., 1990)
Egypt	2006	(El-Kholy et al., 2008)
Ethiopia	1983, 2000/2001, 2003/2004, 2006/2007, 2010/2011	(Farah, 2017, Ayelet et al., 2014) and reviewed by Abera et al. (2015))
Oman	2009	(Kumar, 2011)
Israel	2006, 2012	(Tuppurainen and Oura, 2012)
Lebanon, Jordan	2012/2013	Reviewed by Alkhamis and VanderWaal (2016)
Turkey, Iraq, Iran, Cyprus	2013-2015	Reviewed by Tuppurainen et al. (2017)
Bulgaria, Greece	2015/2016, Serbia	OIE 20151005.3692103,(Sihvonen and Depner, 2016, Toplak et al., 2017)
Russia	2015	OIE 20151016.3720589, Reviewed by Tuppurainen et al. (2017)

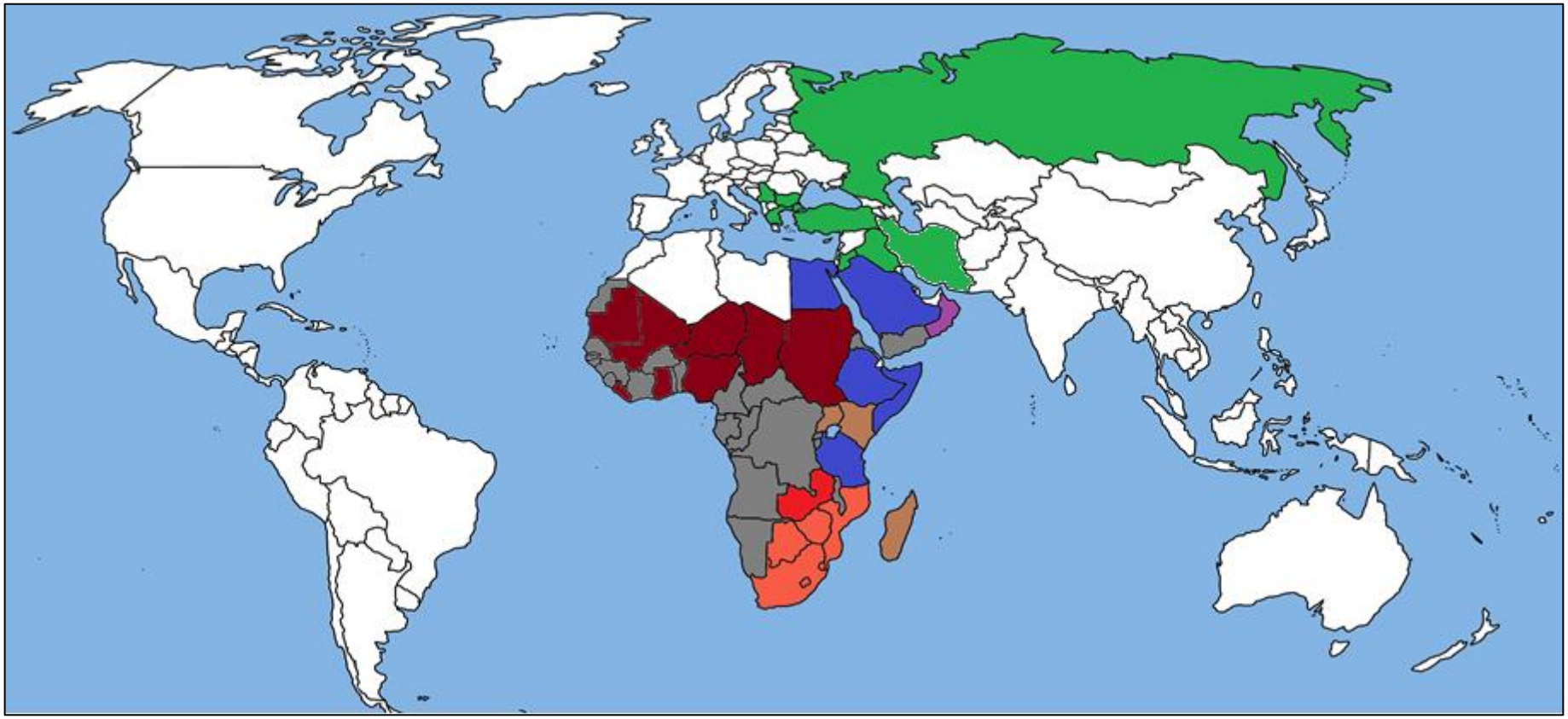

Figure 1.2. Geographical distribution of LSDV. LSDV used to be endemic to Africa and particularly Sub-Saharan Africa. More recently LSDV has spread to the Middle East and into Europe. The different colours represent the times of introduction into different countries. Grey - unknown; red - 1920-1930; pink - 1941-1950; brown-1951-1960; maroon - 1970-1980; dark blue - 1981-1990; purple - 2009; green - 2011-2018. This figure is based on information from Hunter and Wallace (2001), Weiss (1968), Davies (1982), Abera et al. (2015), Davies (1981), Sihvonen and Depner (2016), OIE (2017), Tuppurainen and Oura (2012), Beard (2016).

1.1.3 Economic Impact

Cattle are reared for different reasons including commercial and private/cultural purposes (Ntombimbini and Klein, 2015). Since LSDV can spread rapidly with serious economic impact, LSD is classified as a notifiable disease by the World Organisation for Animal Health (OIE). A notifiable disease is defined as a disease that is required by law to be reported to government authorities. The primary economic losses are due to weight loss, a sharp decline in milk production, loss of traction (morbidity), poor growth, in some cases abortion, damage to hides and temporal to permanent infertility (reviewed by Abera et al. (2015), Tuppurainen and Oura (2012) and Gari et al. (2011). There are also other losses resulting from LSDV infection of cattle, namely, meat losses when infected animals are incinerated and costs of treating secondary infections (Abera et al., 2015).

1.1.4 Clinical Signs of LSD

Infected cattle present a biphasic, febrile response with skin nodules appearing before and during the second episode of the disease (Coetzer, 2004). In cattle, infection with LSDV causes a fever of up to 40-41^0 C (Carn and Kitching, 1995a). The other clinical symptoms include depression, salivation, ocular and nasal discharges (Coetzer, 2004). After 4 to 10 days, lesions appear and these are characterised by erythematous raised foci (Mercer et al., 2007a). These lesions appear all over the body, head, neck, udder, scrotum and vulva and range in size from 0.5 to 10 cm in diameter (Coetzer, 2004, Rovid, 2012, Prozesky and Barnard, 1982). Lesions are circumscribed, firm, rounded and raised. They may exude serum. The lesions are characterised by regions of necrosis which permeates the epidermis and dermis and underlying muscle tissue. Regions of necrosis separate the lesion from the skin creating nodules (Rovid, 2012). These nodules can be removed when clasped between fingers (Figure 1.3) and they leave ulcerative lesions.

Grouping of skin nodules causes the formation of larger plaques which lead to skin sloughing in the lower abdomen and limbs (Weiss, 1968, Von Backstrom, 1945). Secondary nodules can also form along with lymphadenopathy (inflammation of the lymph nodes), conjunctivitis (inflammation of the eyes) and rhinitis (inflamed nasal cavity) (Carn and Kitching, 1995a). Bulls can suffer from temporal or permanent infertility whilst infection of cows in their udders and teats can result in bacterial infections causing mastitis (Mercer et al., 2007a, Tuppurainen and Oura, 2012). There is significant reduction of milk production in infected animals (OIE,

2017). Lesions are not only localised to the skin but may appear in the stomach, uterus, vagina, udder and testes. Necrotic areas can be found in the respiratory tract and pneumonia can develop if pieces of necrotic tissue are inhaled (Coetzer, 2004).

The severity of infection is generally dependant on the animal's age, breed (host genotype) and the state of its immune system upon contracting the disease (OIE, 2017). In one experiment where cattle were infected intravenously with a virulent LSDV strain, Dexter breed of cattle showed severe clinical disease, whereas the Friesian breed showed mild disease and the Dexter cross breed had unapparent clinical signs (Tuppurainen et al., 2005). In a retrospective study based on a questionnaire from farmers in Ethiopia, the cattle breeds Holstein Friesian (HF) and Jersey were found to be more vulnerable to LSDV infection than their locally bred Zebu cattle. In the same study LSDV related mortality was lower in the Zebu cows relative to the HF cows (Gari et al., 2011).

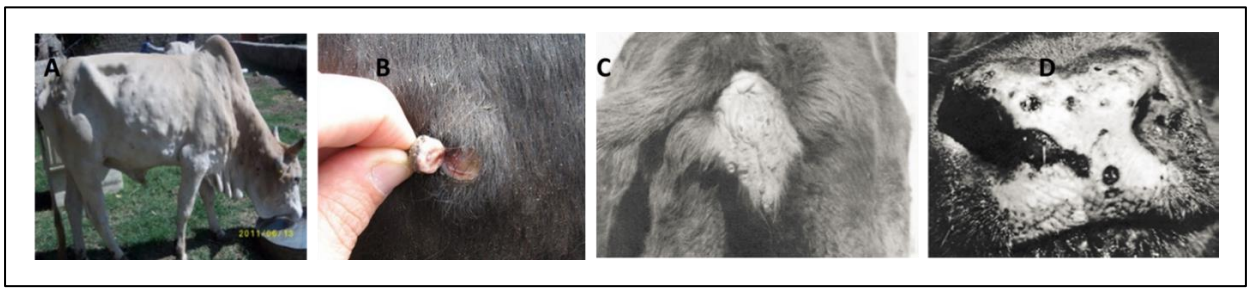

Figure 1.3. Symptoms of lumpy skin disease. Cow with lesion on hide (A), sit fast lesions (B), lesions on vulva (C), necrotic lesions on the muzzle (D). A and B taken from Abutarbush et al. (2015) and C and D taken from Coetzer (2004).

1.1.5 Histopathology

Histological examination of lesions from LSDV infected animals shows differences depending on the stage of infection. During the course of infection, histological examination of lesions and skin sections from animals infected by LSDV show ballooning degeneration in the epidermal layers, the presence of intracytoplasmic inclusion bodies, vasculitis and proliferation of fibroblasts (Mercer et al., 2007a, Alexander et al., 1957, Neamat-Allah, 2015). Acute infection of cattle is associated with vasculitis and lymphangitis, which causes thrombosis and infarction with the subsequent effect of necrosis combined with immune infiltration (Prozesky and Barnard, 1982). Hence, the late stages of infection are characterised by fibroplasia where the dead cells (from necrosis) in the initial stages of infection were replaced by the inflammatory cells and fibroblasts. The last stage of disease also shows hyperkeratosis in the

epidermis. Necrotic cells appear oedematous with vesicles forming inside them. Appearance of inclusion bodies is also characteristic of late stage infection (Prozesky and Barnard, 1982).

1.1.6 Diagnosis

Characterisation of the clinical presentation of LSD, differential diagnosis and laboratory based tests are used routinely to diagnose LSD (Abera et al., 2015). There are many laboratory tests that are used to identify LSDV infection and the key tests that are recommended by OIE are summarised in Table 1.2. Some serological tools for the detection of LSD infected cattle have been developed. The only limitation is that these tests cannot differentiate between infected and vaccinated animals.

Table 1.2. Diagnostic methods used to detect capripoxviruses for different purposes. Modifications to some of the tests included in this table have been made in the current methods of diagnosis and will be reviewed below.

Method	Purpose					
	Population free from infection	Individual animal freedom from infection prior to movement	Contribute to eradication policies	Confirmation of clinical cases	Prevalence of infection-surveillance	Immune status in individual animals or populations post-vaccination
Agent identification						
Virus Isolation	+	++	+	+++	+	N/A
Antigen detection	++	++	++	++	++	N/A
PCR	++	+++	++	+++	++	N/A
Detection of immune response						
VN	++	++	++	++	++	++
IFAT	+	+	+	+	+	++

*A combination of agent identification methods applied on the same clinical sample is recommended.
+++ (recommended method); ++ (suitable method); + (used in some situations, but cost, reliability, or other factors severely limits its application); N/A (not applicable); PCR (polymerase chain reaction); VN (virus neutralisation); IFAT (indirect fluorescent antibody test).

An indirect fluorescence antibody test (IFAT) is routinely used to diagnose LSD (Tuppurainen et al., 2005, OIE, 2017). This test identifies LSDV antibodies in cattle serum (Gari et al., 2008). Western blot analysis using antibodies to structural proteins in the virus can also be used to detect LSDV (OIE, 2017). Innovative diagnostics (ID.vet) has developed the first commercially available ELISA for the detection of LSDV (ID Screen® Capripox Double

Antigen Multi-species available at https://www.id-vet.com/produit/id-screen-capripox-double-antigen-multi-species/).

One of the standard tools for the identification of capripoxviruses involved growth of the virus in a permissive cell line such as primary lamb or bovine cells and observing cytopathic effects (CPE) (Mercer et al., 2007b). However, this does not distinguish between sheeppoxvirus, goatpoxvirus or lumpy skin disease virus. With developments in molecular assay techniques, several polymerase chain reaction (PCR) based methods have been described (Armson et al., 2017, El-Kholy et al., 2008). PCR is the most sensitive in the detection of poxviruses (Mercer et al., 2007a). One of the first PCR based assays to diagnose LSDV made use of primers that were designed to amplify the gene encoding the immunodominant P32 protein (Heine et al., 1999). Other PCR tests have been based on amplification of the viral attachment protein gene (Ireland and Binepal, 1998, Albayrak et al., 2018). Bowden et al. (2008) described a highly sensitive real time qPCR to detect capripoxviruses based on amplification of a region of ORF 74. A limitation of this test was that it could not distinguish between LSDV and the other two capripoxviruses (Bowden et al., 2008). PCR has therefore been coupled with Sanger sequencing of the PCR product, to confirm the presence of LSDV (El-Kholy et al., 2008).

The newer PCR based methods for detection of LSDV have focused mainly on the rapid detection of LSDV, amenability of the test in outbreak areas and distinction between LSDV vaccine strains from wild type virulent LSDV. Menasherow et al. (2014) developed a PCR test based on three differences between the Neethling vaccine strain and the circulating wild type virus in Israel. Virulent LSDV was shown to have 27 nucleotides more compared to the vaccine. Secondly, there was a difference in the primer annealing temperature using LSDV specific primers between the two strains and lastly, a unique restriction site (MboI site) next the ORF 126 (EEV gene) in the vaccine strain was identified. A high-resolution melting assay (HRM) was developed which recognises the 27 base-pair deletions in the vaccine strain (Neethling prototype), which also uses a thermal gradient to detect a product at 65 °C for the vaccine and not WT. Primers were used with 3’ ends unique to the vaccine strain. They also used MboI restriction enzyme digestion to distinguish and confirm the LSDV strains (Menasherow et al., 2014).

Another sensitive PCR based test was recently developed in the Balkans. Similar to the Israeli group, in this PCR, primers specific to the circulating strains and a vaccine strain (Lumpyvax) were used (Vidanović et al., 2016). More recently, Agianniotaki et al. (2017) described a new

diagnostic duplex PCR technique that can differentiate infected animals from vaccinated animals. The presence of a 12 base-pair deletion in the G-protein-coupled chemokine receptor (CPGR) in the vaccine strain is used to differentiate vaccine from WT virulent LSDV (Agianniotaki et al., 2017).

There are efforts being made, using serological and PCR assays, to differentiate vaccinated animals from virulent LSDV infected animals (DIVA) in non-endemic areas (Tuppurainen and Oura, 2012, Tuppurainen and Galon, 2016). The inability to distinguish the antibody response following infection with wild type capripoxvirus from vaccination has made it difficult to conduct serosurveillance of LSDV in capripoxvirus endemic areas. For this reason PCR based techniques have become more important (Tuppurainen et al., 2017).

1.1.7 Transmission

Carn and Kitching (1995) demonstrated that LSDV transmission between infected animals and uninfected animals housed together was inefficient but that intravenous inoculation of animals using a field isolate was extremely efficient in establishing disease. They therefore postulated that infection was established by arthropods (Carn and Kitching, 1995b). Mechanical LSDV transmission by *Aedes aegypti* female mosquitoes from infected cattle to susceptible cattle has been demonstrated (Chihota et al., 2001). Tuppurainen et al. (2013) showed that LSDV could be vertically transmitted by *Rhinecephalus decolarutus* ticks and confirmed the role of Ixodid ticks in both transstadial (*A. hebraeum*) and transovarial (*Rhipicephalus (Boophilus) decolora*tus) transmission of lumpy skin disease virus (Tuppurainen et al., 2013, Tuppurainen et al., 2011, Lubinga et al., 2013, Lubinga et al., 2014).

Transmission of LSDV via semen has also been demonstrated (Annandale et al., 2014). The intrauterine spread of LSDV has been reported in premature calves from infected cows (Rouby and Aboulsoud, 2016). Transmission to suckling calves via infected milk and in cattle sharing drinking troughs has also been implicated as a possible route of transmission (Coetzer, 2004).

1.2 Vaccination against LSDV

1.2.1 Vaccines against LSD

All the LSDV vaccines available commercially are live attenuated vaccines (Abutarbush et al., 2016, Tuppurainen and Oura, 2012, Tuppurainen et al., 2017). The three members of the genus

capripoxvirus, namely, sheeppox, goatpox and LSDV are antigenically the same with a similar precipitating antigen (Kitching et al., 1986). Thus, attenuated LSDV, sheeppox virus and goatpoxvirus have been used as vaccines for LSD (Hunter and Wallace, 2001). The SPPV and GPV based vaccines are often used at a much higher dosage in cattle compared to the LSDV based vaccines (Tuppurainen et al., 2017). The disadvantage of using sheeppox or goatpox virus-based vaccines is that they are confined for use in areas where sheeppox and goatpox are endemic. This is because, the vaccine can be a source of infection for vulnerable sheep or goats (Coetzer, 2004). Recently, the Kenyan sheep and goatpox virus vaccine was actually shown to be LSDV (Tuppurainen et al., 2014). This LSDV strain has not been highly attenuated and may be a source of clinical disease in vaccinated cattle (Tuppurainen et al., 2014). The other disadvantage of using sheeppox virus as a vaccine against LSD is the lack of adequate protection upon LSDV challenge. In a recent study which used a sheeppox virus (RM65) as a vaccine against LSDV in cattle in Israel, RM65 was shown to be less efficacious in protecting animals when compared to the Neethling vaccine strain from South Africa (Ben-Gera et al., 2015).

Whilst vaccination remains the best way of controlling infection and transmission of LSDV, different factors may affect its efficacy. Firstly, local reactions associated with the vaccine may hinder the uptake of the vaccines by farmers. This is because LSD symptoms have been noticed in vaccinated cattle (Ben-Gera et al., 2015). Secondly, the efficacy of the vaccine is complicated by the need to have a cold chain (EFSA, 2015). Thirdly, because some animals remain asymptomatic when infected, transmission of wild type virulent LSDV during vaccination can occur. The use of the same needles during mass vaccination in resource constrained communities can spread wild type LSDV. Fourthly, the presence of maternal antibodies in calves born to either immunised or LSDV-infected cows may lower the protection conferred by vaccination. Lastly, incorrect dosages from incorrect formulations may also render the vaccine ineffective (EFSA, 2015). Because LSD has been confined to Africa until recently, there have not been many commercial producers of the vaccine. For this reason there may be shortages of vaccine during acute endemics where a lot of doses are required in short notice periods (EFSA, 2015).

The most widely used vaccine against LSDV is the South African Neethling strain produced by Onderstepoort Biological Products - OBP Neethling (reviewed by Hunter and Wallace (2001). This attenuated form of LSDV vaccine was made by passaging LSDV (Neethling strain)

fifty times in lamb cells and passaging twenty times in fertilised hens' eggs (reviewed by Davies (1991)). The Neethling vaccine strain of LSDV has been shown to confer neutralising antibodies to other virulent strains of LSDV (reviewed by Hunter and Wallace (2001)). This vaccine is recommended by the manufacturer to be given at 6 months of age and then annually (OBP, South Africa). Vaccination is recommended to be done in the spring (MSD, South Africa). Other vaccines for LSD that are used in South Africa include Herbivac (Deltamune) and Lumpyvax (MSD Animal Health). Both these vaccines have sequences almost identical to LSDV (Neethling strain) (Mathijs et al., 2016).

The Kenyan sheeppox, goatpox (KSGP) vaccine is the standard vaccine used in Kenya for cattle (Carn, 1993). However, as previously noted, molecular characterisation of the Kenyan sheeppox and goatpox virus vaccine (KSGP) O-240 revealed that this vaccine was not sheeppox as previously described, but a strain of LSDV (Tuppurainen et al., 2014). More recently, a goatpox virus strain (Gorgan strain) was shown to effectively protect calves against LSDV challenge (Gari et al., 2015). Other vaccines for LSDV exist, namely the Yugoslavian RM-65 sheeppox virus strain and the Romanian sheeppox virus (Coetzer, 2004). The sheeppox and goatpox virus-based vaccines cannot be used in South Africa because sheeppox is not endemic to South Africa.

1.2.2 Vaccine efficacy

Since vaccination remains the best way to control LSD, there is a great need for efficacious vaccines. As shown in Table 1.3 there are some serious concerns over the different types of LSDV vaccines used and their efficacy. Vaccine failure and the reinfection of vaccinated animals complicate LSD control and eradication (Gari Jimolu, 2011). Interpretation is complicated by the different sources and dosages of the vaccines used. The live attenuated LSDV vaccine provides good protection in cattle and is generally superior to the sheeppox virus-based vaccines. In a field study done in Israel the LSDV Neethling vaccine was significantly more effective at preventing LSD compared to the attenuated sheeppox vaccine (RM 65) (Ben-Gera et a., 2015).

Table 1.3. List of vaccines used against LSD, efficacy data and adverse reactions reported to date.

Vaccine	Manufacturer	Country/Region used	Notes	Reference
Neethling vaccine strain (OVI, SA)	Ondersteport Biologicals (OBP), South Africa	Widely used -Africa and the Middle East	Made by passaging LSDV (Neethling strain) fifty times in lamb cells and passaging twenty times in fertilised hens' eggs i) Provides good protection against LSD. ii) Immunity speculated not to be lifelong therefore annual vaccinations recommended. iii) More adverse reactions in European breeds compared to African breeds iv) More effective than sheeppox virus vaccine RM65.	Weiss, 1968 Van Rooyen et al, 1969 Reviewed by Hunter and Wallace, (2001) (Katsoulos et al., 2018) (Ben-Gera et al., 2015)
Yugoslavian RM65 SPPV		Middle East	Incomplete protection in Israeli trial and some clinical signs of LSD in vaccinated cattle in a trial in Jordan	
Romanian SPP		Egypt		
Kenyan sheep and goatpox (KSGP)	National Veterinary Institute (NVI)	Northern Africa, Middle East, Turkey, Iraq, Iran	KSGP O-240 associated with incomplete protection in Egypt. Failed to protect in Ethiopian cattle. KSGP O-180 failed to protect. This vaccine is actually LSDV.	Davies, 1991; Brenner et al., 2009; Somasundaram, 2011; Abutarbush, 2014, Ayelet, 2013
LSDV Neethling	National Veterinary Institute (NVI)	Ethiopia	Failed to protect in an Ethiopian trial.	
Gorgan GTP strain vaccine	Jordan Bio-Industries Centre (JOVAC)	Middle East	More effective than the Ethiopian Neethling and KSGPO-180.	Gari et al., 2015
Bakirköy SPPV		Turkey	Currently used in Turkey.	Tuppurainen et al., 2017
LSDV Neethling strain	MCI Sante Animale, Morocco		South African Neethling vaccine	Tuppurainen et al., 2017
Romanian SPPV strain	MCI Sante Animale, Morocco		To be tested in a trial	Tuppurainen et al., 2017
Herbivac	Deltamune, South Africa	South Africa	Derived from LSDV Neethling OPB	Personal communication and also Sequenced by Mathjis, 2015
Lumpyvax	MSD, South Africa	South Africa	No available data	Sequenced by Mathjis, 2015

The Kenyan sheep and goatpox virus failed to protect animals in Egypt in the 2006 LSD outbreak; and, the Yugoslavian RM 65 sheeppox virus failed to offer complete protection in Israel in the 2006/2007 LSD outbreak (reviewed by Tuppurainen and Oura (2012)

In Ethiopia a comparison was done with three different vaccines to determine if they could protect from virulent LSDV. The Ethiopian Neethling vaccine strain and KSGPO-180 strain were both produced in an Ethiopian factory and the Gorgan goatpox virus vaccine was produced in Jordan. Vaccine failure was observed in 70 per cent animals vaccinated with the Ethiopian Neethling vaccine and 50 per cent after vaccinating with KSGPO-180 when experimentally challenged with a virulent LSDV strain (Gari et al., 2015). The virulent field strain came from naturally infected cattle and was passaged three times to bulk up virus for challenge. The Gorgan goatpox virus vaccine was shown to elicit better delayed hypersensitivity scores and antibodies as well as much better protection upon challenge with virulent LSDV. It was shown that vaccine failure was intimately linked to the inability of the Ethiopian Neethling and KSGPV O-180 to elicit a strong immune response in sentinel animals (Gari et al., 2015). This may have been due to manufacturing issues.

1.2.3 Adverse reactions after vaccination

Different studies with different vaccines against LSD have reported a range of adverse reactions. The adverse reactions with LSDV (Neethling) vaccine were relatively minimal in a study done on Holstein-Friesian cattle in Greece. Pronounced swelling was seen at the injection site in 26/215 adult cows, but not in calves. This indicated that the vaccine was safer in calves than in adult animals. The swelling found in adult cows, which resolved within 10 days, was acceptable given the serious morbidity observed in virulent infection. Milk production was reduced for 12 days post-vaccination (Katsoulos et al., 2018).

1.3 Poxviruses as vaccine vectors

Poxviruses have been used for vaccination with the first record being the use of Cowpox virus to confer immunity against Variola virus (reviewed by (Riedel, 2005)). The eradication of smallpox, due to the elimination of the causal agent of the disease, Variola virus, was an important milestone in the history of medicine (Fenner, 1977, Fenner, 1980, Fenner, 1982). This goal was achieved after a global vaccination campaign using Vaccinia virus (VV), a virus that is antigenically similar to Variola virus (Fenner, 1982, Smith, 2013). Since then,

poxviruses continue to be researched for use as vaccine vectors (Sanchez-Sampedro et al., 2015). Viral attenuation of poxviruses is also possible (Paoletti, 1996). These attenuated strains are known not to replicate and hence be safer for use as human vaccines (Schnell, 2001).

Highly attenuated vaccines which are currently being used as vaccine vectors have been produced from vaccinia virus. New York Vaccinia (NYVAC), a highly attenuated strain of the Copenhagen strain of vaccinia virus was made by the deletion of 18 open reading frames (ORFs). These deleted ORFs included 2 genes involved in nucleotide metabolism, a viral haemagglutinin, serine protease inhibitors, genes responsible for formation of type A inclusion bodies, a functional complement 4b binding protein and viral host range genes (Tartaglia et al., 1992b). This vaccine vector is highly desirable as it does not disseminate in immunocompromised hosts (Pastoret and Vanderplasschen, 2003).

Modified vaccinia Ankara (MVA) was produced by passaging vaccinia virus for more than 530 times in an unnatural host. Chick embryo fibroblast cells were used to passage the virus (Mayr et al., 1975). Attenuation caused the deletions of 6 genes (approximately 30 000bp). One of the deleted genes included a host range gene which causes the virus not to complete its replication cycle in cells permissive to vaccinia virus (Meyer et al., 1991). Sutter and Moss (1992) managed to show that whilst MVA does not multiply in human cells, early and late viral protein synthesis and DNA replication takes place. This feature makes MVA ideal for heterologous protein expression. MVA was shown to produce similar levels of heterologous protein when compared with vaccinia virus (Carroll et al., 1997) (Sutter et al., 1994). The use of MVA as a vaccine vector has been reviewed by Altenburg et al. (2014). Some studies have shown MVA to upregulate more immunomodulatory genes than NYVAC (Guerra et al., 2007). MVA presents a great safety profile and was used successfully to immunise over 120 000 individuals against smallpox without any serious side effects (Mayr et al., 1978).

The canarypox-based vaccine vector, ALVAC has been used widely. This is a host cell derived vaccine which is naturally restricted to grow in avian species. No infectious progeny has been demonstrated in non-avian species (Tartaglia et al., 1992a). Canarypox virus has been shown to be immunogenic in animals and human recombinant vaccines (Kyriakis et al., 2009, Fries et al., 1996). When MVA, NYVAC and ALVAC were compared as vaccine vectors against simian immunodeficiency virus (SIV), ALVAC induced a higher immune response followed by MVA and then NYVAC (Teigler et al., 2014). To date, the most successful HIV vaccine

with 31% efficacy, employed the use of a canarypox based vaccine in a prime boost regime with HIV gp120 protein (Rerks-Ngarm et al., 2009).

1.3.2 Use of lumpy skin disease virus as a vaccine and recombinant vaccine vector

LSDV is attractive as a vaccine vector due to its ability to express foreign antigens (Fick and Viljoen, 1999). As a poxvirus, it has a large genome of 150kbp, which, like that of vaccinia virus, can accommodate large insertions and therefore be used in the construction of recombinant vaccines (Moss, 1996, Smith and Moss, 1983, Panicali and Paoletti, 1982). LSDV induces both cellular and humoral immune responses (Boshra et al., 2013) and has been used as a vaccine vector for cattle, sheep and non-permissive hosts. Recombinant LSDV vaccines have been made against rabies and tested in animals (Aspden et al., 2002). High levels of antibody were obtained in vaccinated cattle. A recombinant LSDV against rinderpest was developed and it was found to be protective against rinderpest and lumpy skin in a challenge experiment in cattle (Romero et al., 1993). Using the thymidine kinase insertion site, Wallace et al. (2005) expressed Rift Valley Fever antigens in LSDV. In a mouse challenge model with Rift Valley Fever virus, protection against Rift Valley Fever disease was demonstrated (Wallace and Viljoen, 2005). A vaccine against Bovine Ephemeral Fever viral (BEFV) disease was developed using LSDV as a vaccine vector. However, in a small cattle challenge experiment, the vaccine was shown not to be protective against BEFV challenge although antibodies and cellular immunity was detected (Wallace and Viljoen, 2005). LSDV was also used as a vector for a vaccine against heartwater disease in sheep. It was used in a prime boost regime with a DNA vaccine and 90% of the sheep survived needle administered heartwater challenge (Pretorius et al., 2008).

LSDV is an attractive vaccine vector in that the vaccine strain could not be passed between vaccinated and non-vaccinated animals (Carn and Kitching, 1995b).

The other attractive feature of LSDV is its host-restriction to ruminants and inability to complete the replication cycle in non-ruminants including humans (Fick and Viljoen, 1999). LSDV expressing rabies virus glycoprotein protected mice from rabies virus challenge demonstrating that the vaccine was effective in a non-permissive host (Aspden, 2004). LSDV has been shown to be safe in two strains of immunocompromised mice, namely RAG mice and CD4 T cell knockout mice (Shen et al., 2011). LSDV expressing HIV genes were immunogenic in mice and non-human primates (Shen et al. 2011, Burgers et al. 2014).

LSDV has suitable sites on its genome which allows for insertion of foreign genes (Boshra et al., 2013). The region encoding the thymidine kinase enzyme has been successfully used as an insertion site (Wallace and Viljoen, 2005). Other sites for insertion have now been identified which include a ribonucleotide reductase gene and one intergenic region between ORFs 091 and 092 (Aspden et al., 2002, Cohen et al., 1997). More recently, our group has successfully used other intergenic regions as insertion sites for generating recombinants (unpublished). All these features make LSDV suitable for use as a recombinant vaccine vector.

1.4 Virus structure and genomic organisation

1.4.1 Virus structure

Poxviruses have been studied extensively with most of the work having been done on vaccinia virus (Cox et al., 1995, Moss, 2013). Using electron microscopy, poxviruses appear as brick shaped virions with dimensions of approximately 360 x 270 x 250 nm (Cyrklaff et al., 2005). Figure 1.4 shows an electron micrograph of LSDV. LSDV, like Orthopoxviruses is brick shaped (Babiuk, 2018) with a dumbbell shaped viral core. Poxviruses contain a dumbbell shaped viral core and two lateral bodies (reviewed by Laliberte and Moss (2010) and Condit (2007)). The core consists of a large double stranded molecule of DNA and approximately 80 proteins. Twenty of the proteins are linked with transcription and mRNA modification (Moss, 2012). The core is flanked by two lateral bodies which fit into the concavities of the core (Cyrklaff et al., 2005) and (reviewed by Laliberte and Moss (2010)). The lateral bodies are attached to the surface of the core and contain proteins with immunomodulatory function, e.g. vaccinia virus gene H1 (VH1), which enables the virus to evade host antiviral defences (Schmidt et al., 2013).

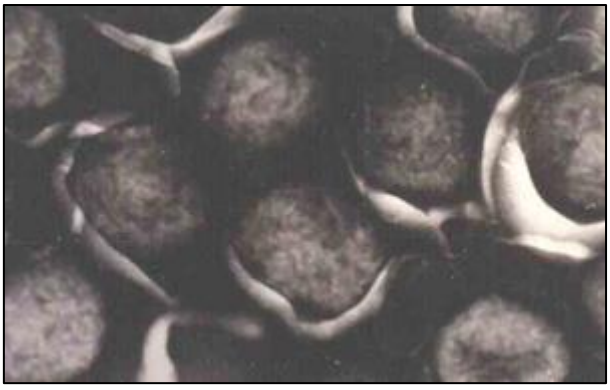

Figure 1.4. Electron micrograph of LSDV. (X100 000 magnification). Taken from ARC, South Africa (http://www.arc.agric.za/arc-ovi/Pages/Vectors-and-Delivery-systems.aspx).

There are two distinct forms of the virus particles of poxviruses. One is the intracellular mature virus (MV) which contains a single membrane and the other the extracellular enveloped virus (EV) which contains two membranes (Hollinshead et al., 1999, Cyrklaff et al., 2005, Moss, 2012). Section 1.4.2. describes the viral life cycle and indicates how the virus acquires the different membranes. After much controversy over the source of the innermost membrane, recent imaging techniques have revealed it to be the host endoplasmic reticulum (Weisberg et al., 2017).

1.4.2 Life cycle of poxviruses

Poxviruses replicate in the cytoplasm of their host cell (Dales, 1962, Dales, 1963) . A lot of knowledge on entry, replication and morphogenesis of poxviruses is based on studies done on vaccinia virus (Quemin et al., 2018). Figure 1.8 summarises key stages in the poxvirus life cycle. Poxviral entry is defined as the step where the viral core gets into the cytoplasm (Moss, 2016). This can be achieved in one of two ways, fusion or endocytosis (Kilcher and Mercer, 2015, Quemin et al., 2018).

Understanding entry of the extracellular enveloped virus (EV) was previously complicated by the fact that it contains an extra membrane. Studies have shown that the outer membrane is dissolved prior to fusion of the MV with the plasma membrane or endosomal membrane. Law et al. (2006) discovered that when EV encounters the host cell membrane, cellular polyanionic molecules complex with viral proteins A34 and B5 to damage part of the outer viral membrane. The outer envelope is thus not incorporated into the host cell but partially dissolves to release the single enveloped virus (Law et al., 2006, Roberts et al., 2009).

The inner membrane fuses with the plasma membrane of a host cell introducing the viral core into the cell (Carter et al., 2005). Entry of the mature virions (MVs) was shown to be facilitated by 5 viral proteins namely, D8, A27 (Hsiao et al., 1999, Kochan et al., 2008, Vazquez and Esteban, 1999), H3, A26 and L1 (Moss, 2016, Foo et al., 2009). Entry of the viral core has been shown to be signalling dependant and is associated with actin/ezrin containing finger like protrusions (Locker et al., 2000).

Upon entry, viral early proteins are produced to initiate synthesis of viral progeny (Liem and Liu, 2016). Transcription of intermediate genes happens simultaneously with DNA replication. The viral cores move towards the periphery of the nucleus where DNA replication ensues

(Condit, 2007). DNA replication occurs in the cytoplasm in specialised units called viral factories (Dales, 1962) and (reviewed by Moss (2013)). This segregation and compartmentalisation favours viral replication and possibly helps evade pathogen pattern recognition receptors (Liem and Liu, 2016). The viral factories contain transcription factors, viral mRNA, RNA-binding protein, translation related complexes, the eukaryotic translation initiation factors (eIF4E and eIF4G), and ribosomal proteins (Katsafanas and Moss, 2007). These, together with cellular proteins, are involved in translating early mRNA into proteins (Liem and Liu, 2016).

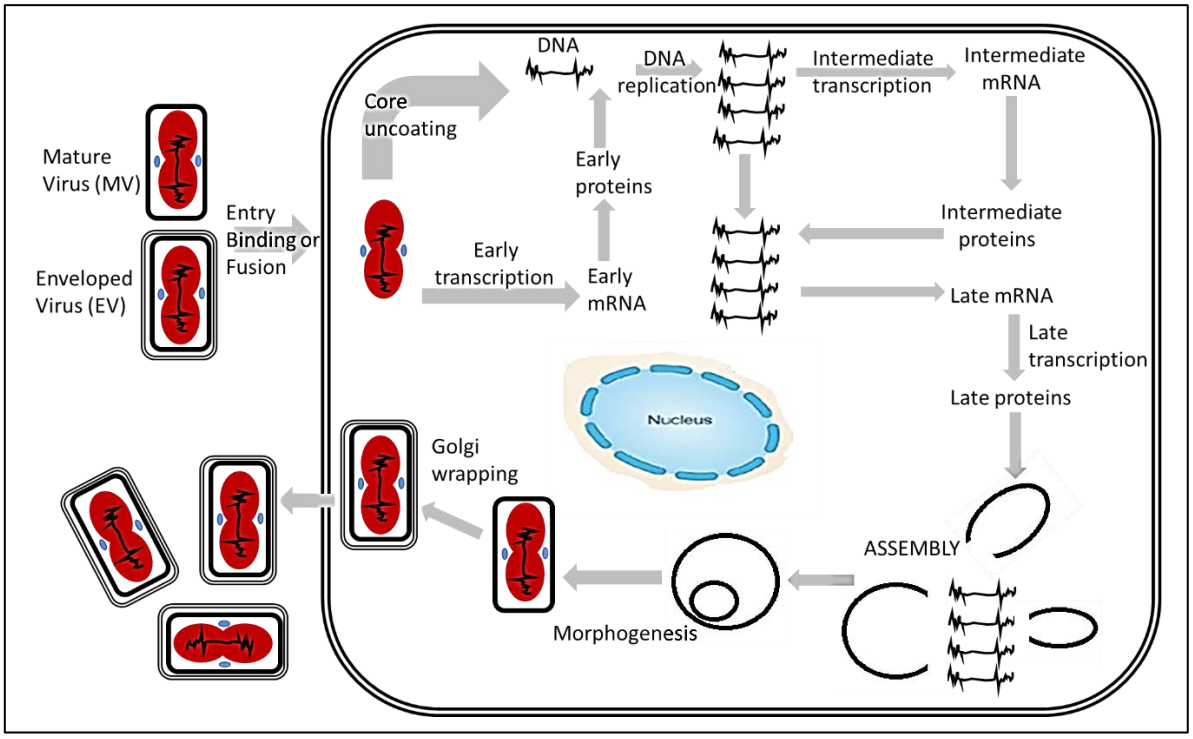

Figure 1.5. The life cycle of a poxvirus. The extracellular enveloped virus (EV) binds the plasma membrane of a target cell. The outer envelope is not incorporated into the cell membrane. The viral core is introduced into the cytoplasm where uncoating of the viral core happens. Early mRNA is transcribed and assists in DNA replication. Early proteins that include viral growth factors and cytokine inhibitors are produced. These favour viral growth. Other proteins that inhibit the cell antiviral machinery are also made. DNA replication occurs and through subsequent events a single enveloped intracellular mature virus is assembled. The IMV is trafficked to the Golgi apparatus where envelope wrapping occurs to yield intracellular enveloped virus (IEV). The IEV is released from the cell as extracellular enveloped virus (EV) which can go on to infect other cells. Adapted from McFadden (2005).

Poxvirus DNA replication occurs in the cytoplasm and starts as early as 2 hours post infection (Moss, 2013). DNA replication starts with a nick of pox DNA on one of the terminal hairpins. The hairpin on the terminus is unravelled allowing for DNA polymerase to bind. DNA replication produces concatemeric DNA molecules which are resolved by nucleases and packaged. About 10 000 copies of the genome are released from one cell although only half are packaged (Mercer et al., 2007a). Interestingly, it has been discovered that circular DNA

(like transfer vectors) also replicate in viral factories; this is advantageous in the construction of recombinant poxviruses (DeLange et al., 1986).

DNA is packaged into a particle surrounded by a single membrane, derived from the endoplasmic reticulum, which matures to MV. Studies done on vaccinia virus have shown that A17, A14 and a scaffolding molecule D13 participate in membrane biogenesis with expression repression of these molecules being linked to accumulation of the viral cores in the cytoplasm of infected cells. H7 and L2 have also been involved in membrane biogenesis (Meng et al., 2013, Maruri-Avidal et al., 2011). L2 has been shown to co-localise with the endoplasmic reticulum and confer stability to some poxviral proteins (Maruri-Avidal et al., 2011). Some of the MV is retained in the cell cytoplasm and some goes into the Golgi to make intracellular enveloped virus (IEV) with 3 membranes. When IEV fuses with the cell membrane, EV is released (Moss, 2006). Deep sequencing of VV and host cell transcriptomes (RNA-seq) has been used to map viral transcription start and stop sites precisely. It has also been insightful in understanding the different classes of mRNA and host response to virus (Yang et al., 2010, Yang et al., 2011).

1.4.3 Genome organisation of LSDV

The LSDV genome is 151kbp in length and includes 2.4kbp inverted repeats in the terminal regions. The genomic organisation of poxviruses is linear with the 5' and 3' ends joined together by means of a phosphodiester bond. Capripoxviruses are AT rich with LSDV having an AT content of 73% (Tulman et al., 2001b). The genome organisation of poxviruses does not include introns and mRNA is not spliced (Condit, 2007). LSDV encodes 156 putative proteins. Conserved coding regions in LSDV are centrally located in the genome flanked by the terminal repeats (Tulman et al., 2001b). Figure 1.6 shows the arrangement of genes in LSDV.

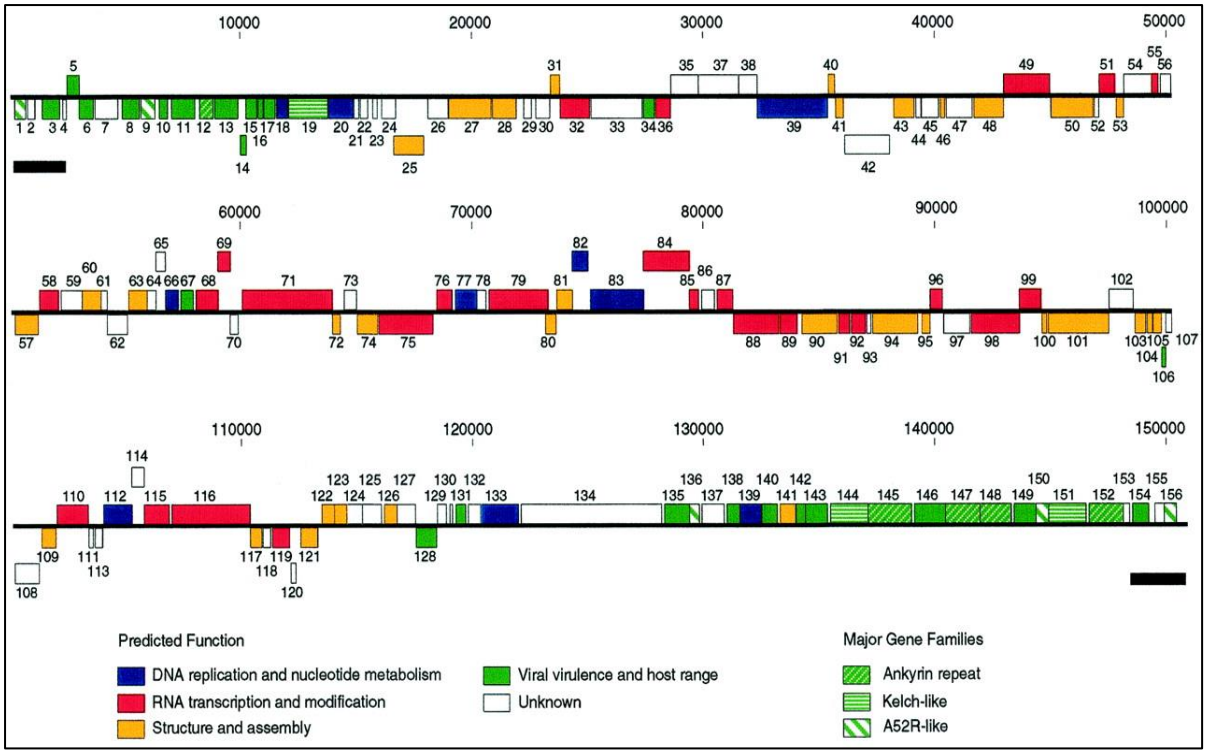

Figure 1.6. A linear representation of the virulent LSDV genome (based on the Kenyan Nl2490 virulent field strain) with genes transcribed to the right being above and those to the left, below the long black line representing the genome. Genes are colour coded according to function and the internal terminal repeats (ITR) are shown below the open reading frame map as black blocks. Taken from Tulman et al. (2001b). Permission to reuse image was granted.

Poxviruses express genes temporally in four phases (Assarsson et al., 2008), namely, immediate early, early, early-late and late. The early gene products are termed so because they are expressed early in infection, before DNA replication and the late gene products are expressed late in infection after DNA replication (Broyles, 2003). There are distinct promoters for early and late gene expression; it is not clear what regulatory factors distinguish immediate early from early gene expression. The early genes encode proteins which are important as virulence factors which alter the host cell response, whereas the late genes encode structural proteins and proteins important for morphogenesis. They also encode core proteins required for transcription and other functions required immediately upon infection. (Assarsson et al., 2008).

1.4.3.1 LSDV sequence comparisons

As observed in other poxviruses LSDV encodes 26 proteins involved in translation, transcription and post-transcription. Seven homologues present in LSDV are important for DNA replication. LSDV also contains enzymes involved in nucleotide biosynthesis like homologues of thymidine kinase and ribonucleotide reductase. Thirty genes encode proteins

important in viral structure which include putative homologues of A36R, B5R and VV A4L which have been identified as genes encoding structural proteins of vaccinia virus.

Studies on LSDV genomes have shown that the genomes of virulent LSDV are highly conserved. LSDV isolated from the Balkans recently was sequenced. Results showed that the genome was 99.95% similar to the virulent Neethling strain that was isolated in South Africa in 1999 (Toplak et al., 2017).

Kara et al. (2003) compared the sequences of 2 virulent LSDVs and one attenuated LSDV (Table 1.4). Comparing the two virulent strains, the Kenyan (Kenyan 2490) and the South African (LD) isolates, mutations were found in the variable terminal regions of the genome (Kara et al., 2003).

Significant differences were found between the Warmbaths virulent LSDV and the attenuated vaccine strain (nLSDV). 114 genes out of 156 had nucleotide changes that resulted in 438 different amino acid changes. Of interest were the frameshift mutations which led to the truncation of 4 genes (Table 1.4). Amongst 9 frameshift mutations observed (see Table 1.4) were ORF 134 (a homologue of the B22R gene in Vaccinia virus) and ORF 131 (superoxide dismutase homologue (Kara et al., 2003). The relevance of these mutations becoming apparent in the DNA comparison of Herbivac and Neethling vaccine, described later.

Most of the changes are found in ORFs belonging to Kelch like repeat motif family. These proteins have been shown to be involved in virulence and their disruption in nLSDV may be the source of attenuation. SPPV019 was shown to be linked to virulence and SPPV019 knock-out viruses were shown to be attenuated (Balinsky et al., 2007). Proteins containing the mutT motif (nudix hydrolases) are important in host range and studies have shown that knocking out this domain results in defects in replication in mutant vaccinia virus (Liu et al., 2015).

More recently, three South African produced vaccines, namely, nLSDV (OBP), Herbivac (Deltamune) and Lumpyvax (MSD) were sequenced (Mathijs et al., 2016). The published sequence of the Neethling vaccine strain from Onderstepoort was used as a reference sequence (Kara et al., 2003). The genomes of the three vaccines were found to be almost identical with 99.9% homology. All three vaccines were shown to have comparable genome sizes. The termini of these genomes were however, not sequenced. (Mathijs et al., 2016).

Table 1.4. List of ORFs found to be different between a virulent LSDV (Warmbaths strain) and an attenuated strain (Neethling vaccine strain). Table modified from Kara et al. (2003).

Open reading frame	Position in Virulent Warmbaths LSDV (length, codons)	Position in South African LSDV Neethling vaccine strain (nLSDV) (length, codons)	Functional domain
ORF019	12073-12945 (291) 12972-13784 (271)	11961-13283 (441) 13217-13669 (151)	Kelch-like domain
ORF144	135541-137193(551)	135320-136129 (270) 136120-136965 (282)	Kelch-like domain
ORF026	18034-18495 (154) 18619-18942 (108)	17909-18817 (303)	Kelch-like domain
ORF134	122187-128264(2026)	121991-124156(722)	Kelch-like domain
ORF013	8932-9918 (329)	8784-9809 (342)	interleukin-1 receptor-like protein
ORF035	28592-29797(402)	28541-29671(377)	hypothetical protein
ORF131	119272-119754(161)	119076-119402(108)	Copper/zinc superoxide dismutase homologue
ORF086	79895-80533(213)	79767-80396(210)	*mut*T motif
ORF087	80536-81297 (253)	80409-81008(200)	*mut*T motif

All three vaccine sequences resembled one another but differed from the published sequence in that they contained two amino acid changes namely T/M in ORF 56, V/A in ORF 116 and a further two nucleotide changes in a non-coding region of the genome. In addition to these changes Herbivac differed from nLSDV in that it contained a two-base pair deletion which caused a frame shift mutation and subsequent restoration of the ORF LW134 from LW134a and LW134b (Mathijs et al., 2016, Mathijs et al., 2017). ORF134 was previously reported to encode a putative protein similar to B22R, an ORF present in Orthopoxviruses (Kettle et al., 1995). Deletion of vaccinia virus B22R causes attenuation, thereby increasing its safety profile (Legrand et al., 2004). A homologue of B22R (C15) in Ectromelia virus was shown to contribute to pathology in an animal model (Reynolds et al., 2017). The restoration of ORF134 may have improved the immunogenicity of Herbivac but may also have increased its virulence.

Based on confidential unpublished data, Herbivac LSDV was regarded as being more immunogenic than nLSDV, from which it was derived (personal communication). The Herbivac genome was sequenced by Dr Nicola Douglass (unpublished) and compared to the SA Neethling vaccine sequence (LSDV LW) (Kara et al., 2003). The genomic sequences were almost identical with only 2 single nucleotide changes (SNPs) and 1 deletion of 2bp. The SNPs were found in LSDV genes LW056 (hypothetical protein) and LW116 (RNA Polymerase subunit). Both these SNPs resulted in conservative amino acid changes, unlikely to affect the function of the putative proteins.

The deletion of 2bp was found in the homologue of the superoxide dismutase (SOD) open reading frame (ORF). This difference in Herbivac was confirmed by PCR and sequencing across the SOD homologue region. Since the mutation in the SOD locus was the only functional difference noted, the improved immunogenicity of Herbivac compared to LSDV LW is therefore most likely due to the mutation in the SOD locus. As stated above, the nLSDV vaccine SOD is truncated relative to virulent LSDV (LSDV Neethling 2490) due to a frameshift mutation. The nLSDV putative SOD protein is only 108 aa in length as opposed to 161 aa for the virulent nLSDV (Figure 1.8). The further deletion of two nucleotides from nLSDV in Herbivac results in the restoration of the SOD ORF in Herbivac (160aa) such that it resembles the SOD homologue from the more virulent Neethling strain 2490 (Tulman et al., 2001a) (Figures 1.7 & 1.8). The mutation of 2bp is found in a run of TA dinucleotides which could render this region unstable.

It would appear as if the full-length SOD homologue benefits the virus in an animal host, as it was lost upon passage during the attenuation of nLSDV yet re-emerged upon passage in a bovine host. The sequencing data showed 60% of the raw reads to contain the deletion and 40% to resemble nLSDV (unpublished). Putting the results from our laboratory together with the published sequence of Herbivac (Mathijs et al., 2016, Mathijs et al., 2017) it is likely that two different seed lots of Herbivac were produced, which differed in the two loci (ORF 131 and ORF 134).

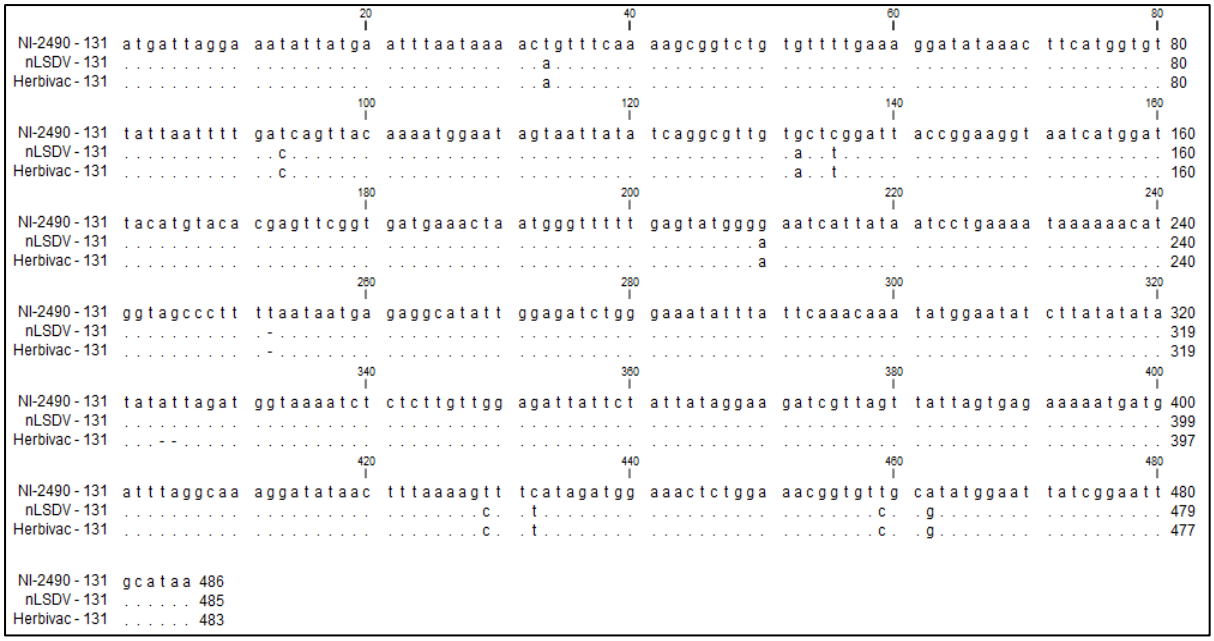

Figure 1.7. Nucleotide alignment of ORF 131 of LSDV Nl 2490, nLSDV, and Herbivac. CLC (Qiagen, USA) alignment programme available on CLC main workbench was used to align the SOD homologue ORFs from the virulent Nl 2490, the Neethling vaccine (nLSDV) and the LSDV vaccine Herbivac. Dots represent matching residues. Gaps are shown by dashes.

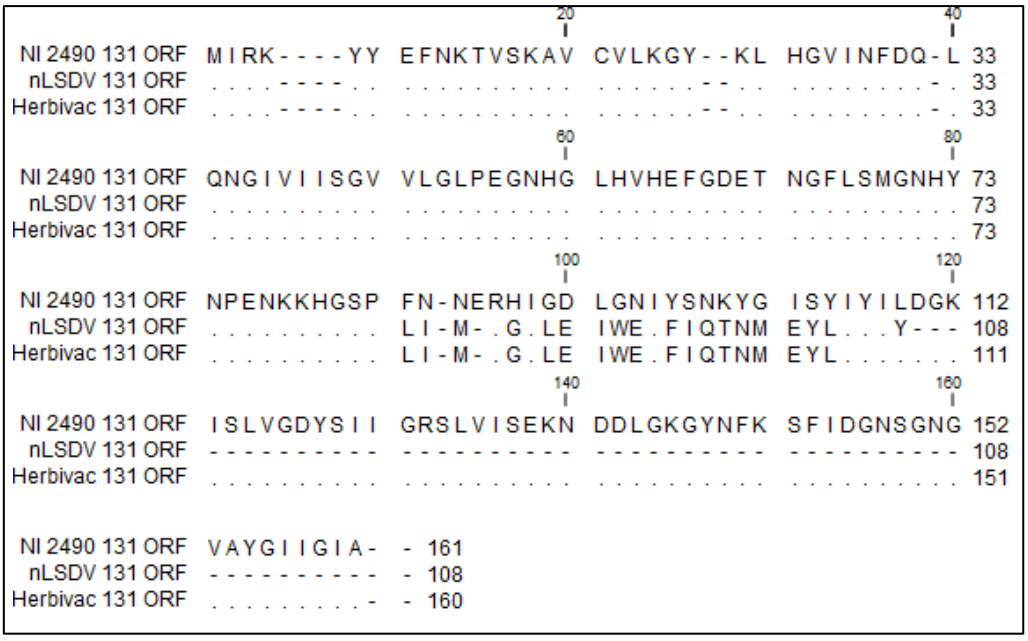

Figure 1.8. Alignment of putative amino acid sequences of SOD homologue genes from the virulent Neethling 2490 strain, Herbivac and LSDV LW (Neethling vaccine- nLSDV) strain (parent of Herbivac). Alignment was done using CLC workbench (Qiagen, USA).

1.5 Virus host interaction: Innate immunity against viral infections

In order to detect foreign pathogens that include viruses, cells employ pathogen associated molecular patterns (PAMPs) (Kawai and Akira, 2008) and damage associated molecular patterns (DAMPs) (Ma and Damania, 2016). The effect of the action of these pattern

recognition receptors (PRRs) includes production of type 1 interferons and many different cytokines and chemokines which can alter cell development (growth and death) as well as recruitment of the adaptive arm of the immune system (Ma and Damania, 2016, Delaloye et al., 2009).

Antiviral sensing mechanisms include Toll-like receptors, nucleotide binding and oligomerisation domain like receptors (NLRs), retinoic acid inducible gene-1 like receptors (RLRs), cGMP-AMP (cGAMP) synthase (cGAS) and absent in melanoma 2 (AIM2) receptors (ALR) (Akira et al., 2006, Orzalli and Kagan, 2017, Ma and Damania, 2016). Sensing of the virus using TLRs occurs at the cell surface and the cytoplasmic-endosomal compartment. The aforementioned antiviral sensing receptors then employ adaptors through which their activity is exerted as shown in Figure 1.9.

TLRs contain a homotypic protein-protein interaction with adaptor molecules, or procaspase thereby causing its proteolytic activation. Caspase-recruitment domain (CARD) and Pyhin domain (PYD) are some of the effectors. NLRs can bind viral RNA directly (Hong et al., 2012). NLRs combine with other proteins like procaspase-1 and an adaptor protein apoptosis-associated speck-like protein containing a CARD (ASC) to form the inflammasome. The inflammasome multiprotein complex leads to cytokine production, in particular, IL1β and IL18 which leads to activation of NF-κB. The inflammasome is activated after infection with DNA viruses like Vaccinia virus (Delaloye et al., 2009), (reviewed by Jacobs and Damania (2012)) and is implicated in inflammatory, caspase dependant programmed cell death (pyroptosis). During a viral infection, nucleotide oligomerisation domain (NOD 2) complexes with mitochondrial antiviral signalling protein (MAVS) to induce type 1 interferons via the activation of the interferon regulatory factors IRF3 and IRF7 (Figure 1.9) (Kanneganti, 2010). The activity of Nod-like receptors (NLRs) has been reviewed by (Jacobs and Damania, 2012). These NLRs, like TLRs, mediate their function through their interaction with NLR effector domains via protein-protein interactions. However, direct binding between viral PAMPs and ssRNA has been suggested (Jacobs and Damania, 2012).

Other molecules can also form the inflammasome without NLRs and these include absent in melanoma 2 (AIM2) and retinoic acid inducible gene-I (RIG 1). Vaccinia virus was shown to trigger the AIM2 inflammasome with concomitant release of IL-1β, cleavage of caspase-1 and IL-1β maturation (Rathinam et al., 2010). AIM2, part of the PYHIN family plays a vital role

in sensing cytosolic dsDNA (Thompson et al., 2011). AIM2 binds dsDNA in the cytoplasm and forms the AIM2 inflammasome with concomitant activation of caspase 1 in pro-IL-Iβ containing cells, with subsequent maturation of pro-IL-Iβ to IL-Iβ (Schroder et al., 2009).

Poxviruses have evolved many mechanisms of immune evasion (Bidgood and Mercer, 2015). LSDV is no exception and has homologues of cellular and viral gamma interferon (IFN-γ) receptor (R), IL-18 binding protein, IL-1R, IFN-α/β binding protein and interleukin-10 (IL-10). LSDV also encodes membrane bound immunomodulatory proteins that act like chemokine receptors, binding intracellular or extracellular factors. These include LSDV010.

Other viral proteins like LSDV014 and LSDV034 are potent in inhibiting the antiviral effects of interferon (IFN). Serine proteinase inhibitors (serpins) exert an immunomodulatory role. In cowpox virus, Serpin CrmA was shown to block caspase activation leading to a reduction in IL-1β secretion (Ray et al., 1992). LSDV also encodes a gene class similar to the A52R gene family which encode proteins which act as Toll like receptor antagonists. These include LSDV001, LSDV009, LSDV136, LSDV150, and LSDV156. LSDV encodes proteins with ankyrin repeat motifs. These genes have been implicated in host range functions (Tulman et al., 2001a).

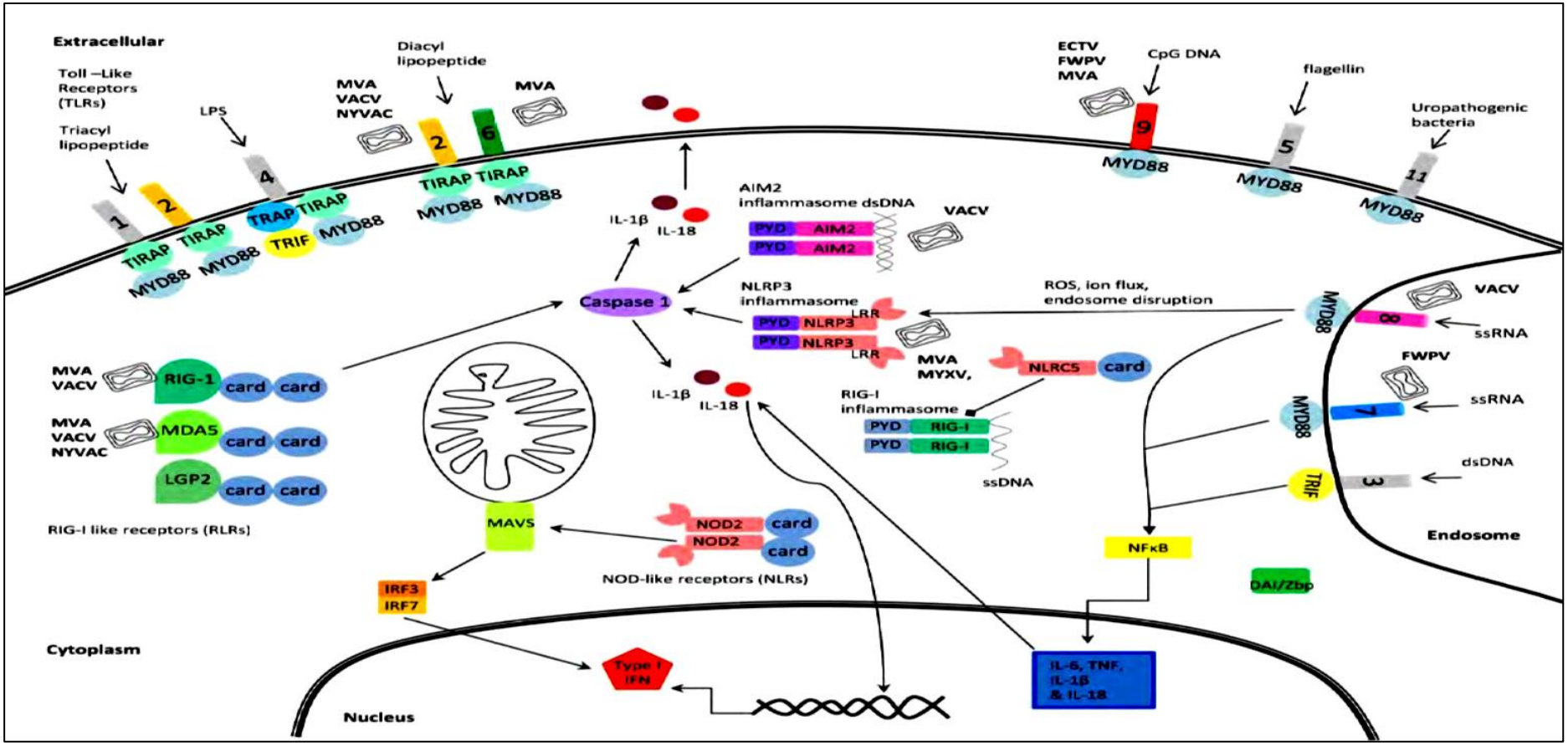

Figure 1.9. Innate immune system recognition of different antigens including poxviruses. Pathogen recognition receptors (PRRs) that are employed by the host against poxviruses include members of the Toll like receptor family, retinoic acid inducible gene-1 (RIG-1)-like receptors (RLRs), nucleotide oligomerisation domain (NOD)-like receptors (NLRs) and inflammasomes. Indicated by cartoon representations of poxviruses are known sites of interaction of poxvirus proteins with the host pathogen sensing mechanisms. Toll like receptors are important in sensing viral/viral related products (TLR 3,4,7,8 &9), bacteria via lipopeptides (TLR 1&2), fungi and drugs. TLRs trigger production of type 1 interferons, inflammatory cytokines (TNF α, IL 6, IL 1 β and IL 12) and chemokines, which subsequently activate the NFkB pathway and Type 1 interferon response. They use their leucine rich domains to sense pathogens and make use of intracellular adaptor molecules like myeloid differentiation protein 88 (MyD88), Toll/Interleukin-1 receptors domain (TRIP), TIR domain-containing adapter protein (TIRAP) and TIR domain-containing adapter inducing IFNβ (Trif)) and Trif-related adapter molecule (TRAM). Specific TLRs are numbered in the diagram together with their adaptors molecules. The RIG-like receptor family uses 3 different receptors namely, melanoma differentiation-associated gene 5 (MDA5), laboratory of genetics and physiology 2 (LGP2) and RIG 1 which have adaptor molecules MAVS and IPS-1. Nod like receptors and the AIM2 like receptor family sense viral nucleotides and activate the inflammasome. The effect of the action of these PRRs leads to the production of Type 1 interferons (IFN) and IL1β/18 (Ma and Damania, 2016). This response ultimately constitutes an antiviral response. Taken from Offerman (2014), which was adapted from (Kawai and Akira, 2006) and (Kanneganti, 2010).

1.5.1 The interferon stimulated genes (ISG)

Interferons play a role as antiviral cytokines (Baldanta et al., 2017). They exert their function through induction of interferon stimulated genes (ISGs) (Schoggins, 2014). This is mediated by the recruitment and activation of Janus Kinases (JAKs), activation of signal transducers and activators of transcription (STATs) whose activity once translocated into the nucleus is to drive the translation of interferon stimulated genes (ISGs) (Mercer et al., 2007a). Table 1.5 below shows ISGs expressed following virus infection and the function of these ISGs.

Table 1.5. Interferon Stimulated Genes that are activated by Type 1 interferons. Modified from (Bowie and Unterholzner, 2008, Chawla-Sarkar et al., 2003, Baldanta et al., 2017)

Interferon Stimulated Gene	Function	References
ISG15	Modification of viral proteins by ubiquitylation	(Zhang and Zhang, 2011, Baldanta et al., 2017)
APOBEC3, ADAR	RNA editing	(Sharma et al., 2015, Smith et al., 1997)
Mx PROTEIN	Transcription and trafficking of other ISGs	(Verhelst et al., 2013)
PKR	Inhibition of translation	(Krishnamoorthy et al., 2001)
RNaseL, 2'5' OAS	RNA degradation	(Chawla-Sarkar et al., 2003)
TRIM proteins	Host response regulation and inhibition of viral transcription	(van Tol et al., 2017)
MicroRNAs	Gene regulation	(Sedger, 2013)
MDA-5, RIG-1, DAI	Pathogen recognition	(Bowie and Unterholzner, 2008)
TRAIL, Fas, caspase 4, RIDs, PKR, DAP kinase	Apoptosis	(Chawla-Sarkar et al., 2003)

1.5.2 Apoptosis as an antiviral mechanism

Apoptosis is a programmed cell death with innate immune function that is specifically activated to remove unwanted cells which can either be defective or virus infected (reviewed by Seet et al. (2003), (Veyer et al., 2017) (Everett and McFadden, 1999). Cytotoxic T-lymphocytes (CTLs) and natural killer cells (NK) mediate this process via the perforin/granzyme pathway. There are two pathways of apoptosis namely the intrinsic and extrinsic pathways (reviewed by Nagata (2018) (Figure 1.10). The extrinsic apoptotic pathway uses an external stimulus to induce apoptosis. CTLs employ death receptors on the surfaces of infected cells to induce apoptotic cell death via the extrinsic pathway. The intrinsic pathway of apoptosis does not involve receptors like the extrinsic pathway. Stimuli for death via the intrinsic pathway include use of positive or negative intracellular signals. Absence of growth factors, cytokines or hormones

which naturally inhibit cell death is one way negative signalling promotes apoptosis. Thus, loss of any signals that favour cell survival leads to cell death. Positive signalling of cell death include radiation, hypoxia, reactive oxygen species (free radicals), hyperthermia and, importantly, virus infections (reviewed by Elmore (2007)). Once these stimuli are detected, mitochondrial membrane permeabilization (MMP) occurs and pro-apoptotic factors are released from the intermembrane space (IMS). One of the factors released is cytochrome C. Cytochrome C activates the apoptosis protease-activating factor 1 (APAF-1) and ATP/dATP to generate the apoptosome. The apoptosome in turn activates caspase 9 which activates other caspases leading to apoptosis (Figure 1.10).

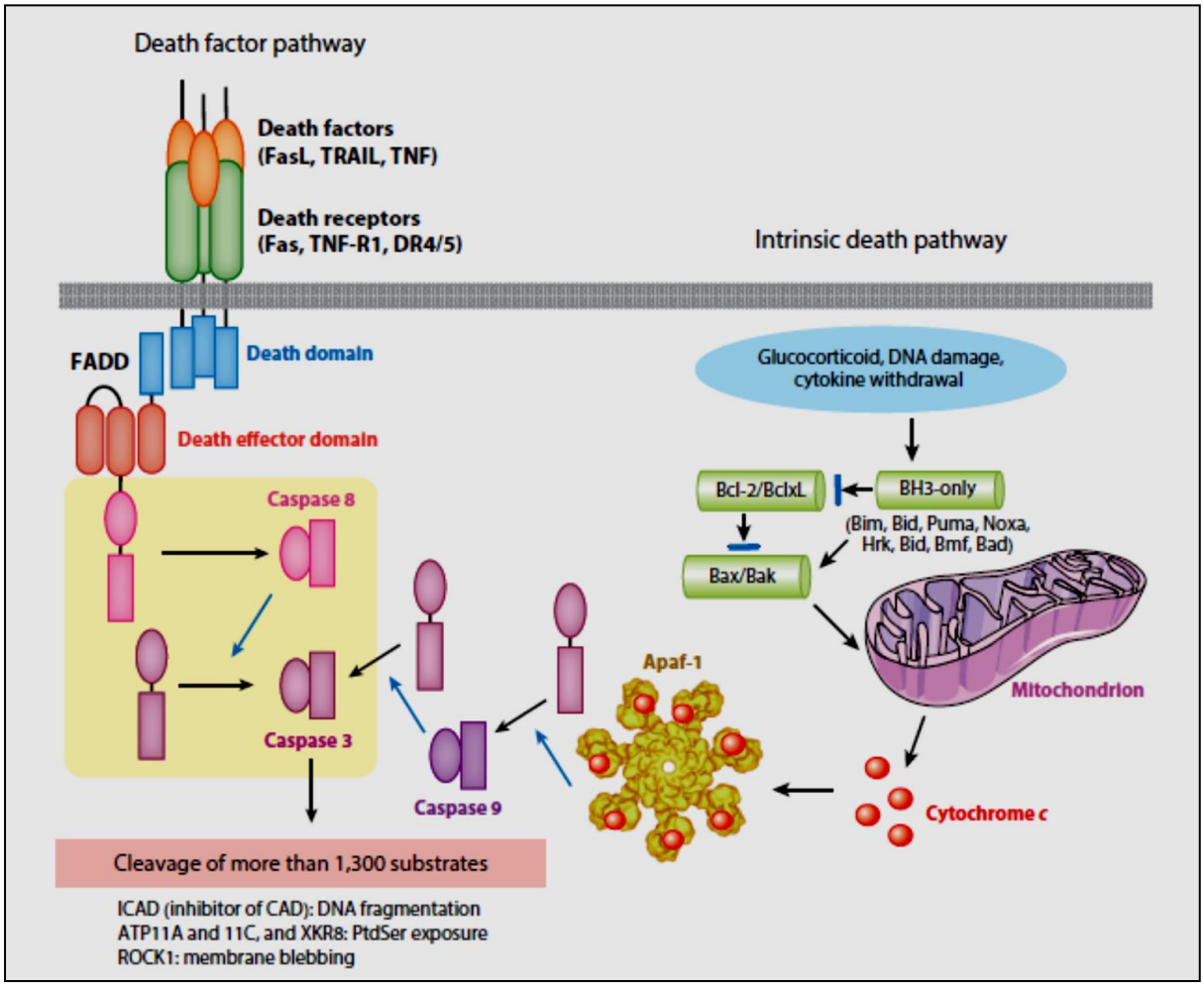

Figure 1.10. Pathways of apoptosis. The extrinsic apoptotic pathway uses death ligands that include FAS, TRAIL and TNF-α via their respective death receptors. The death receptor includes a transmembrane domain which is linked to the different death effectors like Fas-associated protein with death domain (FADD). The intrinsic apoptotic pathway does not use membrane bound death receptors but has sensing mechanisms to various intracellular stimuli that include DNA damage. B cell lymphoma proteins, Bcl-2 and Bclxl are antiapoptotic whereas members of the BH3 family are pro-apoptotic. The B cell lymphoma 2 homology 3 (BH3) proteins interact with Bax and Bak to effect apoptosis. Bak and Bax affect mitochondrial outer membrane potential (MOMP) leading to the release of cytochrome c. Cytochrome c multimerises with pro-caspase 9 and apoptotic protease-activating factor 1 (Apaf-1) to form the apoptosome which activates procaspase 9 to caspase 9. Both the intrinsic and extrinsic pathway eventually lead to the activation of caspase 3 which acts on a variety of substrates to cause apoptosis (Taken from Nagata (2018)). Permission to reuse image was granted.

1.5.3 The different mechanisms of cell death

The known forms of cell death are depicted in Figure 1.11. The unique feature of apoptotic cell death is nuclear fragmentation well before cell lysis (Duke and Cohen, 1986). When cells die via apoptosis, apoptotic bodies are formed which are engulfed by phagocytic cells (Arandjelovic and Ravichandran, 2015). Efferocytosis refers to the removal of apoptotic cells by macrophages, though recent literature has shown that this can be extended to other forms of cell death (Karaji and Sattentau, 2017). No inflammatory response is induced following apoptosis. Necrosis is a form of cell death which involves swelling of cells, nuclear and cytoplasmic disintegration and cell rupture (reviewed by (Gamrekelashvili et al., 2015)). In this form of cell death, damage associated molecular patterns (DAMPs) bound to nucleosomes are released (Yoon et al., 2014) and an inflammatory response is elicited. Both forms of cell death result in the cleavage of DNA, however apoptosis results in the cleavage of DNA into nucleosomal units in the cell (Nagata, 2000). Due to the activation of multiple lysosomes in necrotic cell death, initially cleavage was thought to be disorderly (reviewed by De Duve and Wattiaux (1966)); but later early necrosis was shown to be ordered with cleaved DNA containing predominantly 5' overhangs (Didenko et al., 2003). Apoptosis results in the release of poly- or oligonucleosomes in contrast with necrosis, which results in degraded DNA and histones (Yoon et al., 2014). Unlike apoptosis, necrosis activates the inflammasome via the activation of IL-1β and IL-18 (Griffith and Ferguson, 2011). Inhibition of necrosis has been implicated in poxvirus dissemination (reviewed by Chan et al. (2015)).

Pyroptosis is an inflammatory form of cell death characterised by caspase-1 activation and IL-1β secretion. Necroptosis has been identified as a form of programmed cell death that augments or is a salvage mechanism for apoptosis, especially when drivers for apoptosis are blocked (reviewed by (Walsh, 2014)). Necroptosis is chiefly driven by receptor interacting protein kinase (RIPK3) and does not use caspases (Dunai et al., 2011). Necroptosis, a form of necrosis, involves the leakage of cellular contents into the extracellular milieu (reviewed by Gamrekelashvili et al. (2015)) and, like pyroptosis, elicits an inflammatory response (reviewed by Rock and Kono (2008)) and (Tait et al., 2014).

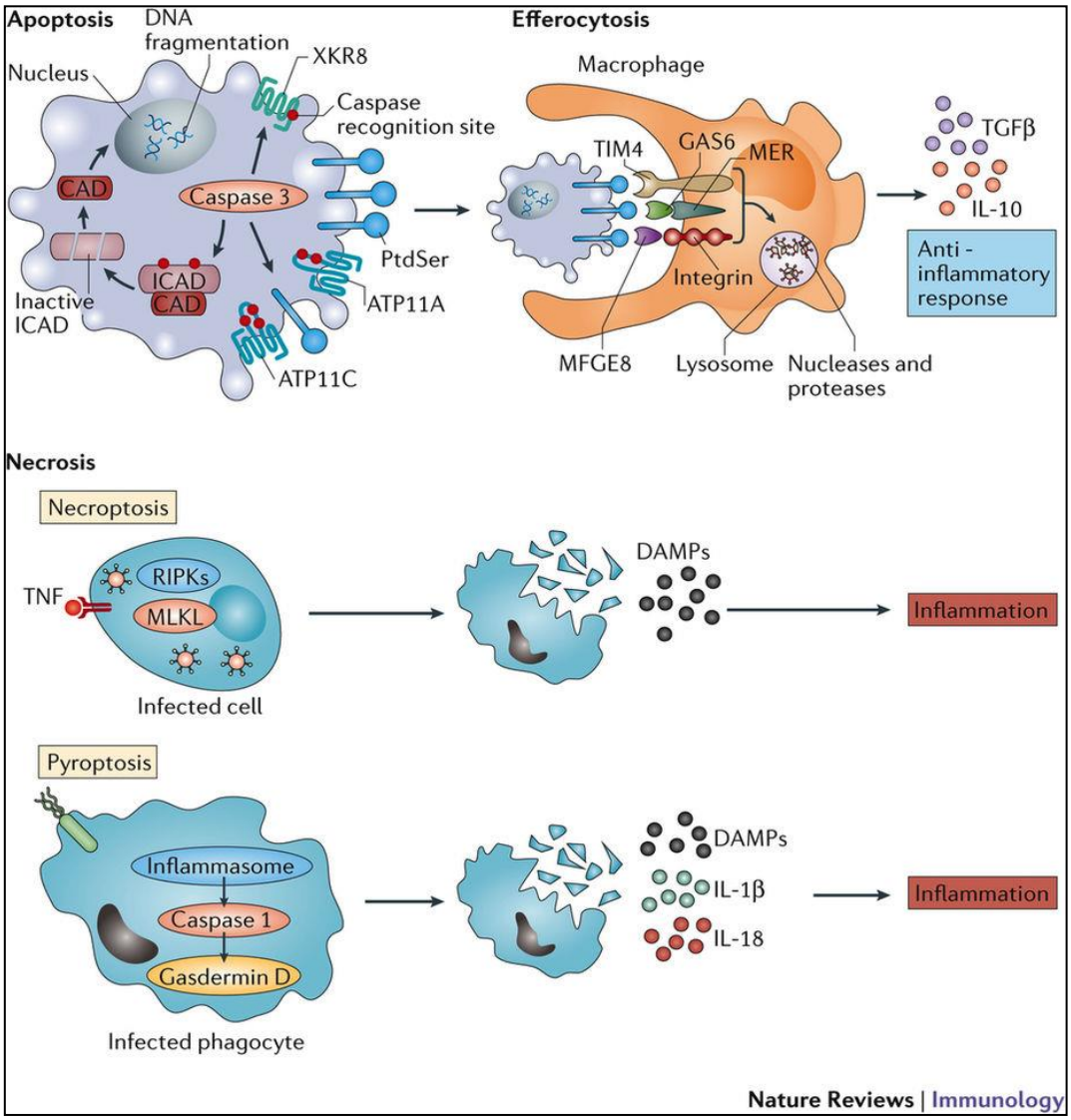

Figure 1.11. Different forms of cell death elicit either an anti- or pro- inflammatory response. Apoptosis is characterised by DNA fragmentation which is mediated by caspase activated DNases. These introduce DNA breaks. Macrophages release transforming growth factor-β (TGFβ) and interleukin 10 (IL10) which inhibit inflammation. Necroptosis and pyroptosis are two different forms of necrosis which promote inflammation. This inflammatory response is mediated by the release of damage associated molecular patterns (DAMPs). The DAMPs activate the inflammasomes which in-turn activate the caspases. The DAMPs cause cells to release cytokines which are chemoattractant for immune cells (Taken from Nagata and Tanaka (2017). Permission to reuse image was granted.

1.5.4 Inhibition of apoptosis

Evasion of apoptosis can be advantageous to the virus as the virus can persist to complete its replication and produce progeny (reviewed by Zhou et al. (2017). Whilst some viral infections will inhibit apoptosis, others use it to aid viral dissemination (Zhou et al., 2017). In the case of a vaccine vector, evasion of apoptosis can help ensure that foreign antigens are expressed for a longer length of time. In the case of a vaccine, evasion of caspase mediated cell death can be beneficial since the infected cell will then engage in programmed necrosis (necroptosis) and an

inflammatory response will be induced. Figure 1.12 shows some of the sites and molecules targeted by viral proteins in the evasion of apoptosis.

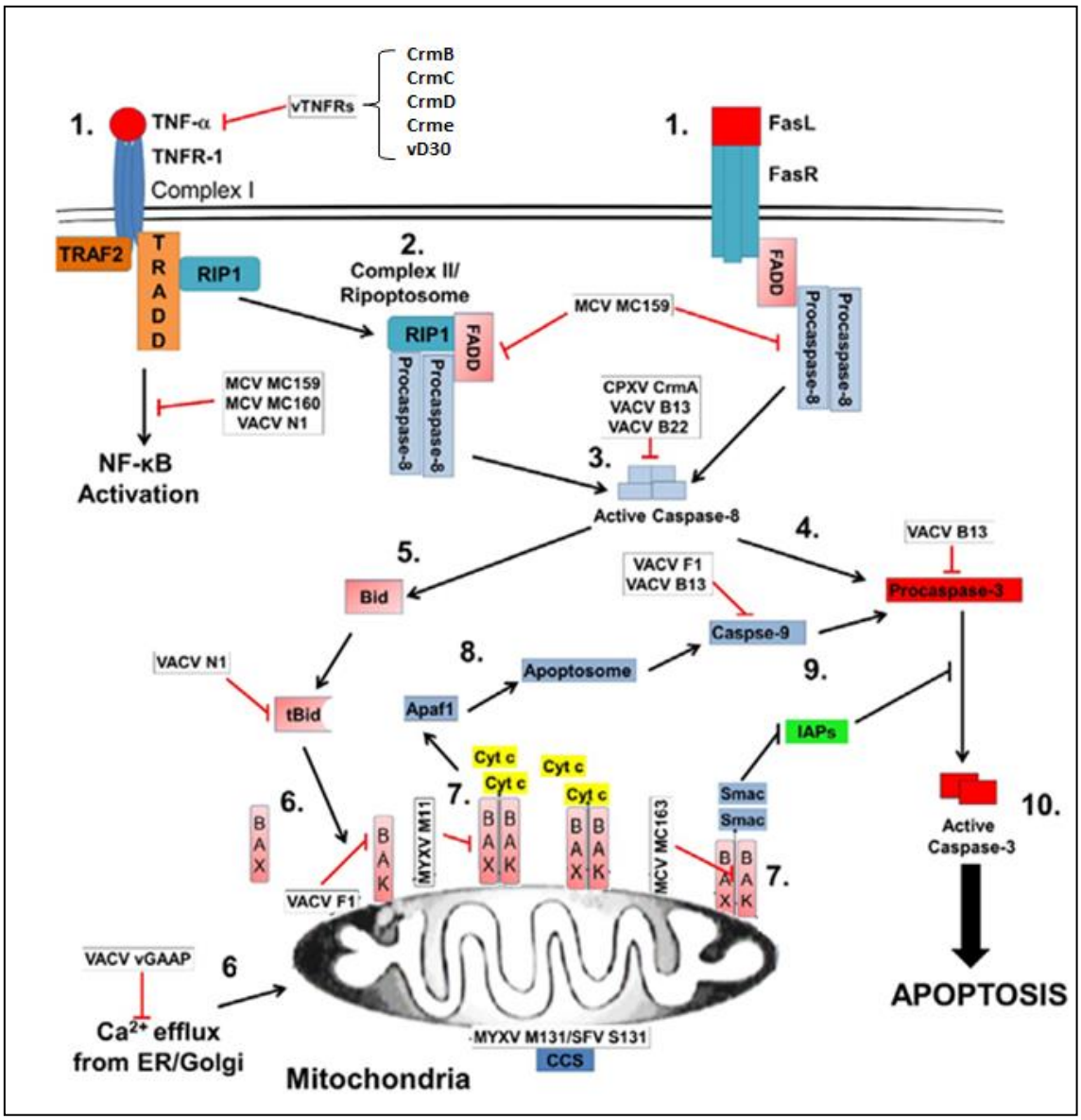

Figure 1.12. Outline of both the extrinsic and intrinsic apoptotic pathways showing sites at which viral proteins inhibit these pathways. (1) Binding of tumour necrosis factor (TNF) to the TNF-receptor (TNFR-1) triggers association of its cytoplasmic regions death domain (DD) with TNFR associated death domain protein (TRADD) which leads to nuclear κB activation. Binding of FasL to FasR also causes recruitment of the procaspase 8 via its Fas associated death domain (FADD). (2) TNF can also induce apoptosis when receptor interacting protein RIP interacts with FADD and procaspase-8. (3) Oligomerisation of the procaspase-8 results in cleavage resulting in activation of caspase-3 in (4) or (5) cleavage of BH3 interacting domain death agonist (Bid) to its cleavage products truncated Bid (tBid). (6) tBid can either activate Bcl-2 homologous antagonist killer (Bak)/Bcl-2 associated protein (Bax) in the mitochondria or Bak/Bax can make the mitochondria porous in response to calcium ions (Ca^{2+}) from the endoplasmic reticulum or Golgi apparatus. (7) Permeabilization of the mitochondria is the result of Bak/Bax and this makes the mitochondria extrude cytochrome C and other caspases from the inner mitochondrial membrane to the cytoplasm. (8) Formation of the apoptosome from cytochrome c binding Apaf1 and subsequent activation of initiator caspase 9 (9) whose role is to activate effector caspases (Caspase 3). Smac from the inner membrane of the cytoplasm binds inhibitor of apoptosis proteins (IAPs) which further activates caspase 3 which in (10) cleaves target proteins resulting in the induction of apoptosis. The poxviral proteins from Myxoma virus (MYX) – M11, MYXV, M131, Vaccinia virus (VV) F1, Molluscum contagiousum MC163 and Shope Fibroma virus (SFV) S131R antagonise the apoptotic immune response. CrmA is a powerful inhibitor of apoptosis which inhibits the activated caspases. The same serpin was also shown to protect cells from FAS and TNF mediated cell death. CrmA is also integral at preventing perforin dependant apoptosis by inhibiting the effect of the serine protease granzyme B (reviewed by Seet et al. (2003)). Modified from Nichols et al. (2017). Permission to reuse image was granted.

1.5.5 Cell death and immunogenicity

Evasion or induction of cell death can affect immunogenicity. There has been contradicting views on whether apoptosis is immunogenic or not (Griffith and Ferguson, 2011). Being a non-inflammatory form of cell death, which clears a host of virally-infected cells, apoptosis is not an obvious mechanism to exploit to induce/improve immunogenicity of a live vaccine. However, a recombinant live rabies vaccine expressing cytochrome C, a pro-apoptotic protein, was shown to induce protective immunity by induction of apoptosis (Dietzschold et al., 2006). Damage associated molecular patterns (DAMPs), induced by necrosis, cause an inflammatory response, which would enhance immunogenicity (reviewed by Griffith and Ferguson (2011). There is no report to date implicating the involvement of LSDV SOD homologues with improved immunogenicity.

1.5.6 Modulation of host factors as a mechanism for immune evasion and host range

The host first interacts with a virus at the cell surface. The second point of interaction is when a virus undergoes replication inside the cytoplasm of the infected cell. Early gene products often carry an immune evasion role and are also known as virulence factors. These molecules help subvert the host antiviral system and therefore determine virus tropism. As mentioned above, cell viral sensing mechanisms include the use of PRRs to inhibit viral replication. Therefore, in order to replicate inside a cell, poxviruses must inactivate certain anti-viral mechanisms such as dsRNA sensing mechanisms designed to supress viral replication, which include 2′,5′-oligoadenylate synthetase (OAS/RNase) and double stranded RNA dependent protein kinase R (PKR) (Sadler and Williams, 2008). Vaccinia virus produces an enzyme E3 which antagonises the activity of OAS and PKR (McFadden, 2005, Chang et al., 1992). Vaccinia virus E3 is an early viral protein with a double stranded RNA (dsRNA) binding domain that suppresses the interferon response by preventing activation of the dsRNA-activated protein kinase R (PKR) (Chang et al., 1992, Watson et al., 1991). The same enzyme is encoded by the ORF034 in lumpy skin disease virus and has been reported to inhibit the activity of PKR (Tulman et al., 2001b). LSDV encodes a repertoire of genes that determine its host range including homologues of VV C7L, N1L virulence, Myxoma (MYX) 004, an anti-apoptotic gene product M011L and a rabbit fibroma virus p28 host range factor (Tulman et al., 2001a). Studies show that the Kelch-like proteins expressed by capripoxviruses differ slightly and probably account for the strict host restriction of these viruses (Balinsky et al., 2007). LSDV contains homologues of all the genes in sheeppox and goatpox viruses and, in addition,

has 9 more ORFs, one or more of which possibly confer the ability of LSDV to grow in bovine cells. One of the unique genes expressed by LSDV is LSDV132 which was postulated to play a role in virulence and host range (Tulman et al., 2002).

Vaccinia virus D9 and D10 are decapping enzymes which remove the 5' cap on mRNA (Liem and Liu, 2016). This leads to degradation of host mRNA, thereby preventing synthesis of host proteins important in antiviral defence. Also, the degradation of mRNA limits the amount of RNA and dsRNA before final assembly of genomic DNA into immature viruses. This helps evade antiviral mechanisms against dsRNA which gets produced by DNA viruses (Burgess and Mohr, 2015, Silverman, 2015).

Twelve host range gene families that help a virus replicate in a host have been identified and are shown in table 1.6. Much work has been done on vaccinia virus and this is thought to apply to other poxviruses (reviewed by Bahar et al. (2011)). Table 1.7 documents known LSDV proteins that could modulate the host cell function or antiviral immune response.

1.6 Generation of the superoxide anion in response to viral infection

Poxviral infection activates processes that have been implicated in the generation of reactive oxygen species (ROS) including the superoxide anion (Liem and Liu, 2016). The amount of superoxide anion is also increased by the action of macrophages and lymphocytes which have been shown to produce superoxide anion as a defence mechanism against pathogens (Johnston et al., 1978). Phagolysosomes, which are cytoplasmic bodies formed between the fusion of a phagosome and a lysosome, are involved in the catabolism of pathogens, particularly bacteria (Armstrong and Hart, 1971, Klionsky et al., 2014). They produce superoxide which is complexed with nitrogen species (NO_2) to form highly reactive oxygen species, namely, peroxynitrite ($ONOO^-$). Action of superoxide or hydrogen peroxide can remove iron from iron clusters (4Fe-4S) and it is this iron that can also cause damage when it combines with hydrogen peroxide to form a highly reactive hydroxyl anion which can damage DNA. The product of superoxide dismutation, hydrogen peroxide, can also oxidise cysteine residues present in proteins of the pathogen (reviewed by Slauch (2011)).

Table 1.6. List of Poxvirus host range gene families and how they mediate their function (Oliveira et al., 2017, Bratke et al., 2013, Werden et al., 2008, Iyer et al., 2002).

Host range gene family	Putative proteins encoded by other poxviruses	Role	Reference
K3L	SWPV - C8, VV-WR K3L	Inhibits antiviral PKR	(Davies et al., 1993, Carroll et al., 1993)
E3L	VV E3L	Inhibitor of PKR	(Davies et al., 1993, Beattie et al., 1996, Langland and Jacobs, 2002)
C7L/M063R	CPXV-GRI-90, VV-C7L, MYXV-M062R, M063R & M064R	Inhibits interferon	(Meng et al., 2009, Meng et al., 2012)
TNF receptor (R) II homologue T2 (Crm)	MYXV T2, Crm B, C, D, E, CPXV-GRI D13L, ECTV-009, HSPV-010 and DPV-W84-005	Antiviral, anti-inflammatory response	(Smith et al., 1990, Smith et al., 1991, Saraiva and Alcami, 2001, Panus et al., 2002)
Apoptosis inhibitor T4 family	CPXV-203, CMLV-188, TATV-195, CPXV-GRI (B8R) & MPXV (B10R)	Anti-apoptotic	(Hnatiuk et al., 1999)
Bcl-2/M11L	VV N1L, A52 and B14	Anti-apoptotic by sequestering apoptotic factors Bak & Bax	(Everett et al., 2000, Wasilenko et al., 2003)
Pyrin domain M13L	MYXV 13L, RFV 13L, SWPV 014, DPV 024, YLDV 18L and TPV 18L	Inhibit caspase 1 activation & subsequent cytokine production	(Johnston et al., 2005, Bratke et al., 2013)

Host range gene family	Putative proteins encoded by other poxviruses	Role	Reference
Serpin (Serine Protease Inhibitors)	SPI-1, SPI-2 (CrmA) and SPI-3, MYXV 151R/SERP2 and 152R/SERP3 genes	Regulate biological processes	(Silverman et al., 2001, van Gent et al., 2003)
Short complement-like repeats containing B5R/VCP family	VV B5R	Involved in cell to cell spread	(Wolffe et al., 1993)
KilA-N/RING domain-containing p28/N1R protein family	ECTV p28-012, CNPV 0022 and RFV N1R-143	ubiquitin ligase-independent role	(Iyer et al., 2002)
ANK/F-box proteins (CP77/T5)	CPXV-BR 017/025, 220, 011, 213,	Mediate protein -protein interactions using their repeat domains	(Mercer et al., 2005, Sonnberg et al., 2008, Werden et al., 2008)
Orthopoxvirus K1L family	VV K1L	Supports viral replication through interactions with protein factors	(Ramsey-Ewing and Moss, 1996, Shisler and Jin, 2004)

CPXV-cowpox virus, VARV-Variola virus, VV-Vaccinia virus, MYXV-myxoma virus, ECTV- Ectromelia virus, SWPV-Swinepox virus, TATV-Taterapoxvirus, CMLV-Camelpox virus, YLDV-Yaba-like disease virus, TPV-Tanapox virus, DPV-Deerpox virus and RFV- Rabbit fibroma virus.

Table 1.7. Viral genes in LSDV that could be involved in modulating the immune response, host function and apoptosis. Adapted from (Tulman et al., 2001b, Kara et al., 2003).

ORF	Gene(s) related with ORF	Putative Function based on other poxvirus proteins
LSDV005, LSDV006, LSDV135, LSDV013, LD008	Homologues of IL 10, IFN-ϒ receptor (IFN-R), IL-1R, IFNα/β binding protein and IL-18 binding protein respectively	Modulation of host immune responses
LSDV010, LSDV011, LSDV138	Homologues of G protein-coupled CC chemokine receptor (GPCR), CD47 and OX-2 like proteins respectively	Affect intracellular signalling transduction and or bind extracellular factors to evade the immune system and contribute to host range
LSDV014, LSDV034	Homologues of VV PKR inhibitors	Intracellular roles in immune modulation or evasion by conferring resistance to antiviral effects of IFN
LSDV149	Similar to Vaccinia virus C12L and Myxoma M151R	Poxvirus serine protease inhibitors which have anti-inflammatory roles and block Caspase 1 activation
LSDV001, LSDV009, LSDV136 and LSDV150, LSDV156	Similar to VV A52R	Antagonist for host cell IL-1, Toll like receptor signalling, Toll-like receptor 4 and IL-18R induction of NF-kβ
LSDV0067	Homologues of epidermal growth factor (EGF), VV C7L host range, N1L virulence protein and A14.5l virulence protein, MYX M004&M011L anti-apoptosis, rabbit fibroma virus (RFV) N1R virus host range factor	Host range function
LD102, LSDV145, LSDV147, LSDV067, LK152	Genes that contain Akyrin repeats	Host range functions, inhibition of viral induced apoptosis
LSDV141	Similar to MYX144R	EEV host range
LSDV146, LSDV131, LSDV143	VV K4L phospholipase D-like protein, cellular Cu Zn superoxide dismutase and tyrosine protein kinase	LSDV131 function to be investigated and LSDV143 (tyrosine proteinase kinase-like protein)
LSDV019, LSDV 144, LSDV151	VV A55R, A52R Kelch like protein	Host range function and virulence (Kochneva et al., 2005)
LSDV003, LSDV 017	Similar to Leporipoxvirus M011L	Apoptosis regulator, inhibition of apoptosis

LSDV- virulent field strain 2490 (Tulman), LD – Warmbaths strain-Kara, and LK-Neethling Kenyan 2490 strain.

1.6.1 Function of the superoxide anion

Reactive oxygen species activate mitogen activated kinases such as MEK or MAPK which control cellular proliferation (Behrend et al., 2003). The role of superoxide in apoptosis and inflammation has been complicated by the fact that the superoxide radical behaves differently depending on its concentration (Teoh et al., 2005). In a pro-oxidative state, the superoxide radical has been shown to be anti-apoptotic (Teoh et al., 2005). Mild increases in superoxide can inhibit cell death signalling with a shift towards H_2O_2 causing an apoptotic response (Pervaiz and Clement, 2002b) (Kumar et al., 2007). This probably explains the varying effects reported regarding its role in apoptosis and inflammation.

The ratio of superoxide to hydrogen peroxide in tumour cells firmly regulates apoptotic death (Kumar et al., 2007). In one experiment, Clement and Stamenkovic showed that preincubation of Jurkat cells with a SOD inhibitor diethyldithiocarbamide (DDC) raised superoxide concentration and consequently inhibited Fas mediated cell death (Clement and Stamenkovic, 1996). Fas (also known as CD95) is a cell surface cell death receptor which is involved in inducing apoptosis (Krammer, 2000). Other reports have shown that the intracellular redox state of a cell affects its fate. This redox state is regulated through the function of a Na^+/H^+ exchanger (NHE). It actively extrudes H^+. Superoxide anion activates NHE1 promoter activity while H_2O_2 inhibits NHE1 promoter activity which promotes survival (Akram et al., 2006, Kumar et al., 2007).

1.6.2 The role of the superoxide anion in apoptosis

Recent studies have shown that small increments in the superoxide anion tend to promote survival whereas an increase in hydrogen peroxide (a product of superoxide dismutation) promotes cell death. Table 1.8 below summarises some evidence for the claim.

Table 1.8. A summary of reports supporting the notion that the superoxide anion is anti-apoptotic and hydrogen peroxide is pro-apoptotic.

Superoxide anion (O_2^-) ANTIAPOPTOTIC	**Hydrogen peroxide (H_2O_2) APOPTOTIC**
At low levels superoxide can inhibit cell death [Pervaiz & Clément, 2002]	H_2O_2 activates Caspases 3&6 [Kumar et al., 2007] which induces apoptosis
Superoxide activates NHE promoter activity [Akram, et al 2006]	H_2O_2 inhibits NHE 1 promoter activity [Kumar et al, 2007], which induces apoptosis
Mitochondrial superoxide cannot be translocated into the cytoplasm [Novo and Parola, 2008]	H_2O_2 can pass through mitochondrial membranes causing cytotoxic damage [Novo and Parola, 2008]
Superoxide activates mitogen activated kinases such as MEK or MAPK which control cellular proliferation [Behrend et al., 2003]	Myelorexidase of phagocytic cells can use H_2O_2 to form highly reactive hypochlorite [Novo and Parola, 2008] which kills infected cells
Superoxide is a natural inhibitor of Fas-mediated cell death [Clement and Stamenkovic, 1996]	H_2O_2 induces apoptosis in Hela cells via the mitochondrial pathway [Singh et al, 2007]

1.6.3 Role of antioxidants

Antioxidant mechanisms exist in a cell with the primary role of removing reactive oxygen species like the superoxide anion. One of the antioxidants is superoxide dismutase (SOD) which is involved in the dismutation of the superoxide anion (O_2^-) to hydrogen peroxide (H_2O_2) and oxygen (O_2) as per the equation below:

$$O_2^{\cdot -} + O_2^{\cdot -} + 2H^+ \xrightarrow[SOD]{} O_2 + H_2O_2 \text{ (McCord and Fridovich, 1969)}$$

Different types of SOD exist. There are SODs that contain copper and zinc (Cu, Zn SOD), manganese (MnSOD) and iron (FeSOD) (Scandalios, 1993). These enzymes perform the same function which is to catabolise the superoxide anion to oxygen and hydrogen peroxide. They differ in localisation. Cu Zn SOD is found in the cytosol, the mitochondrial intermembrane space and in peroxisomes. Mn SOD is found only in the mitochondria (Fukai and Ushio-Fukai, 2011).

1.6.3.1 Structure and activity of Cu Zn SOD

The activity of SOD is intimately related to the structure of the enzyme. Copper zinc SOD is a homodimer with each subunit containing a β barrel which is made up of 8 β strands in an antiparallel fashion to make a Greek Key motif. This motif is indispensable for electrostatic guidance, dimerization and dismutation of the anion using the transition metal copper (reviewed by Perry et al. (2010). The hydrophobic motifs form the internal core and direct the β barrels into the active sites. Cu is held in the active sites by 3 histidines in the reduced state whereas Zn is bound by three histidines and one aspartic acid. The size of the pocket of the active sites poses steric hindrances to other molecules like phosphate which otherwise could occupy the active site. Presence of the hydrophobic core and the main chain β sheet give structure to the enzyme (reviewed by Perry et al. (2010). Figure 1.13 shows the structural form of cellular Cu Zn SOD.

Cu Zn SOD is activated from its apo state when the copper ion is docked onto the enzyme (Culotta et al., 2006). Copper is supplied by the copper chaperone for SOD (CCS) (Rae et al., 2001). In Cu, Zn SOD, the zinc is supplied by passive diffusion (Teoh et al., 2003). Before docking of copper to Cu Zn SOD and subsequent activation, a CCS-SOD 1 heterodimer is formed (Torres et al., 2001, Rae et al., 2001, Culotta et al., 2006, Lamb et al., 2001). Figure 1.14 summarises the steps involved in activation of SOD from its apo state to a fully active SOD dimer.

1.6.3.2 Activation of SOD

During activation of SOD apo state, dimerization of SOD with the copper chaperone CCS is important for the transfer of Cu. The amino acids of SOD and CCS facilitates dimerization through protein to protein interactions (Casareno et al., 1998). Domains that facilitate dimerization in SOD and CCS have been identified (Schmidt et al., 2000). Amino acids of Domain II of CCS are homologous to some residues in Cu Zn SOD such that this domain was once called SOD 4 by some authors (Schmidt et al., 1999, Culotta et al., 1997). Copper is important for stabilising the heterodimer and copper transfer is achieved when Cysteine rich copper donor sites interact with histidine rich acceptor sites of SOD (Torres et al., 2001).

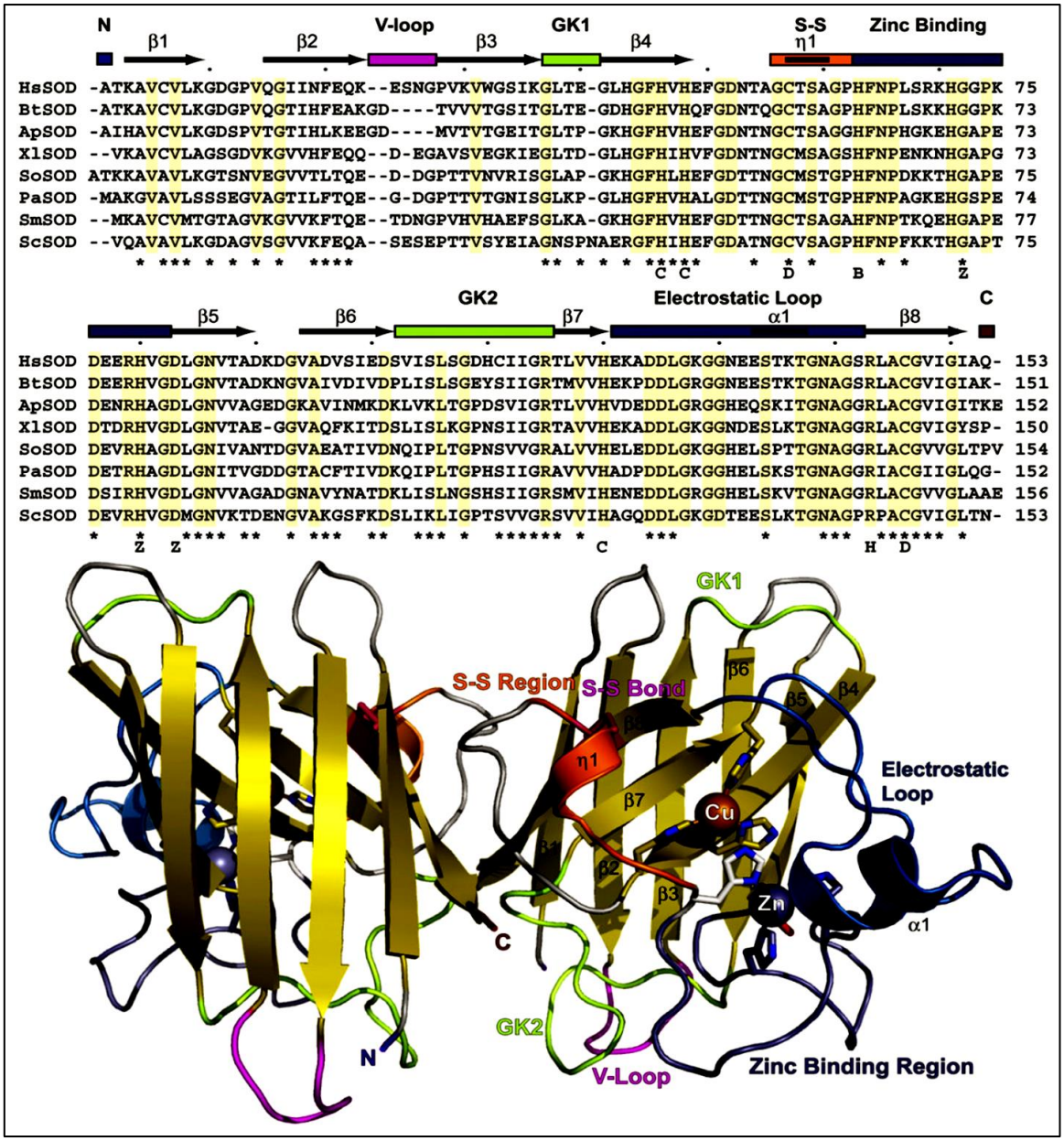

Figure 1.13. Functional domains in Cu, ZnSOD are shown and the preservation of structure between different SOD 1 proteins. Homo sapiens SOD (Hs), B taurus (Bt), A. pompejana (ApSOD), X laevis (XISOD), S oleracea (SoSOD), P. atrosanguina (PaSOD), S mansoni (SmSOD), S cerevisiae (ScSOD). Elements that are important in structure and the formation of the secondary structure are annotated above the amino acid sequence alignment. C represents the Copper binding ligand, D cysteine, B, the bridging histidine, Z zinc binding domain. The second image shows the structure of HsSOD (1PUO). The structural elements are in colour and encoded with abbreviations (V-loop for variable loop. GK1 and GK2 for Greek loops 1 and 2 and S-S, disulphide region). N denotes the amino terminal and C the carboxyl terminal. The metal binding ligands are represented as sticks with the bridging Histidine on position 61 in white. Taken from (Perry et al., 2010). Permission to reuse image was granted.

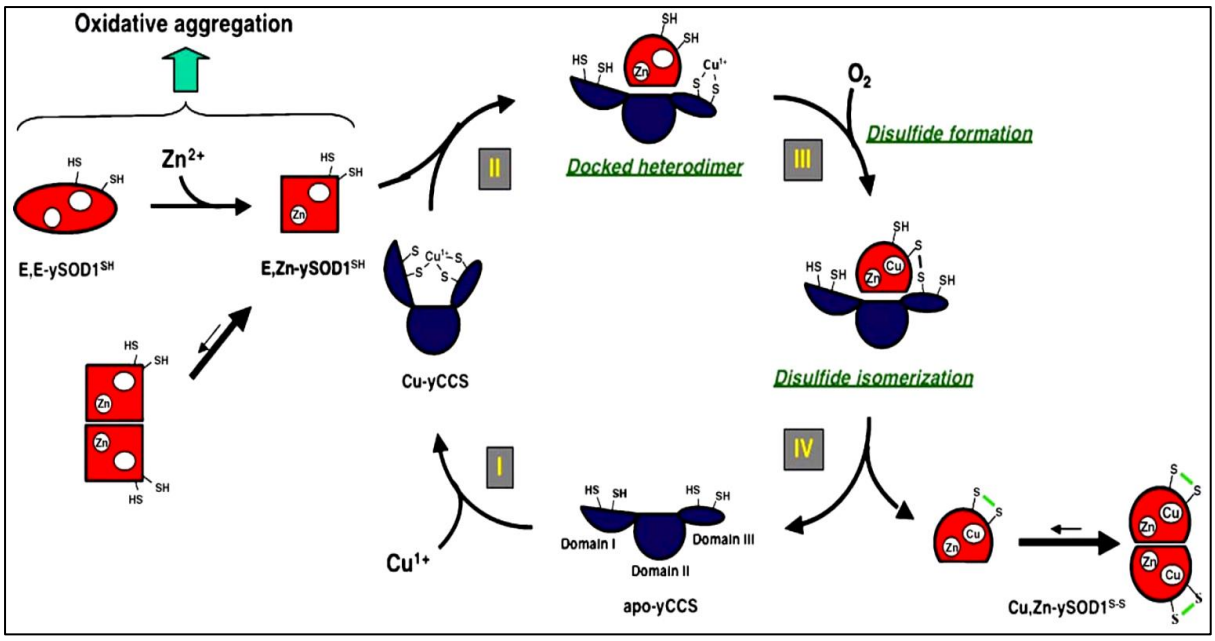

Figure 1.14. Putative mechanism for docking of copper onto SOD 1 by the chaperone, CCS. Step I and II- Copper is acquired by the chaperone and SOD 1 heterodimerises with CCS to form a CCS-SOD1 heterodimer. Step III- the heterodimeric complex is activated when exposed to molecular oxygen or the superoxide anion. Copper transfer occurs. Step IV- the complex isomerises to an intramolecular disulphide. Taken from (Culotta et al., 2006).

1.7 SOD homologues

Many viruses encode SOD-like proteins. Baculoviruses, Orthopoxviruses including vaccinia virus and variola, Leporipoxiviruses (shope fibroma virus and myxoma virus), Entomopoxviruses like *Amsacta moorei*, chloroviruses and some viruses belonging to the *Mimiviridae* family encode SOD-like proteins (Cao et al., 2002, Teoh et al., 2003, Almazan et al., 2001, Becker et al., 2004, Kang et al., 2014, Lartigue et al., 2015). SOD homologues that have the same function as SOD enzymes have been reported for *Megavirus chilensis* and the Entomopoxvirus *Amsacta moorei* (Becker et al., 2004, Lartigue et al., 2015). Alignment of these SOD proteins show preservation of certain catalytic residues. However other SOD homologues which have not retained the ability to function as SOD enzymes but that have residues important in dimerization with the copper chaperone have been reported (Cao et al., 2002, Teoh et al., 2005, Teoh et al., 2003). These SOD homologues inhibit the proper function of cellular Cu Zn SOD. An alignment of these SOD proteins reveals putative binding sites between the SOD homologues and the copper chaperone which may affect the proper metalation and activity of Cu Zn SOD (Figure 1.15).

Recombinant Leporipoxviruses myxoma virus (MYX) and SFV expressing SOD decoys M131R and S131R respectively were shown in in-situ gel assays to be catalytically inactive (Cao et al., 2002). The authors used a 6-hydroxydopamine test to investigate the activity of cellular Cu Zn SOD, after infecting cells with wild type MYX, SFV, SOD-knock-out and SOD knock-in viruses. They found that the cells infected with wild type virus and knock-in mutants had lower SOD activity compared to cells only suggesting a role of SOD in inhibiting activity of cellular SOD (Cao et al., 2002). Teoh et al, 2003 showed that the SOD expressed by SFV and MYX bind the copper chaperone for SOD (CCS). They also showed by immunoprecipitation, that when they used CCS specific polyclonal antibodies, they recovered SFV SOD (Teoh et al., 2003). Protein alignments showed SFV SOD contained a cysteine molecule at position 67, which could assist in the dimerization of CCS and SOD (Teoh et al., 2003). The ability of Leporipoxviruses' SOD to inhibit SOD activity was also shown through SOD activity assays which showed that infection of cells with viruses expressing SOD from SFV/MYX caused a 10-15% inhibition of cellular SOD activity (Teoh et al., 2005). On the other hand, SOD from vaccinia virus was shown to be inactive as a functional enzyme or decoy (Almazan et al., 2001). This was done by generating A45R knock-out and revertant A45R knock-in viruses which were investigated for SOD activity or inhibitory activity. In summary, Leporipoxviruses encode SOD homologues which are catalytically inert but bind the copper chaperone for SOD (Teoh et al., 2003). Shope fibroma virus (SFV) SOD acts in a way to perturb levels of the superoxide radical (Teoh et al., 2005). Thus, these SOD homologues act as decoy proteins binding the copper chaperone thereby depleting the amount of copper available for use by the Cu, Zn SOD (Teoh et al., 2003). This causes an intracellular increase in the superoxide anion. An increase in intracellular superoxide concentration through the inhibition of the SOD free radical scavenger has been shown to inhibit apoptosis in mammalian cells (Pervaiz and Clement, 2002a).

More recently *Molluscum contagiosum* virus was shown to encode a protein (MC163) which contains a mitochondrial localisation domain, a transmembrane domain and a Cu Zn SOD domain (Coutu et al., 2017). MC163 Cu Zn SOD domain is 19% similar to full-length SOD from Herbivac. MC163 was shown to localise in the mitochondrion and reduce apoptosis. It is postulated that the SOD homologue binds proapoptotic proteins (Bak or Bax) thereby inhibiting them. Cellular and mutant Cu Zn SOD has also been shown to localise in the mitochondrion (Kawamata and Manfredi, 2008). The effect of this is to reduce mitochondrial membrane potential which is key to apoptosis (Coutu et al., 2017).

Table 1.9 shows a summary of tests that have been conducted on different SOD homologues and the results.

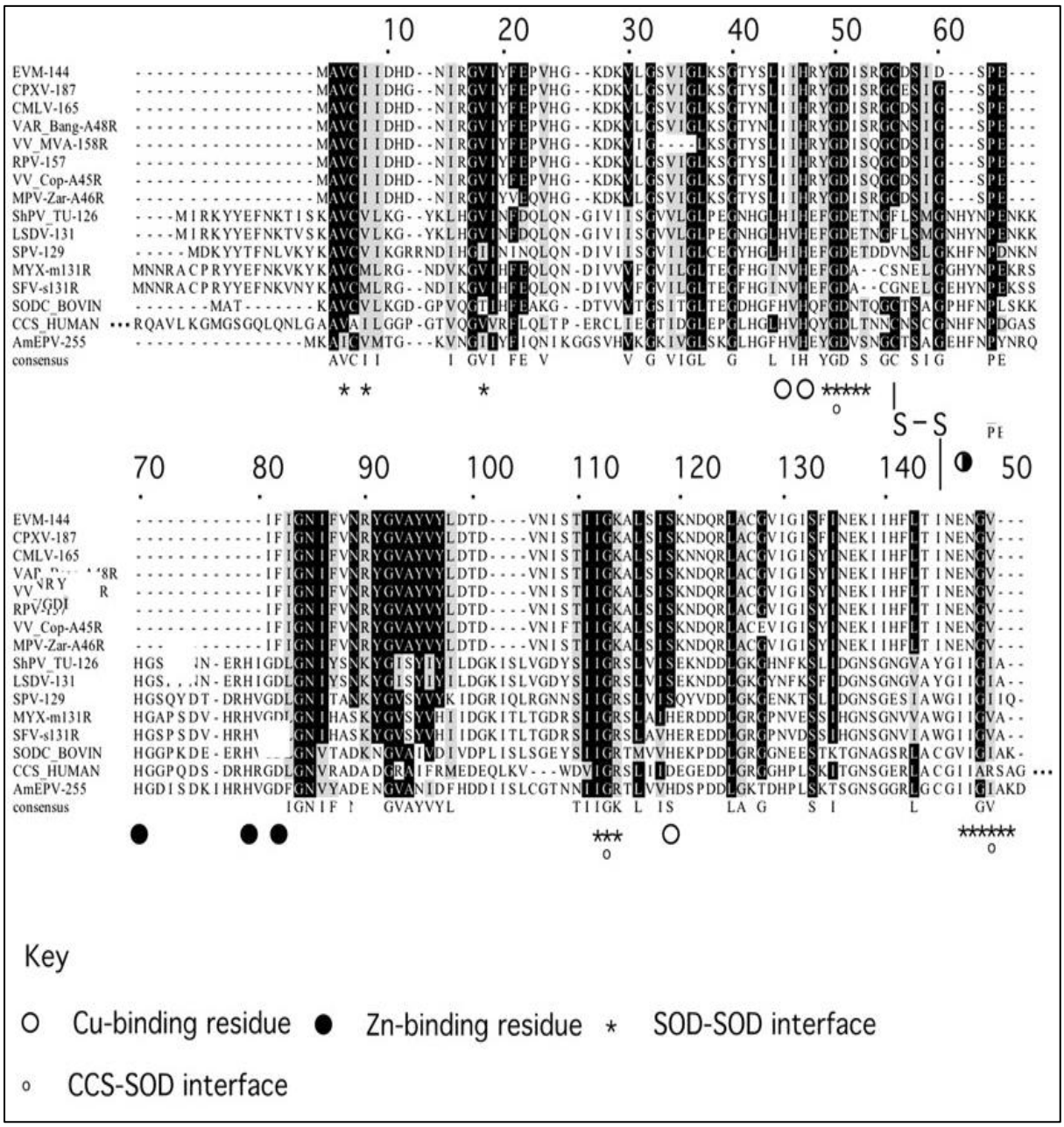

Figure 1.15. Amino acid alignment of viral SOD-like proteins from ectromelia virus (EVM-144), cowpox virus (CPXV-187), camel pox (CMLV-165, variola (VAR_Bang_A45R, vaccinia strain MVA (VV_MVA-158R), rabbitpox (RPV-157), vaccinia strain Copenhagen (VV_Cop-A45R), and monkey pox (MPV-Zar-A46R) viruses. Capripoxviruses include sheeppox (ShPV_TU-126), lumpy skin disease virus (Nl 2490) (LSDV-131), and swinepox (SPV-129) viruses. Leporipoxviruses are myxoma (MYX-m131R) and Shope fibroma (SFV-s131R) viruses. Included in the alignment is a known active SOD enzyme from Amsacta moorei (AmEPV-255), bovine (SODC_BOVIN), residues from domain II of the copper chaperone for SOD (CCS_HUMAN) and human cellular Cu Zn SOD. Symbols below the consensus sequence are shown in the key. Taken from Cao et al. (2002). Permission to reuse image was granted.

Table 1.9 summarises the studies done on SOD homologues to characterise them as active enzymes or SOD decoys which inhibit the activity of cellular SOD.

Table 1.9. Summary of all the tests done on poxvirus SOD homologues to determine whether they act as functional SOD enzymes or decoy proteins.

SOD homologues tested	Summary of results	Authors
Myxoma virus and Shope fibroma virus (Leporipoxviruses). Wild type viruses, recombinant MYX and SFV expressing a decoy (M131R and S131R respectively)	Myxoma and Shope Fibroma virus encode a decoy that does not function as an enzyme but as a functional decoy in cells	(Cao et al., 2002, Teoh et al., 2005, Teoh et al., 2003)
Vaccinia virus and recombinant vaccinia virus expressing a decoy (*A45R*)	Vaccinia virus SOD homologue is not functional as an enzyme or as an inhibitor in cell culture. The homologue is packaged in the viral core.	(Almazan et al., 2001)
Amsacta Moorei virus (an Entomopoxvirus), protein expressed in bacterial system and purified	SOD from AMV is a functional SOD enzyme.	(Becker et al., 2004)
Chlorovirus PBCV-1. WT virus was used and purified GST-tagged protein from bacterial plasmids were also used.	Chloroviruses SOD (*a245r*) is packaged in the viral core and is a functional SOD enzyme.	(Kang et al., 2014)
Megavirus Chilensis purified protein	A functional SOD was purified which does not use a copper chaperone to insert copper and does not need copper for activity.	(Lartigue et al., 2015)
Molluscum contagiosum - transient expression of the MC163 protein.	The gene product was shown to localise to the mitochondrion and inhibit apoptotic cell death.	(Coutu et al., 2017)

1.8 Project motivation

At the University of Cape Town (UCT) it was found that the SOD homologue gene in Herbivac differed from that of nLSDV. Herbivac contained a mixture of viruses, some with a full-length SOD homologue and others with the truncated SOD homologue resembling that of nLSDV.

The first objective of the project was to determine if there was a difference between nLSDV and Herbivac in the innate response induced at 24 hours post infection in mouse spleens.

On confirmation of the different response in mice the second objective of the project was to construct viruses with a deleted SOD gene and an improved, more stable SOD gene (SOD knock-out and SOD knock-in LSDVs).

The third objective of the project was to characterise the different recombinant viruses and compare them to Herbivac and nLSDV. Growth curves were done on chorioallantoic membranes (CAMs) of fertilised hens' eggs and in cell culture (MDBK cells) to determine if the viruses differed from each other and nLSDV, which had a truncated SOD homologue gene. CAMs infected with the different vaccines and recombinants were analysed histologically to determine how they may differ with respect to pathogenicity and immunogenicity.

In silico structural alignments of SOD were done to determine the presence of putative residues important in the activity or absence of activity of SOD homologues. The fourth and last objective was to investigate the role of the full-length SOD homologue in cell death. Using a known cell death inducer, the role of the full-length SOD homologue in inhibition of camptothecin induced cell death was investigated. Camptothecin is a known cancer drug that induces apoptosis in neoplastic cells. Camptothecin binds topoisomerase which is involved in maintaining the integrity of DNA during replication. Topoisomerases remove tension created in DNA by supercoiling. To allow for the replication fork and polymerases to act, topoisomerases create breaks in DNA which are resolved once DNA replication has occurred. Camptothecin inhibits type 1 topoisomerases (Xu and Her, 2015, Hsiang et al., 1989). When these topoisomerases are inhibited, tension in the DNA as well as stalling of DNA replication occurs causing DNA damage and thereby inducing apoptosis via the intrinsic pathway. Thus, observing behaviour of cells in the presence of camptothecin can be informative in understanding induction or inhibition of apoptotic cell death. Two types of cell death, namely apoptosis and necrosis were analysed. We hypothesised that the presence of the full-length SOD homologue would cause inhibition of apoptosis which would lead to viral persistence and increased immune response to the virus.

Chapter 2 Comparison of the innate host transcriptome induced in mice after infection with nLSDV and Herbivac

2.1 Introduction 51
2.2 Methods 54
2.2.1 Viruses 54
2.2.3 RNA extraction 54
2.2.4 Microarray hybridisation and data analysis 55
2.3 Results 57
2.3.1 Comparative differential host gene expression following infection with Herbivac or nLSDV 57
2.3.2 Host processes and pathways activated by Herbivac and nLSDV. 69
2.4 Discussion 74

List of figures

Figure 2.1. A Heatmap showing differential expression induced in mouse spleens obtained from mice infected with MVA, nLSDV or Herbivac. 57

Figure 2.2. Venn diagram showing a set of uniquely differentially regulated transcripts and genes that were differentially expressed by both viruses in response to infection with Herbivac, nLSDV and MVA.. 65

Figure 2.3. Radial plot showing differences in the level of expression of immune system related genes.. 66

Figure 2.4 Radial plot showing differences in the level of expression of (A) interferon related genes and (B) genes involved in pathogen pattern recognition. 67

Figure 2.5 Radial plot showing differences in the level of expression of genes related to cell death.. 67

Figure 2.6 Venn diagram showing GO processes associated with Herbivac and nLSDV. In each circle, the number of differentially expressed processes are shown.. 70

Figure 2.7 Graphical presentation of top canonical pathways intercepting with genes affected by Herbivac infection..... 72

Figure 2.8 Graphical presentation of top canonical pathways intercepting with genes affected by nLSDV infection.. 73

List of tables

Table 2.1. Differentially expressed genes in response to Herbivac, MVA and nLSDV infection..... 58

Table 2.2 List of genes uniquely differentially expressed in response to nLSDV and Herbivac infection.. 68

Table 2.3 Summary of processes unique to nLSDV AND Herbivac..... 71

Table 2.4. Summary of pathways unique to nLSDV AND Herbivac.. 74

Chapter 2 Comparison of the innate host transcriptome induced in mice after infection with nLSDV and Herbivac

2.1 Introduction

The advent of systems biology and use of high throughput genomics and proteomics makes it possible to delineate vaccine induced immune responses that are predictive of the overall immune response (reviewed by Six et al. (2012)). Microarray technology uses knowledge of DNA hybridisation. Gene specific probes which are impregnated onto a glass or silicon chip by a robot are hybridised to cDNA molecules which have been reverse transcribed from mRNA and mixed with fluorescent probes or dyes (reviewed by Dhiman et al. (2001)). The value of microarrays is that they can simultaneously analyse the whole transcriptome on a single chip.

Microarrays have been used to study host responses to vaccination (reviewed by Furman and Davis (2015) and Pepini et al. (2017)) as well as virus host interaction, reviewed by Law et al. (2013). In one study, MVA was used to infect HeLa cells and the host transcriptomic response was analysed. Whilst MVA does not complete its replication cycle in HeLa cells, morphogenesis is blocked at the stage where immature virus is formed, which is after MVA early gene expression. MVA infection resulted in differential expression of 410 host genes including 20 immune related genes and five cytokines. The authors suggest that some of the upregulated genes, including NF-κB, could be responsible for antigen specific immune responses after vaccination with recombinant MVA (Guerra et al., 2004).

The spleen contains the interface for the innate and adaptive immune system. T cell zones are present in the spleen and antigen presenting cells (APCs) present antigens to T cells. Dendritic cells drain in the spleen and so the spleen presents a unique organ to investigate host responses to vaccination. Studying the transcriptome of splenocytes following vaccination can be insightful in understanding the immunogenicity of a vaccine. In a recent study where subunit vaccines against *Fasciola hepatica* were made, the authors identified the best antigen formulation in their vaccine based on splenic gene expression (Rojas-Caraballo et al., 2017). In another study, a DNA vaccine against H5N1 with an extended NF kappa B site was shown, by microarray analysis of the genes expressed by splenocytes, to downregulate a gene, *Lyst*, which, they postulated would protect vaccinated animals from an inflammatory reaction that

could be deleterious (Redkiewicz et al., 2017). These studies show that the spleen is a suitable organ to use in the investigation of immunomodulatory responses of the host to a virus infection.

In another study, an early innate immune molecular signature with a predictive score of 90% accuracy in predicting the humoral response to influenza was shown (Nakaya et al., 2011). Earlier, the same scientific group, analysed a repertoire of 30 000 genes and proteins to elucidate a unique molecular signature with a predictive value for the strength of the immune response to the successful yellow fever vaccine (YF-17D) (Querec et al., 2009). In that study, microarray analysis was used to understand the transcriptome on peripheral blood mononuclear cell (PBMC) stimulated using the YF-17D vaccine (Querec et al., 2009). The results showed upregulation of 50 interferon and antiviral genes. An increase in the expression of the translation initiation factor *Eif2ak4* was also shown to be predictive for a good cellular immune response to YF-17D (Querec et al., 2009).

The role of the innate immune response in determining the magnitude and quality of adaptive immune response has resulted in a focus on understanding the innate response. Understanding the role of pathogen recognition receptors (PRRs) which are present on innate immune cells provides a unique insight into the overall immune response. These PRRs are inducible upon interacting with pathogen associated molecular patterns (PAMPs) (reviewed by Six et al. (2012)). Upon infection, viral nucleic acids often trigger PRRs (Sparrer and Gack, 2015). Intracellular DNA sensors have been described and include leucine-rich repeat flightless-interacting protein 1 (Lrrfip1), Ifi16 (which is part of the PyHIN – pyrin and HIN200 family), RNA polymerase III, DExD/H box RNA helicases 9/36 (DDX9/36) and DNA dependant activator of IFN regulatory factors (DAI), which play a role in type 1 IFN production and cytokine production (Thompson et al., 2011). The molecule stimulator of interferon genes (STING) plays a role in TLR 9 independent production of type 1 interferons and other cytokines (Barber, 2014). Virus sensing by PRRs activates type 1 interferons which in turn upregulate major histocompatibility (MHC) Class 1 molecules. This makes virus infected cells targets for cytotoxic T lymphocytes (CTLs) and TNF-like death ligands (Upton and Chan, 2014). Natural killer cells and cytotoxic cells make use of granzymes and perforin to kill cells. Granzyme B is the most documented and a classical example of an apoptosis inducer. Granzyme A, on the other hand, is involved in caspase independent cell death (Upton and Chan, 2014).

An antiviral response by an infected cell includes cell death which could take the form of apoptosis or necrosis (Orzalli and Kagan, 2017). It has also been shown that approximately 300 genes are induced by the action of interferons with some of those genes being involved in apoptosis (reviewed by Kaminskyy and Zhivotovsky (2010)). MVA induces apoptosis in macrophages with a concomitant release of IFN β production (Royo et al., 2014).

Traditionally, necrosis was thought of as an unorderly form of death, in contrast to apoptosis. However, there is a growing body of knowledge which supports the notion of necroptosis being a programmed form of cell death (reviewed by Nikoletopoulou et al. (2013), (Orzalli and Kagan, 2017)). This form of death is induced in addition to apoptosis or becomes pertinent in instances where apoptosis is inhibited by viral anti-apoptotic gene products (Chan et al., 2003). Unlike apoptosis, necroptosis is a highly inflammatory form of cell death (reviewed by Orzalli and Kagan (2017)).

The aim of this part of the study was to compare changes in virus host interactions following infection of mice with either Herbivac or nLSDV. As nLSDV is being used as a vaccine for lumpy skin disease and as a vaccine vector, it will be important to establish whether the 2bp deletion in ORF131, which restores the gene encoding a SOD homolog, plays a role in modulation of the host immune response.

MVA was used as a control in this experiment as it has been shown to induce a distinct gene expression profile following its use as a vaccine vector (Altenburg et al., 2014, Guerra et al., 2004, Guerra et al., 2007, Guzman et al., 2012, Nájera et al., 2006, Teigler et al., 2014, Offerman et al., 2015). Our laboratory works with MVA and so it was available to use.

In this study, RNA from spleens of mice infected with nLSDV or Herbivac was reverse transcribed and hybridised to Affymetrix© arrays containing DNA probes specific to all the genes present in a mouse. Mice that received PBS were used as a control to compute fold change of expression. Understanding host gene expression profiles following infection will be instrumental in understanding how LSDV works as a vaccine vector for both human and veterinary vaccine purposes.

2.2 Methods

2.2.1 Viruses

The Neethling vaccine strain used in this study is a commercial vaccine strain from Onderstepoort Biological Products (OBP), Onderstepoort, Pretoria. Herbivac LS (batch 008) was supplied to us by Deltamune, Pretoria. In this thesis, Herbivac LS will be called Herbivac. Both viruses were grown on chorioallantoic membranes (CAMs) of 7-day old embryonated specific pathogen free (SPF) White Leghorn chicken eggs (AviFarms, South Africa). Titration of the two lumpy skin disease viruses was done using the immunostaining method. Sera from cattle immunised with Herbivac was used detect LSDV. LSDV to be titrated was serially diluted from 10^{-1} to 10^{-8}. Virus (100µl) was added to MDBK cells. After 72 hours of incubation, virus was removed, and cells washed using PBS. A primary antibody raised against cattle and conjugated to a peroxidase was then added. Hydrogen peroxide and di-anisidine dye were added. After washing off the substrate, LSDV positive foci stained brown and were counted to determine the titre in plaque forming units for the LSD virus. Streaking of virus cultures was done on Luria agar to check for bacterial contamination of the virus stocks.

MVA was originally obtained from Prof Keith Dumbell, who obtained it from Prof. A. Mayr (Veterinary Faculty, University of Munich, Germany). It was grown and titrated on chick CAMs by Dr Offerman (Offerman, 2014).

Ethics approval for the use of embryonated eggs was granted by the University of Cape Town (ethics number 013/016).

2.2.2 RNA extraction

2.2.2.1 Inoculation of mice

Naïve BALB/c female mice were divided into four groups of three mice. The different groups received an intravenous inoculation of 100µl of 10^5 pfu/100µl of the following vaccines/controls 1) nLSDV, 2) Herbivac 3) Modified vaccinia Ankara (MVA) or 4) 100µl phosphate buffered saline (PBS). MVA was used as an experimental control and PBS a negative control. After 24 hours of infection, the mice were sacrificed by cervical dislocation in the absence of anaesthesia. Spleens were collected and stored in RNAlater (Qiagen, Venlo, Limburg, NL). All virus inoculations, animal handling and sacrificing of mice was done by Mr

Rodney Lucas at the UCT Research Animal Facility. Ethics approval for the mouse work was granted by The University of Cape Town ethics committee (ethics number 013/017)

2.2.2.2 RNA extraction from mouse spleens

Three spleens from 3 animals which received the same virus were pooled and homogenised using TissueRuptor blender (Qiagen) in TRIzol® reagent (Life Technologies, USA). From this pooled homogenate RNA was prepared in triplicate. DNase treatment was done using On-column PureLink® according to the manufacturer's guidelines. RNA was isolated using the RNA extraction kit (Qiagen) and eluted in ultra-pure water. RNA quality and concentration were determined using the Nanodrop ND1000 (Thermo Scientific, USA) and the Agilent Bioanalyser at CPGR (South Africa).

2.2.3 Microarray hybridisation and data analysis

For microarray hybridisations, 200ng of RNA was used to make cDNA. The samples were fragmented and labelled according to the Affymetrix WT PLUS protocol. Hybridisation of the targets was done on the Affymetrix Mouse Gene ST 2.0 arrays followed by incubation overnight. After washing and staining of the chip, the chip was scanned using the GeneChip® Scanner 3000 7G.

2.2.3.1 Generation of gene lists

Dr Armin Darfur and Dr Kristy Offerman from UCT provided the bioinformatic analysis pipeline and support for this study. The output from the microarray readings were *CEL files and these served as input for differential expression analysis. CEL files were normalised using Robust Multi-array averaging (RMA) (Irizarry et al., 2003) and similar probes on different arrays were used to do the averaging. RMA is available from Bioconductor as a component of the Affymetrix 'affy' package (Gautier et al., 2004). The result was $\log_2$ transformed data which was annotated using the Mouse Gene ST 2.0 and filtered in the first filtering step using the Genefilter package. This filtration step included an intensity filter which reported only genes that were $>\log_2$ in 20% of the samples (Gentleman et al., 2011). Another filtration step using a variance filter was done and this filter only enriched for genes whose interquartile ranges of the log transformed data was less than 0.5. Differential gene expression was measured using a linear regression model approach using the R package, Limma (Smyth, 2005). A heatmap was made using heatmap.2 from the CRAN package gplots (Warnes et al., 2009) and depicted the

unsupervised hierarchical clustering based on the genes with p-value < 0.05 and $\log_2$ fold change (FC) above or below cut-off (±1). Note, genes with a p-value of <0.05 and absolute fold change of >1 and above was noted whereas genes with a p-value of >0.05 and absolute fold change of <1 were assigned 0. See Appendix 1 for the R script used.

A tool for drawing Venn diagrams was used (Venny, available at http://bioinfogp.cnb.csic.es/tools/venny/). This enables visualisation of genes, biological processes and pathways that are common or unique to Herbivac or nLSDV infection (Oliveros and Venny, 2007).

2.2.3.2 GO processes

The MGI Gene Ontology Term Finder available at http://www.informatics.jax.org/gotools/MGI_Term_Finder.html was used to find GO terms associated with a set of differentially expressed genes. Gene ontology allows for the creation and maintenance of a structured, curated database of genes and related information based on evidence found in the literature. For this study, biological processes which represent an orderly amalgamation of molecular functions is reported (GO Ontology Consortium). To do this, the gene list from R containing all the differentially expressed genes was loaded onto the MGI Gene ontology tool. Biological processes were listed for each virus.

2.2.3.3 Pathway analysis

Ingenuity pathway analysis IPA® (QIAGEN Inc., https://www.qiagenbioinformatics.com/products/ingenuitypathway-analysis) was used to find pathways that were either activated or inhibited following infection with Herbivac or nLSDV. The gene list generated by the R program along with the $\log_2$ FC values was imported onto the IPA console. Top canonical pathways were determined. The Z score was used to determine whether a pathway is activated, inhibited or whether the information on the pathway is unknown. The number of genes present in the data set was expressed as a ratio of the total number of genes in that pathway.

2.3 Results

2.3.1 Comparative differential host gene expression following infection with Herbivac or nLSDV

Host gene expression in response to Herbivac and nLSDV was investigated using microarrays. RNA was isolated from spleens of BALB/c mice 24 hours after infection. The group of mice that received PBS only was used for baseline expression and expression of genes in the virus-infected groups was investigated for up/down regulation against the expression data of mice that were inoculated with PBS. RNA from mice infected with MVA was used as an experimental positive control. Genes that were significantly up or down regulated (with an adjusted p-value of < 0.05) and a fold $\log_2$ fold change of greater than 0 were described as up regulated and smaller than 0, down regulated.

Figure 2.1 shows a heatmap of the genes that were differentially expressed by MVA, Herbivac and nLSDV. Unsupervised hierarchical clustering of the differentially expressed genes demonstrated that the viruses induced distinct, overall transcriptomic responses in mouse spleens (Figure 2.1).

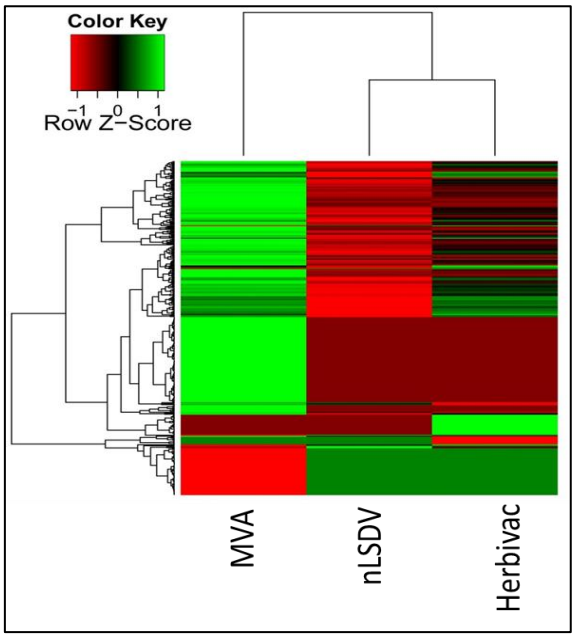

Figure 2.1. A Heatmap showing differential expression induced in mouse spleens obtained from mice infected with MVA, nLSDV or Herbivac. Only genes (with p-value < 0.05) with $\log_2$ fold change of above or below the set cut off of >0 or < 0 as compared to the PBS group are shown. Unsupervised hierarchical clustering of the samples is shown by the dendrograms. Heatmap analysis was performed in the R package, gplots (Warnes et al., 2009).

2.3.1.1 Herbivac and nLSDV induce a different host transcriptome

The differentially expressed genes induced after nLSDV or Herbivac infection are listed in Table 2.1 with their levels of up or downregulation. The gene lists produced from data analysis showed that Herbivac and nLSDV induced largely similar host responses in mice (97 genes) and a few dissimilar responses – 36 unique to Herbivac and 6 unique to nLSDV. Infection with Herbivac caused differential gene expression of more genes than infection with nLSDV. The genes that were differentially expressed after MVA infection correlated with those reported by Offerman et al. (2015).

Table 2.1. Differentially expressed genes in response to Herbivac, MVA and nLSDV infection. The differences in Log_2 fold changes (FC) between virus and control are shown.

Full list of annotated up & down regulated genes					
Symbol	**Name**	**Herbivac**	**MVA**	**nLSDV**	**Herbivac-nLSDV ratio**
Sp100	nuclear antigen Sp100	1.49	0.95	1.02	1.46
Sp100	nuclear antigen Sp100	1.49	1.78	1.02	1.46
Sp100	nuclear antigen Sp100	1.49	1.5	1.02	1.46
Ms4a4c	membrane-spanning 4-domains, subfamily A, member 4C	1.58	1.74	1.11	1.42
BC094916	cDNA sequence BC094916	1.52	1.97	1.1	1.38
Ifit2	interferon-induced protein with tetratricopeptide repeats 2	1.66	1.92	1.22	1.36
Trim12c	tripartite motif-containing 12C	1.44	1.24	1.07	1.35
Ifih1	interferon induced with helicase C domain 1	1.73	2.06	1.28	1.35
Plac8	placenta-specific 8	1.44	1.59	1.08	1.33
Pyhin1	pyrin and HIN domain family, member 1	1.78	1.83	1.35	1.32
Ifi44l	interferon-induced protein 44 like	2.34	2.96	1.8	1.3
Eif2ak2	eukaryotic translation initiation factor 2-alpha kinase 2	1.64	1.97	1.26	1.3
Cmpk2	cytidine monophosphate (UMP-CMP) ki0se 2, mitochondrial	1.89	1.85	1.47	1.29
Fcgr4	Fc receptor, IgG, low affinity IV	1.62	1.99	1.26	1.29
Isg15	ISG15 ubiquitin-like modifier	1.99	2.09	1.56	1.28
Herc6	hect domain and RLD 6	1.8	2.08	1.41	1.28
Ifi202b	interferon activated gene 202B	1.86	2.04	1.45	1.28
Rtp4	receptor transporter protein 4	1.52	2.31	1.2	1.27
Ifit1	interferon-induced protein with tetratricopeptide repeats 1	2.67	2.91	2.12	1.26
Ifi44	interferon-induced protein 44	2.21	2.94	1.75	1.26
Phf11b	PHD finger protein 11B	1.96	1.88	1.55	1.26
Slfn8	schlafen 8	1.29	1.77	1.02	1.26

Symbol	Name	Herbivac	MVA	nLSDV	Herbivac-nLSDV ratio
Trim30a	tripartite motif-containing 30A	1.72	2.31	1.39	1.24
Phf11c	PHD finger protein 11C	2.24	2.96	1.81	1.24
Gm20559	predicted gene, 20559	1.28	1.78	1.03	1.24
Ddx60	DEAD (Asp-Glu-Ala-Asp) box polypeptide 60	2.09	2.69	1.7	1.23
Gm14446	predicted gene 14446	2.99	3.39	2.43	1.23
Znfx1	zinc finger, NFX1-type containing 1	1.48	1.8	1.2	1.23
Irf7	interferon regulatory factor 7	2.32	2.88	1.93	1.2
Oas1b	2'-5' oligoadenylate synthetase 1B	1.54	1.92	1.28	1.2
Klrk1	killer cell lectin-like receptor subfamily K, member 1	1.46	1.44	1.23	1.19
Pydc3	pyrin domain containing 3	1.7	2.36	1.43	1.19
Setdb2	SET domain, bifurcated 2	1.6	2.21	1.36	1.18
Ddx58	DEAD (Asp-Glu-Ala-Asp) box polypeptide 58	1.25	1.79	1.06	1.18
Mx2	myxovirus (influenza virus) resistance 2	2.69	3.45	2.28	1.18
Oas3	2'-5' oligoadenylate synthetase 3	1.96	2.55	1.68	1.17
Bst2	bone marrow stromal cell antigen 2	2.25	2.73	1.92	1.17
Pydc4	pyrin domain containing 4	2.24	2.98	1.91	1.17
Tdrd7	tudor domain containing 7	1.19	1.36	1.03	1.16
Ms4a4a	membrane-spanning 4-domains, subfamily A, member 4A	1.71	1.93	1.47	1.16
Oas1g	2'-5' oligoadenylate synthetase 1G	2.55	3.31	2.21	1.15
Parp12	poly (ADP-ribose) polymerase family, member 12	1.73	2.51	1.52	1.14
Mov10	Moloney leukemia virus 10	1.23	1.68	1.08	1.14
Oasl1	2'-5' oligoadenylate synthetase-like 1	2.45	2.86	2.15	1.14
Trim30c	tripartite motif-containing 30C	2.78	3.42	2.43	1.14
Trafd1	TRAF type zinc finger domain containing 1	1.35	1.66	1.18	1.14
Apol9b	apolipoprotein L 9b	2.97	2.85	2.64	1.13
Helz2	helicase with zinc finger 2, transcriptional coactivator	1.26	1.65	1.12	1.13
Fcgr1	Fc receptor, IgG, high affinity I	1.82	1.79	1.61	1.13
Ly6c2	lymphocyte antigen 6 complex, locus C2	2.08	2.17	1.86	1.12
Slfn1	schlafen 1	1.31	1.98	1.17	1.12
Ms4a6d	membrane-spanning 4-domains, subfamily A, member 6D	2.22	2.47	1.98	1.12
Daxx	Fas death domain-associated protein	1.66	2.05	1.48	1.12
Gca	Grancalcin	1.24	1.37	1.12	1.11
Trim30d	tripartite motif-containing 30D	2.24	2.23	2.01	1.11
Mx1	myxovirus (influenza virus) resistance 1	3.3	3.89	2.96	1.11
Tlr3	toll-like receptor 3	1.24	1.33	1.13	1.1
Dhx58	DEXH (Asp-Glu-X-His) box polypeptide 58	1.6	2.23	1.45	1.1
Oasl2	2'-5' oligoadenylate synthetase-like 2	2.55	3.29	2.31	1.1
Tor3a	torsin family 3, member A	1.62	2.12	1.49	1.09

Symbol	Name	Herbivac	MVA	nLSDV	Herbivac-nLSDV ratio
Irgm1	immunity-related GTPase family M member 1	1.22	2.13	1.12	1.09
Cxcl11	chemokine (C-X-C motif) ligand 11	2.3	3.08	2.11	1.09
Usp18	**ubiquitin** specific peptidase 18	**2**.48	**3**.14	**2**.27	**1.09**
Zbp1	Z-DNA binding protein 1	1.52	3.16	1.39	1.09
Gm12185	predicted gene 12185	1.68	2.49	1.56	1.08
Ly6a	lymphocyte antigen 6 complex, locus A	2.1	3.34	1.95	1.08
Gm15056	predicted gene 15056	2.28	2.61	2.11	1.08
Tnfsf10	tumor necrosis factor (ligand) superfamily, member 10	1.63	1.86	1.53	1.07
Xaf1	XIAP associated factor 1	1.44	2.11	1.34	1.07
Tuba8	tubulin, alpha 8	2.05	2.14	1.94	1.06
BC147527	cDNA sequence BC147527	1.65	1.9	1.56	1.06
Xdh	xanthine dehydrogenase	2.01	2.48	1.9	1.06
Rnf213	ring finger protein 213	1.53	2.71	1.46	1.05
Slfn4	schlafen 4	1.93	2.67	1.84	1.05
Parp14	poly (ADP-ribose) polymerase family, member 14	1.06	2.01	1.01	1.05
Parp11	poly (ADP-ribose) polymerase family, member 11	1.26	1.84	1.2	1.05
Stat2	signal transducer and activator of transcription 2	1.26	2.2	1.2	1.05
Phf11d	PHD finger protein 11D	2.3	2.44	2.19	1.05
Cd69	CD69 antigen	1.45	1.8	1.41	1.03
Slfn5	schlafen 5	1.78	2.77	1.73	1.03
I830012O16Rik	RIKEN cD0 I830012O16 gene	2.29	1.97	2.22	1.03
Oas2	2'-5' oligoadenylate synthetase 2	2.29	3.46	2.25	1.02
Gm12250	predicted gene 12250	1.14	2.94	1.12	1.02
Pi4kb	phosphatidylinositol 4-kinase, catalytic, beta polypeptide	1.69	1.68	1.65	1.02
Ccl3	chemokine (C-C motif) ligand 3	1.39	1.22	1.38	1.01
Sp100	nuclear antigen Sp100	1.03	1.5	1.02	1.01
Sp100	nuclear antigen Sp100	1.03	1.78	1.02	1.01
Sp100	nuclear antigen Sp100	1.03	0.95	1.02	1.01
Gm5431	predicted gene 5431	2.7	3.33	2.67	1.01
Mlkl	mixed lineage kinase domain-like	1.52	2.1	1.54	0.99
Sgcb	sarcoglycan, beta (dystrophin-associated glycoprotein)	1.12	1.29	1.13	0.99
Gm6904	predicted gene 6904	1.52	1.98	1.53	0.99
AW011738	expressed sequence AW011738	1.21	1.66	1.23	0.98
AI607873	expressed sequence AI607873	1.12	1.47	1.15	0.97
Cd274	CD274 antigen	1.12	2.01	1.15	0.97
Pde7b	phosphodiesterase 7B	1.45	1.68	1.54	0.94
Chic1	cysteine-rich hydrophobic domain 1	1.12	1.66	1.2	0.93
Gzmb	granzyme B	2.63	3.44	2.85	0.92

Symbol	Name	Herbivac	MVA	nLSDV	Herbivac-nLSDV ratio
Cxcl10	chemokine (C-X-C motif) ligand 10	1.5	3	1.68	0.89
Gm4951	predicted gene 4951	1.04	2.55	1.26	0.83
Gbp10	guanylate-binding protein 10	1.21	3.24	1.5	0.81
Gbp11	guanylate binding protein 11	1.63	3.47	2.04	0.8
Slfn3	schlafen 3	**1**.7	**0**	**0**	**N/A**
Gzma	granzyme A	1.64	0	0	N/A
F830016B08Rik	RIKEN cDNA F830016B08 gene	1.63	2.01	0	N/A
Mndal	myeloid nuclear differentiation antigen like	1.53	1.34	0	N/A
Tlr7	toll-like receptor 7	1.53	1.41	0	N/A
Apol11b	apolipoprotein L 11b	1.48	0	0	N/A
AW112010	expressed sequence AW112010	1.38	0	0	N/A
Zufsp	zinc finger with UFM1-specific peptidase domain	1.34	1.48	0	N/A
Lgals9	lectin, galactose binding, soluble 9	1.31	1.55	0	N/A
Rsad2	radical S-adenosyl methionine domain containing 2	1.3	0.79	0	N/A
Ifitm3	interferon induced transmembrane protein 3	1.28	1.75	0	N/A
Lgals3bp	lectin, galactoside-binding, soluble, 3 binding protein	1.28	1.66	0	N/A
Anxa4	annexin A4	1.21	1.33	0	N/A
Gm6548	eukaryotic translation elongation factor 1 alpha 1 pseudogene	1.19	1.35	0	N/A
Nmi	N-myc (and STAT) interactor	1.15	1.4	0	N/A
Tmem184b	transmembrane protein 184b	1.14	1.17	0	N/A
Iigp1	interferon inducible GTPase 1	1.13	2.64	0	N/A
Epsti1	epithelial stromal interaction 1 (breast)	1.12	1.63	0	N/A
Trim21	tripartite motif-containing 21	1.12	1.27	0	N/A
Nampt	nicotinamide phosphoribosyltransferase	1.11	1.59	0	N/A
Nt5c3	5'-nucleotidase, cytosolic III	1.11	0	0	N/A
Gm6637	predicted gene 6637	1.1	0	0	N/A
Il15	interleukin 15	1.1	0.97	0	N/A
Parp9	poly (ADP-ribose) polymerase family, member 9	1.1	1.93	0	N/A
Stxbp3a	syntaxin binding protein 3A	1.09	0	0	N/A
Atp10a	ATPase, class V, type 10A	1.08	1.47	0	N/A
Gm1966	predicted gene 1966	1.07	1.86	0	N/A
H2-T24	histocompatibility 2, T region locus 24	1.06	1.19	0	N/A
Tspo	translocator protein	1.06	0	0	N/A
Pkib	protein kinase inhibitor beta, cAMP dependent, testis specific	1.05	1.69	0	N/A
Lgmn	Legumain	1.03	0	0	N/A
Ascc3	activating signal cointegrator 1 complex subunit 3	1.01	1.01	0	N/A
1600014C10Rik	RIKEN cD0 1600014C10 gene	0	0.96	0	N/A
A530099J19Rik	RIKEN cD0 A530099J19 gene	0	-1.38	0	N/A

Symbol	Name	Herbivac	MVA	nLSDV	Herbivac-nLSDV ratio
Adar	adenosine deaminase, RNA-specific	0	1.12	0	N/A
Ank	progressive ankylosis	0	-0.95	0	N/A
Aqp1	aquaporin 1	0	-1	0	N/A
Arid5a	AT rich interactive domain 5A (MRF1-like)	0	0.78	0	N/A
Atm	ataxia telangiectasia mutated homolog (human)	**0**	**1**.24	**0**	**N/A**
Atp8b4	ATPase, class I, type 8B, member 4	0	1.41	0	N/A
B4galt5	UDP-Gal:betaGlcNAc beta 1,4-galactosyltransferase, polypeptide 5	0	1.38	0	N/A
BC023969	cDNA sequence BC023969	0	0.85	0	N/A
Btnl10	butyrophilin-like 10	0	-0.91	0	N/A
C130026I21Rik	RIKEN cD0 C130026I21 gene	0	0.8	0	N/A
C2	complement component 2 (within H-2S)	0	1.23	0	N/A
Ccnb2	cyclin B2	0	-1.06	0	N/A
Cd209b	CD209b antigen	0	-1.2	0	N/A
Cd24a	CD24a antigen	0	-1.01	0	N/A
Cd55	CD55 antigen	0	-1.07	0	N/A
Cdkl1	cyclin-dependent kinase-like 1 (CDC2-related ki0se)	0	-0.89	0	N/A
Cebpb	CCAAT/enhancer binding protein (C/EBP), beta	0	0.92	0	N/A
Cers6	ceramide synthase 6	0	0.96	0	N/A
Cfb	complement factor B	0	2.02	0	N/A
Ctsc	cathepsin C	0	1.29	0	N/A
Ctse	cathepsin E	0	-0.99	0	N/A
Cxcl9	chemokine (C-X-C motif) ligand 9	0	2.7	0	N/A
Depdc1a	DEP domain containing 1a	0	-1.26	0	N/A
Ear1	eosinophil-associated, ribonuclease A family, member 1	0	-2.31	0	N/A
Etnk1	ethanolamine kinase 1	0	1.06	0	N/A
Fam26f	family with sequence similarity 26, member F	0	1.55	0	N/A
Fbln5	fibulin 5	0	-1.05	0	N/A
Gas6	growth arrest specific 6	0	-0.86	0	N/A
Gbp2b	guanylate binding protein 2b	0	2.42	0	N/A
Gbp3	guanylate binding protein 3	0	1.69	0	N/A
Gbp4	guanylate binding protein 4	0	2.36	0	N/A
Gbp7	guanylate binding protein 7	0	1.98	0	N/A
Gbp8	guanylate-binding protein 8	0	1.29	0	N/A
Gdap10	ganglioside-induced differentiation-associated-protein 10	0	1.79	0	N/A
Glipr2	GLI pathogenesis-related 2	0	1.13	0	N/A
Gm19763	predicted gene, 19763	0	1.23	0	N/A
Gm614	predicted gene 614	0	0.87	0	N/A
Gm7609	predicted pseudogene 7609	0	1.35	0	N/A

Symbol	Name	Herbivac	MVA	nLSDV	Herbivac-nLSDV ratio
Hemgn	Hemogen	0	-1	0	N/A
Hmbs	hydroxymethylbilane synthase	0	-0.88	0	N/A
Hmgcs2	3-hydroxy-3-methylglutaryl-Coenzyme A synthase 2	0	-1.23	0	N/A
Hpse	Heparanase	0	1.25	0	N/A
Hsh2d	hematopoietic SH2 domain containing	0	1.26	0	N/A
Hsp90ab1	heat shock protein 90 alpha (cytosolic), class B member 1	**0**	**0**.97	**0**	**N/A**
Hspa8	heat shock protein 8	0	1	0	N/A
Hsph1	heat shock 105kDa/110kDa protein 1	0	1.23	0	N/A
Ifi27	interferon, alpha-inducible protein 27	0	-0.97	0	N/A
Igfbp3	insulin-like growth factor binding protein 3	0	-1.43	0	N/A
Igtp	interferon gamma induced GTPase	0	1.8	0	N/A
Il33	interleukin 33	0	0.84	0	N/A
Irf1	interferon regulatory factor 1	0	1.3	0	N/A
Irgm2	immunity-related GTPase family M member 2	0	1.39	0	N/A
Itk	IL2 inducible T cell kinase	0	0.74	0	N/A
Keap1	kelch-like ECH-associated protein 1	0	0.89	0	N/A
Kel	Kell blood group	0	-1.16	0	N/A
Klf1	Kruppel-like factor 1 (erythroid)	0	-0.8	0	N/A
Lrat	lecithin-retinol acyltransferase (phosphatidylcholine-retinol-O-acyltransferase)	0	-1.34	0	N/A
Ly6e	lymphocyte antigen 6 complex, locus E	0	1.09	0	N/A
Marco	macrophage receptor with collagenous structure	0	-1.04	0	N/A
Mgst3	microsomal glutathione S-transferase 3	0	-0.92	0	N/A
Mid1	midline 1	0	1.08	0	N/A
Mif	macrophage migration inhibitory factor	0	1.14	0	N/A
Mrc1	mannose receptor, C type 1	0	-1.17	0	N/A
Ms4a6c	membrane-spanning 4-domains, subfamily A, member 6C	0	1.39	0	N/A
Msh3	mutS homolog 3 (E. coli)	0	0.93	0	N/A
N4bp1	NEDD4 binding protein 1	0	0.92	0	N/A
0a25	N(alpha)-acetyltransferase 25, NatB auxiliary subunit	0	1.16	0	N/A
Nlrc5	NLR family, CARD domain containing 5	0	2.1	0	N/A
Nxpe2	neurexophilin and PC-esterase domain family, member 2	0	-1	0	N/A
Ogfr	opioid growth factor receptor	0	1.27	0	N/A
Pfkfb3	6-phosphofructo-2-kinase/fructose-2,6-biphosphatase 3	0	1.12	0	N/A
Pigq	phosphatidylinositol glycan anchor biosynthesis, class Q	0	-0.9	0	N/A
Pkhd1l1	polycystic kidney and hepatic disease 1-like 1	0	-1.01	0	N/A
Ppa1	pyrophosphatase (inorganic) 1	0	1.9	0	N/A

Symbol	Name	Herbivac	MVA	nLSDV	Herbivac-nLSDV ratio
Ppm1k	protein phosphatase 1K (PP2C domain containing)	0	1.03	0	N/A
Prg2	proteoglycan 2, bone marrow	0	-1.58	0	N/A
Psmb10	proteasome (prosome, macropain) subunit, beta type 10	0	1.34	0	N/A
Psmb9	proteasome (prosome, macropain) subunit, beta type 9 (large multifunctio0l peptidase 2)	0	1.1	0	N/A
Rhd	Rh blood group, D antigen	0	-0.91	0	N/A
Sepw1	selenoprotein W, muscle 1	0	0.93	0	N/A
Slc7a11	solute carrier family 7 (cationic amino acid transporter, y+ system), member 11	**0**	**0**.93	**0**	**N/A**
Smchd1	SMC hinge domain containing 1	0	1.27	0	N/A
Socs1	suppressor of cytokine sig0ling 1	0	1.65	0	N/A
Sp110	Sp110 nuclear body protein	0	1.21	0	N/A
Stat1	signal transducer and activator of transcription 1	0	1.76	0	N/A
Tfrc	transferrin receptor	0	-0.8	0	N/A
Tlcd1	TLC domain containing 1	0	-0.78	0	N/A
Tlr11	toll-like receptor 11	0	-1	0	N/A
Tmem120b	transmembrane protein 120B	0	-0.84	0	N/A
Tnf	tumor necrosis factor	0	1.15	0	N/A
Trim25	tripartite motif-containing 25	0	1.08	0	N/A
Ubr4	ubiquitin protein ligase E3 component n-recognin 4	0	1.18	0	N/A
Vps54	vacuolar protein sorting 54 (yeast)	0	1.1	0	N/A
Vwa5a	von Willebrand factor A domain containing 5A	0	1.02	0	N/A
Wars	tryptophanyl-tRNA synthetase	0	1.37	0	N/A
Fcer2a	Fc receptor, IgE, low affinity II, alpha polypeptide	0	-1.64	-1.21	0
Gbp5	guanylate binding protein 5	0	2.59	1.04	0
Gbp9	guanylate-binding protein 9	0	1.91	1.03	0
Irg1	immunoresponsive gene 1	0	1.31	1.01	0
Zcchc2	zinc finger, CCHC domain containing 2	0	1.53	1.05	0
Lilrb4	leukocyte immunoglobulin-like receptor, subfamily B, member 4	0	0	1.25	0

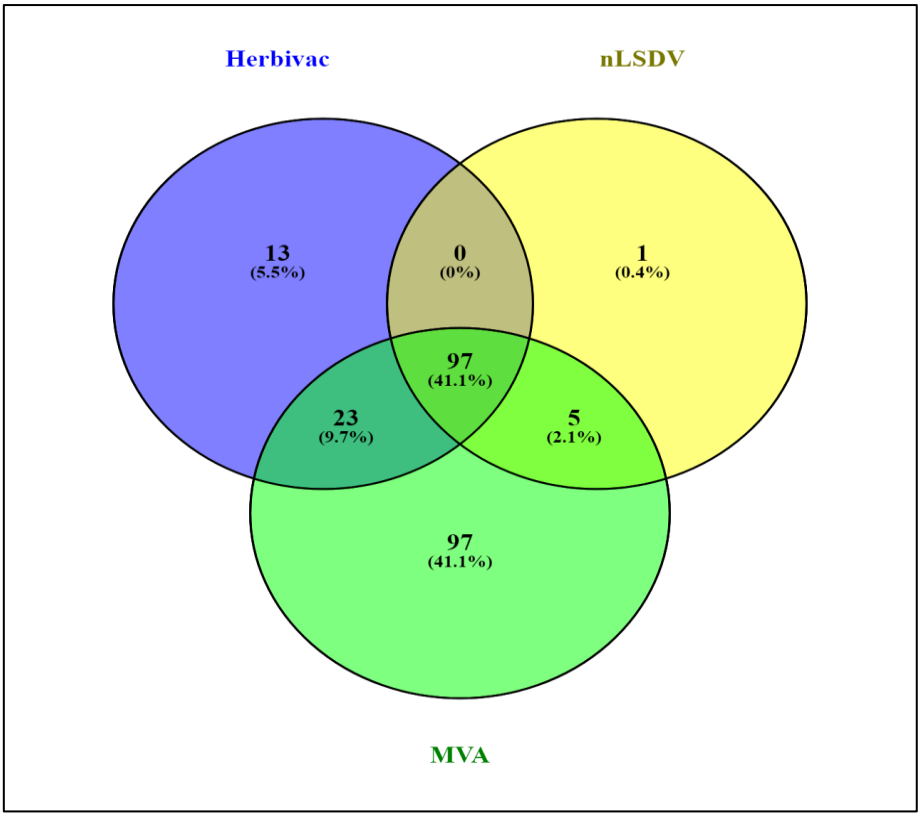

Figure 2.2. Venn diagram showing uniquely differentially regulated transcripts in response to infection with Herbivac, nLSDV and MVA. In each circle, the numbers of differentially expressed genes are indicated. The numbers inscribed inside the blue, yellow and green circles show the number of genes uniquely up/down regulated in response to Herbivac, nLSDV and MVA respectively. The intersections show the numbers of genes that were differentially expressed in response to two or three viruses.

Where Herbivac and nLSDV caused differential expression of host genes in common the level of upregulation was, in general, higher after infection with Herbivac than with nLSDV, but the significance of this is not clear (Figures 2.1 and 2.2).

Herbivac and nLSDV both upregulated genes associated with the immune response. Three clusters based on the function of the differentially expressed genes were constructed (figures 2.3 and 2.4). Immune related genes were similarly regulated by both viruses (Herbivac and nLSDV) (figure 2.3). Herbivac downregulated two immune related genes (*Olfr430* and *Fcamr*) whilst nLSDV infection was associated with downregulation of one gene only (*Fcer2a*) (Figure 2.3).

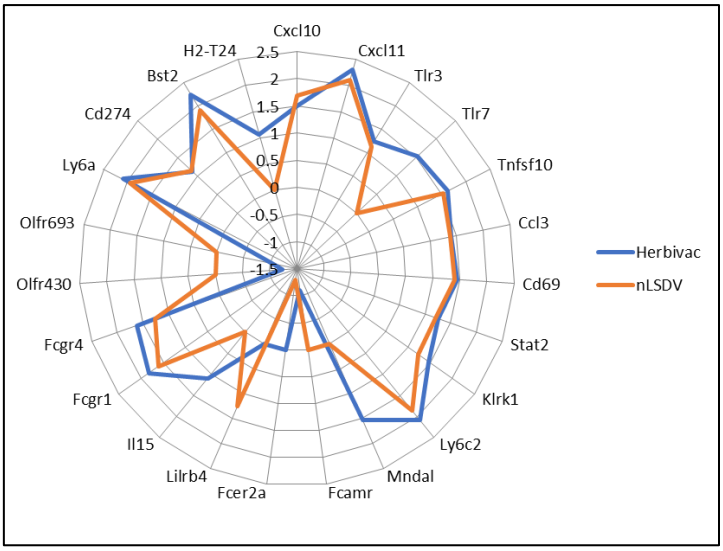

Figure 2.3. Radial plot showing differences in the level of expression of immune system related genes. This radial plot shows genes whose $\log_2$ fold change was > 1 (upregulated) and <1 (downregulated). Genes that were not significantly up/down regulated were assigned 0.

Genes associated with an interferon response, pathogen recognition receptors and cell death were identified. Again, Herbivac and nLSDV induced the upregulation of the same host genes, although Herbivac infection appeared to upregulate the equivalent genes to a greater degree than nLSDV (figure 2.4). The significance of this difference was not ascertained. Thirty-six genes were differentially expressed after Herbivac infection only (table 2.2). Interferon related genes - *Ifitm3, Iigp, Il15, F830016B08Rik, Gm 1966, Gm 6548, Nmi, Gm6637* and *A530099119Rik* were only upregulated after Herbivac infection and not nLSDV (figure 2.4A). The trend of regulation was also consistent between Herbivac and nLSDV for pathogen pattern recognition. Only one gene -*Trim 21* - was upregulated in response to Herbivac alone (Table 2.2 and figure 2.4B)). Genes of the Pyrin and HIN domain (Pyhin), Pyrin Domain Containing (*Pydc*), Interferon 1 (*Irf 1*) and Oas (2'-5'-oligoadenylate synthetase 1) families appeared more highly upregulated following inoculation with Herbivac compared to nLSDV (Figure 2.4B). The statistical significance of these differences were not ascertained.

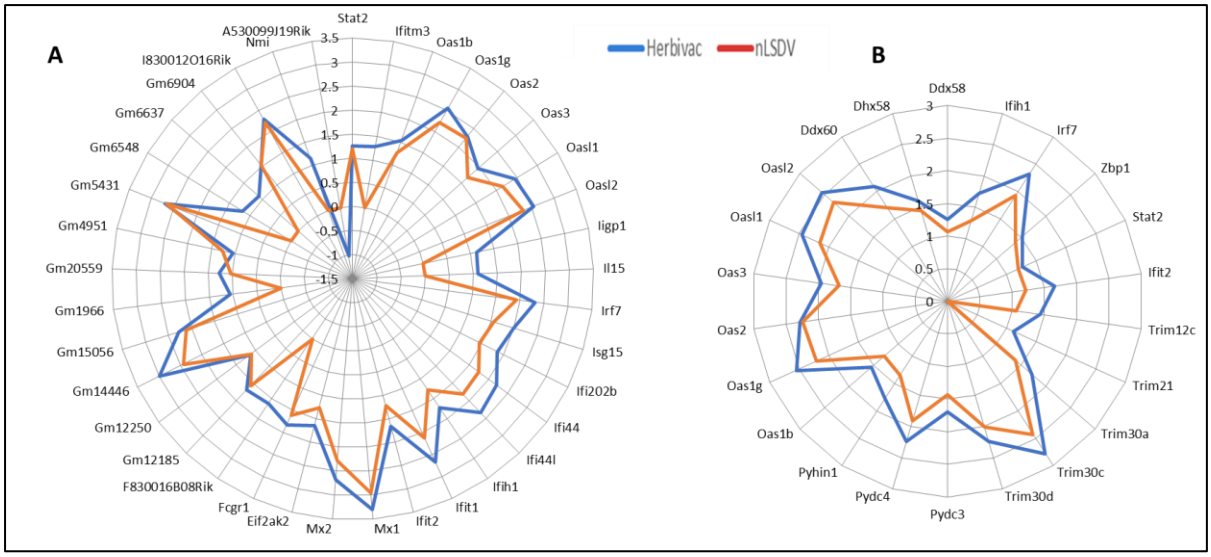

Figure 2.4 Radial plot showing differences in the level of expression of (A) interferon related genes and (B) genes involved in pathogen pattern recognition. This radial plot shows those genes with a $\log_2$ fold change > 1 (upregulated) and <1 (downregulated). Genes that were not significantly up/down regulated were assigned 0.

The most striking difference between Herbivac and nLSDV was the upregulation of two genes associated with cell death, *Parp 9* ($\log_2$ FC of 1.1) and *Gzma* ($\log_2$ FC of 1.93) by Herbivac only and not nLSDV (Figure 2.5).

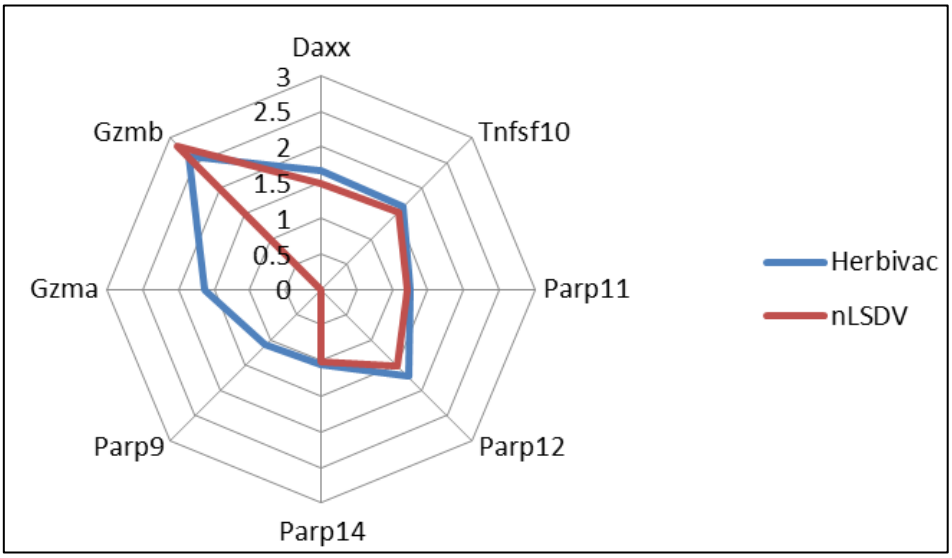

Figure 2.5 Radial plot showing differences in the level of expression of genes related to cell death. The genes shown in this radial plot were upregulated with a $\log_2$ fold change > 1 and downregulated with a $\log_2$ fold change of <1. Genes that were not significantly up/down regulated were assigned 0.

The genes uniquely dysregulated by nLSDV or Herbivac infection are listed in table 2.2.

Table 2.2 List of genes uniquely differentially expressed in response to nLSDV and Herbivac infection. Blue coded genes were downregulated, and black coded genes upregulated.

Genes uniquely differentially expressed by nLSDV		
Gene Symbol	**Gene name**	**Description**
Fcer2a	Fc receptor, IgE, low affinity II, alpha polypeptide	positive regulation of humoral immune response mediated by circulating immunoglobulin
Gbp5	guanylate binding protein 4	negative regulation of interferon-alpha production
Gbp9	guanylate-binding protein 9	cellular response to interferon-gamma
Irg1	interferon, alpha-inducible protein 27	RNA polymerase II activating transcription factor binding
Lilrb4	leukocyte immunoglobulin-like receptor, subfamily B, member 4A	integral component of membrane
Zcchc2	zinc finger, CCHC domain containing 2	phosphatidylinositol binding
Genes uniquely differentially expressed by Herbivac		
Gene Symbol	**Gene name**	**Description**
Olfr430	olfactory receptor 430	G-protein coupled receptor signalling pathway
Fcamr	Fc receptor, IgA, IgM, high affinity	adaptive immune response
Olfr693	olfactory receptor 693	G-protein coupled receptor signalling pathway
A530099J19Rik	RIKEN cDNA A530099J19 gene	
Anxa4	annexin A4	negative regulation of NF-kappaB transcription factor activity
Apol11b	apolipoprotein L 11b	
Ascc3	activating signal cointegrator 1 complex subunit 3	cell proliferation
Atp10a	ATPase, class V, type 10A	nucleotide binding
AW112010	expressed sequence AW112010	
Epsti1	epithelial stromal interaction 1 (breast)	
F830016B08Rik	RIKEN cDNA F830016B08 gene	cellular response to interferon-beta
Gm1966	predicted gene 1966	
Gm6548	predicted gene 6548	
Gm6637	predicted gene 6637	
Gzma	granzyme A	apoptotic process
H2-T24	histocompatibility 2, T region locus 24	antigen processing and presentation of peptide antigen via MHC class I
Ifitm3	interferon induced transmembrane protein 3	type I interferon signalling pathway
Iigp1	interferon inducible GTPase 1	cellular response to interferon-beta
Il15	interleukin 15	interleukin-15-mediated signalling pathway
Lgals3bp	lectin, galactoside-binding, soluble, 3 binding protein	

Gene Symbol	Gene name	Description
Lgals9	lectin, galactose binding, soluble 9	negative regulation of interferon-gamma production
Lgmn	legumain	cysteine-type endopeptidase activity
Mndal	myeloid nuclear differentiation antigen like	negative regulation of cell growth
Nampt	nicotinamide phosphoribosyltransferase	NAD biosynthetic process
Nmi	N-myc (and STAT) interactor	cellular response to interferon-gamma
Nt5c3	5'-nucleotidase, cytosolic III	transferase activity
Parp9	poly (ADP-ribose) polymerase family, member 9	double-strand break repair
Pkib	protein kinase inhibitor beta, cAMP dependent, testis specific	cAMP-dependent protein kinase inhibitor activity
Rsad2	radical S-adenosyl methionine domain containing 2	CD4-positive, alpha-beta T cell activation
Slfn3	schlafen 3	negative regulation of cell proliferation
Stxbp3a	syntaxin binding protein 3	cellular response to interferon-gamma
Gene Symbol	**Gene name**	**Description**
Tlr7	toll-like receptor 7	toll-like receptor 7 signalling pathway
Tmem184b	transmembrane protein 184b	transporter activity
Trim21	tripartite motif-containing 21	negative regulation of NF-kappaB transcription factor activity
Tspo	translocator protein	negative regulation of tumor necrosis factor production

2.3.2 Host processes and pathways activated by Herbivac and nLSDV.

The clustering of genes based on molecular function was done manually using knowledge of the genes and their function (Figures 2.3 - 2.5). However, a curated database exists where gene ontology terms have been defined. The gene lists were analysed on a gene ontology server (MGI) and gene ontology (GO) processes associated with the gene lists were elucidated. Both Herbivac and nLSDV shared 58 GO processes (Figure 2.6) with 16 processes being unique to Herbivac and eight to nLSDV (Table 2.3). Processes that involve pattern recognition receptors were identified. These pathways were however common between Herbivac and nLSDV infection. Since most biological processes were similar, emphasis was put on dissimilar processes.

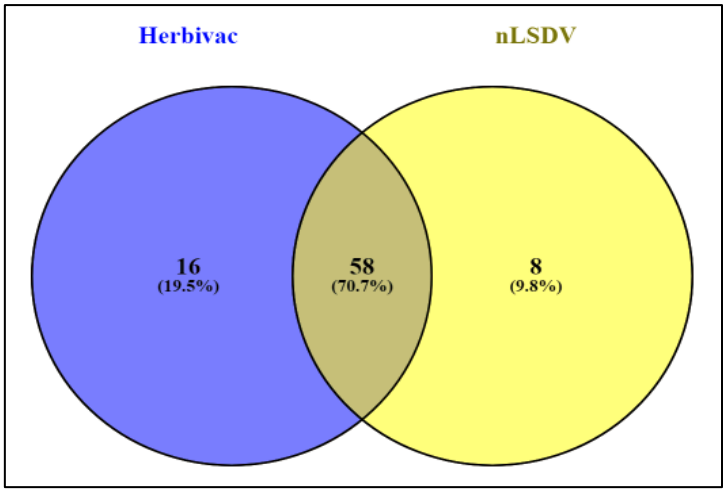

Figure 2.6 Venn diagram showing GO processes associated with Herbivac and nLSDV. In each circle, the number of differentially expressed processes are shown. The number inscribed inside the blue and yellow circles show the number of processes uniquely up/down regulated in response to Herbivac and nLSDV respectively. The intersection shows the number of processes that were upregulated in response to both viruses. Only processes showing a p value of < 0.05 are shown.

Herbivac infection was associated with immune response regulation and processes relating to apoptosis (table 2.3). Of interest was the large number of processes related to cell death, immune response and interferon response that were activated following Herbivac infection compared to those activated following nLSDV infection. nLSDV surprisingly had GO processes that pointed towards a bacterial infection such as response to lipopolysaccharide and responses to stimuli of bacterial origin. This was an unexpected finding as the virus used to inoculate these animals was tested for bacterial contamination by streaking viral stocks on Luria Agar. No contamination was detected.

Ingenuity pathway analysis (IPA) was used to analyse pathways that were activated or inhibited by the genes that were differentially regulated after infection with Herbivac or nLSDV. IPA was also used to identify biological processes; the same results that were obtained by the MGI GO annotation tool were identified (results not shown). Pathway analysis revealed that the two viruses affected the same pathways (Figure 2.7 and 2.8). Fourteen pathways were affected by both Herbivac and nLSDV (Figures 2.7 and 2.8). Pathway analysis revealed that the genes involved in the interferon response were similar after the two viral infections further supporting results presented in Figure 2.4. The number of differentially expressed genes affecting a pathway were expressed as a fraction of the total number of genes involved in that particular pathway and presented as a ratio (orange line in Figures 2.7 and 2.8). The ratio of genes involved in PRRs, death receptor signalling, and apoptosis signalling were similar for the two viral infections, again showing that the two viruses induced the differential expression of the

same genes and consequentially, the same pathways. No pathway was shown to be downregulated.

Table 2.3 Summary of processes unique to nLSDV AND Herbivac. The gene lists were used to determine processes likely to be affected by nLSDV and Herbivac infection. Processes exclusive to nLSDV or Herbivac are listed.

Herbivac	nLSDV
1. type I interferon biosynthetic process	1. cellular response to interferon-gamma
2. interferon-alpha biosynthetic process	2. cellular response to organic substance
3. regulation of interferon-alpha biosynthetic process	3. cellular response to biotic stimulus
4. toll-like receptor signaling pathway	4. cellular response to lipopolysaccharide
5. pattern recognition receptor signaling pathway	5. response to lipopolysaccharide
6. regulation of interferon-gamma production	6. cellular response to molecule of bacterial origin
7. interferon-gamma production	7. response to molecule of bacterial origin
8. interferon-beta biosynthetic process	8. regulation of multi-organism process
9. regulation of interferon-beta biosynthetic process	
10. positive regulation of apoptosis	
11. positive regulation of programmed cell death	
12. positive regulation of cell death	
13. immune response-activating signal transduction	
14. positive regulation of chemokine production	
15. immune response-regulating signaling pathway	
16. negative regulation of cytokine production	

The activation scores indicated by the colour of the bars (orange – upregulation, blue for downregulation and grey for unknown activation status), were very similar following Herbivac and nLSDV infection. Herbivac and nLSDV infection had the same activation score for pathways involved in pathogen recognition receptors in recognition of viruses and bacteria, interferon signalling, death receptor signalling and retinoic acid mediated apoptosis signalling. Only UVA induced MAPK signalling was activated following Herbivac infection and unknown following nLSDV infection (Figures 2.7 and 2.8).

The number of pathways unique to Herbivac were greater than those unique to nLSDV (Table 2.4), again suggesting that Herbivac causes an elevated host response in mice compared to nLSDV. Pathways unique to Herbivac are those involved in metabolism and immunity whereas those unique to nLSDV infection were involved in the immune response only. No information on the activation level (denoted by an orange colour) was associated with these unique pathways. It is therefore impossible to infer whether there was upregulation or downregulation

of these pathways. This pattern of activation was noticed for most of the pathways that were identified by IPA (grey bars in Figures 2.7 and 2.8).

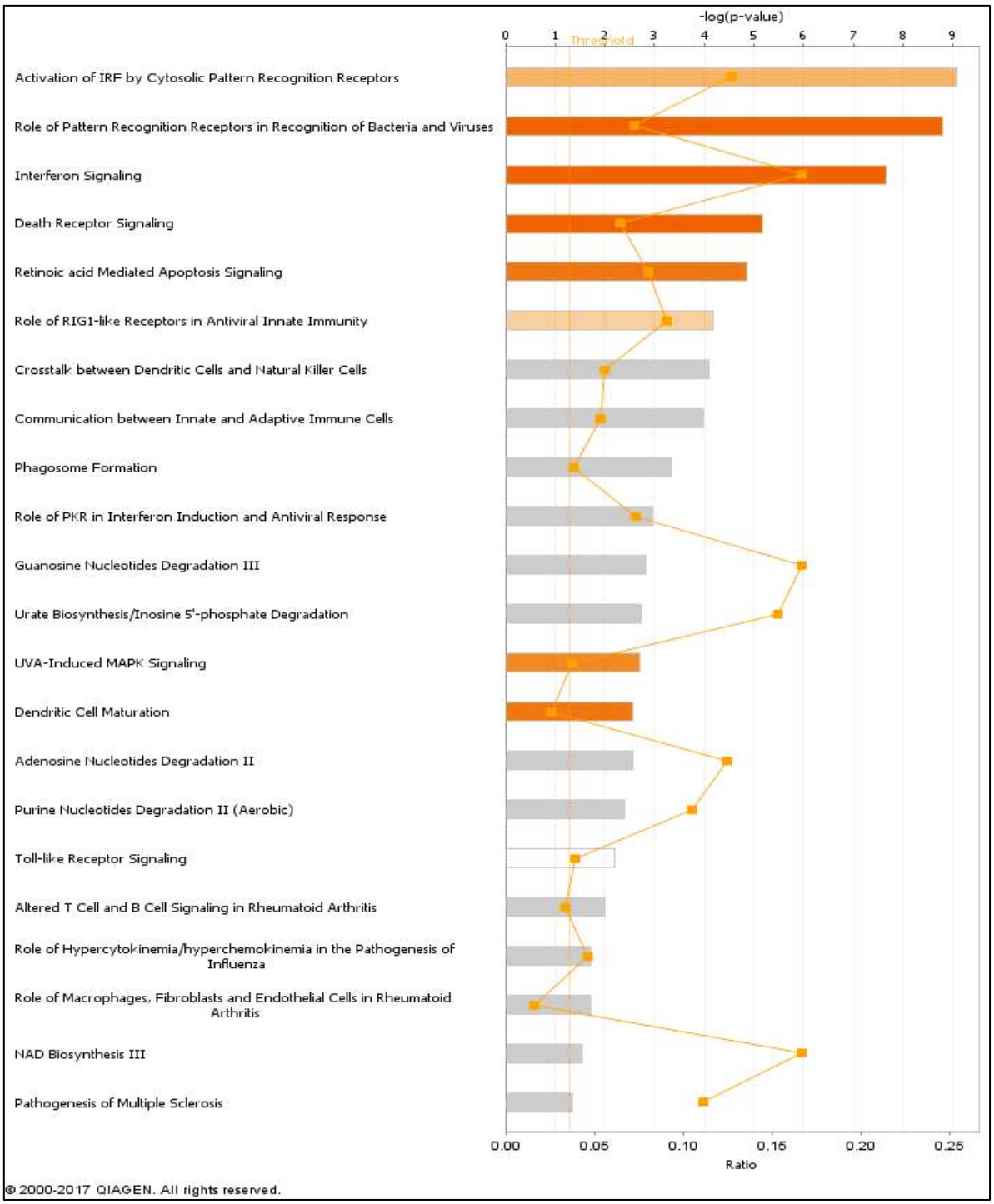

Figure 2.7 Graphical presentation of top canonical pathways intercepting with genes affected by Herbivac infection. The Z score uses the fold change to compute whether a pathway is upregulated (activated) ORANGE or unknown GREY. No pathways were downregulated. The ratio (orange line) presents the number of genes identified from the experimental gene lists in relation to the total number of genes involved in that pathway. The inverted (–log scale) shows the level of significance with molecules having a low p value having the highest –log values.

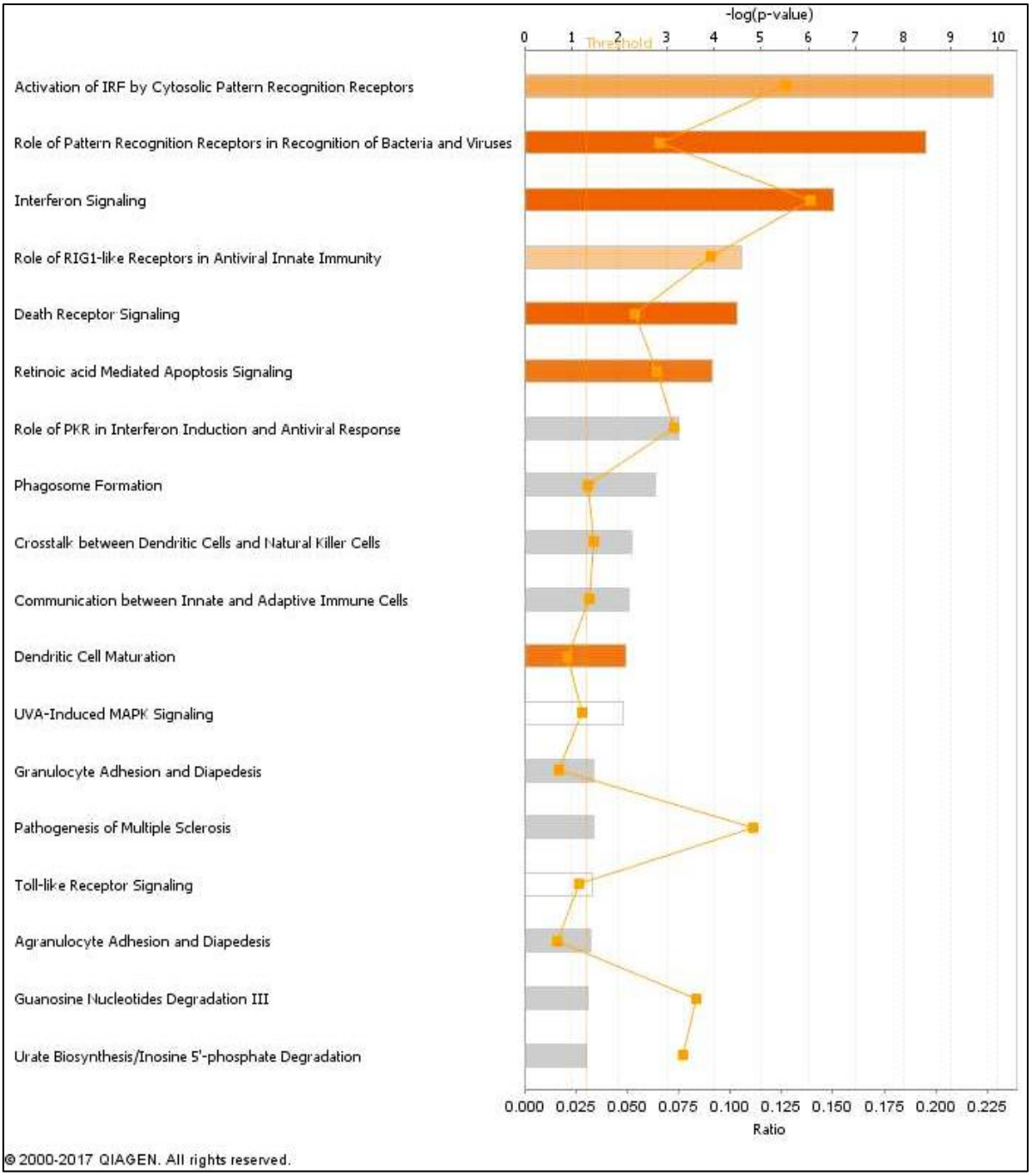

Figure 2.8 Graphical presentation of top canonical pathways intercepting with genes affected by nLSDV infection. The Z score uses the fold change to compute whether a pathway is upregulated (activated) ORANGE or unknown GREY. No pathways were downregulated. The ratio (orange line) presents the number of genes identified from the experimental gene lists in relation to the total number of genes involved in that pathway. The inverted (–log scale) shows the level of significance with molecules having a low p value having the highest –log values.

Table 2.4. Summary of pathways unique to nLSDV AND Herbivac. The gene lists were used to determine pathways likely to be affected in response to nLSDV and Herbivac infection.

Herbivac	nLSDV
1. Adenosine Nucleotides Degradation II 2. Purine Nucleotides Degradation II (Aerobic) 3. Altered T cell and B cell signalling in Rheumatoid Arthritis 4. Role of hypercytokinemia and hyperchemokinemia in influenza 5. Role of macrophages fibroblasts and endothelial cells in rheumatoid arthritis 6. NAD biosynthesis IIII	1. Granulocyte Adhesion and Diaspedisis 2. Agranulocyte Adhesion and Diaspedisis

2.4 Discussion

Whole gene expression profiling using microarrays provides a systematic approach to understanding virus host interactions. To date, no study has been done to compare the host transcriptome after infection with nLSDV and Herbivac. Host gene expression was analysed in mouse spleens 24 hours post infection. Compared to the PBS control, nLSDV and Herbivac induced differential expression of 97 genes in common, largely related to response to viral infection, and which have been shown in other poxvirus studies (Offerman et al., 2015, Royo et al., 2014). nLSDV infection resulted in the differential expression of 6 unique genes and Herbivac infection resulted in the differential expression of 36 unique genes. MVA and Herbivac both induced differential expression of 23 genes whereas nLSDV and MVA both induced differential expression of 5 genes (Figure 2.2). In comparison, Herbivac and not nLSDV could thus perform slightly more similar to the greatly documented MVA.

There were more upregulated genes following all viral infections than downregulated genes which is most likely due to the non-permissive nature of the infection. In a non-permissive host, some viral proteins may not be able to target host antiviral machinery as they do in a permissive host. The antiviral K3L genes from the three different capripoxviruses have been shown to

inhibit PKR (a host sensor of viral double stranded RNA) differently depending on the host. These differences may play a role in determining host range (Park and Peng, 2018). Guerra et al. (2003) showed that after VV infection, almost 90% of the host transcripts were downregulated compared to mock controls, maybe due to the permissive nature of infection (Guerra et al., 2003). Also, in this study Guerra et al. (2003) looked at 6 and 10 hours post infection in HeLa cells which is unlike this study that was done *in vivo* after 24 hours. Looking at earlier time points may therefore be informative but due to the non-permissive nature of infection this remains only speculative. In another study, in HeLa cells as well, MVA was shown to induce a distinct gene profile with induction of genes involved in cell structure (Guerra et al., 2004). Such genes were not detected in this study, possibly because of the nature of target cells in the spleen. Most of the genes that were differentially expressed after MVA infection were associated with an immune response. This is not unique to this study as Guerra et al. (2004) showed that infection with MVA caused differential expression of 20 transcripts associated with cytokines, members of the tumour necrosis factor and Nuclear kappa B family (Guerra et al., 2004).

Offerman et al. (2015) investigated the host gene expression profile of mice that were infected intravenously with Herbivac, Canarypoxvirus (CNPV), Fowlpox virus (FWPW), MVA and two novel Avipoxviruses. Herbivac was shown to induce upregulation of 463 genes and induce downregulation of 85 genes. In that experiment MVA induced the increased expression of 299 genes and downregulation of 177 genes (Offerman et al., 2015). This also supports findings in the present study which demonstrated that LSDV induced mainly upregulation as opposed to downregulation of genes.

Genes that were differentially expressed which were associated with an enrichment of specific processes and pathways are discussed below. Although Herbivac uniquely upregulated the expression of activating signal cointegrator 1 complex subunit 3 (*Ascc3*), which is important for cell proliferation (Dango et al., 2011), Herbivac also upregulated a negative regulator for cell proliferation schlafen 3 (*Slfn 3*) (reviewed by Mavrommatis et al. (2013)). Whether the upregulation of Ascc3 contributed to the cell proliferation observed (chapter 3, figure 3.29) is not known. There was no enrichment of processes relating to proliferation.

Toll-like receptor (TLR)

TLRs are part of the antiviral sensing mechanism (as reviewed in section 1.5). TLRs are important in evoking immune effector responses with TLRs 3, 4, 7, 8 and 9 playing a role in the induction of type 1 interferons (Kawai and Akira, 2006). TLRs 3 and 7 were induced following Herbivac infection whereas only TLR3 was induced following nLSDV infection in mice. TLR3 activation is mediated by dsRNA which is abundantly present during the bidirectional RNA transcription of different DNA strands or as an intermediary product in DNA replication (Thompson et al., 2011, Weber et al., 2006, Kawai and Akira, 2006). DsRNA is a potent activator of the innate antiviral immune system (Weber et al., 2006). TLR7 is located inside the cell in the endosomal compartment where it senses ssRNA (Petes et al., 2017) and is critical to the induction of a potent innate immune response. TLR7 can cooperate with other antiviral mechanisms like RIG 1 (Szabo et al., 2014). TLR7 induction leads to the production of proinflammatory cytokines (Petes et al., 2017). TLRs 3,7,8 and 9 are found mostly inside the cell and it would be logical to find TLRs 3 and 7 upregulated following a poxviral infection (reviewed by (Buonaguro et al., 2011).

Signalling via the TLR pathway is important in dendritic cell maturation which is indispensable for B lymphocyte activation. TLR signalling has been linked to both IgM and IgG secretion (Pasare and Medzhitov, 2005) as well as the consequent induction of inflammatory cytokines like TNF-β, IL-1β, IL-6 and IL-12 (reviewed by Buonaguro et al. (2011). The ability of Herbivac to induce the activation and upregulation of two Toll like receptor genes (*Tlr 3* and *7*) leads one to speculate that the interferon response would be greater after Herbivac than nLSDV which only induced the upregulation of *Tlr 3.* This is supported by the finding that there were more interferon related processes induced after infection with Herbivac compared to nLSDV (Table 2.3).

Interferon

The induction of pathogen pattern recognition receptors like TLRs is important in the development of an interferon response (Kawai and Akira, 2008). Both vaccine strains, Herbivac and nLSDV, influenced the upregulation of several genes involved in pathogen pattern recognition and the interferon response (Figure 2.4). Both Herbivac and nLSDV induced the same profile of interferon related pathways (Figure 2.7 and 2.8). The number of differentially regulated genes involved in the IFN response was higher in mice infected with

Herbivac (37 genes) compared to those induced by nLSDV (28 genes) (Figures 2.4). A study comparing the transcriptome of macrophages infected by a panel of different poxviruses showed that MVA induced a strong interferon response (Royo et al., 2014). This may be why MVA is widely used successfully as a vaccine vector (Pavot et al., 2017) and a vaccine (Volz and Sutter, 2017). Though both LSDVs induced a strong IFN response, and will potentially perform well as vaccines/vectors, because Herbivac induced expression of more IFN related genes it could possibly perform better as a vaccine/vector.

IFN activation has been shown to increase the ability of macrophages to phagocytose (Royo et al., 2014). Both virus infections were associated with the upregulations of ISG15 which has been shown to be a potent interferon stimulated gene with potent antiviral activity (Yángüez et al., 2013). ISG15 can bind viral proteins directly and has been associated with *in vitro* activation of macrophages and reduction of vaccinia virus titre (Baldanta et al., 2017). Since both nLSDV and Herbivac upregulated this potent ISG they are likely to activate macrophages leading to an elevated antiviral response. It can thus be inferred that when used as a vector, LSDV can lead to the phagocytosis of the heterologous antigen being expressed by the viral vaccine, leading to subsequent major histocompatibility class presentation.

Of note Herbivac and not nLSDV infection induced the expression of *Trim 21*. Though there have been conflicting reports regarding its role, its expression has been associated with a modest increase in IFN β production (Yángüez et al., 2013). Trim 21 was shown to lead to about 20% increase in IFN-β production in dendritic cells stimulated by different immunogens (Zhang et al., 2013). The mechanism of action of Trim 21 is that it binds the antiviral DNA sensor DDX41 causing its ubiquitination and subsequent degradation. The effect is that DDX41 will not be able to detect DNA (Yángüez et al., 2013). It appears the virus hijacks this regulatory mechanism to evade PRRs like DDX41.

Querec et al. (2009) showed that the immunogenic and successful yellow fever vaccine (YF-17D) had a gene signature with a high predictive value of an effective immune response. Their study identified most of the antiviral, immune system and interferon genes that were differentially expressed in our vaccinated mice. These genes included *Oas1-3, Tlr7, DDX58, Ifihi, Cxcl10, DHX58, Eif2ak2*, and *Mx1*. The response was predictive of a CD8+ T cell response. It can therefore be inferred that both nLSDV and Herbivac would induce a strong T cell response. The MVA control has been associated with the induction of interferon induced proteins (IFIT1 and ISG15) which were also upregulated in the present study (Guerra et al.,

2007) which increase confidence in the results of this study. The same study by Guerra et al. (2007) also showed that MVA infection was associated with the differential expression of OASL, RIG 1 and MDA5.

Immune response

The immune response is regulated largely by type 1 IFN genes (Trinchieri, 2010). Both nLSDV and Herbivac induced the upregulation of very similar genes associated with the innate immune response (Figure 2.3). A few transcripts were uniquely regulated by Herbivac which included interleukin 15 (*Il15*) and *Tlr7* (Table 2.2). Il15 is a cytokine produced by monocytes and macrophages in response to viral infection and causes proliferation of natural killer cells (Mak and Saunders, 2006, Ekmekcioglu et al., 2008, Verbist et al., 2012). This interferon related cytokine was upregulated after Herbivac infection only (Table 2.2). A multivalent influenza protein expressed by vaccinia virus which also expresses Il15 was shown to induce T cells and consequently protect animals against lethal challenge (Valkenburg et al., 2014).

A few transcripts were downregulated after infection with Herbivac and these included olfactory receptors (*Olfr430* and *Olfr693*) and Fc IgA, IgM, high affinity receptor (*Fcamr*). Of the Fc receptors, IgE low affinity II and alpha polypeptide (*Fcer2a)* was downregulated after nLSDV infection. Downregulation of *Fcamr* has been previously reported (Offerman et al. (2015). MVA and Herbivac downregulated *Fcamr* and all 6 poxviruses (CNPV, FeP2, FWPV, PEPV, Herbivac and MVA) downregulated *Fcer2a* in their experiment. Fc receptors are important in the humoral immune response (Sun, 2014). Binding of an immunoglobulin to Fc receptors mediates antibody dependent cell mediated cytotoxicity which aids in killing virally infected cells (Reid et al., 2011). Downregulation of *Fcer2a* may be an immune evasion strategy employed by LSDV against the adaptive immune system. This may be desirable for a vector as it may reduce anti-vector immunity and antibody dependant enhancement of infection.

Cell death

A strong interferon and immune response leads to activation of different host antiviral mechanisms including cell death, which, is in turn inhibited by the infecting virus. Overall, Herbivac induced an increased interferon response and immune response. It is thus interesting to establish which antiviral response is either activated or inhibited by Herbivac or nLSDV to understand the role of the full-length SOD homologue on virus host interaction.

There was an increased induction of cell death related genes after Herbivac infection and consequently more cell death processes than those induced by nLSDV. The presence of necrotic nodules (sometimes known as sit-fasts which are zones of necrosis) on skin of infected animals supports the finding that LSDV infection induces cell death (Abutarbush et al., 2015). Upon histological examination of lesions on CAMs, van Rooyen et al. (1969) showed regions of necrosis on the superficial cell layer of the ectoderm. LSDV is known to encode genes that are thought to inhibit cell death in a productive infection (Kara et al., 2003). Viruses may, however, inhibit cell death in the early stages of replication to allow for maturation of the virus before dissemination (Danthi, 2016). The poxviruses MVA and NYVAC were reported to induce apoptotic cell death in HeLa cells, dendritic cells and macrophages (Guerra et al., 2006, Guerra et al., 2007, Royo et al., 2014).

The cell death related genes upregulated after Herbivac infection included the granzymes A and B (*Gzma* and *Gzmb),* Poly (ADP-ribose) polymerase (*Parp 9,11,12* and *14*), TNF-Related Apoptosis Inducing Ligand (Tnfsf10) and Death-associated protein 6 (*Daxx*). In contrast, nLSDV did not show upregulation of *Parp 9* and *Gzm A* (Figure 2.5). Upregulation of Parp has been shown to recruit nicotinamide adenine dinucleotide (NAD^+) which eventually leads to necrosis (Ha and Snyder, 1999). NAD is produced when a cell undergoes oxidative stress (Di Lisa and Ziegler, 2001). Interestingly, pathway analysis demonstrated that the NAD biosynthetic pathway was somewhat affected after Herbivac infection alone (though the activation profile was unknown; see Figure 2.7). When cleaved by caspases, Parp is known to cause the release of the apoptosis inducing factor from the mitochondria leading to cell death (Hong et al., 2006). Granzyme A is present in CD8+ CTLs and NK cells and is the most abundant granzyme. It affects apoptotic cell death by cleaving Arginine or Lysine residues. Gzma elicits a caspase independent mode of apoptosis (reviewed by Lieberman (2010).

The presence of a SOD homologue in leporipoxviruses was shown to inhibit cell death in a permissive host (Cao et al., 2002, Teoh et al., 2005, Teoh et al., 2003). Since Herbivac and nLSDV differed in only one locus, it could be inferred that LSDV SOD was playing a role in cell death. This appears to suggest that the antiviral immune response employed other means of cell death to clear Herbivac which were not engaged to eliminate nLSDV. The host may employ caspase independent programmed cell death in the presence of apoptosis inhibitors. Poxviruses are known to encode proteins from the Serpin protease family that include CrmA which inhibits caspase activity (reviewed by Nichols et al. (2017)). Thus, the host may engage

other caspase independent mechanisms like necrosis. However, since these two viruses were similar with the exception of the SOD homologue, the additional arm of cell death employed could be attributed to the presence of the full-length SOD homolog in Herbivac. Since LSDV does not replicate in mice, the full-length SOD homologue present in Herbivac could have conferred survival or inhibition of cell death which resulted in the host engaging in other forms of cell death and increasing transcripts associated with cell death.

Results from the MVA experiment were congruent to literature which shows that MVA induces apoptosis in dendritic cells (Guzman et al., 2012). Upregulation of genes involved in cell death was also observed after MVA infection. MVA had 16 genes upregulated which are important in apoptosis. Parp 1 cleavage was shown by Guerra et al. (2007) after MVA infection. This provides further confidence in the dataset that was generated by this study. However, it is important to note that due to the algorithm used, assignment of no fold change (0) could have been as a result of variations in the replicate experiment hence a p value of >0.05. Also, since only genes with an absolute change of >1 were noted, some genes whose individual expression level was not as high but whose contribution to a pathway in concert with other genes, could be significant, may have been missed or under represented by assigning 0. For comparative purposes though, and hypothesis generation, noted differences will be used as a basis for future studies.

In summary, our results showed that in a non-permissive host, Herbivac and nLSDV induced upregulation of many interferon and immune related genes but Herbivac infection resulted in expression of a unique profile of cell death related genes. Due to unique upregulation of transcripts involved in caspase independent cell death and necrosis related cell death (Gzma and Parp 9) which was associated with Herbivac, we postulate that the improved immunogenicity that is seen in cattle in Herbivac compared to nLSDV may be due to an immunogenic form of cell death linked to the presence of a full-length SOD decoy. In the following chapter, recombinant viruses in which the truncated SOD from nLSDV is knocked out or replaced with a SOD resembling SOD from Herbivac are characterised with respect to growth of virus in cell culture and eggs, histological presentation of infected CAMs, and cell death.

Chapter 3 Characterisation of the impact of the LSDV SOD homolog on viral growth, SOD activity and cell death

3.1 Introduction 85
3.2 Methods 88
3.2.1 Viruses 88
3.2.2 Alignment of different SOD homologues 89
3.2.3 Construction of transfer vectors 89
3.2.4 Generation of recombinant LSDVs with and without SOD 92
3.2.5 Preparation of LSDV stocks 96
3.2.6 Growth curves of the different LSDV viruses in cell culture 96
3.2.7 Growth curves of different LSDV viruses on chick chorioallantoic membranes (CAMs). 96
3.2.8 CAM Histology 97
3.2.9 Preparation of homogenates for SOD activity determination 97
3.2.10 Reactive Oxygen Species (ROS) assay 98
3.2.11 Apoptosis assays 99
3.2.12 Statistics 101
3.3 Results 102
3.3.1 Comparison of the LSDV SOD homologue amino acid sequences 102
3.3.2 Construction of transfer vectors to insert an improved SOD gene into LSDV and to delete SOD in LSDV 104
3.3.3 Isolation of recombinant viruses 108
3.3.4 Growth of parent LSDV vaccines and recombinants in cell culture. 115
3.3.5 Growth of vaccines and recombinants on CAMs 116
3.3.6 Histopathology of CAMs infected with viruses 118
3.3.7 Effect of the LSDV SOD homologues on activity of cellular SOD activity 122
3.3.8 Induction or inhibition of apoptosis / necrosis by viruses 123
3.4 Discussion 127

List of Figures

Figure 3.1. Schematic of the generation of a recombinant poxvirus via homologous recombination. 87

Figure 3.2. Diagram showing the binding sites of primers.....90

Figure 3.3. Schematic showing how homologous recombination can occur between the transfer vector pHM1 and viral DNA of nLSDV to generate nLSDVdSOD-M.. 92

Figure 3.4. Diagram to show strategy of insertion of SODis and mCherry into nLSDVdSOD-M to generate nLSDVSODis-M. 93

Figure 3.5. Mechanism of the SOD determination kit..98

Figure 3.6. Mechanism of the cell death ELISA kit.. 100

Figure 3.7. Structural alignment of SOD and SOD homologues..103

Figure 3.8. Construction of transfer vector pHM1.. 105

Figure 3.9. Transfer vector pHM1.. 105

Figure 3.10. Insert DNA sequence synthesised and ligated into a pUC57-Simple vector. ...106

Figure 3.11. Plasmid map of transfer vector to insert an improved SOD gene into LSDV-pHM2v3.. 107

Figure 3.12. Confirmation of pHM 2v3 by restriction enzyme digestion. 107

Figure 3.13. Transient expression of GFP following infection with nLSDV and transfection with pHM1 108

Figure 3.14. A - Diagram to show primer binding sites and fragments they generate. 109

Figure 3.15. Appearance of MDBK cells infected with nLSDVdSOD-M recombinant.....110

Figure 3.16. Transient expression of mCherry. 111

Figure 3.17. Fluorescence microscopy of cells infected with nSDVSODis-M.. 111

Figure 3.18. Confirmation of nLSDVSODis-M by PCR analysis.. 112

Figure 3.19. A – Diagram to show primer binding sites and fragments generated from recombinants nLSDVSODis-M and nLSDVdSOD-M.. 113

Figure 3.20. A – plasmid map of transfer vectors pHM1dSOD and B - pHM1-SOD_pos used to construct nLSDVdSOD-UCT and nLSDVSODis-UCT respectively.. 114

Figure 3.21. Diagram to show primer binding sites and fragments generated from recombinants nLSDVdSOD-UCT and nLSDVSODis-UCT. 114

Figure 3.22. Appearance of MDBK cells uninfected or infected with nLSDVdSOD-UCT, nLSDVSODis-UCT or nLSDV. 115

Figure 3.23. Growth curves of nLSDV, nLSDVSODis-UCT and nLSDVdSOD-UCT in MDBK cells.. 116

Figure 3.24. Macroscopic appearance of infected chick CAMs on day 5 post infection. 117

Figure 3.25. Growth curves of nLSDV, nLSDVdSOD-UCT and nLSDVSODis-UCT on CAMs. 117

Figure 3.26. H&E staining of fixed membranes post inoculation with PBS nLSDV, Herbivac, nLSDVdSOD-M and nLSDVSODis-M. 119

Figure 2.27. H&E staining of fixed membranes 5 days post inoculation with PBS, nLSDV, nLSDVdSOD-UCT, nLSDVSODis-UCT. 120

Figure 3.28. Immune infiltration in H&E stained sections. 122

Figure 3.29. Total SOD activity.....123

Figure 3.30. Apoptotic cell death detection.. 124

Figure 3.31. Apoptotic cell death detection.. 125

Figure 3.32. Necrotic cell death detection.. 126

Figure 3.33. Apoptosis enrichment factor of HeLa S3 cells 24 h.p.i.....127

List of Tables

Table 3.1. Primers used to amplify flanking sequences of LSDV 130 and LSDV 132 and the marker genes from pRO-2. 90

Table 3.2. Primers used to detect presence of recombinant nLSDVdSOD-M. 109

Table 3.3. Histology of CAM sections 121

Chapter 3 Characterisation of the impact of the LSDV SOD homolog on viral growth, SOD activity and cell death.

3.1 Introduction

Poxvirus replication occurs in the cytoplasm (section 1.4.2) where poxviruses encode their own transcription machinery which makes it possible for viral replication and transcription to occur in specialised viral factories (Liem and Liu, 2016). When a poxvirus uncoats and DNA replication occurs, this stage can be manipulated to generate recombinant poxviruses (Yao and Evans, 2003). The knowledge of homologous recombination between the genomes of two replicating poxviruses and the subsequent finding that DNA can recombine with pox viral DNA has accelerated the generation of recombinant poxviruses (Weir et al., 1982, Sanchez-Sampedro et al., 2015).

Panicali and Paoletti (1982) first described the generation of recombinant vaccinia virus. In that study, they inserted the thymidine kinase gene from herpes simplex virus. This was made possible by the co-transfection of the thymidine kinase gene (containing vaccinia virus flanking sequences) and vaccinia virus. Other studies have successfully shown that huge inserts can be added to pox genomes owing to the large genomes of poxviruses. In one study, up to 25 kb of foreign DNA was successfully inserted into a vaccinia virus genome Recombination in vaccinia virus occurs with near to perfect accuracy and the virus remains infectious after manipulation of DNA (if essential genes are not disrupted) (Carroll and Moss, 1997, Smith and Moss, 1983). LSDV, like other poxviruses, has a large genome which replicates in the cytoplasm of permissive cells and can be manipulated in the same way as vaccinia virus.

The process of generating recombinant poxviruses makes use of a transfer vector containing the gene of interest fused with a poxvirus promoter and start codon, stop codon and a pox terminator sequence - TTTTTNT (Mackett et al., 1984, Yuen and Moss, 1987) and flanked by regions homologous to the insertion site in the poxvirus (Souza et al., 2005, Mackett et al., 1982, Wyatt et al., 2017). These flanking regions aid in homologous recombination for insertion of the gene(s) into genomic DNA during viral replication. Vaccinia virus has been shown to use as little as 12bp of homologous sequence for recombination (Yao and Evans, 2001).

To select for recombinant viruses over wild type viruses, marker and selection genes are usually inserted, either within the flanking regions of DNA or outside the flanks (Souza et al., 2005). DNA recombination occurs in the cytoplasm as the poxvirus DNA undergoes replication (Mercer et al., 2007). In this thesis, the *E. coli* xanthine (guanine) phosphoribosyltransferase (*ecoGPT*) was used as a metabolic selection marker (Boyle and Coupar, 1988). The *ecoGPT* gene encodes a phosporibosyltransferase that helps supply guanine from xanthine available in the media as a salvage pathway for guanine synthesis (Mulligan and Berg, 1981). Hence, in the presence of an antiviral agent, mycophenolic acid (MPA), which is an inhibitor of purine biosynthesis, expression of *ecoGPT* allows for the synthesis of purines from xanthine/hypoxanthine via the salvage pathway (Falkner and Moss, 1988). MPA is an antiviral agent that inhibits inosine monophosphate dehydrogenase, which catalyses the synthesis of xanthine monophosphate. The depletion of xanthine monophosphate leads to inhibition of cell growth due to lack of purine nucleotides (Falkner and Moss, 1988).

Different expression markers are useful in the selection of recombinant viruses with or without metabolic selection (Rice et al., 2011, Morrow et al., 2012). Fluorescent proteins (FPs) have been used as reporters of gene expression (Paszkowski et al., 2016, Marzook et al., 2014, Al Ali et al., 2016). GFP was isolated in 1961 and it has been used a lot in recombinant DNA technology (Shimomura, 2005). The whole structure of the fluorescent protein is key to its generation and maintenance of fluorescence (Kremers et al., 2011). Selection of recombinant viruses can therefore be done by picking fluorescent foci of cells or by cell sorting. The reporter genes eGFP and mCherry were used in this thesis. GFP absorbs at 488 nm and emits at 507nm and GFP transfected cells fluoresce within 16-24 hours post infection (Zhang et al., 1996). mCherry absorbs 587 nm and emits at 610 nm and is a useful FP due to its brightness and photo stability (Shaner et al., 2005). Figure 3.1 shows a simplified diagram of how a poxvirus recombinant is made.

To understand the role of different viral genes, mutants can be generated where the gene under investigation is deleted or reintroduced (in a revertant virus). In 1991, Blasco et al, characterised a profilin homologue by creating a knockout with *GPT* in place of profilin (Blasco et al., 1991). Similar strategies have been used to determine roles of genes and homologues (Almazan et al., 2001, Cao et al., 2002, Teoh et al., 2005, Teoh et al., 2003).

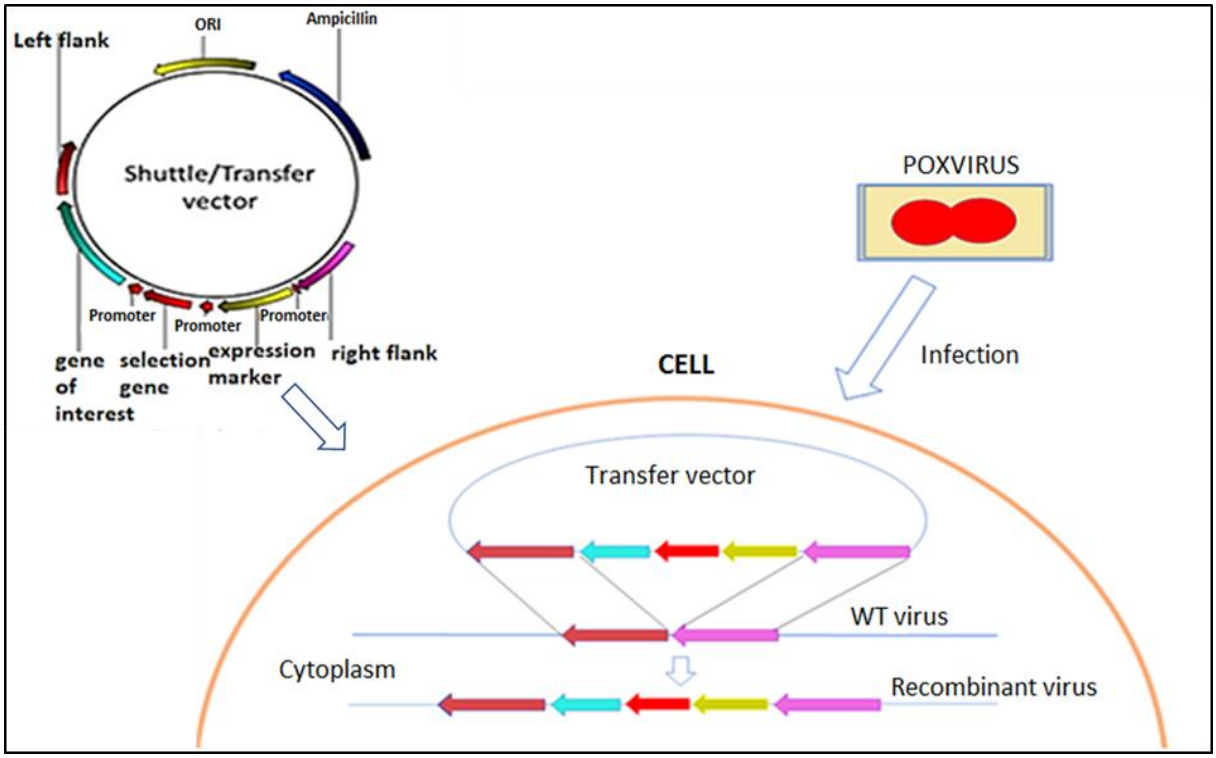

Figure 3.1. Schematic of the generation of a recombinant poxvirus via homologous recombination. Homologous recombination takes place between homologous poxviral sequences in a transfer vector and the poxviral genome. Cells are infected with a poxvirus and transfected with a transfer vector. The transfer/shuttle vector contains sequences of homology to poxvirus DNA at the site of insertion (left flank and right flank). After infection, DNA from the poxvirus replicates in the cytoplasm where homologous recombination occurs within the flanking seuqences. The transfer vector contains a cassette containing the target gene being inserted, a selection marker and an expression marker within the flanks. Expression of the target gene, as well as the marker and selection genes, is driven by a poxviral promoter.

Poxviruses express a SOD homologue which is a late protein that is packaged in the viral core (Almazan et al., 2001, Cao et al., 2002, Teoh et al., 2003) and most likely exerts its effect from the early stages of infection. SOD homologues are known to perturb the levels of the superoxide anion through interference with the activity of SOD (Cao et al., 2002, Teoh et al., 2005, Teoh et al., 2003). Hydrogen peroxide, the product of SOD catalysis has been implicated in apoptotic cell death, whereas the superoxide anion, the substrate for SOD catalysis has been noted to be pro-survival (Pervaiz and Clement, 2002a, Kumar et al., 2007). SOD homologues have been implicated in the pathogenesis of leporipoxviruses. The presence of a SOD homologue in a revertant Shope Fibroma Virus (SFV) was shown to be associated with increased diameter of lesions *in vivo*, when inoculated into rabbits. Microscopic investigation revealed that there was proliferation of fibroblasts, necrosis and leukocyte infiltration in animals infected with wild type SFV containing a SOD homologue (Teoh et al., 2005). In addition, the SOD knockout virus did not protect infected Jurkat cells from mitochondrial and Fas-associated cell death (Teoh et al., 2005). The SOD knock-out mutants resulted in increased growth capabilities in

cell culture yielding ten times more virus than the revertant virus (Cao et al., 2002, Teoh et al., 2005).

Herbivac encodes a full-length SOD homologue whereas nLSDV does not. Herbivac SOD is almost similar in size to the SOD found in the virulent field strain of LSDV (160 aa). SOD from the virulent strain has several substitution mutations when compared with nLSDV and Herbivac. There is a 1bp deletion in nLSDV and Herbivac which in nLSDV caused a frameshift mutation resulting in a truncation. SOD was put back in frame by the additional 2bp deletion in Herbivac. The 1bp deletion caused several amino acid differences (Figure 1.7). The further 2bp deletion in Herbivac SOD is the reason why it is a full-length SOD.

The objective of this chapter was to investigate if the presence of SOD had an impact on the phenotype of LSDV on infected cells or CAMs. This chapter describes the generation of recombinant viruses in which i) SOD was deleted and ii) SOD resembling that of Herbivac was reintroduced into the SOD locus. The *SOD* gene used here was modified in the region where the 2bp deletion had occurred. Careful analysis revealed that there were AT dinucleotide repeats and this region was suspected to be highly unstable. Modifications in the SOD ORF were made to make it more stable. The recombinant viruses were compared to one another as well as the parent nLSDV and Herbivac for growth in cell culture and on chorioallantoic membranes of fertilised hens' eggs (CAMs). The viruses were also compared with respect to histological changes in infected chick CAMs. The activity of cellular SOD from cell lysate derived from cells that had been infected with recombinant viruses expressing full-length SOD or the truncated SOD was also investigated.

A further objective was to characterise the apoptotic and necrotic activity of the different viruses expressing either the truncated or the full-length SOD homologue and to compare them to LSDV with SOD knocked out.

3.2 Methods

3.2.1 Viruses

The Neethling vaccine strain (nLSDV) and Herbivac were grown and titrated as described in section 2.2.1.

3.2.2 Alignment of different SOD homologues

Different SOD or SOD-like protein sequences were aligned. These included full length active SOD from humans and cow obtained from GenBank. The protein sequence of a stabilised form of SOD (section 3.3.2.2) and Herbivac (UCT), which are not available on NCBI, were deduced by translating their respective nucleotide sequences using CLC Bio (Qiagen©). SOD-like ORFs from variola virus, vaccinia virus, sheeppox virus, myxoma virus, LSDV (Neethling vaccine strain, Nl 2490, Neethling vaccine LW 1959, Herbivac and nLSDVSODis) and Amsacta Moorei entomopoxvirus were included in the alignment. The sequence of human copper chaperone CCS was also included in the alignment. The chaperone is homologous to SOD and dimerises with SOD during its activation from the apo state. The structures for bovine and human SOD were obtained from the protein databank (1SOS and 1EQ9). SOD alignment was done using the TCoffee Expresso program available on the TCoffee server. Structural alignment was done on ESPript 3.0 Server.

3.2.3 Construction of transfer vectors

3.2.3.1 Construction of transfer vector pHM1 (for generating nLSDVdSOD-M) by overlapping PCR and cloning

To delete SOD (ORF131) from nLSDV, a transfer vector was constructed (see Figures 3.3 and 3.9). This transfer vector (pHM1) contained LSDV ORFs 130 and 132 as flanking sequences, with a positive marker for selection (ecoGPT) and the eGFP marker gene placed between the flanking sequences. Overlapping PCR was used to assemble three DNA fragments into one large fragment (see Figure 3.2). The primers used for these PCR reactions are listed in Table 3.1. The three plasmids pZG1, pZG2 and pZG4 were constructed by Zek Gimbot. pZG1 and pZG2 contain LSDV ORFs 130 and 132 respectively inserted into pGEM®-T easy (Promega, USA). pZG4 contains a gene cassette of ecoGPT and eGFP constructed from the plasmid pRO2-DNA. The pSS promoter was placed upstream of eGFP whilst the p7.5 promoter was used for eGPT expression.

Table 3.1. Primers used to amplify flanking sequences of LSDV 130 and LSDV 132 from pZG1 and pZG2 respectively, and the selection and marker genes from pRO-2. The nucleotides are colour coded to correspond to figure 3.2. Primer 130 LEFT FLANK REV is complementary to primer pRO-2-GPT FOR and primer pRO-2-eGFP REV is complementary to primer 132 RIGHT FLANK FOR. Primers were designed such that the three products produced could be joined by overlapping PCR using the outermost primers to amplify one single large fragment.

Name	Primer
130 LEFT FLANK FOR	5'- GGTACCGGAGACAACATTGAACAAACCGATAATG -3'
130 LEFT FLANK REV	5'- GGAATTAGTGATCACTCGAGGCATGCATCGATCTATAGTTTGTTATTATCAGTTGCATG -3'
pRO-2-GPT FOR	5'- CATGCAACTGATAATAACAAACTATAGATCGATGCATGCCTCGAGTGATCACTAATTCC -3'
pRO-2-eGFP REV	5'- GCAATTCCGATAATTCCATATGCAACGAATTCCATCCGATCCAATGTCGACGTATACAG -3'
132 RIGHT FLANK FOR	5'- GTATACGTCGACATTGGATCGGATGGAATTCGTTGCATATGGAATTATCGGAATTGC -3'
132 RIGHT FLANK REV	5'- ACTAGTGATACATCACACAATGTAACAAGTTCAG -3'

Figure 3.2. Diagram showing the binding sites of primers described in Table 3.1. Primer sequences are indicated by coloured arrows above and below the cassette pointing in the direction of amplification. Primer segments coloured red indicate sequences complementary to LSDV 130 (left flank) and LSDV 132 (right flank). Primer segments coloured blue indicate the nucleotides that were added to facilitate assembly of the PCR fragments and are complementary as shown in the diagram. Red text within the cassette indicates the location of restriction sites and highlighted blue text indicates the location of the EcoGPT promoter (p7.5kDa) and the GFP promoter (pSS).

The schematic of primer binding sites and the resultant assembly product is shown in Figure 3.2. PCR amplification using primer sets for the left and right flanking sequences of LSDV, as well as the GPT and eGFP genes, were used to amplify linear products to use in the subsequent assembly and PCR reaction. The reverse primers for the left flanking (LSDV 130 REV) sequence were designed with an additional oligonucleotide sequence complementary to the selection and marker gene cassette (blue in Figure 3.2 and Table 3.1). The pRO 2 DNA forward primers also contained a region complementary to the left flank (colour coded red in Figure 3.2 and Table 3.1). The reverse primer (pRO 2 eGFP REV) included oligonucleotides complementary to a region in the right flank (colour coded red). The right flank forward (LSDV 132 FOR) primers also contained an overlapping sequence which was complementary to a region in the marker gene cassette (colour coded blue).

Three PCR reactions were carried out using the KAPA Hifi Polymerase master mix (Kappa Biosystems, SA) to amplify the Left flank, Right flank and pRO-2 DNA. The cycling

conditions included an initial denaturation step at 95 °C for 5 minutes, 25 cycles of: denaturation at 95 °C for 30 seconds, annealing for 30 seconds at 55°C for the left and right flank, and 60°C for the marker genes, and extension at 72°C for 30 seconds for the left and right flanks and 2 minutes for the marker genes. The final extension time was 7 minutes at 72°C. After amplification, the PCR products were gel purified, quantified using the nanodrop and used in the subsequent assembly reaction.

The left flank forward and the right flank reverse primers were used to assemble the three genes into one fusion product. Equimolar amounts of DNA were added into the same tube for the overlapping PCR. The primers used for the assembly reaction were LSDV 130 forward and LSDV 132 reverse. The conditions for the overlapping PCR included an initial denaturation step at 95 °C for 5 minutes, 25 cycles of: denaturation at 95 °C for 30 seconds, annealing for 30 seconds at 55°C and extension time at 72°C for 3 minutes. A final extension time of 7 minutes was done.

The product from the overlapping assembly PCR was cloned into pJET (ThermoScientific, USA) (Appendix 1) according to standard methods and manufacturers' recommendations (Thermo Fisher, USA). pJET is a blunt end (open) cloning vector. It is compatible with most laboratory strains of E coli. It contains *eco471R* gene which is a lethal gene that enables positive selection for recombinant plasmids only. pJET also contains an ampicillin resistance gene which enables cells which take up bacteria expressing it to survive in the presence of ampicillin.

3.2.2.2 Construction of transfer vector pHM2v3 (for generating nLSDVSODis-M)

To generate recombinant SOD knock-in (nLSDVSODis-M), a transfer vector, pHM2v3 (Figure 3.11), containing the SOD gene flanked by GPT and LSDV 132 was designed. Part of the GPT gene was used as the left flanking sequence and LSDV 132 was used as the right flanking sequence. The SOD of Herbivac contains AT dinucleotide repeats in the region of the 2bp deletion relative to nLSDV. This region was speculated to be unstable. In order to stabilise this region, the degeneracy of the genetic code was utilised. Nucleotides encoding the same amino acids were used to replace the AT rich area. The chain of ATs was replaced with ATCTACATAC to produce the improved *SOD*. The final vector included *SODis*, an expression marker mCherry downstream of the mH5 promoter and flanking sequences for

homologous recombination (Figure 3.11). GenScript (New Jersey, USA) synthesised the insert and cloned it into pUC 57 simple vector.

3.2.4 Generation of recombinant LSDVs with and without SOD

3.2.4.1 Isolation of nLSDVdSOD-M

Figure 3.3 below shows how recombination can take place between the transfer vector pHM1 and nLSDV. Primary lamb testes cells were grown in a 12-well culture plate overnight until they were 70% confluent. Parent LSDV (Neethling vaccine strain – Onderstepoort SA), at a multiplicity of infection of 0.004 was used to infect cells for two hours. X-tremeGENE™ Hp transfection reagent (Roche, Switzerland) was warmed to room temperature and mixed with the plasmid (3ug) at a ratio of 1:1. After removing virus, the transfection complex was added. After 48 hours of incubation, DMEM with 10% FCS was added to the cells. Cells were viewed using a fluorescence microscope and images were taken (Figure 3.13). The cells were incubated for an additional 24 hours after which virus was extracted from the cells through 3 cycles of freeze-thaw.

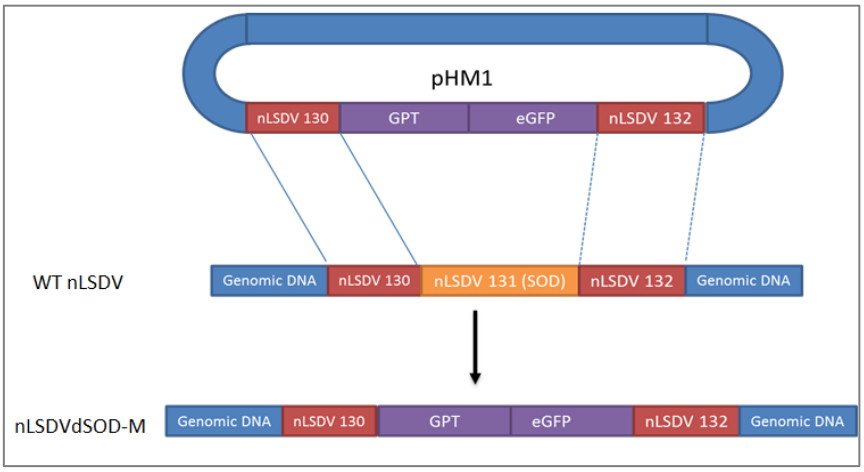

Figure 3.3. Schematic showing how homologous recombination can occur between the transfer vector pHM1 and viral DNA of nLSDV to generate nLSDVdSOD-M. The left (130) and right (132) flanks can recombine to delete the *SOD* homologue gene present in nLSDV and replace it with GPT and eGFP.

After infection and transfection in primary LT cells, virus was passaged in MDBK cells in the presence of selection medium. Selection medium contained mycophenolic acid at a concentration of 2.5ug/ml MPA in complete media and was supplemented with 15µg hypoxanthine and 250µg xanthine (Sigma-Aldrich, USA). The virus was passaged 7 times in

the presence of MPA. At the eighth passage, a serial dilution to isolate a single fluorescing recombinant virus was done. The virus from the single focus was expanded in a 6-well plate. The recombinant virus was confirmed to be correct by PCR. MDBK cells were infected with cell lysate from the single focus propagated in a 6 well plate and incubated without MPA for 3 days. The media was removed from the 6 well plate and cells were washed with 1X PBS. Solution A (100 mM KCl, 10 mM Tris-HCl pH 8.3 and 2.5 mM $MgCl_2$) was added first. Proteinase K (final concentration 120 µg/ml; Sigma-Aldrich, USA) was added to Solution B (10 mM Tris-HCl pH 8.3, 2.5 mM $MgCl_2$ and 1.5% Tween-20). Solution B was added and using a sterile cell scraper the cells were removed from the well. The lysate was incubated at 60^0C for 1 hour followed by10 minutes incubation at 95^0C. 5ul of the lysate was used for PCR, as described in section 3.2.4.4.

3.2.4.2 Isolation of nLSDVSODis-M

The plasmid pHM2v3 (Figure 3.11) was used to transfect cells infected with nLSDVdSOD-M. The schematic below (Figure 3.4) shows how the recombinant nLSDVSODis-M was made.

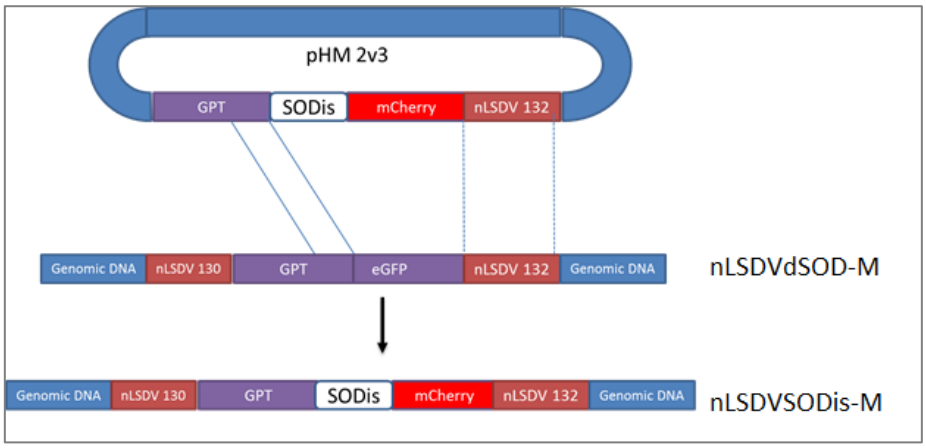

Figure 3.4. Diagram to show strategy of insertion of SODis and mCherry into nLSDVdSOD-M to generate nLSDVSODis-M. Part of the GPT gene and right flank (132) can recombine to insert *SODis* and mCherry replacing it with eGFP.

A 70 – 90% confluent layer of lamb testes cells in a 12 well plate was infected with nLSDVdSOD-M at an MOI of 0.05. X-tremeGENE™ Hp transfection reagent (Roche, Switzerland) was warmed to room temperature and mixed with plasmid pHM2v3 (3 µg) at a ratio of 1:1. After 2 hours, virus was removed, and the transfection complex was added. After 48 hours of incubation, DMEM with 10% FCS was added to the cells. Cells were viewed using a fluorescence microscope. After a further 48 hours, the cells containing recombinant virus

were lysed in 1mM Tris and used to infect MDBK cells. Red fluorescing foci were picked, and the virus grown in MDBK cells. A total of 3 rounds of picking was done. Since both the parent and recombinant viruses contained the GPT gene, MPA selection could not be used to select nLSDVSODis-M. PCR, as described in section 3.2.4.4, was used to confirm that the recombinant was correct **(**Figure 3.18**)**.

3.2.4.3 Isolation of recombinant SOD knock-in and SOD knock-out viruses without marker genes

To confirm that the differences identified from experiments using nLSDVSODis-M and nLSDVdSOD-M were not due to the presence of marker genes, recombinants without marker genes were constructed. The SOD knock-out virus without marker genes nLSDVdSOD-UCT and the SOD knock-in virus, nLSDVSODis-UCT were constructed.

A plasmid without the marker genes and the *SOD* gene - pHM1dSOD was made by Ruzaiq Omar by excising GPT and eGFP from within the flanks by treating pHM1 with NsiI and EcoRI and blunting it using T4 polymerase (New England BioLabs, Massachusetts, USA). This plasmid was circularised using T4 ligase (New England BioLabs, Massachusetts, USA).

A plasmid containing *SODis* between the flanking sequences (130 and 132) was made by excising the marker genes from pHM1 as described above. pHM1 was treated with NsiI and EcoRI to remove GPT and GFP. The linear vector backbone was blunted. *SODis* along with its promoter sequence was excised from pHM2v3 and blunted. A blunt end ligation was then used to generate pHM1-SOD_pos containing *SODis* between LSDV 130 and 132 flanking sequences. Competent *E..Coli* cells (Lucigen, USA) were transformed by pHM1dSOD or pHM1-SOD_pos. These transfer vectors were confirmed to be correct by Sanger DNA sequencing (CAF, Stellenbosch University, SA).

To construct and isolate nLSDVdSOD-UCT (SOD knock-out without markers), primary lamb testes cells were seeded into a 6-well plate at a total of $5x10^5$cells/well. Cells were infected with nLSDVdSOD-M (expressing eGFP) at an MOI of 0.05 within two hours of seeding. 24 hours post seeding and infecting, cells were transfected with 3µl XtremeGeneHP + 6µg pHM1dSOD (Figure 3.20). Six days post transfection a lysate was prepared by two rounds of freeze-thawing (37°C/-80°C). Virus from this lysate was passaged in MDBK cells and single

non-fluorescing foci were picked. This was done five times before a serial dilution was made in a 96-well plate and a single non-fluorescing focus was isolated for large scale preparation of the virus.

For the construction of nLSDVSODis-UCT (SOD knock-in without markers), a monolayer of primary lamb testes cells were infected with nLSDVdSOD-M (expressing eGFP) at an MOI of 0.001 and transfected with 6ug of transfer vector pHM1-SOD_pos (Figure 3.20). Cells were lysed by three cycles of freezing and thawing 48 hours post infection and transfection. The lysate was passaged in MDBK cells and three rounds of picking of non-fluorescing foci were performed. A single non-fluorescing focus was isolated on a 96-well plate and expanded in MDBK cells. PCR analysis confirmed the recombinant to be nLSDVSODis-UCT.

3.2.4.4 PCR

All recombinant LSDV viruses were confirmed to be correct by PCR using appropriate primer pairs. Primer set A binds in the LSDV 130 and LSDV 132 regions which flank the *SOD* gene region. Primer set A comprised forward primer HM 130 FW (5'-GGAGCACCATTTCCATATAC-3') and reverse primer HM 132 REV (5'-AGTAGCTTAAAAGGAGGGAAG-3'). Primer set B binds in the SOD ORF (131). Primer set B included forward primer HM131 FW (5'-CGAGTTCGGTGATGAAAC-3') and reverse primer HM 131 REV (5'-AATTCCATACGCGACACC-3').

The PCR conditions for both primer sets were: an initial denaturation step at 95°C for 5 minutes, 25 cycles of: denaturation at 95 °C for 30 seconds, annealing for 30 seconds at 55°C and extension time at 72°C for 1 minute. A final extension time of 7 minutes at 72°C was done. The PCR ready mix ImmoMix™ Red (Bioline, USA) was used.

PCR was also performed which used primers that bind outside the left flank, LSDV 129 forward (5'-GAGCCCTGTAATTCACTTTT-3') and within the right flank LSDV 132 reverse (5'-ATCGATGGAAAAGATCCG-3') (Figure 3.19). The conditions for the PCR included an initial denaturation step at 95°C for 5 minutes, 25 cycles of: denaturation at 95°C for 30 seconds, annealing for 30 seconds at 59°C and extension time at 72°C for 3 minutes. A final extension time of 7 minutes at 72°C was done. For this PCR, Phusion® High-Fidelity DNA Polymerase (New England BioLabs, Massachusetts, USA) was used.

3.2.5 Preparation of LSDV stocks

The Neethling vaccine (nLSDV) and recombinant LSDV viruses were bulked up in 500ml hyperflasks (Corning® HYPERFlask®). MDBK cells in a hyperflask were infected at an MOI of 0.01 and incubated for a fortnight. After the cells had lifted, virus was harvested by 3 cycles of freeze-thawing. The lysate was subjected to centrifugation at 800 rpm for 10 minutes. The supernatant was collected and centrifuged through a 36 % sucrose cushion at 11000 rpm for 1 hour at 4°C using a Sorvall RC5C Plus centrifuge and Sorvall S534 rotor. After centrifugation, the supernatant was decanted, and the pellet was suspended in 500ul PBS per tube. Aliquots of 200ul were made and stored at -80 °C.

3.2.6 Growth curves of the different LSDV viruses in cell culture

The viruses nLSDV, nLSDVdSOD-UCT and nLSDVSODis-UCT were compared for growth in tissue culture. MDBK cells were seeded at a concentration of $5x10^5$ cells per well of a 12 well plate. Cells were infected at an MOI of 0.015 in triplicate and lysates were prepared 2 hours post infection and at subsequent 1-day intervals from days 1 to 5. At each time point a plate was frozen. All the plates were frozen and thawed three times in total to release virus. The Reed and Muench (1938) endpoints dilution method was used to determine the virus titre. Titrations in $TCID_{50}$ units were converted to focus forming units per ml (ffu/ml).

3.2.7 Growth curves of different LSDV viruses on chick chorioallantoic membranes.

Viruses nLSDV, nLSDVdSOD-UCT and nLSDVSODis-UCT were compared for growth on chick chorioallantoic membranes (CAMs). Seven-day-old specific pathogen free eggs (SPF) from Leghorn chickens Avifarms (Pty) Ltd (Lyttelton, South Africa) were used and inoculated as described by Offerman et al. (2013). CAMs were inoculated with PBS, nLSDV, nLSDVdSOD-UCT and nLSDVSODis-UCT. Viral titrations were done from 2 days to 5 days post infection. Membranes were dropped by making a hole at the air sac and dorsal area. Care was taken to make a hole in a well vascularised area. A pipette bulb was used to move the air sac to the dorsal area where viral inoculation was done. Two hours post dropping membranes, viruses were diluted to a concentration of 10^4 $TCID_{50}$/ml. A tuberculin insulin syringe was used to inject 100 µl of virus (10^3 $TCID_{50}$) to each egg. Once eggs were infected, they were incubated at 34°C. Eggs were harvested daily from Day 0 to Day 5 and membranes were pooled (3 per

virus per time point). A low speed spin was done (800 rpm for 1 minute) and the supernatant was titrated using the $TCID_{50}$ method (Reed and Muench, 1938). Titrations were performed in triplicate.

3.2.8 CAM Histology

The method described by Offerman et al. (2013) was used to prepare CAMs for histology. The first experiment compared CAM sections from eggs inoculated with nLSDV, Herbivac, nLSDVdSOD-M and nLSDVSODis-M. Six days post infection, 3 membranes per virus were harvested. At this point, all membranes had a mean titre of 10^6 TCID50/ml. The membranes were fixed in 10% buffered formalin (formaldehyde (37–40%), $NaH_2PO_4.H_20$ (35.03 M), Na_2HPO_4 (anhydrous, 21.84 M)). The membranes were rolled into small cylinders which were embedded in paraffin. Thin sections were cut into 5µm thick sections on an approximately 5-6 cm long x 1-2 cm wide block. Haematoxylin and Eosin staining (H&E) was done as described by Fischer and colleagues (Fischer et al., 2008). Images were taken using a light microscope.

The same experiment was done using the recombinant viruses without marker genes. Seven-day-old CAMs were infected with 10^3 $TCID_{50}$/100µl nLSDV, nLSDVdSOD-UCT or nLSDVSODis-UCT. A single representative membrane (n=1) was harvested from each treatment on days 1, 3 and 5. The CAMs were fixed in 10% buffered formalin and embedded as described above. Five sections per membrane per day were stained using H&E, evaluated under the light microscope and blinded tissue scoring was done based on immune infiltration, hyperplasia, ballooning degeneration and presence/absence of inclusion bodies in the chorionic or allantoic epithelium. Scoring was done by a specialist veterinary pathologist Dr. Sophette Gers (PathCare VetLab, Cape Town South Africa).

3.2.9 Preparation of homogenates for SOD activity determination

To perform the SOD activity assay, cellular homogenates were made from uninfected and infected cells. MDBK cells were infected with nLSDV, Herbivac, nLSDVSODis-M and nLSDVdSOD-M at an MOI of 10 for 2, 6 and 24 hours. After the stipulated time, cells were washed with PBS and homogenised in 2X lysis buffer (Abcam - ab179835, Lot # GR292167-16) containing 2mM EDTA. The homogenate was clarified by centrifugation at 1500 rpm for 5 minutes. The supernatant was used for SOD activity determination and protein quantification.

3.2.10 Reactive Oxygen Species (ROS) assay

Most commercially available kits involve the use of hypoxanthine/xanthine and xanthine oxidase to generate superoxide anions. SOD present in cell lysates or homogenate then acts on the superoxide anion dismutating it to hydrogen peroxide. The SOD determination kit (19160) (Sigma, USA) based on a highly soluble tetrazolium salt WST-1 (2-(4-Iodophenyl)- 3-(4-nitrophenyl)-5-(2,4-disulfophenyl)- 2H tetrazolium monosodium was used in this experiment to determine SOD activity. This direct method of detecting SOD activity uses a tetrazolium salt which reacts with the superoxide anion released by the xanthine oxidase system. If there is a lot of functional SOD in the homogenate, there is a decline in the amount of the superoxide anions available to react with the dye hence the absorbance drops. When there is an inhibitor or a functional SOD decoy, the superoxide anion is continually produced and therefore the absorbance increases. The assay measures the activity of SOD present in cell lysate.

The 19160 SOD determination kit (Sigma, USA) was used according to the manufacturer's protocol. The assay measures directly the amount of superoxide produced by xanthine oxidase when it metabolises xanthine. The produced superoxide radical reacts with the water-soluble tetrazolium salt (WST-1) to form a soluble dye (WST-1 formazan) (see Figure 3.5). If there is a functional SOD enzyme, the produced superoxide is dismutated to hydrogen peroxide resulting in a decrease in absorbance.

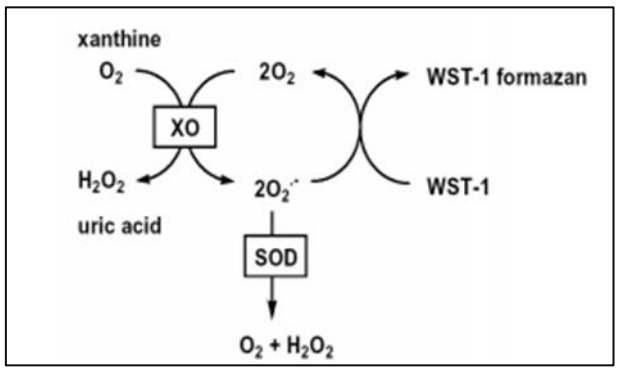

Figure 3.5. Mechanism of the SOD determination kit. Xanthine oxidase (XO) is used to generate superoxide anions from xanthine. The generated superoxide anions are dismutated to oxygen and hydrogen peroxide by cellular Cu Zn SOD. The rate of inhibition of this reaction by the reaction of WST and the superoxide anion is inversely related to the amount of superoxide anion present in the cell lysate. An increase in WST 1-formazan, a coloured product is inversely proportional to the amount of SOD present in the lysate. In the presence of an inhibitor like a SOD decoy there is an increase in WST-1 formazan (increase in absorbance). Figure taken from Sigma SOD determination kit 19160, USA.

In the presence of a SOD inhibitor, the levels of the superoxide anion increase resulting in an increase in absorbance. Clarified homogenate (20µl) was loaded into the assay. A kinetic assay at one-minute intervals was selected and absorbance was measured at 450nm. SOD activity was calculated in the linear phase of the reaction i.e. in the first 20 minutes. The absorbance reading at 5 minutes was subtracted from the absorbance reading at 15 minutes. SOD activity was calculated according to the equation below:

$$\text{Percentage SOD activity} = \left(\frac{\text{Change in Absorbance of Blank} - \text{Change in Absorbance of Sample}}{\textit{Change in Absorbance of Blank}}\right)*100$$

SOD activity was given as a percentage of the blank. Different amounts of bovine SOD were used to monitor the assay. Units used included 5.6 mU, 56 mU, 5.6 U and 56 U.

3.2.10.1 Protein Quantification

Protein quantification was done using the Bio-Rad DC protein assay kit as per manufacturer's manual (Solution A Cat # 500-0113 and Solution B Cat # 0114) (Bio-Rad, USA). Absorbance readings were obtained using a Versa Max spectrophotometric reader (Molecular Devices, USA) at 750 nm. The amount of protein was used to normalise the activity of SOD and activity of SOD was expressed as percentage activity/mg of total protein.

3.2.11 Apoptosis assays

3.2.11.1 Induction of apoptosis/necrosis by viruses

MDBK cells were first seeded into a 96 well plate at a seeding density of 1 x 10^4 cells/well. After overnight incubation, cells were infected with the four viruses. The infected cells were then incubated for 24 hours. Apoptotic cell death was measured over a period of 2, 6 and 24 hours post infection to investigate the death profile over time. For the 2 and 6-hour time points, an MOI of 10 was used. For the 24-hour time point, an MOI of 1 was used. A monolayer of cells was infected with nLSDV, Herbivac, nLSDVdSOD-M or nLSDVSODis-M. After 2, 6 and 24 hours, cell death via the apoptotic pathway was investigated by removing all the medium in which the cells were grown and using the cell lysate to determine the amount of apoptosis induced.

To investigate necrosis, the media in which the infected cells were growing was collected and added directly to the microplate to measure the amount of oligonucleosomes released into the milieu by dying cells. Oligonucleosomes released both into the cytoplasm because of apoptotic cell death and into the media along with dying cells (necrosis) were measured using the Cell death detection ELISAPLUS assay (Ref No. 11774425001, Roche, Switzerland).

Figure 3.6 shows the mechanism of the cell death ELISA kit in determining oligonucleosomes released into the milieu by dying cells. Readings were taken using a VersaMax™ ELISA Microplate Reader (Molecular Devices, USA). Measurements were done at 405nm and a reference wavelength of 490nm was used.

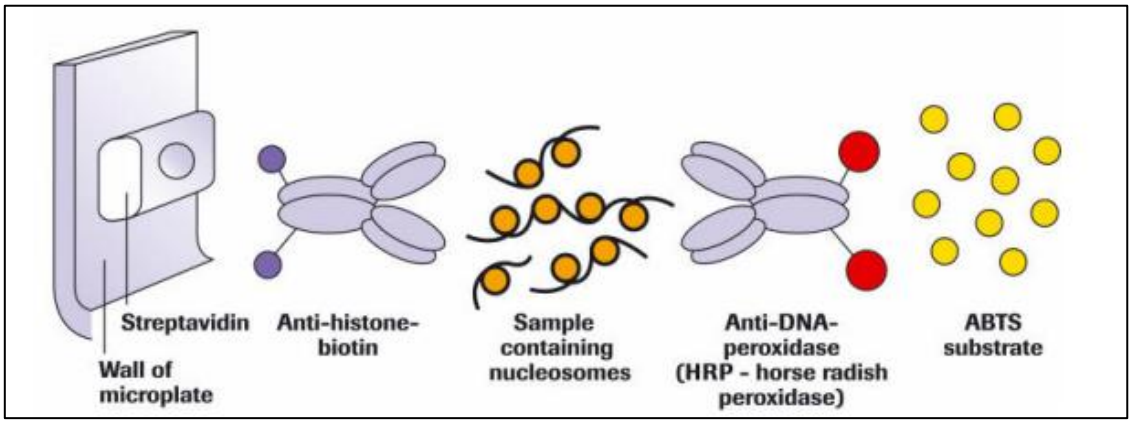

Figure 3.6. Mechanism of the cell death ELISA kit. A sample containing nucleosomes from the apoptotic or necrotic fraction is added to the streptavidin microplate. An immunoreagent composed of anti-histone biotin which immobilises the nucleosomes to the streptavidin plate and anti-DNA antibody conjugated to horse radish peroxidase is then used in quantifying the number of bound nucleosomes. After incubation and washes, 2,2'-Azino-bis (3-ethylbenzthiazoline-6-sulfonic acid) - ABTS substrate is added for 20 minutes. A stop solution is then added to stop the reaction. Reading is done at 405 and 490 nm on a spectrophotometer. Figure taken from Roche Cell Death Detection ELISA^{PLUS}, USA.

Apoptosis and necrosis were also investigated in a non-permissive cell line – HeLa S3 cells (ATCC, USA). An M.O.I of 10 was used in the non-permissive cell line. Apoptosis and necrosis were investigated as described above at 24 hours post infection.

3.2.11.2 Inhibition of apoptosis by viruses after camptothecin induction

To measure the ability of a virus to inhibit apoptosis or necrosis, a known inducer of apoptosis and necrosis called camptothecin was used. A dilution series of camptothecin was performed initially to determine the ideal concentration to induce apoptosis. For MDBK cells, a concentration of 1µg/ml was selected as able to induce both apoptosis and necrosis. In HeLa

S3 cells, a concentration of 100µg/ml camptothecin was found to be the concentration to use in inducing apoptosis/necrosis.

Cells were seeded and infected as described above, in duplicate. Camptothecin was added to one set of wells, so that there were wells that were infected but had no camptothecin added and wells which were infected and had camptothecin added. After 24 hours, the assay for determining apoptosis or necrosis as described above, was used.

3.2.11.3 Calculation of the amount of mono/oligonucleosomes released after induction of apoptosis/necrosis and enrichment factor.

To ascertain the exact number of oligonucleosomes being released into the cytoplasm (apoptosis) or media (necrosis) after camptothecin induced apoptosis/necrosis a mathematical formula was used. Enrichment refers to the amount of oligonucleosomes released into in the cytoplasm or medium following induction of apoptosis or necrosis respectively. The formula for calculating this is given below:

$$\text{Enrichment factor} = \frac{mU\ of\ the\ sample\ with\ camptothecin\ added}{mU\ of\ the\ corresponding\ treatment\ without\ camptothecin\ added}$$

mU – Absorbance

Once the enrichment factor was computed, an investigation into the fold decrease or fold increase in the amount of apoptosis or necrosis was done. The formula for calculating fold reduction in apoptosis is given below.

$$\text{Fold decrease in apoptosis} = \frac{Enrichment\ factor\ [uninfected\ cells]}{Enrichment\ factor\ of\ infected\ cells}$$

3.2.12 Statistics

All statistics, unless specified, used one-way ANOVA followed by Tukey's test for differences between groups. This was performed using GraphPad Prism version 5.0 for Windows (GraphPad Software, La Jolla California USA, www.graphpad.com). The significant p value was set at $p < 0.05$.

3.3 Results

3.3.1 Comparison of the LSDV SOD homologue amino acid sequences

The putative amino acid sequences of the SOD homologues from nLSDV and Herbivac were compared to other published SOD and SOD decoy genes from poxviruses and animals. Figure 3.7 shows an alignment of a selection of different SOD homologues. The homologue from nLSDV is a truncated protein (108 aa) lacking some key residues described below. SOD from Herbivac was shown to be 160 aa. The LSDV SOD from the virulent field strain Nl 2490 contain 161 aa. None of the LSDV putative SOD protein sequences (from the virulent and vaccine strains of LSDV) had the catalytic arginine at position 142 in Figure 3.7. An R-to-G amino acid substitution is present at this site in both the virulent strain and Herbivac. Eight metal binding residues, mostly histidine and aspartic acid, are important for catalytic activity and binding metals (Perry et al., 2010). The virulent strain of LSDV, nLSDV and Herbivac contained 6 of these residues. All the LSDV strains contained all the Zn binding sites. The much studied myxoma virus SOD homologue contained 7 out of the 8 metal binding residues and 2 copper binding residues. Vaccinia virus SOD on the other hand contained only 1 copper binding site and no Zn binding site.

The cysteine at position 56, which is present in bovine SOD, human SOD, CCS, myxoma SOD homologue (position 55) and AMV SOD was absent from all the LSDV strains. LSDV Nl 2490 and Herbivac contained all the 8 antiparallel strands and helical turns whereas nLSDV contained 6 out of the 8 strands present in functional SOD. Regions of homology between CCS and SOD homologues from LSDV were present. However, the SOD homologue from nLSDV contained only 1 out of the three residues that are important in SOD-CCS heterodimerisation. All the SOD homologues (with the exception of A45R from VV) and enzymes from different hosts contained all 3 residues important for dimerization, namely glycine at positions 50 and 114, and isoleucine at position 152. Lastly, cysteine residues at positions 56 and 145, responsible for maintenance of structure by intramolecular bond formation, were absent from all LSDV SOD homologues, but present in those with known SOD activity (AMV, human and bovine SOD).

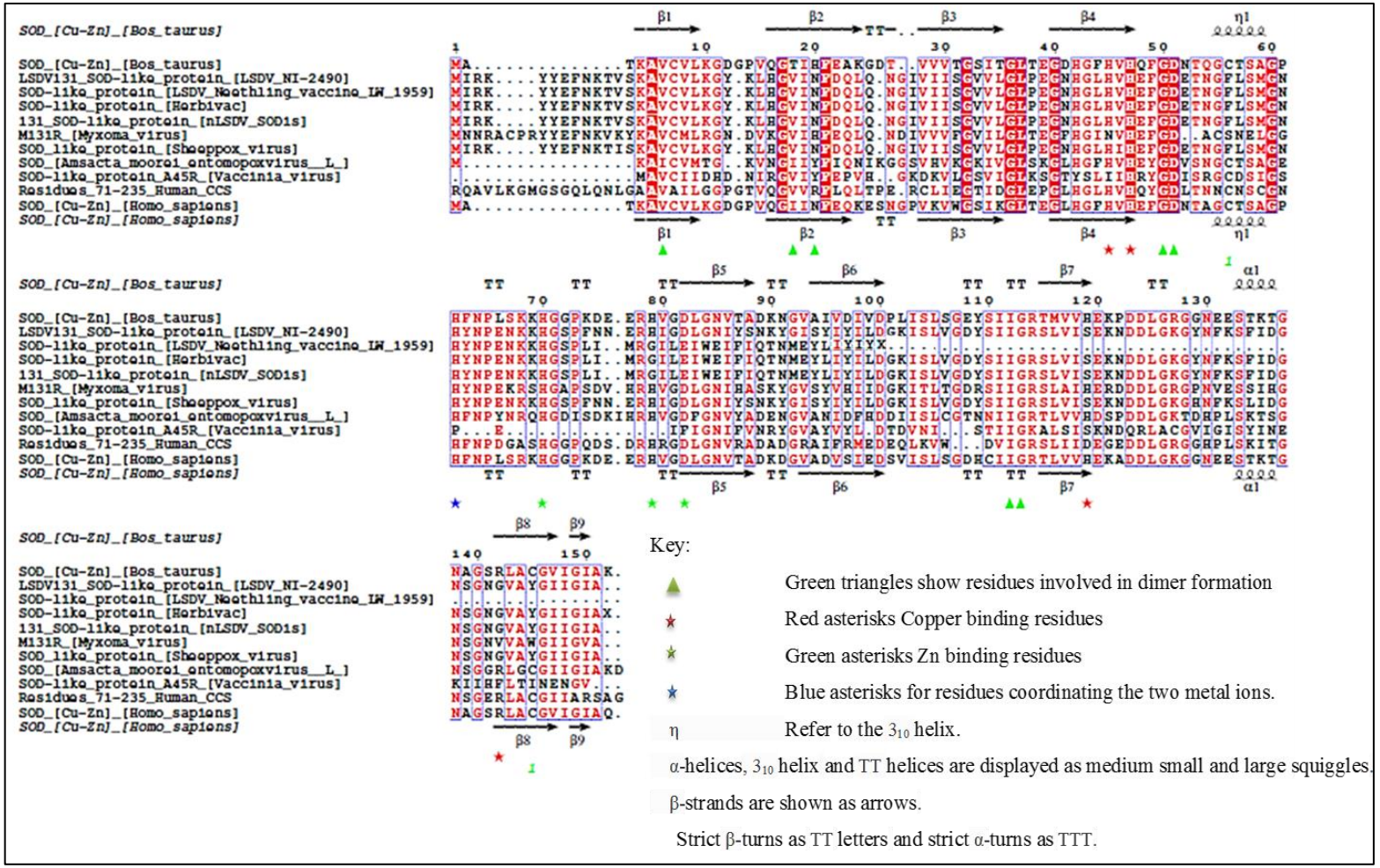

Figure 3.7. Structural alignment of SOD and SOD homologues. SOD-like proteins from LSDV (Neethling vaccine strain, virulent Nl 2490, Neethling vaccine LW 1959, Herbivac and nLSDVSODis), Myxoma virus, variola virus, sheeppox virus, vaccinia virus, Amsacta Moorei Entomopoxvirus and vaccinia virus were included in the alignment. Also included in this alignment are residues 71 to 235 of Human CCS and the human as well as bovine SOD. The structures for bovine and human SOD were obtained from the protein databank (1SOS and 1EQ9). SOD alignment was done using the TCoffee Expresso program available on the TCoffee server. Structural alignment was done on ESPript 3.0 Server. A key showing some of the residues of interest is shown in the alignment.

3.3.2 Construction of transfer vectors to insert an improved SOD gene into LSDV and to delete SOD in LSDV

Initially two transfer vectors were designed that included reporter genes and selection markers. The first transfer vector included an improved SOD gene that had been redesigned to improve stability. The second transfer vector deleted SOD. Later on in the project, recombinant LSDVs without the marker or selection genes were constructed to ensure that the differences observed between viruses with and without the SOD gene were due to the changes in SOD and not the marker genes.

3.3.2.1 Construction of transfer vector to delete the SOD gene in LSDV (pHM1)

The transfer vector pHM1 was designed to delete the SOD homologue gene from the Neethling strain of LSDV. This plasmid was constructed by overlapping PCR fragments (Figures 3.8 and 3.9). Initially 3 individual PCR fragments were generated from pZG1, pZG2 and pZG4 (section 3.2.3.1) to produce the left flank, right flank and gpt-GFP respectively. Figure 3.8B shows PCR fragments of 466bp (lane 1) for the left flank, 405bp (lane 2) for the right flank and 1505bp (lane 3) for the marker and selection genes. These products were purified and subjected to overlapping PCR as depicted in Figures 3.2 and 3.8. PCR products of approximately 2.2kbp were obtained (Lanes 4, 5 and 6), as expected. BamHI digestion linearised the plasmid to produce a fragment of 5224bp (Figure 3.9). DNA sequencing confirmed the transfer vector to be correct (see Appendix for sequence).

3.3.2.2 Construction of transfer vector to insert an improved SOD gene into LSDV (pHM2v3)

It was hypothesized that the *SOD* gene in Herbivac was unstable due to the AT repeats and so this gene was redesigned to improve the stability of the gene. *SODis* (*i*mproved *s*tability) was designed in such a way that the AT repeats were replaced by other nucleotides coding for the same amino acids (see Figure 3.10).

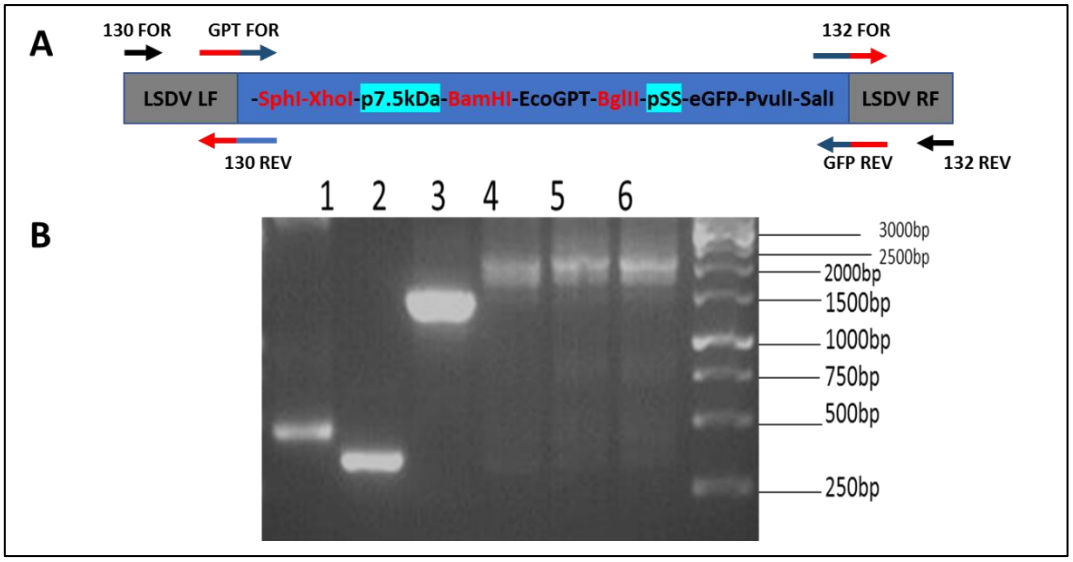

Figure 3.8. Construction of transfer vector pHM1. A – Schematic showing the binding sites of primers designed and used in the assembly of the three fragments. Primer 130 forward was designed to bind in LSDV 130. Primer 130 reverse was designed to bind inside LSDV 130 with additional oligonucleotides complementary to the GPT-GFP cassette. This cassette carries a selection marker (GPT) and an expression marker (GFP). Another primer was designed, GPT forward, which binds in the selection cassette but also includes some oligonucleotides complementary to LSDV130. Primer GPT reverse binds in the GPT GFP cassette with oligonucleotides complementary to LSDV 132. LSDV 132 forward binds in the LSDV 132 region and contains additional nucleotides complementary to the GPT-GFP cassette. 132 reverse binds in the 132 region. **B – 1% Agarose gel electrophoresis of PCR fragments**: amplification of the left flank (1) using primers 130 FOR and 130 REV, right flank (2) using primers 132 FOR and 132 REV and pRO-2 DNA /cassette (3) using primers GPT FOR and GFP REV (130 FOR and 132 REV). The PCR products from lanes 1,2 and 3 were fused in an overlapping PCR using primers 130 FOR and 132 REV (Table 3.1) to generate a fusion product of approximately 2.2.kbp (Lanes 4,5,6).

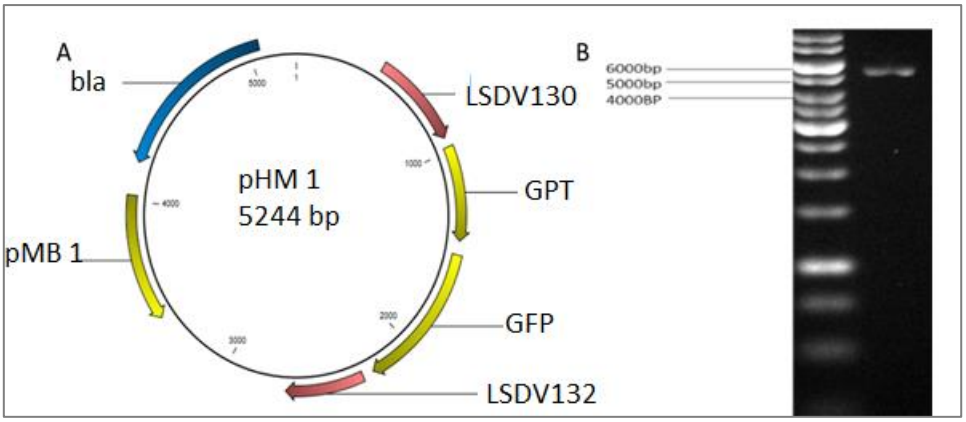

Figure 3.9. pHM1. A – Plasmid map of transfer vector pHM 1, used to delete the SOD gene in nLSDV. LSDV 130 and 132 are open reading frames that flank the LSDV SOD homologue, ORF 131. GPT, xanthine-guanine phosphoribosyltransferase, GFP, green fluorescent protein. **B – 1% agarose gel electrophoresis of pHM 1 subjected to BamHI restriction enzyme digestion**.

The transfer vector pHM2v3 was designed to reintroduce the full-length *SOD* homologue gene into the SOD knock-out virus to generate the SOD knock-in virus nLSDVSODis-M. *SODis* was synthesised and ligated into pUC57-Simple by GenScript (New Jersey, USA). The plasmid map is shown in Figure 3.11.

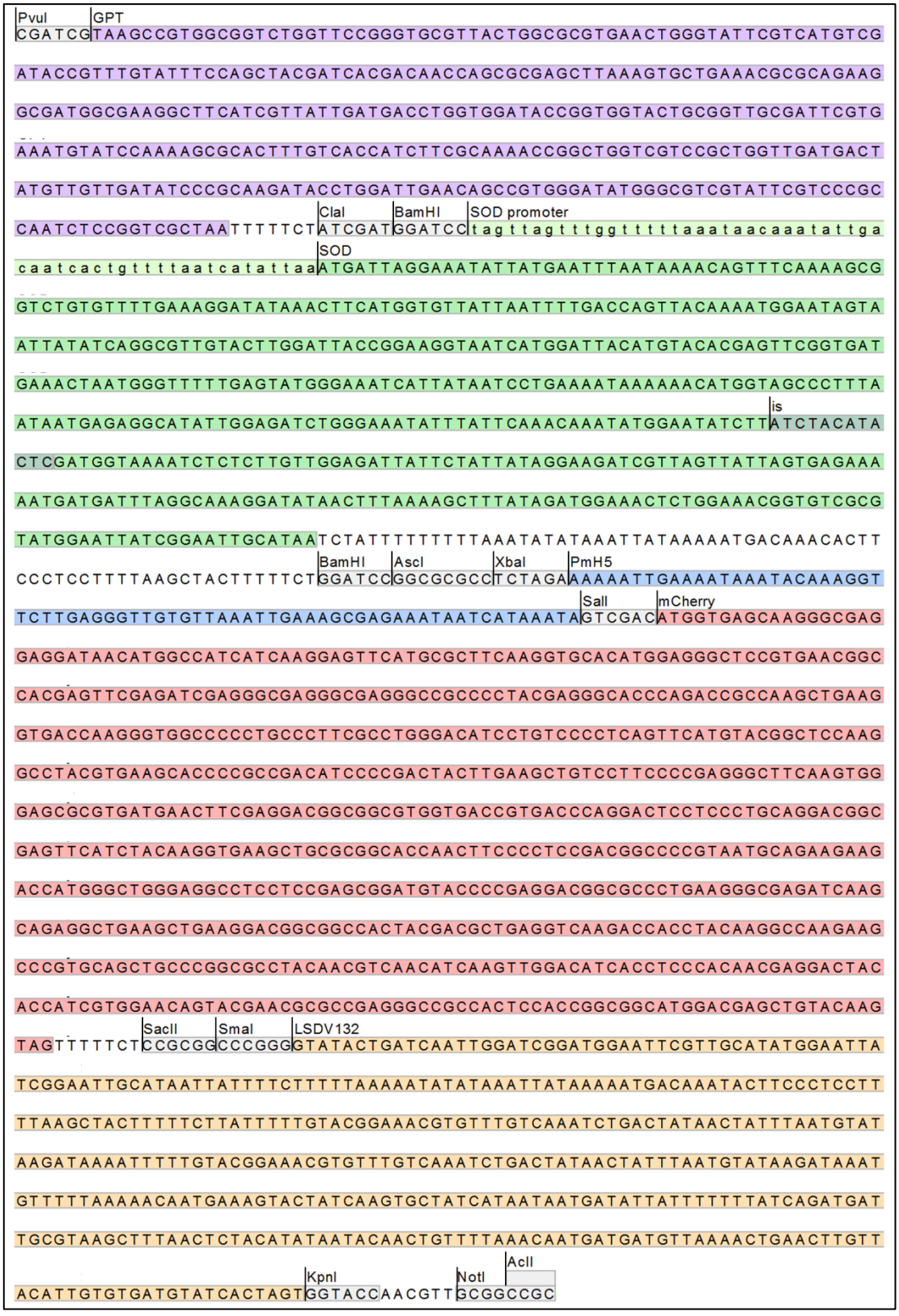

Figure 3.10. DNA sequence synthesised and ligated into a pUC57-Simple vector by GenScript (New Jersey, USA) to generate transfer vector pHM2v3. The purple section is the section of homology to GPT, light green sequence contains the *SOD* promoter region, the green region shows the *SOD* gene, the region in blue font is the mH5 promoter and the region in red represents the mCherry gene. The right flanking sequence is highlighted in orange and represents LSDV 132.

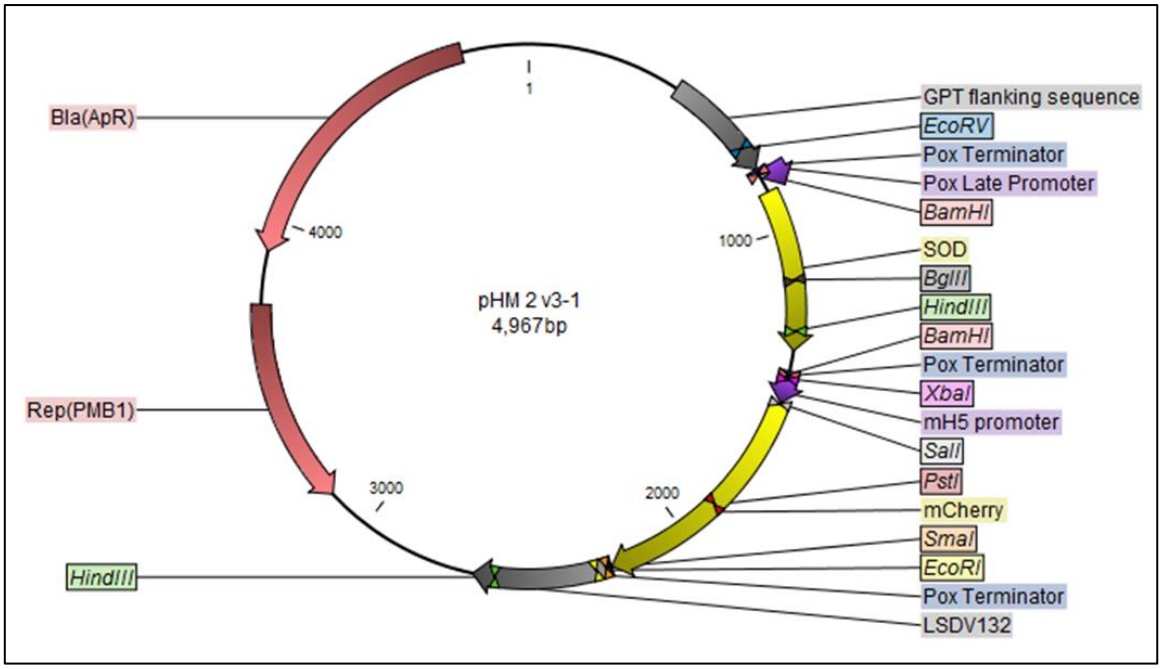

Figure 3.11. Plasmid map of transfer vector to insert an improved *SOD* gene into LSDV- pHM2v3. Modified *SOD* homologue gene based on LSDV 131. The transfer vector pHM2v3 contains part of GPT and nLSDV 132 as flanking sequences. *SODis* and *mCherry* are placed within the flanks.

Restriction digestion was performed on pHM2v3 **(**Figure 3.12**)**. There are single XbaI and SalI sites in pHM2v3. BamHI sites are located on each side of the *SOD* gene (see figure 3.11).

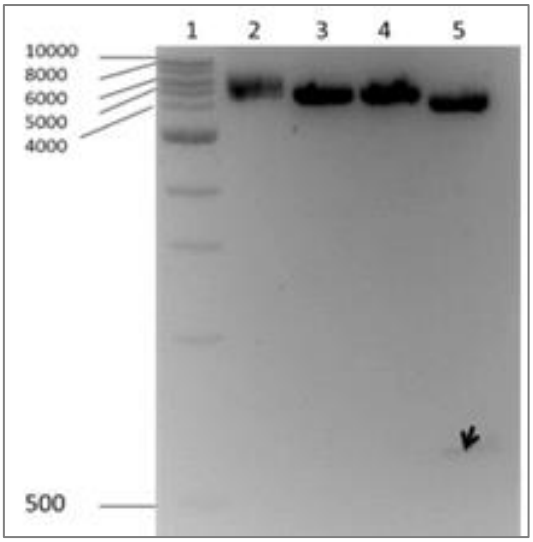

Figure 3.12. Confirmation of pHM 2v3 by restriction enzyme digestion. Plasmid pHM2v3 was untreated (lane 2) or treated with XbaI (lane 3), SalI (lane 4) and BamHI (lane 5). Lane 1 is a marker (Thermofisher O'GeneRuler, SM0312). Samples were subjected to 1% agarose gel electrophoresis.

3.3.3 Isolation of recombinant viruses

3.3.3.1 Isolation of nLSDVdSOD-M (SOD knock-out).

The SOD homologue ORF was completely removed from nLSDV by homologous recombination of nLSDV with transfer vector pHM1. Figure 3.13 shows expression of eGFP in infected cells showing that the pSS promoter was recognised by LSDV. Recombinant nLSDVdSOD-M was isolated after 7 passages, of which 6 were done in the presence of mycophenolic acid (MPA).

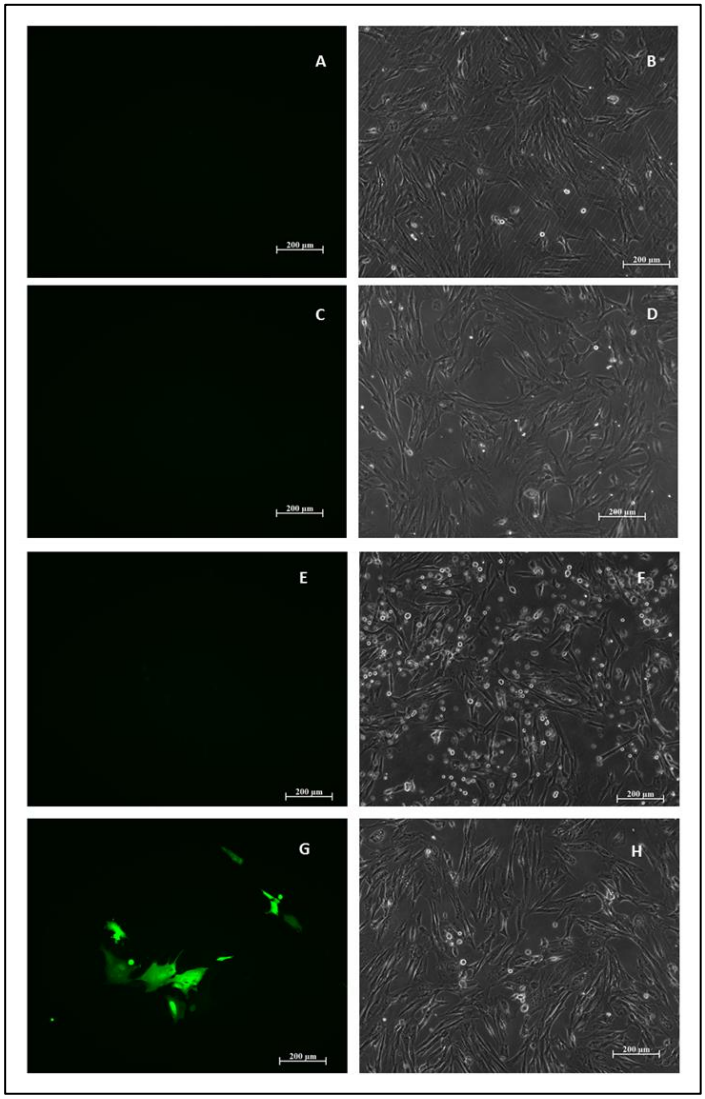

Figure 3.13. Transient expression of GFP following infection with nLSDV and transfection with pHM1. Primary lamb testes cells were infected with nLSDV at an MOI of 0.04 and transfected with 3 ug of pHM 1 (G and H). Cells were photographed after 48 hours using UV light and a green filter (A, C, E, G) and phase contrast (B, D, F, H). Controls included uninfected and untransfected lamb testes cells (A and B), uninfected transfected cells (C and D) and infected cells not transfected with plasmid (E and F). Imaging was done using a fluorescence microscope (Zeiss, Germany) using the 10X objective and the scale bar depicts 200µm.

PCR was used to confirm the recombinant was indeed the desired knockout virus. The sequences of the primers used in the screening of recombinant viruses can be found in section 3.2.4.2. Primers that bind in the left and right flank (HM 130 FW and HM 132 respectively) and those that bind in the SOD region (131 FW and 131 REV) were used (Figure 3.14). The primer set 130 FW and 132 REV generated a fragment of 1745 in the recombinant and 808 in the parent virus. The primer set 131 (FW and REV) generated a fragment of 300bp in the parent virus and no fragment in the recombinant, showing that the SOD gene is not present in this virus. Results confirm that the *SOD* gene was successfully knocked out.

Table 3.2. Primers used to detect presence of recombinant nLSDVdSOD-M. The respective fragment sizes are also listed. Primer sequences are found in section 3.2.4.2. The positions of the primer binding sites are given in Fig 3.14.

	Forward Primer	Reverse Primer	Size of fragment
nLSDVdSOD-M	HM 130 FW	HM 132 REV	1745
	HM 131 FW	HM 131 REV	0
nLSDV	HM 130 FW	HM 132 REV	808
	HM 131 FW	HM 131 REV	300

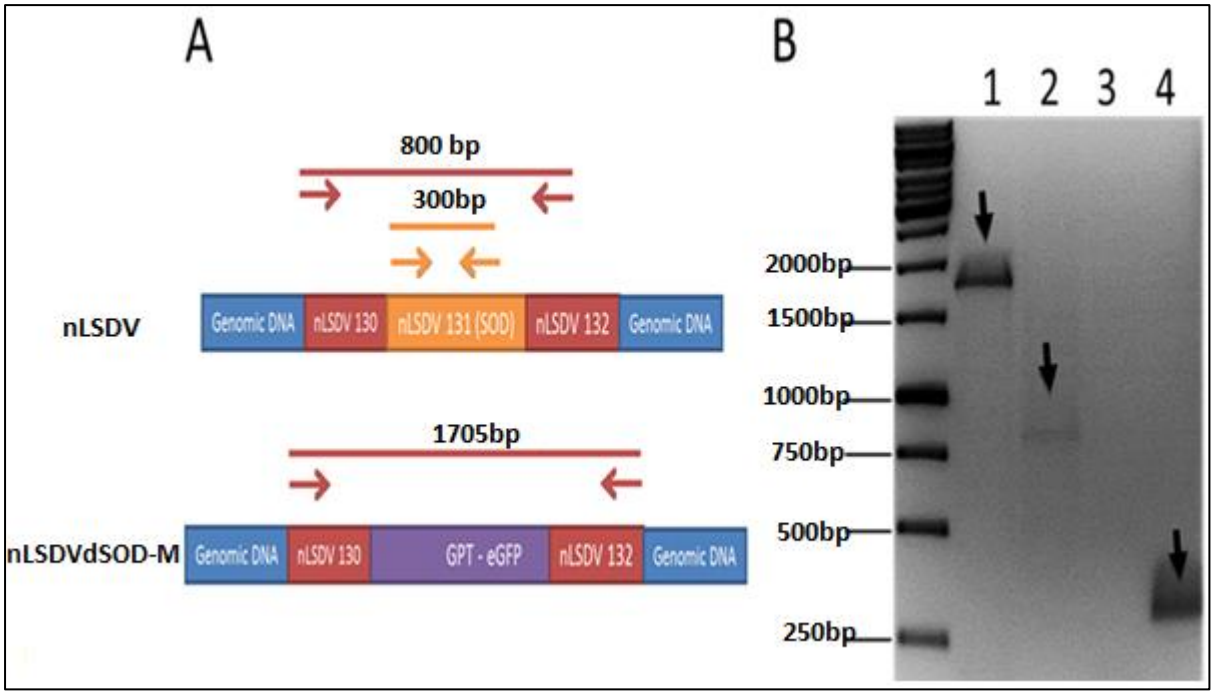

Figure 3.14. A - Diagram to show primer binding sites and fragments they generate. The primer sets are colour coded and Table 3.2 shows the names of the primers used. **B - 1% agarose gel electrophoresis of PCR products**. Lanes 1 and 2 – products generated from primer set HM 130 FW&132 REV on recombinant virus and parent virus respectively. Lanes 3 and 4 - PCR products from primer set HM 131 FW and 131 REV on recombinant virus and parent virus respectively.

Since this recombinant contained a green fluorescent protein as an expression marker, green fluorescence was used to establish the presence of the recombinant. The recombinant nLSDVdSOD-M was grown to a titre of $10^{8.5}$ $TCID_{50}$ per ml (see section 3.2.5 for method) in MDBK cells. This stock was confirmed to be a pure culture of recombinant nLSDVdSOD-M by PCR and sequencing. No product of 300bp could be detected using primers which amplify the *SOD* gene. In addition, sequencing across the region of insertion of GPT and eGFP using primers Left Flank FW, Right Flank REV, and GPT FOR confirmed *SOD* was replaced by the marker eGFP and selection marker (GPT) genes. Figure 3.15 shows the appearance of nLSDVdSOD-M at passage 7. Figure 3.19 shows PCR confirmation of this virus stock.

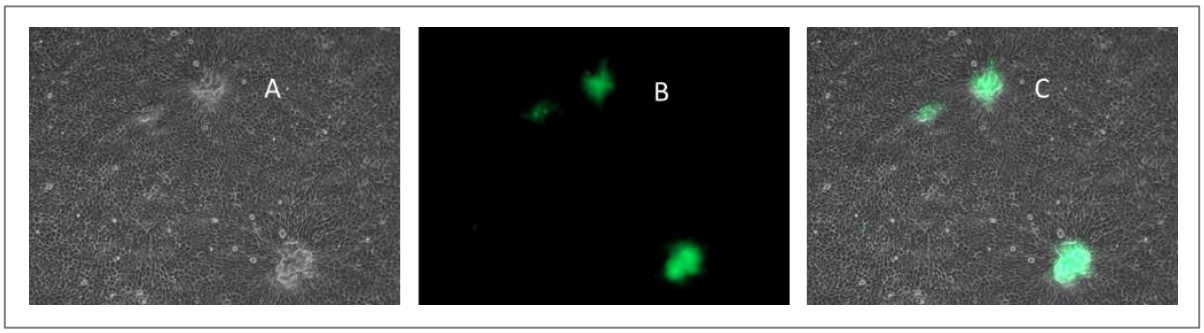

Figure 3.15. Appearance of MDBK cells infected with nLSDVdSOD-M recombinant virus after 7 passages (6 were done in the presence of MPA). A - phase contrast image, B - fluorescent image and C - a merged image. Imaging was done using a fluorescence microscope (Zeiss, Germany) using the 10X objective.

3.3.2.2 Isolation of nLSDVSODis-M

Once nLSDVdSOD-M was successfully made, this recombinant virus was used as parent virus in the generation of a SOD knock-in virus. Since nLSDVdSOD-M contains GPT and GFP, within the flanking regions 130 and 132, the second recombinant containing the stabilised form of *SOD* was inserted using part of the GPT gene and the right flank (132) as sites of homologous recombination. Included in this insert was mCherry which is a red fluorescing protein gene. After infecting lamb testes cells with nLSDVdSOD-M and transfecting with pHM2v3, red fluorescing cells were observed less than 24 hours post transfection (see Figure 3.16). The red fluorescing virus was purified by 2 rounds of picking. At passage 4, a single fluorescing focus was identified in a 96 well plate and expanded for further analysis.

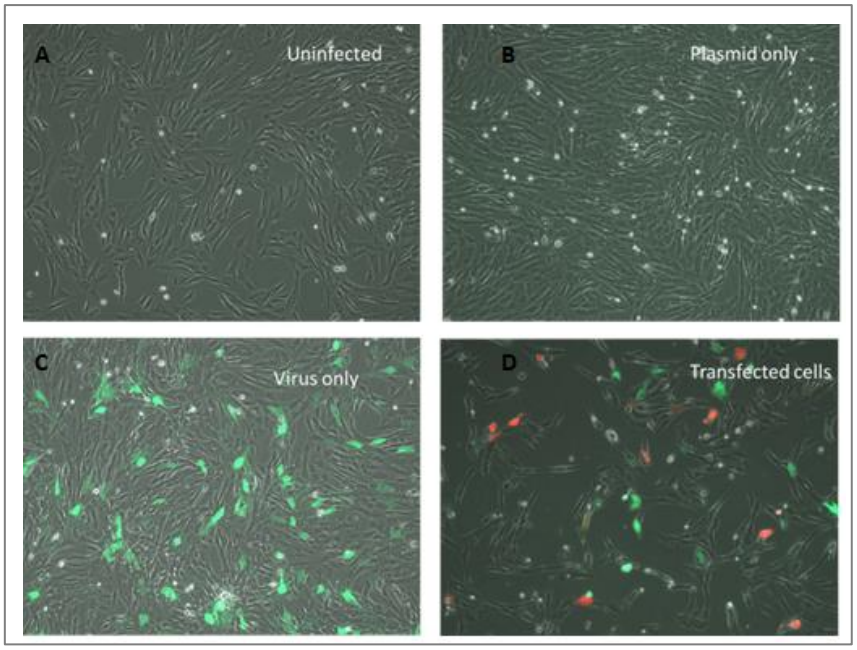

Figure 3.16. Transient expression of mCherry. Primary lamb testes cells were infected with nLSDVdSOD-M (which expresses GFP – green) at an MOI of 0.01 (C and D) and transfected with 3 ug of pHM 2v3 (B and D). Plasmid pHM2v3 contains mCherry which causes infected cells to fluoresce red. Figures show merged images. Appearance of uninfected cells (A), cells with plasmid only (B), infected cells with parent virus (C) and infected, transfected cells (D). Imaging was done using a fluorescence microscope (Zeiss, Germany) using the 10X objective.

After isolating the recombinant nLSDVSODis-M the virus was grown up to high titres in MDBK cells. Viral titration using TCID50 was done and the viral titre was determined as 10^8 $TCID_{50}$/ml. MDBK cells infected with nLSDVSODis-M were shown to express mCherry and not eGFP using fluorescence microscopy. This indicated that there was no parent virus present in the nLSDVSODis-M stock (Figure 3.17).

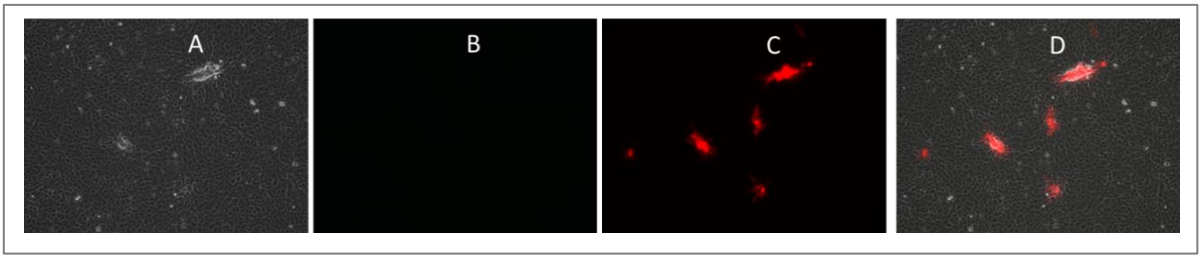

Figure 3.17. Fluorescence microscopy of cells infected with nSDVSODis-M. Appearance of cells infected with recombinant nLSDVSODis-M after 3 passages of cell lysate from Phase contrast (A), green fluorescence (B), red fluorescence (C) and a merged image (D). Infected MDBK cells were photographed 72 hours post infection. Imaging was done using a fluorescence microscope (Zeiss, Germany) using the 10X objective.

PCR confirmed that the desired insert was present in the LSDV genome and that no parent virus was present in the stock of recombinant nLSDVSODis-M (Figure 3.18). Primers that bound in the left flank and SOD region (130 FW and 131 REV), right flank and SOD region

(131 FW and 131 REV) were used to check if the desired recombinant was obtained. Primer set 130 FW and 131 REV generated a fragment of 1365bp (lane 4) from the recombinant and a fragment of 730bp from nLSDV (lane 2). The primer set 131 FW and 131 REV generated fragments of 300bp from both the recombinant nLSDVSODis-M and nLSDV (lanes 3 and 5) indicating the presence of the *SOD* gene in both these viruses.

Table 3.3 Primers used to detect presence of recombinant nLSDVSODis-M. Primer set A binds in the left flank and the *SOD* gene and primer set B binds in the *SOD* gene only. Primer set A produced PCR products of 730bp and 1365bp in lanes 2 and 4 in Figure 3.18. Primer set B produces PCR products of 300bp in lanes 3 and 5 (Figure 3.18). The respective fragment sizes are also listed. Primer sequences are found in **section 3.2.4.2**.

	Forward Primer	Reverse Primer	Primer set	Size of fragment	Lane in gel
nLSDV	HM 130 FW	HM 131 REV	A	730	2
nLSDVSODis-M	HM 131 FW	HM 131 REV	B	300	3
	HM 130 FW	HM 131 REV	A	1365	4
	HM 131 FW	HM 131 REV	B	300	5

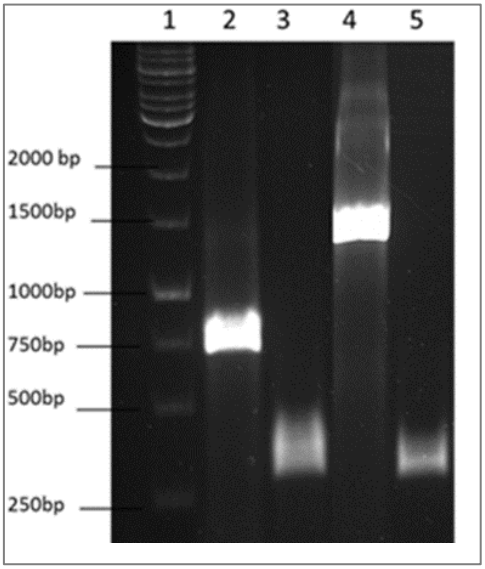

Figure 3.18. Confirmation of nLSDVSODis-M by PCR analysis. 1% gel electrophoresis image of amplified products from nLSDV (lanes 2 and 3) and nLSDVSODis-M (lanes 4 and 5) using primer sets A (lanes 2 and 4) and B (lanes 3 and 5). These primer sets generate fragments of 730bp from nLSDV (lane 2), 300bp from nLSDV (lane 3), 1365bp from nLSDVSODis-M (lane 4) and 300bp from nLSDVSODis-M (lane 5).

The two recombinant viruses nLSDVdSOD-M and nLSDVSODis-M were successfully made. The presence of *SOD* was confirmed by PCR with a forward primer outside the left flank (LSDV 129 FOR) and another inside the right flank (LSDV 132 REV). The regions where

these primers bound and the fragments they generated is shown in Figure 3.19. The gel image in Figure 3.19B shows that the recombinants were successfully obtained.

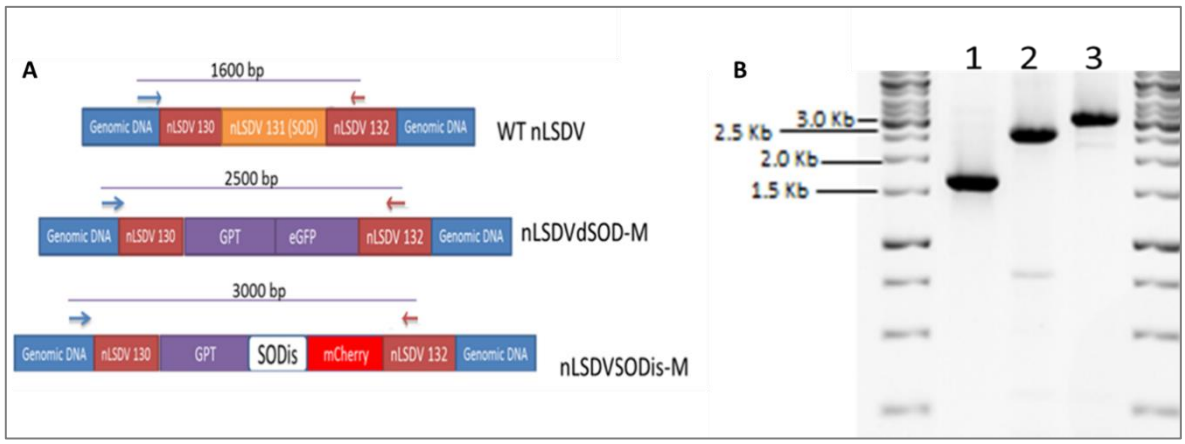

Figure 3.19. A – Diagram to show primer binding sites and fragments generated from recombinants nLSDVSODis-M and nLSDVdSOD-M. Primer 129 forward binds in the LSDV 129 region and Primer 132 reverse in the LSDV132 region. They generate PCR fragments of 1600bp in nLSDV, 2500bp in nLSDVdSOD-M and 3000bp in nLSDVSODis-M. B – 1% Agarose gel electrophoresis of PCR products from nLSDV (lane 1), nLSDVdSOD-M (lane 2) and nLSDVSODis-M (lane 3).

3.3.2.3 Construction of nLSDVdSOD-UCT and nLSDVSODis-UCT

In the final part of the project, two more recombinant LSDVs were constructed, one with the SOD homologue deleted and one with the Neethling SOD homologue replaced by *SODis*, but no reporter genes were present in these recombinants. This was to confirm that the differences observed were due to the SOD homologues and not the two different reporter genes or GPT. Transfer vectors pHM1dSOD and pHM1-SOD_pos were made to generate nLSDVdSOD-UCT and nLSDVSODis-UCT respectively (Figure 3.20). Sanger sequencing confirmed these plasmids.

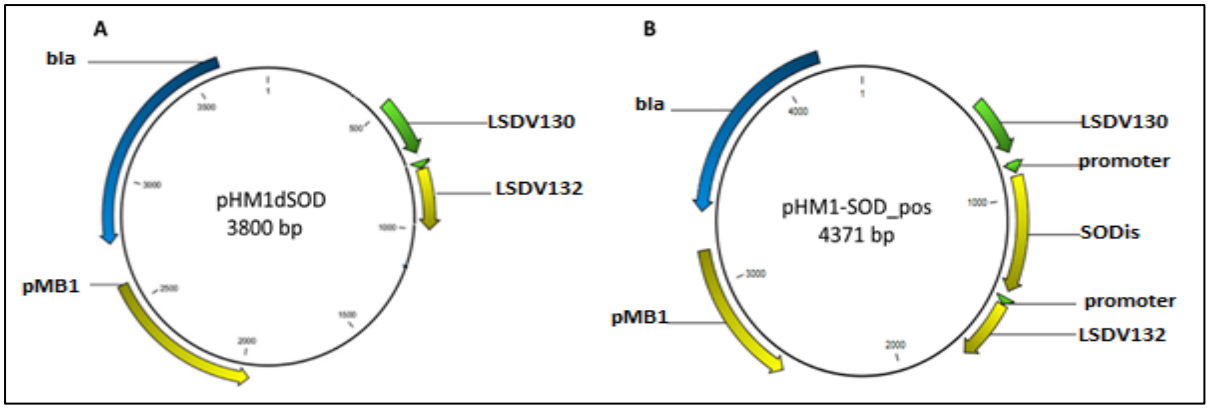

Figure 3.20. A – plasmid map of transfer vectors pHM1dSOD and B - pHM1-SOD_pos used to construct nLSDVdSOD-UCT and nLSDVSODis-UCT respectively. Plasmids contain an ampicillin resistance gene (bla) and an origin for replication (pMB1).

The two recombinant viruses without markers, nLSDVdSOD-UCT and nLSDVSODis-UCT were successfully made as described in section 3.2.4.3. PCR was performed using a forward primer that binds outside the left flank (LSDV 129 FOR) and another inside the right flank (LSDV 132 REV) to confirm the recombinants. The regions where these primers bound and the fragments they generated is shown in Figure 3.21. Figure 3.21 B shows that the recombinants were successfully obtained. nLSDVSODis-UCT produced a PCR fragment of the expected size of 1600bp (lane 1), as did nLSDV (lane 3). The expected fragment of 1100bp was generated from nLSDVdSOD-UCT (lane 4) and a 2500bp fragment was generated from nLSDVdSOD-M (lane 2).

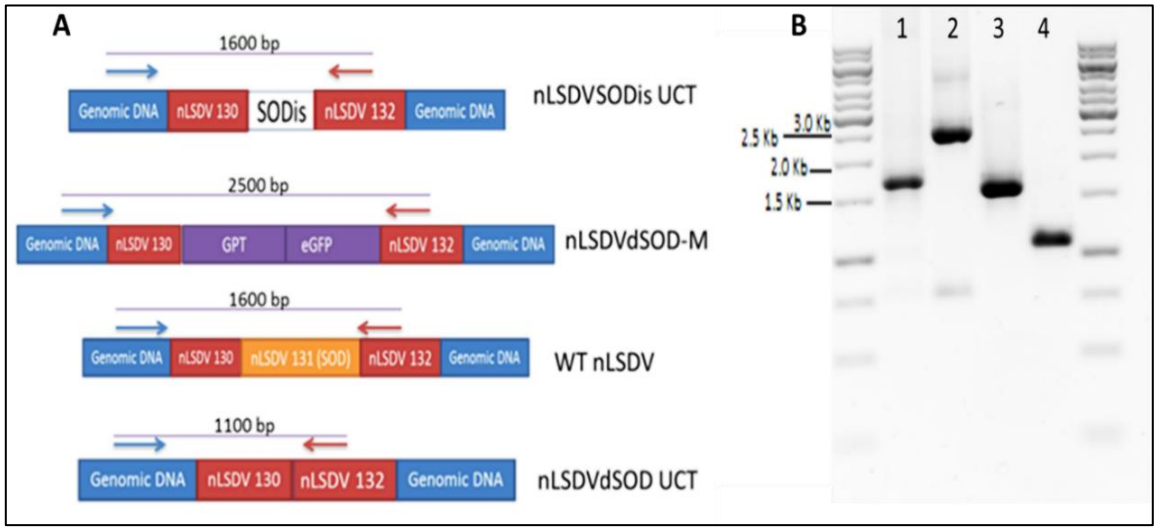

Figure 3.21. A – Diagram to show primer binding sites and fragments generated from recombinants nLSDVdSOD-UCT and nLSDVSODis-UCT. Primer 129 forward binds in the LSDV 129 region and Primer 132 reverse in the LSDV132 region.. **B – 1% Agarose gel electrophoresis of PCR products**. DNA was amplified from nLSDVSODis-UCT (lane 1), nLSDVdSOD-M (lane 2), nLSDV (lane 3) and nLSDVdSOD-UCT using primers 129 forward and 132 reverse.

3.3.4 Growth of parent LSDV vaccines and recombinants in cell culture.

The recombinant viruses without markers, nLSDVdSOD-UCT and nLSDVSODis-UCT were compared with respect to growth in MDBK cells (Figures 3.22 and 3.23). Cytopathic effect, indicated by cell foci and gaps in the monolayer, was seen earlier in MDBK cells infected with nLSDVSODis-UCT compared to nLSDVdSOD-UCT (Figure 3.22). This could have influenced virus yield as at day 5, most nLSDVSODis-UCT infected cells were dead as shown by the morphology of cells and presence of gaps. Hence day 5 was removed from the growth curve shown in Figure 3.22. Virus yield from nLSDVdSOD-UCT infected cells appeared to be lower than that of nLSDVSODis and nLSDV infected cells at 1-day post infection. Days 2-4 post infection, there was an increased growth of nLSDV with significant difference between virus yield from nLSDV infected cells compared to nLSDVdSOD-UCT infected cells ($p<0.01$) and not nLSDVSODis-UCT ($p>0.05$) (Figure 3.23).

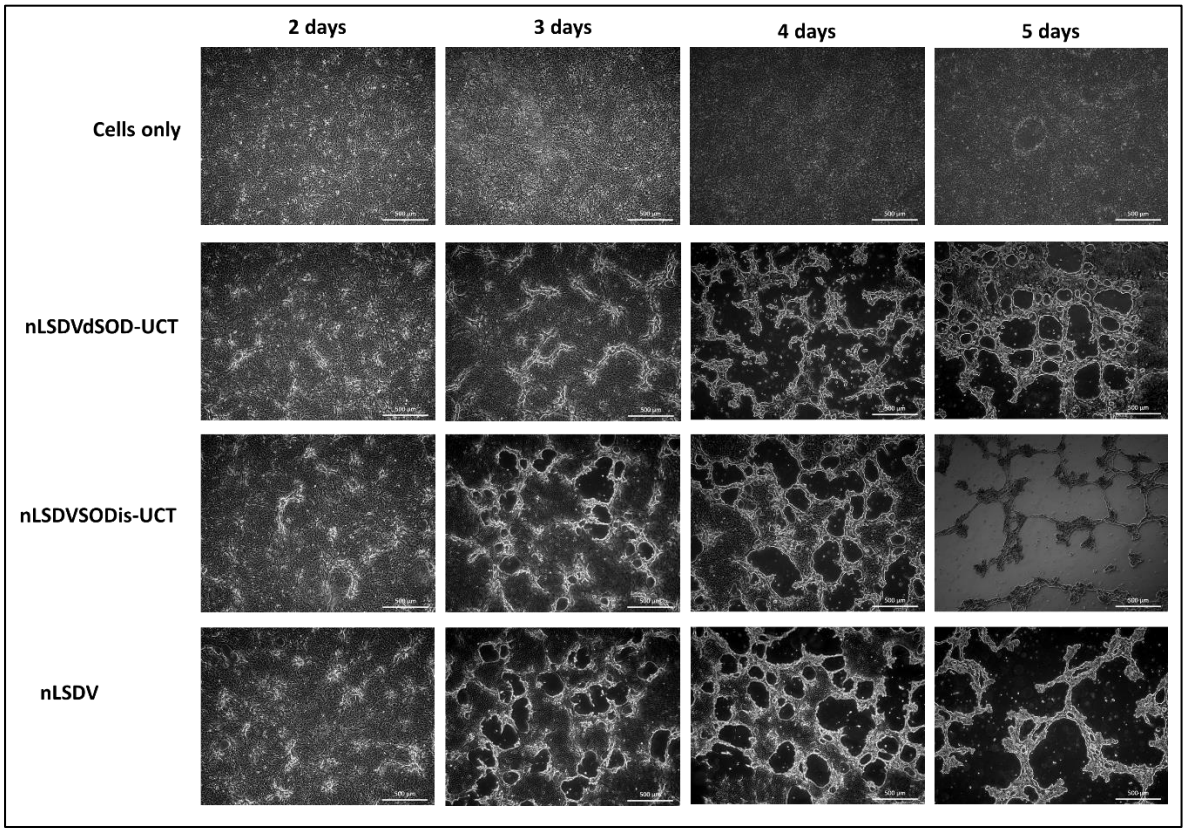

Figure 3.22. MDBK cells uninfected or infected with nLSDVdSOD-UCT, nLSDVSODis-UCT or nLSDV at an MOI of 0.015. A. Monochrome light inverted microscopic images were taken at time points as indicated.

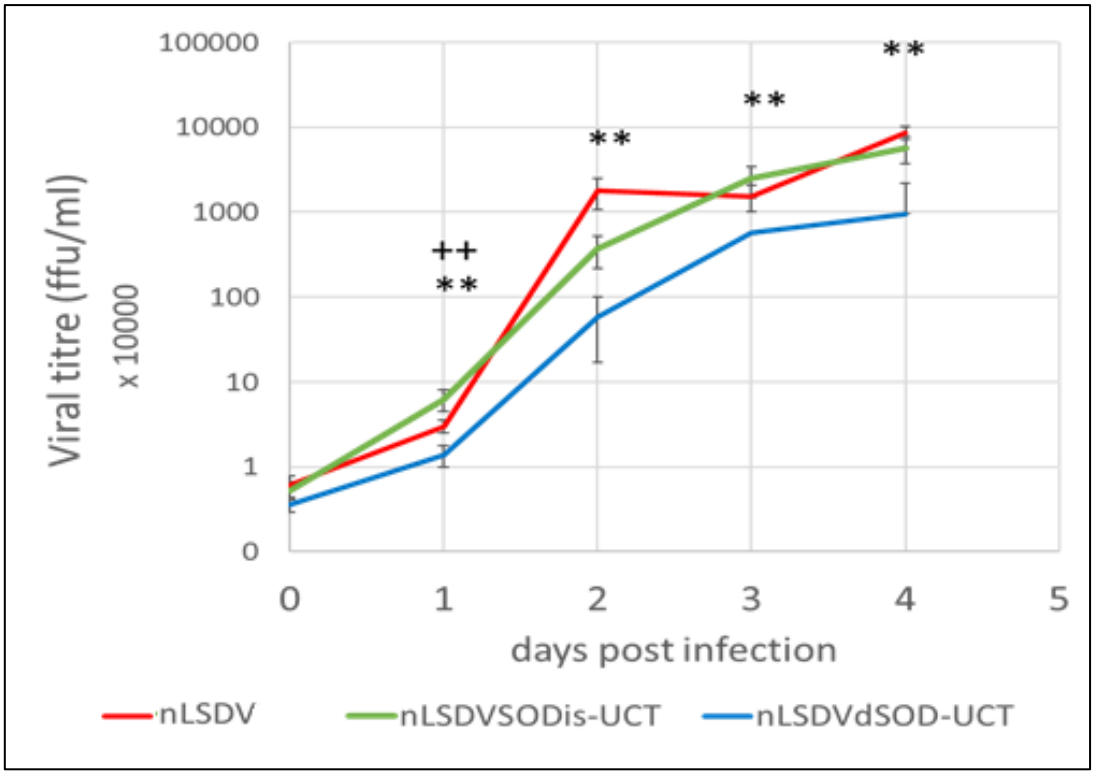

Figure 3.23. Growth curves of nLSDV (red), nLSDVSODis-UCT (green) and nLSDVdSOD-UCT (blue) in MDBK cells. Cells were infected at an MOI of 0.015 in triplicate and lysates were prepared 2 hours post infection and at subsequent 1-day intervals. Titrations were performed using the TCID50 method and titres were converted to ffu/ml. A one-way ANOVA was done on each time point, n=3. Post-hoc T-test was performed to identify which titres at which time points were significantly different from another. The symbol ** represents a significance level of $p<0.01$. The symbol ++ represents a difference between nLSDVdSOD-UCT and nLSDVSODis-UCT at $p<0.01$. Data points denote mean and error bars SEM.

3.3.5 Growth of vaccines and recombinants on CAMs

Virus was isolated and titrated from chorioallantoic membranes (CAMs) of 7-day-old fertilised eggs which were infected with nLSDV, nLSDVdSOD-UCT and nLSDVSODis-UCT. The growth curves of the three viruses, nLSDV, nLSDVdSOD-UCT and nLSDVSODis-UCT are shown in Figure 3.24.

Looking at the virus yield per day, there was lower viral yield from CAMs infected with nLSDVdSOD-UCT compared to nLSDV and nLSDVSODis-UCT at days 4 and 5 (Figure 3.25).

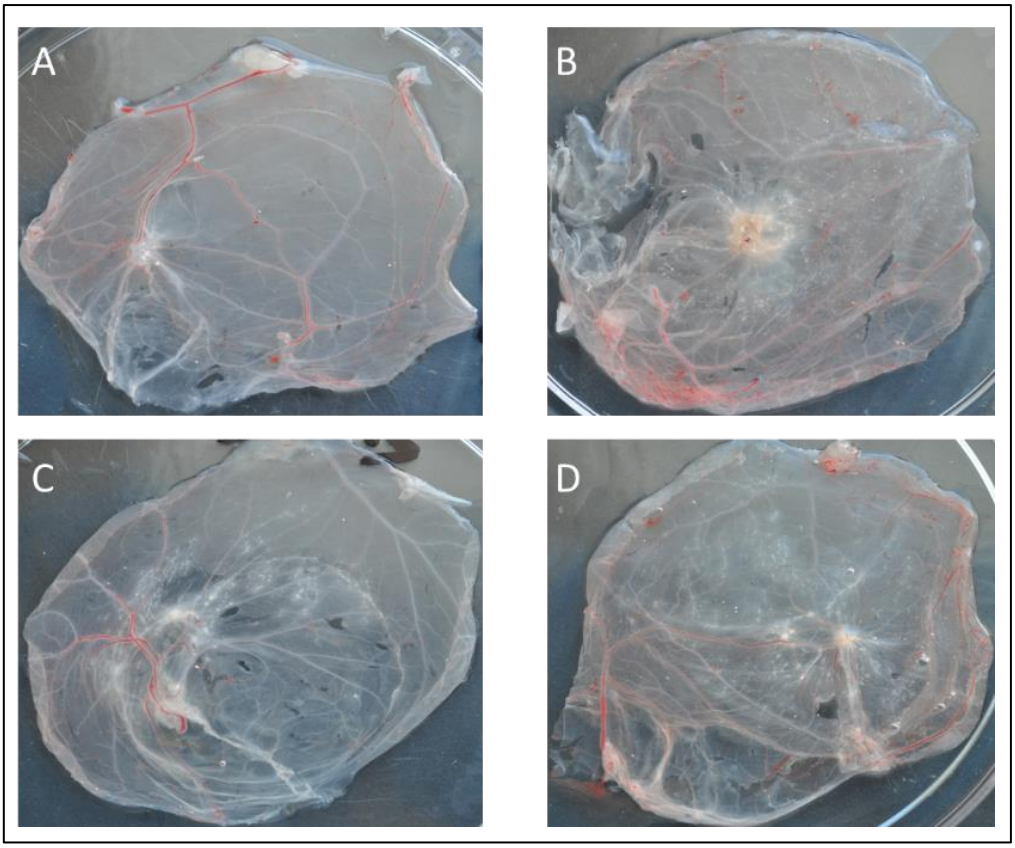

Figure 3.24. Macroscopic appearance of infected chick CAMs on day 5 post infection. 7-day-old embryonated hens' eggs were inoculated with PBS (A), nLSDV (B), nLSDVdSOD-UCT (C), nLSDVSODis-UCT (D). Membranes were collected daily for 5 days in triplicate. Representative images are shown.

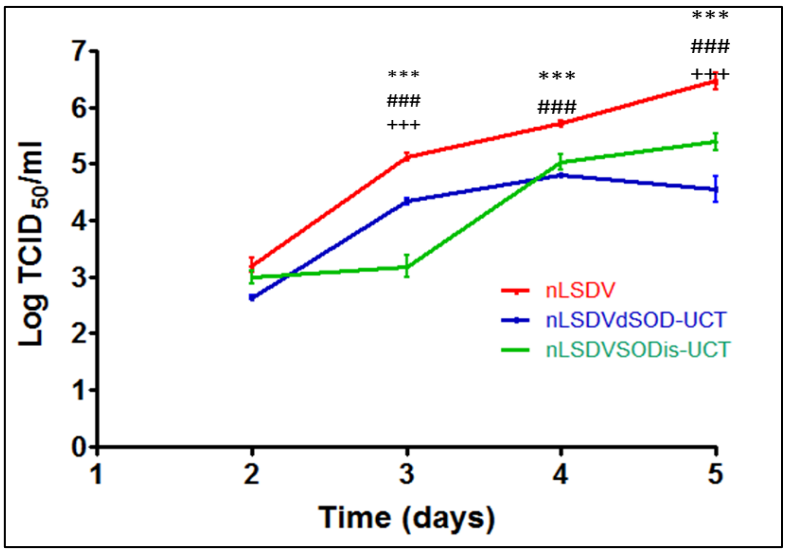

Figure 3.25. Growth curves of nLSDV, nLSDVdSOD-UCT and nLSDVSODis-UCT on CAMs of fertilized hens' eggs. 7-day-old fertilized hens' eggs were infected with virus at 10^3 TCID50 per egg and incubated at 34 °C. Eggs were harvested daily from Day 0 to Day 5, triplicate membranes were pooled and crude virus extracts were titrated. One-way ANOVA was done at each time point and Tukey post-hoc was performed to identify which titres at which time points were significantly different from another. The symbols represent a significance level of $p<0.001$. The symbol * represents difference between nLSDV and nLSDVdSOD-UCT, the symbol # difference between nLSDV and nLSDVSODis-UCT and the symbol + represents the difference between nLSDVdSOD-UCT and nLSDVSODis-UCT. Data points denote mean and error bars SEM.

3.3.6 Histopathology of CAMs infected with viruses

CAMs of fertilised hens' eggs infected with nLSDV, nLSDVdSOD-M, nLSDVSODis and Herbivac (described section 3.2.6) were examined histologically at day 6, when the mean titre of all the viruses were approximately $10^{6.0}$ $TCID_{50}$/ml. Figure 3.26 shows H&E staining of the sections. Comparing nLSDV and Herbivac (Figure 3.26) there was notable proliferation of fibroblasts as well as increased immune cell infiltration in the mesoderm of Herbivac-infected CAMs. When comparing nLSDVdSOD-M and nLSDVSODis-M **(**Figure 3.26**)** there was pronounced ectodermal thickening in CAMs infected with nLSDVSODis-M. There was a loss of fibroblasts in nLSDVdSOD-M infected cells whereas proliferation of fibroblasts in the mesoderm of nLSDVSODis infected CAMs was observed. There was a lot of vacuolation in the mesoderm of nLSDV infected CAMs and nLSDVdSOD-M infected CAMs. There was also ballooning degeneration (cell death) in the epithelial layers of nLSDVdSOD-M and nLSDVSODis-M infected CAMs. The level of ballooning degeneration was comparable in CAMs infected with nLSDVdSOD-M and nLSDVSODis-M. It could not be concluded which infection had the most ballooning degeneration because nLSDVSODis-M had a lot of proliferation in the epithelial layers which could have replaced the dying cells with newer ones.

Recombinant vaccines nLSDVdSOD-UCT and nLSDVSODis-UCT were also characterised based on their differences in histology on CAMs (Figure 3.27). For this experiment 5 sections were prepared from a single membrane collected on days 1, 3 and 5 post infection. The grade of inflammation, epithelial hyperplasia and presence of inclusions progressively increased from day 1 to day 5. Major differences were noted at day 5 post infection (Table 3.3). Inflammation in the mesoderm and chorionic epithelial hyperplasia achieved the highest score by day 5 and in general; the nLSDV and nLSDVSODis-UCT achieved higher scores (more intense inflammation) for each time point - than nLSDVdSOD-UCT (Table 3.3 and Figure 3.27). Hyperplasia and viral inclusions were absent in the control section (PBS). There was increased ballooning degeneration associated with nLSDVdSOD-UCT and nLSDV infection which was absent in nLSDVSODis-UCT infected CAMs. Intracytoplasmic viral inclusions were observed more often in the sections of nLSDVSODis-UCT, compared to nLSDV and nLSDVdSOD-UCT. Vacuolar change (ballooning) often accompanied the inclusions in sections of nLSDV and nLSDVSODis-UCT.

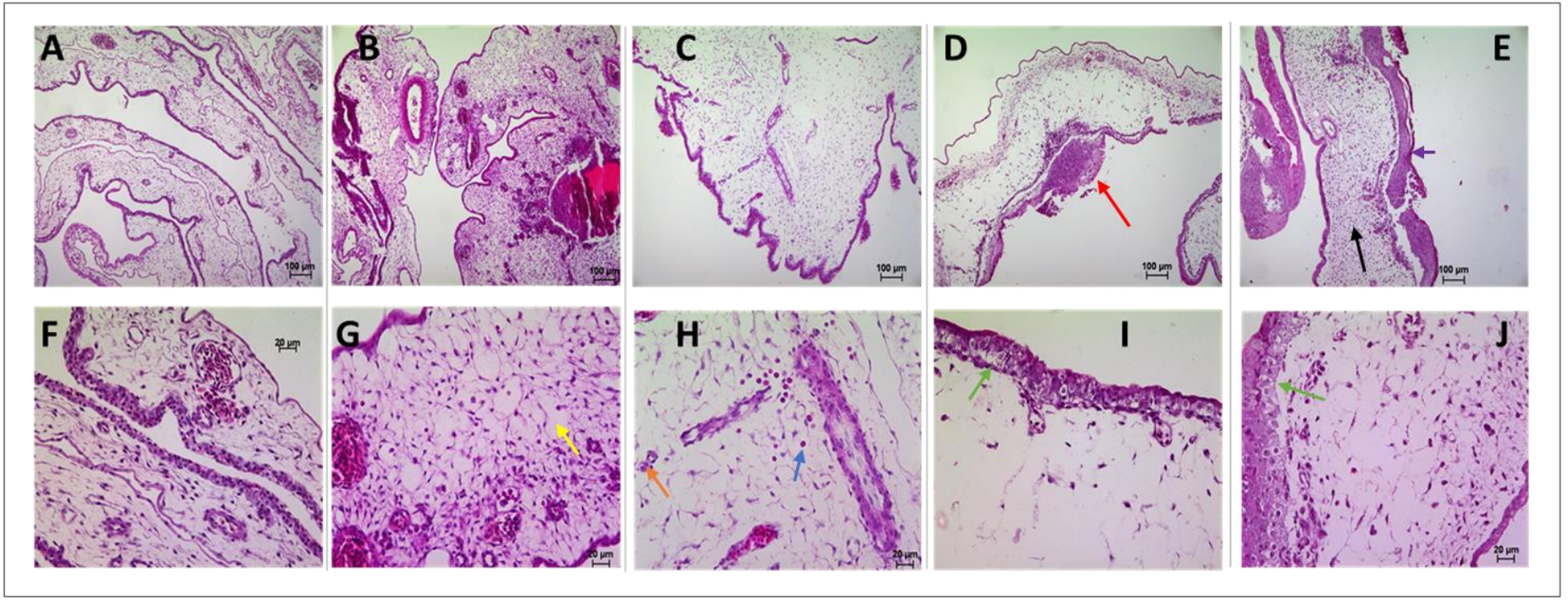

Figure 3.26. H&E staining of fixed membranes 6 days post inoculation with PBS (A & F), nLSDV (B & G), Herbivac (C & H), nLSDVdSOD-M (D & I) and nLSDVSODis-M (E & J). Membranes were fixed in buffered formalin at day 6 where their mean titre was 10^6 $TCID_{50}$/ml. Arrows indicate vacuolation (yellow arrow), angiogenesis/vascularisation (orange arrow), immune cell infiltration (blue arrow), ballooning degeneration/cell death (green arrow) and fibroplasia (black arrow). Purple arrow shows ectodermal thickening and the red arrow shows a pock on the membrane. Upper panel shows low magnification (100X) and the bottom panel higher magnification (400X).

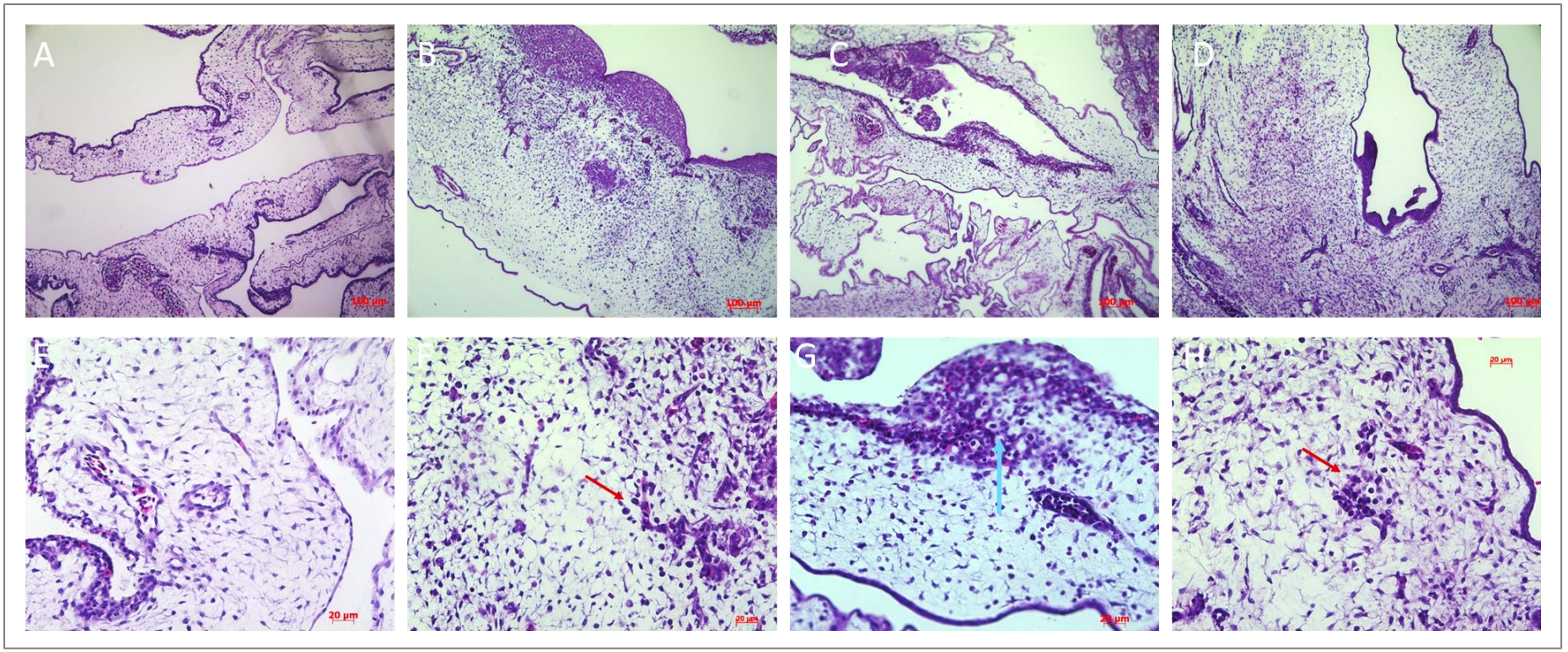

Figure 3.27. H&E staining of fixed membranes 5 days post inoculation with PBS (A & E), nLSDV (B & F), nLSDVdSOD-UCT (C & G), nLSDVSODis-UCT (D & H). Membranes were fixed in buffered formalin at day 5. Arrows indicate immune cell infiltration (red arrow) and ballooning degeneration/cell death (blue arrow). Upper panel shows low magnification (100X) and the bottom panel higher magnification (400X).

Table 3.3. Histology. Chorioallantoic membranes (CAMs) were inoculated with PBS, nLSDV, nLSDVdSOD-UCT and nLSDVSODis-UCT. Day 5 formalin fixed, and paraffin embedded sections were stained by haematoxylin and eosin using routine methods. Scoring was done based on presence of intracytoplasmic inclusions, epithelial hyperplasia and inflammatory changes.

Chorioallantoic membranes: Histological changes						
Sample	**Section**	**Intracytoplasmic inclusions**	**Epithelial hyperplasia**		**Inflammatory changes**	**Additional comments**
			Chorionic	**Allantoic**	**Mesoderm**	
nLSDV	A	+	4	2	5	ballooning and inclusions
	B	+	4	1	4	
	C	+	4	1	5	
	D	+	5	1	5	
	E	+	4	1	5	
nLSDVdSOD-UCT	A	+	2	1	3	-
	B	+	3	2	3	ballooning degeneration
	C	+	3	2	2	ballooning degeneration
	D	+	3	1	3	-
	E	+	3	2	3	-
nLSDVSODis-UCT	A	+	4	1	5	-
	B	+	4	1	4	-
	C	+	2	0	3	-
	D	+	3	0	4	-
	E	+	4	1	5	high numbers of inclusions (chorion)
PBS	A	-	0	0	0	-
	B	NP	NP	NP	NP	-
	C	NP	NP	NP	NP	-
	D	NP	NP	NP	NP	-
	E	NP	NP	NP	NP	-

0 - Not detectable; **1 - Minimal** (Barely detectable in a minority of fields); **2 – Mild** (Barely detectable, but present in most fields); **3 - Moderate** (Clearly visible in at least 50% of fields); **4 - Marked** (Clearly visible in more than 50% of fields); **5 - Severe** (Outspoken changes in the majority of fields); **NP** (Not performed)

The inflammatory scores from each section in Table 3.3 were averaged and the results are presented in Figure 3.28. Bars represent the inflammatory score and standard error of the mean (SD). There is a significant decrease in the inflammatory score of nLSDVdSOD-UCT compared to nLSDV ($p < 0.001$) and nLSDVSODis-UCT ($p < 0.01$). There was no significant difference in the number of immune cells infiltrating the mesoderm of nLSDV and nLSDVSODis-UCT infected CAMs (Figure 3.28). This suggested a role for the truncated SOD in immune infiltration which, when deleted, is lost.

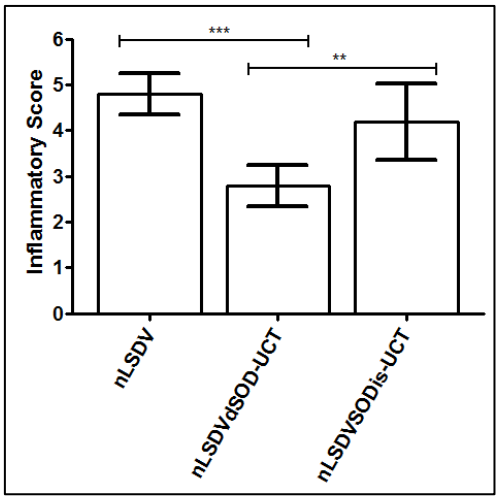

Figure 3.28. Immune infiltration in H&E stained sections. CAMs infected for 5 days were washed, fixed with 4% buffered formalin, embedded, sectioned and stained with haematoxylin and eosin. Five consecutive sections were evaluated under the light microscope and scored for inflammation (oedema, haemorrhage and infiltration with white blood cells). One-way ANOVA and Tukey post hoc testing was used to test for significance. The symbol *, **, *** represents a significance level of $p<0.05$, $p<0.01$ and $p<0.001$ respectively. Bars denote mean and standard deviation.

3.3.7 Effect of the LSDV superoxide homologues on activity of cellular SOD activity

SOD activity in MDBK cells infected with nLSDV, Herbivac, nLSDVdSOD-M and nLSDVSODis-M was measured at 3 different time points post infection using a SOD determination kit (Sigma, USA). No significant difference in SOD activity could be detected between the different viruses at any of the time points post infection (2 hrs, 6 hrs and 24 hours) (Figure 3.29).

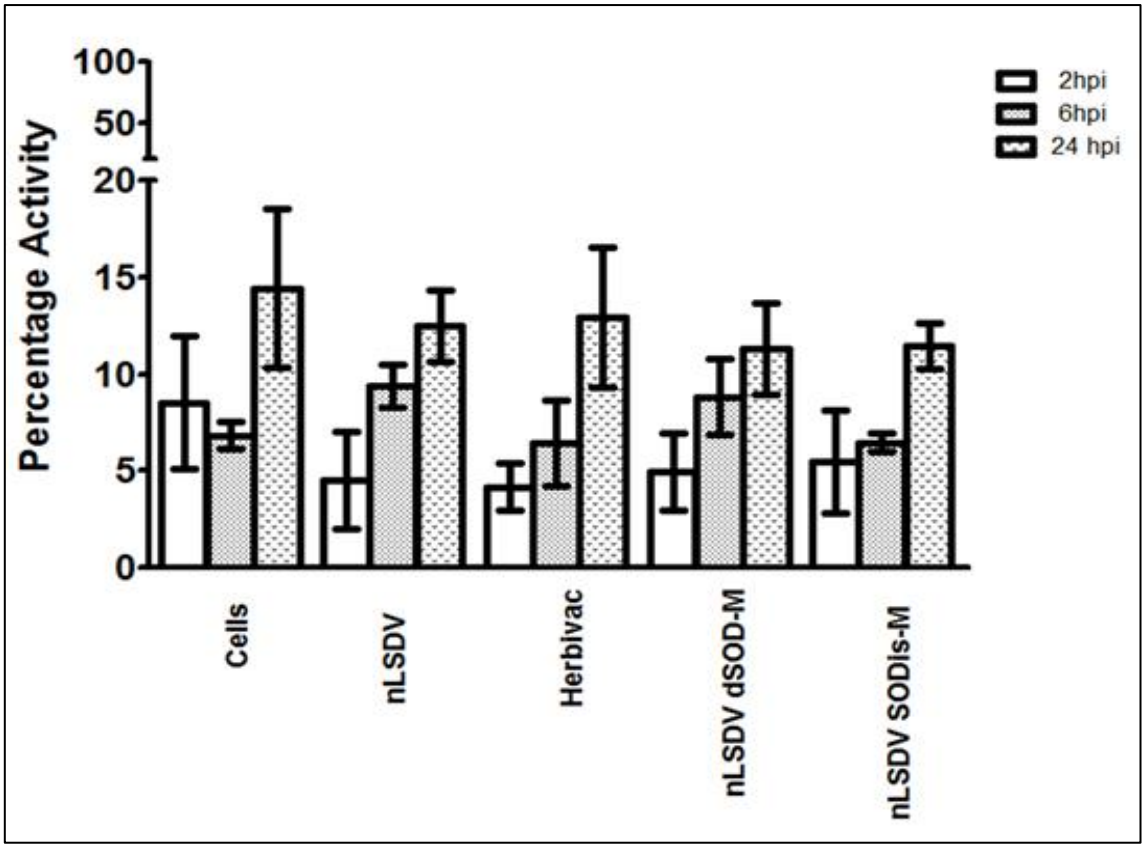

Figure 3.29. Total SOD activity. MDBK cells were infected for 2, 6 and 24 hours and lysed using a lysis buffer and mechanical disruption. SOD activity was normalised to amount of protein loaded. Bars represent mean percentage SOD activity. Experiment was done at 2, 6 and 24 hours post infection (hpi). No significant differences at $p<0.05$ were observed between viral infections at any time (One-way ANOVA). Bars denote mean and error bars SEM.

3.3.8 Induction or inhibition of apoptosis / necrosis by viruses

An experiment to determine the ability of the different LSDVs to induce cell death and to inhibit camptothecin induced cell death was done. At two hours post infection with LSDVs at an MOI of 10, there was significantly increased apoptosis in MDBK cells infected with nLSDVSODis-M ($p < 0.001$) compared to nLSDV, Herbivac or nLSDVdSOD-M (Figure 3.30A). Six hours post infection, there was increased apoptotic cell death induced by Herbivac and nLSDVSODis-M relative to cells, but no significant increase in apoptosis induced by nLSDV and nLSDVdSOD-M (Figure 3.30B).

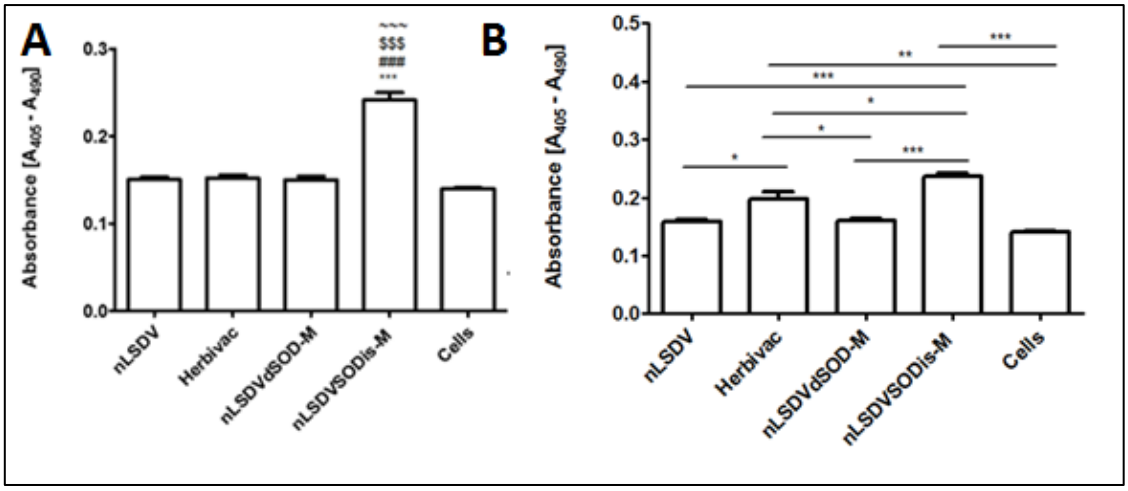

Figure 3.30. Apoptotic cell death detection. MDBK cells were either uninfected or infected with nLSDV, Herbivac, nLSDVdSOD-M and nLSDVSODis-M at an MOI of 10. Bars represent absorbance which is proportional to the amount of oligonucleosomes released in the cytoplasm of apoptotic cells. **A** - After 2 hours of infection, media was removed, and the cells lysed. The Roche cell death detection ELISAPLUS kit was the used to measure the number of nucleosomes released from the cells. The three symbols *** represents a significance level of $p<0.001$. Symbols *, ~, $, #, represent significance level of nLSDVSODis-M compared with cells, nLSDV, Herbivac and nLSDVdSOD-M respectively. **B** - After 6 hours of infection, media was removed, and the cells lysed. The Roche cell death detection ELISAPLUS kit was the used to measure the number of nucleosomes released from infected cells only. The symbol *, **, *** represents a significance level of $p<0.05$, $p<0.01$ and $p<0.001$ respectively. Bars denote mean and error bars SEM.

The effect of virus on apoptosis in MDBK cells was most noticeable at 24 hours post infection (Figure 3.31). Viruses nLSDVSODis-M and Herbivac had comparable induction of cell death by virus only. Viruses nLSDV and nLSDVdSOD-M had comparable induction of cell death, however, the level of induction of apoptosis was lower than the level of induction observed for nLSDVSODis-M and Herbivac.

In addition to measuring the induction of apoptosis by viruses at 24 hours post infection the inhibition of camptothecin induced apoptosis was measured. As can be seen in Figure 3.31 (B-D), all viruses effectively inhibited apoptosis showing that LSDV encodes anti-apoptotic gene products. When the absorbance values for infected cells without camptothecin were taken as baseline values of cell death and the camptothecin induced cell death values were used to denote induction or inhibition of apoptosis, all viruses inhibited camptothecin induced apoptosis (Figure 3.31C). Of note, there was greater inhibition of camptothecin induced apoptosis following infection with Herbivac and nLSDVSODis-M compared to nLSDV and nLSDVdSOD-M (Figure 3.31D) in MDBK cells.

Cell death by necrosis was investigated 24 hours post infection. All viruses tested induced necrosis relative to uninfected cells. However, there was increased necrotic cell death after infection with nLSDVSODis-M and Herbivac compared to nLSDV and nLSDVdSOD-M

(Figure 3.32**)**. Upon inducing cell death with camptothecin (1µg/ml), the ability of viruses to inhibit necrotic cell death was investigated. When necrosis was induced using camptothecin there was inhibition of necrosis by all 4 viruses shown by an enrichment factor of 1 compared to uninfected cells with an enrichment score of 4 (Figure 3.32C).

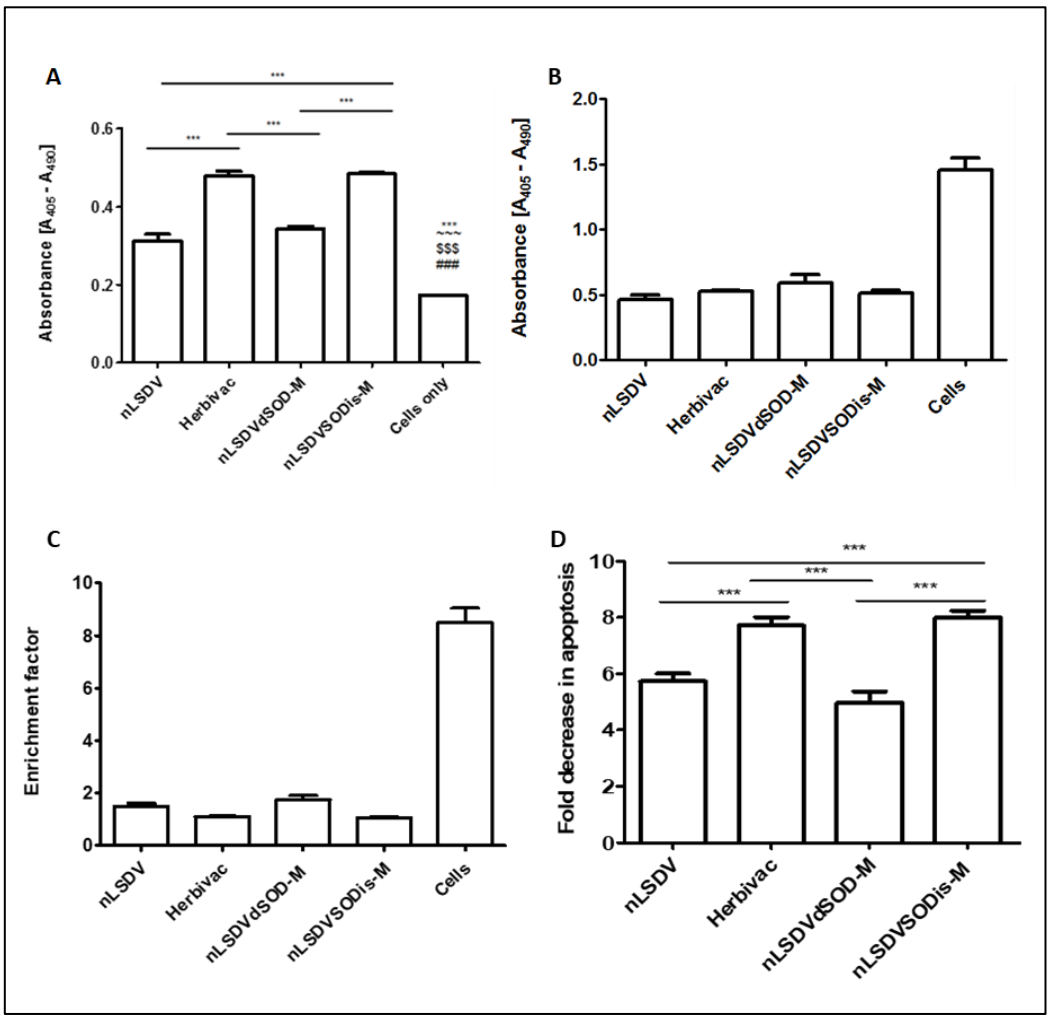

Figure 3.31. Apoptotic cell death detection. **A – Induction of apoptotic cell death.** MDBK Cells were either uninfected or infected with nLSDV, Herbivac, nLSDVdSOD-M or nLSDVSODis-M at an MOI of 1. After 24 hours of infection, media was removed, and the cells lysed. The Roche cell death detection ELISAPLUS kit was the used to measure the number of nucleosomes released. Bars represent absorbance which is proportional to the amount of oligonucleosomes released in the cytoplasm of apoptotic cells. The symbol *, **, *** represents a significance level of $p<0.05$, $p<0.01$ and $p<0.001$ respectively. **B - Inhibition of apoptotic cell death.** MDBK Cells were either uninfected or infected with nLSDV, Herbivac, nLSDVdSOD-M or nLSDVSODis-M and apoptosis induced using 1µg/ml camptothecin. **C - Apoptosis enrichment factor of MDBK cells.** The absorbance of dying cells (CAM induced cell death) was divided by the absorbance of infected cells or cells only (control) without camptothecin to establish the number of mono/oligonucleosomes released after CAM treatment. An enrichment factor of >1 means there was camptothecin induced cell death whereas a value of 1 means there was no camptothecin induced cell death. A value of < 1 shows there was inhibition of camptothecin induced cell death. **D - Inhibition of camptothecin induced apoptosis.** The enrichment factor of infected cells was normalised to the enrichment factor of uninfected cells to obtain the fold decrease in apoptosis. Graphs represent the mean + S.E.M of 3 biological experiments. To compute the fold decrease in absorbance, the enrichment factor after CAM induction of apoptosis for cells was divided by the enrichment factor of virus infected cells A high fold decrease in apoptosis shows the extent to which the virus inhibits camptothecin induced apoptosis. The symbol *, **, *** represents a significance level of $p<0.05$, $p<0.01$ and $p<0.001$ respectively. Bars denote mean and error bars SEM.

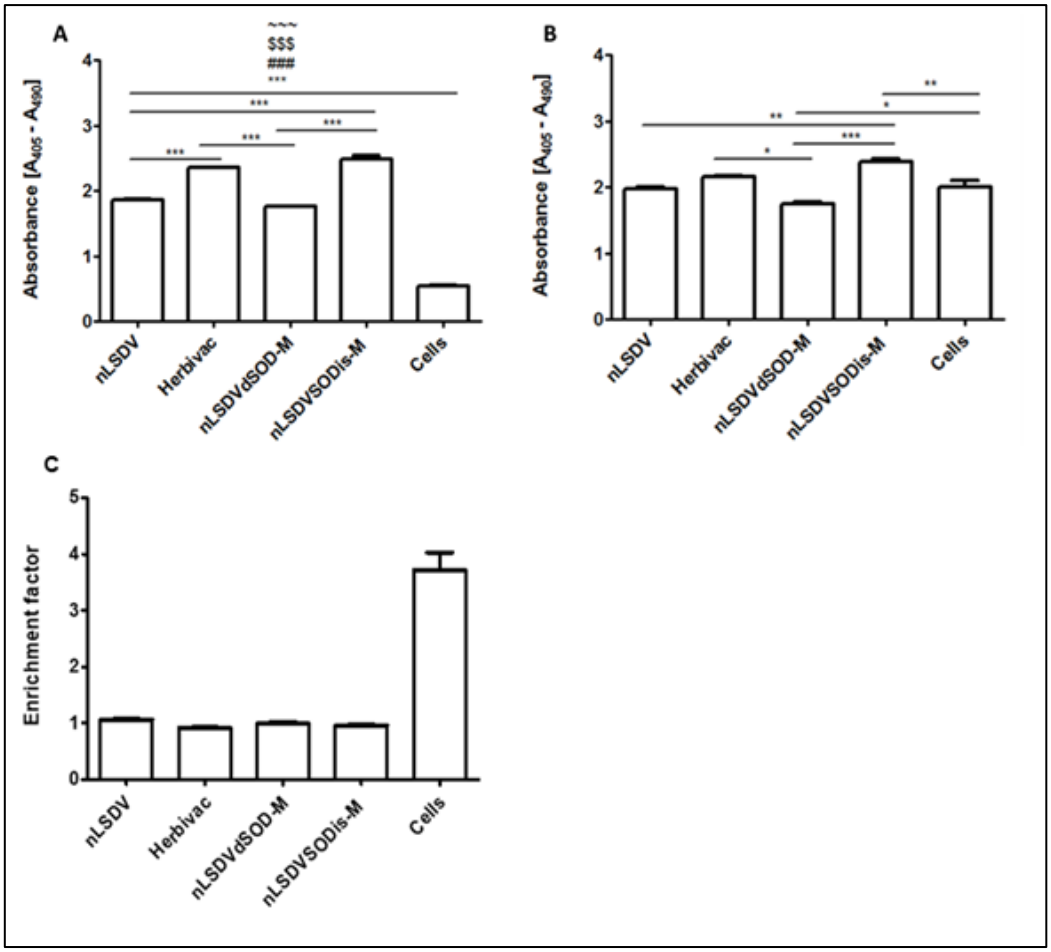

Figure 3.32. Necrotic cell death detection. A – Induction of necrosis by viruses. MDBK cells were either uninfected or infected with nLSDV, Herbivac, nLSDVdSOD-M or nLSDVSODis-M. They were tested for cell death 24 hours post infection. Media in which cells were growing was used to investigate the amount of oligonucleosomes released by necrotic cells. Uninfected cells were used as a negative control. Bars represent absorbance which is proportional to the amount of oligonucleosomes released in the cytoplasm of apoptotic cells. The symbol *, **, *** represents a significance level of $p<0.05$, $p<0.01$ and $p<0.001$ respectively. Symbols *, ~, $, #, represent significance level of necrosis of cells compared with nLSDV, Herbivac and nLSDVdSOD-M and nLSDVSODis-M respectively. **B - Inhibition of necrotic cell death**. MDBK cells were either uninfected or infected with nLSDV, Herbivac, nLSDVdSOD-M or nLSDVSODis-M and necrosis induced using 1µg /ml camptothecin. Note camptothecin in equal amounts was added to all viruses and cells. Measurement was done 24 h.p.i and post CAM addition. **C - Necrosis enrichment factor in MDBK cells.** The absorbance of dying cells (CAM induced cell death) was divided by the absorbance of infected cells or cells only (control) without camptothecin to establish the number of mono/oligonucleosomes released after CAM treatment. An enrichment factor of >1 means there was camptothecin induced cell death whereas a value of 1 means there was no camptothecin induced cell death. A value of < 1 shows there was inhibition of camptothecin induced cell death. The symbol *, **, *** represents a significance level of $p<0.05$, $p<0.01$ and $p<0.001$ respectively. Bars denote mean and error bars SEM.

The first experiments were done in a permissive cell line where LSDV was able to replicate. The ability or inability of the four viruses to induce or inhibit apoptosis in a non-permissive cell line, HeLa S3, was also tested with nLSDV, Herbivac, nLSDVdSOD-M and nLSDVSODis-M at an MOI of 10 with and without camptothecin (100µg/ml). Using the cell death detection ELISA to determine induction or inhibition of apoptosis or necrosis, there was no significant difference in the number of oligonucleosomes released after 24 hours. However,

upon addition of camptothecin, a trend towards inhibition of camptothecin induced apoptosis by nLSDV, Herbivac and nLSDVSODis-M was shown. Virus nLSDVdSOD-M is the only one that did not show a trend in apoptosis inhibition. (Figure 3.33B).

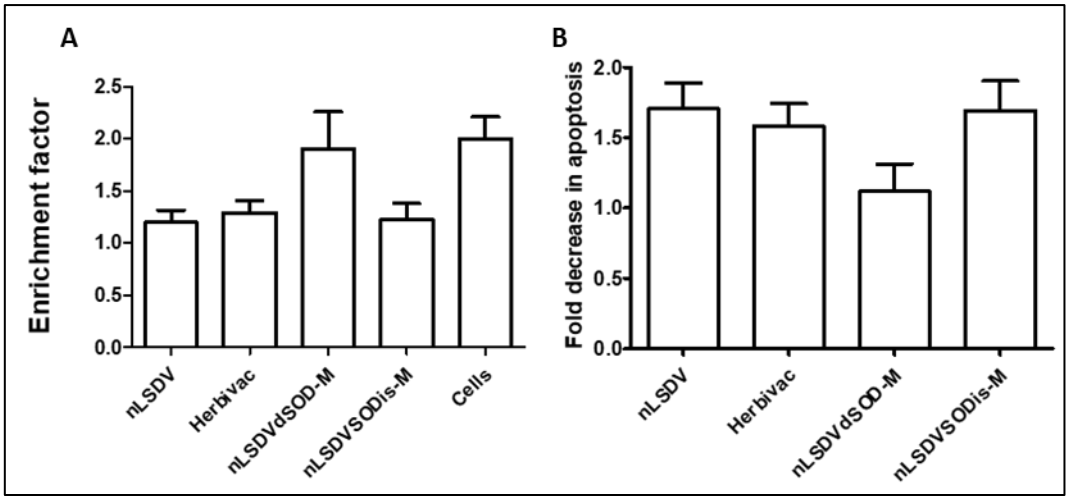

Figure 3.33. Apoptosis enrichment factor of HeLa S3 cells 24 h.p.i. A – Induction of apoptosis. The absorbance of dying cells (CAM induced cell death) was divided by the absorbance of infected cells or cells only (control) without camptothecin to establish the number of mono/oligonucleosomes released after CAM treatment. An enrichment factor of >1 means there was camptothecin induced cell death whereas a value of 1 means there was no camptothecin induced cell death. A value of < 1 shows there was inhibition of camptothecin induced cell death. Camptothecin was used at a concentration of 100µg /ml**. B - Inhibition of camptothecin induced apoptosis.** HeLa S3 cells were infected with nLSDV, Herbivac, nLSDVdSOD-M and nLSDVSODis-M at an M.O.I of 10. Apoptosis was induced by adding camptothecin to infected cells. The fold decrease in apoptosis was measured against uninfected cells. Graphs represent the mean + S.E.M of 3 biological experiments. To compute the fold decrease in absorbance, the enrichment factor after CAM induction of apoptosis for cells was divided by the enrichment factor of virus infected cells A high fold decrease in apoptosis shows the extent to which the virus to inhibits camptothecin induced apoptosis. Significance was set at $p<0.05$. Bars denote mean and error bars SEM.

3.4 Discussion

To fully characterise the full-length LSDV SOD and to investigate whether it has functional domains similar to the leporipoxvirus SOD homologues, a protein domain alignment was done. The amino acid sequence and structural domains of SOD in a virulent field strain LSDV (Nl 2490) were compared with the LSDV vaccine strains (nLSDV and Herbivac), vaccinia virus, myxoma virus, Amsacta Moorei with bovine and human SOD.

An important step in SOD activation (Figure 1.16**)** is the dimerization of the copper chaperone for SOD with monomeric SOD (Culotta et al., 1997). Leporipoxvirus SOD homologues have been reported to bind the copper chaperones and thereby act as inhibitors of the proper metalation of Cu Zn SOD (Cao et al., 2002, Teoh et al., 2005, Teoh et al., 2003). The level of inhibition is at the stage of SOD-CCS dimerization observed in the activation of cellular SOD

(reviewed in Chapter 1) (Teoh et al., 2003, Teoh et al., 2005). Regions of homology between the second domain of CCS and Cu Zn SOD and some homologues including LSDV SOD were shown (Teoh et al., 2003). It is interesting to note that the truncated SOD from nLSDV did not have all the motifs needed to dimerise with CCS. However, Herbivac and the virulent field strain of SOD contained all the residues important in heterodimerisation. These residues have also been reported to be present in leporipoxviruses although they have been shown to also include a cysteine at position 56 homologous to a cysteine at position 57 in CCS which further stabilises the heterodimer (Cao et al., 2002). Myxoma virus contains a small deletion that places cysteine in the 56th position (Cys 56). This cysteine is thought to play a role in dimerization between MYX SOD and CCS because it occupies a similar position as Cys 57 in yeast. (Cao et al., 2002, Teoh et al., 2003). This amino acid plays a role in binding copper and stabilises the formation of the CCS-SOD heterodimer (Culotta et al., 2006). However, this residue was absent from all the LSDV SOD homologues.

There are conserved domains important for SOD enzyme function and these include a catalytic arginine at amino acid position 142 and copper binding residues (Figure 3.7). The absence of this conserved domain in the active site may be the reason LSDV SOD homologues are catalytically inactive as a SOD enzyme. LSDV Nl 2490 and Herbivac contained 5 out of 6 domains required for the active site. SOD from nLSDV however did not show most of the required domains which include residues at position 119 and 142 in bovine SOD (Figure 3.7).

The β sheets are responsible for maintaining the structure of cellular SOD. These β-sheets can aggregate through hydrogen bonding via the interaction of their edges with other β-sheets they encounter (Richardson and Richardson, 2002). The β sheet strand numbers 5 and 6 in nLSDV, Herbivac and LSDV Nl 2490 are known as 'edge strands' and are able to form hydrogen bonds with other edge strands synonymous to the finding in amyloid fibrils. In native SOD 1 (Cu Zn SOD) these edge strands are protected as they bind metals (Valentine and Hart, 2003). However, nLSDV becomes particularly more interesting as it ends at the 6^{th} β sheet and lacks other residues which coordinate metal binding. This, in turn, exposes the β sheet edges which can bind other proteins including cellular SOD 1. Aggregates formed are not generally problematic in mammalian cells as they are sequestered into an aggresome for proteolytic degradation. The exception is when the aggregates are soluble like Cu Zn SOD aggregates which become harder to clear (Valentine and Hart, 2003, Banci et al., 2007). Aggregation of mutant Cu Zn SOD with

low or no affinity to the metals are toxic to cells (Kabashi et al., 2007). These aggregates may lead to cell death possibly through apoptosis (Oh et al., 2008).

SOD homologues from LSDV Nl 2490 have been shown to cluster phylogenetically with other SOD homologues that have been reported to act as decoy proteins (Teoh et al., 2003). A SOD homologue from vaccinia virus was shown to be in a different cluster compared to the homologues from LSDV and the leporipoxviruses (Teoh et al., 2003) which clustered together. It is important to note that vaccinia virus SOD (A45R) has been shown to be inactive as an enzyme and a decoy (Almazan et al., 2001). It was therefore more likely for LSDV to functionally resemble proteins in the same cluster and therefore could potentially retain some decoy activity like the other homologues closely related to it, such as the SOD from leporipoxviruses. This finding was instrumental in doing functional assays to investigate whether full length SOD from Herbivac functioned as a SOD decoy as has been reported for the leporipoxviruses.

Findings from the investigation of the growth of different LSDV viruses in cell culture showed that the presence or absence of the SOD influenced virus yields. The yields of nLSDVdSOD-UCT were lower than those of nLSDV and nLSDVSODis-UCT. This is in contrast to experiments with SOD homologue deletion mutants in recombinant SFV and MYX which were shown in two independent experiments to grow ten times better in a one-step growth curve in tissue culture (Teoh et al., 2005, Cao et al., 2002). Therefore, it can be concluded that the presence of a LSDV SOD homologue (truncated or full-length) contributes to the better growth yields in cells and CAMs. This is important when considering growth of virus for use as vaccine.

Growth curves of LSDV in chick CAMs had a similar growth profile to that shown by van Rooyen et al. (1969). In that experiment virus titres peaked at day 6 and started declining at day 7. Also in agreement with our study, virus yield did not exceed 10^6 $TCID_{50}$/0.2 ml (results not shown). It does appear that there is a limit to the amount of virus one can extract from infected CAMs. Therefore performing growth curves within the first 5 days of experiment can be more informative than after 6 days as viral titres drop.

The presence or absence of SOD in LSDV resulted in different histological changes in CAMS. There were increased numbers of fibroblasts in nLSDV, Herbivac, and nLSDVSODis-M and

not nLSDVdSOD-M infected CAMs when compared to uninfected CAMS. Interestingly, there was ectodermal proliferation in nLSDVSODis-M infected CAMs. Also, CAMs infected with nLSDVSODis-M had the most pronounced epithelial hyperplasia and ectodermal thickening. Inhibition of SOD leads to an increase in the superoxide radical and this has been reported to promote cell proliferation (Behrend et al., 2003). In one study, Teoh and colleagues infected rabbits with SFV, measured the sizes of lesions and performed histological examination of lesion biopsies. They reported that the presence of a decoy SOD was associated with an increase in the size of lesions and microscopically with fibromatous cell proliferation (Teoh et al., 2005). Our results support this as nLSDVSODis-M was shown to induce more fibroplasia compared to nLSDVdSOD-M. Our results also showed a role of the truncated gene product from nLSDV as nLSDV infected CAM sections also contained more fibroblasts compared to nLSDVdSOD-M.

Infiltration of leukocytes was observed in the mesoderm of all infected CAMs with highest amounts shown after infection with Herbivac in the first histology experiment. Scoring in a blinded fashion by an independent specialist veterinary pathologist in a second experiment revealed that there was increased immune infiltration after infection with nLSDV and nLSDVSODis-UCT at day 5. nLSDVdSOD-UCT had the least amount of immune infiltration (Table 3.3 and Figure 3.27**)**. Leukocyte infiltration after infecting CAMs with poxviruses has been reported before and it has been postulated to act as an indicator for an acute inflammatory response (Offerman et al., 2013, Prozesky and Barnard, 1982). The SOD knockout virus therefore appeared to have the least inflammatory response whereas the SOD knock-in (both truncated and full-length SOD) viruses had the highest inflammatory response. This could account for the improved immunogenicity that was observed in cattle (unpublished observations, Deltamune). Lesions from rabbits infected with wild type SFV expressing a SOD homologue showed extensive leukocyte infiltration (Teoh et al., 2005). Because our viruses only differ at the SOD locus, we conclude that the SOD homologue contributes to the differences observed. The presence of marker genes did not appear to influence major differences in histopathology.

Despite nLSDV (containing the truncated SOD) having the same inflammatory score as the SOD knock-in virus, our chick CAM experiment showed some differences in pathology. In fact, nLSDV resembled the SOD knock-out in those pathologies. In both CAM histology

experiments with and without marker genes there was more pronounced ballooning degeneration in CAMs infected with nLSDV and nLSDVdSOD-M/UCT than with nLSDVSODis-M /UCT. (Table 3.3). Fewer cells were observed in the epithelium of CAMs infected with the knock-out than with the SOD knock-in viruses. CAMs infected with nLSDVSODis-M may have compensated for the degenerating cells through cellular proliferation and epithelial hyperplasia. There was pronounced epithelial hyperplasia as well as fibroplasia following infection with nLSDVSODis-M. The presence of a functional decoy SOD has been implicated in survival and proliferation of cells (Teoh et al., 2005). Ballooning degeneration is however not a new finding in LSDV infections. Van Rooyen and colleagues also showed necrosis in CAM sections infected with LSDV (van Rooyen et al., 1969). It is thus evident that infection with LSDV is associated with cell death. However, what makes the SOD knock-in recombinants particularly interesting here, is that their presence was associated with some form of protection from cell death or the dying cells are efficiently replaced.

SOD can have antiviral properties and so many viruses have evolved mechanisms to modulate the host SOD activity (Cao et al., 2002). SOD homologues from leporipoxviruses have been shown to compete for copper thereby inhibiting the activity of SOD. Teoh et al. (2003) showed that the SOD homologues from leporipoxviruses bind the copper chaperone for copper, indirectly inhibiting cellular SOD activity. Since full-length LSDV SOD resembled and clustered with SOD from leporipoxviruses, we investigated whether this SOD was active as an enzyme or whether SOD from LSDV inhibited the activity of cellular SOD. In this experiment, we failed to show any involvement of the truncated or full-length SOD homologue from LSDV in the perturbation of the activity of cellular Cu Zn SOD. The vaccinia virus SOD homologue (product of the A45R) gene is a late gene product which is packaged in the viral core (Almazan et al., 2001) and can exert its effect early in infection. Similarly, LSDV encodes a SOD homologue that is believed to be a late protein because of its promoter sequence (Tulman et al., 2001). However, we were not able to show any significant differences in SOD activity at any time point. This may have been due to the cellular feedback mechanisms which maintain a steady concentration of SOD within the cell making it impossible to determine whether the SOD homolog is acting as a decoy or an active enzyme.

The superoxide anion has been shown to be anti-apoptotic and proliferative (Pervaiz and Clement, 2002b, Behrend et al., 2003). We did not observe any enrichment of the superoxide anion in our *in vitro* SOD assays in LSDV infected cells, but, interestingly, the proliferative nature of viruses

containing the full-length SOD was observed on the histology of infected CAMs (refer to section 3.3.6). There was fibroplasia in the mesoderm of CAMs infected with Herbivac and nLSDVSODis-M compared to nLSDVdSOD-M infected CAMs. There was also epithelial hyperplasia in CAMs infected with nLSDVSODis-M and Herbivac and not nLSDV or nLSDVdSOD-M. Using viruses without markers, increased epithelial hyperplasia associated with nLSDV and nLSDVSODis-UCT was observed though it was not significantly different compared to nLSDVdSOD-UCT.

We showed increased induction of cell death following viral infection with LSDV containing the full-length SOD homologue compared to nLSDV and the SOD knock-out at 24 hours post infection (Figure 3.31). This trend was different at 2 and 6 hours post infection where nLSDVSODis-M infected cells only, had increased induction of apoptosis (Figure 3.30). The differences in induction of cell death between nLSDVSODis-M and Herbivac at these times may be as a result of Herbivac being a mixture of the full-length SOD and truncated SOD observed in nLSDV.

In an experiment to determine the role of the full-length SOD homologue in the inhibition of camptothecin induced cell death, we observed that there was an increased inhibition of camptothecin induced cell death following infection with viruses containing a full-length SOD homologue (Herbivac and nLSDVSODis-M) compared to nLSDV and the SOD knock-out (Figure 3.31D). This observation implies that there were different pathways of apoptosis being affected by virus infection and camptothecin. Virus infection could have induced apoptosis via the extrinsic pathway. Camptothecin is known to induce death via the intrinsic pathway (Zeng et al., 2012). Death via the extrinsic pathway is mediated by cell membrane surface bound death receptors which include tumor necrosis factor receptor 1 (TNF-R1), FAS, TNF-related apoptosis-inducing ligand (TRAIL) (Veyer et al., 2017, Zhou et al., 2017). The intrinsic pathway of apoptosis is triggered by different intracellular stimuli that includes DNA damage, cytokine deprivation, oxidative stress, calcium overload and endoplasmic reticulum stress (Zhou et al., 2017). Once the above stated stimuli are evoked, they all converge to cause mitochondrial outer membrane permeabilization (MOMP). MOMP is highly regulated by proteins belonging to the BCL-2 family. Upon induction of the intrinsic pathway of apoptosis, the BCL-2 homology domains can interact with BCL-2 associated protein X (BAX) or BCL-2 agonist or killer (BAK) (Zhou et al., 2017). Camptothecin causes DNA damage (Horwitz et al., 1972) and consequently evokes the intrinsic form of apoptosis. The involvement of the extrinsic apoptotic death pathway

in nLSDVSODis infection is further substantiated by the fact that immediately after infection (2 and 6 h.p.i) we started to observe a general induction of apoptosis. It can be inferred that virus binding to death ligands on the cell surface may contribute to the induction of the extrinsic cell death pathway.

There was a general trend of inhibition of camptothecin induced cell death by all 4 viruses showing that LSDV contains anti-apoptotic genes or gene products. The observation that the SOD knock-out virus also inhibited camptothecin induced apoptosis indicated that this was not completely dependent on SOD. LSDV has been shown to encode apoptosis regulatory genes such as LSDV003, LSDV017 and LSDV154. LSDV also includes ankyrin repeat genes (Tulman et al., 2001, Kara et al., 2003) which from studies using vaccinia virus *in vitro* (Ryerson et al., 2017) have been shown to be antiapoptotic. Thus, there would be a general anti-apoptotic environment from gene products other than SOD. Interestingly, the truncated form of SOD present in nLSDV did not appear to play a role in inhibition of camptothecin induced cell death as there was no significant difference in the inhibition of camptothecin induced apoptosis between nLSDV infected cells compared to nLSDVdSOD-M infected cells (Figure 3.31D). In addition a SOD decoy from myxoma was shown to mount partial protection against apoptosis and able to mount full defense, possibly in concert with other antiapoptotic gene products like M11L (Teoh et al., 2005).

Camptothecin has been shown to affect both mammalian and poxviral DNA topoisomerases making it a candidate antiviral agent for poxviruses (Horwitz et al., 1972, Da Fonseca and Moss, 2003). Camptothecin could have bound viral topoisomerases thereby inhibiting them. Regardless of this however, our assertions that viruses containing full-length SOD inhibit CPT induced cell death remain true as equal amounts of camptothecin were added to both the knock-out and knock-in viruses but had varying effects. The SOD knock-out was a control showing LSDV without SOD inhibited camptothecin induced cell death and viruses expressing full-length SOD showed even greater inhibition.

In this study, we did not manage to detect SOD decoy activity that was reported of leporipoxviruses, yet we got the same antiapoptotic effects when SOD was present. The likely explanation of this is that SOD from Herbivac could be exerting its effects differently to leporipoxviruses' SOD. *Molloscum Contagiosum* encodes a MC163 whose amino acid residues (46-108) have been shown to possess properties of a Cu Zn SOD (Coutu et al., 2017). MC163

was shown to bind apoptotic factor BAX in the mitochondria thereby inhibiting apoptosis (Coutu et al., 2017). It can be inferred therefore that since the full-length SOD homologue from Herbivac did not appear to interfere with cellular Cu Zn SOD, binding and inactivation of apoptotic factors may be the mechanism by which full length SOD homologues from LSDV exert their antiapoptotic effect. Although Cu Zn SOD is a cytosolic protein, it and its mutant SODs have also been shown to localize to the mitochondria further substantiating the claim that the full length SOD homologue from LSDV could localize to the mitochondrion where it binds apoptotic factors (Sturtz et al., 2001, Magrané et al., 2009).

It can be inferred therefore that the inhibition of apoptosis by Herbivac and possibly nLSDVSODis-M leads to the host increasing antiviral mechanisms to clear the infection. This is however absent in nLSDV and potentially nLSDVdSOD-M infected cells. The implications of this are that Herbivac and nLSDVSODis-M may induce a more potent immune response than nLSDV or nLSDVdSOD-M. This finding is substantiated by the finding from our microarray experiment in Chapter 2 that LSDV infection was characterized by an upregulation of antiviral genes that are associated with pathogen recognition receptors, interferon related genes and immune system related genes. Thirteen genes were unique to Herbivac infection alone (Chapter 2 section 2.3.4.1). Amongst those that were commonly upregulated by both viruses (section 2.3.4.1) though they were not compared statistically against each other, most genes that were upregulated which are associated with an antiviral response had a greater fold change in upregulation after Herbivac infection compared to nLSDV.

In the presence of camptothecin, the full-length SOD homologue expressed by both Herbivac and nLSDVSODis-M could have contributed to better protection of the infected cells from cell death. Inhibition of cell death however is a means by which viruses evade the host's antiviral mechanisms. This aids the virus to complete its replication cycle and produce infectious viral particle (Nichols et al., 2017). Since apoptosis of infected cells is an innate function that is used to remove the infected cell (Everett and McFadden, 1999), its inhibition may result in the infected cells resorting to other means of cell death that include necrosis or necroptosis Walsh (2014). Induction of necroptosis is beneficial in effecting a strong immune response to viral infection (Orzalli and Kagan, 2017). Vaccinia virus was shown to inhibit caspase 8 leading to infected cells inducing necroptosis (Li and Beg, 2000). This inhibition in vaccinia virus was averted by necroptosis (Cho et al., 2009, Veyer et al., 2017). A vaccine/vector that inhibits apoptosis causing the infected cell to engage in necroptosis could be desirable as

necroptosis is an immunogenic form of cell death (Sarhan et al., 2018). It is interesting to note that in a whole system in mice, GO processes relating to cell death were elevated after Herbivac infection and not nLSDV infection (Chapter 2). More interestingly, there was an upregulation of Gzma which is involved in the induction of caspase independent cell death. Taken together, this suggests that infection by Herbivac elicits a more potent immune response possibly due to the type of cell death induced.

We speculate that the viral induction of apoptosis and necrosis that was shown by viruses expressing full-length SOD *in vitro* could account for an increase in transcripts related to cell death that were detected in mice infected with Herbivac. Cellular processes and pathways involved in cell death were activated after Herbivac infection. Also, though paradoxical, the ability of viruses containing full-length SOD to inhibit apoptosis could account for the increased expression of cell death transcripts *in vivo*. Granzyme A and poly (ADP-ribose) polymerase 9 (Parp 9) upregulation was observed after Herbivac infection only. Gzma participates in caspase independent cell death (Martinvalet et al., 2005). Necroptosis has been reported to be caspase independent making our findings striking. Inhibition of apoptosis may result in the induction of a more immunogenic form of cell death. This observation suggests that when apoptosis is inhibited, the host cell/organism activates expression of other cell death machinery. Essentially, the elevated cell death processes and pathways following infection with Herbivac observed from analyzing our microarray data confirms this. More work will need to be done in the way of using different assays/methods to test for different forms of cell death such as necroptosis.

Chapter 4 Conclusion and future work

Chapter 1 of this thesis reviewed literature on the use of LSDV as a vaccine and vaccine vector. A more immunogenic vaccine strain of LSDV, Herbivac was supplied to our group and whole genome sequencing done. Whole genome sequencing revealed that there was a single potential functional difference between Herbivac and the widely used Neethling vaccine strain (nLSDV). The mutation in Herbivac restored the SOD ORF which was truncated due to a single base pair deletion in nLSDV. There was an additional 2 bp deletion which restored the ORF back into frame in Herbivac.

The first objective of this thesis was to establish whether there was a difference between nLSDV and Herbivac in the innate response in mice 24 hours post infection. Initial studies in a mouse model (chapter 2) showed that when mice were infected by either Herbivac or nLSDV, there was differential expression of 98 genes compared to the uninfected mice. These were largely related to the response to a viral infection. A few notable differences were observed. nLSDV differed in the unique expression of 6 genes and Herbivac differed in the unique expression of 36 genes, which included granzyme A and Poly (ADP-ribose) polymerase (Parp 9) (Figure 2.5). A lot more Gene ontology (GO) processes were enriched after Herbivac infection (16) than nLSDV (8) infection (Figure 2.6). The difference observed as alluded to in Chapter 2, could either be as a result of the SOD gene/gene product or experimental variation within the nLSDV group. Gzma was particularly interesting in that it is linked to the caspase independent form of cell death. Also, Parp 9 contributes to necrosis. There has been a new form of immunogenic, programmed necrotic cell death (necroptosis) descibed, which is activated when caspase activity is inhibited (Han et al., 2011). The finding that these transcripts were upregulated following Herbivac infection corroborates the finding in Chapter 3, that Herbivac induced viral apoptosis in infected cells (extrinsic apoptosis). Further studies should be performed to study the response at more time points earlier after infection. The use of a permissive animal/host model may also be more informative.

Even though the transcripts differentially expressed were largely similar, there was a trend towards Herbivac having more immune related transcripts being upregulated compared to nLSDV. This finding in a non-permissive host is interesting as it warrants further studies which

can substantiate the use and advantage of having Herbivac as a vaccine vector. Since, the only functional difference between Herbivac and nLSDV was the presence of a full-length SOD homolog, clonal viruses expressing the full-length SOD, nLSDVSODis-UCT and nLSDVSODis-M may therefore be superior vaccines and vaccine vectors. Testing the vaccine vectors in rabbits and conducting immunogenicity experiments can be informative as to whether viruses expressing full length SOD are more immunogenic than the viruses expressing the truncated SOD homolog or where the SOD homologue was deleted.

In the final experimental chapter, recombinant viruses expressing a full-length SOD homologue (nLSDVSODis) and with SOD knocked out (nLSDVdSOD), were made. When the SOD homologue was deleted from LSDV it could be shown that this virus grew to lower titres in both cell culture and on CAMs. This novel finding presents a possible and exciting manufacturing advantage when growing nLSDVSODis-UCT for use as a vaccine and vaccine vector. Histological analyses also revealed that there was less immune cell infiltration associated with nLSDVdSOD-UCT infection compared to nLSDV and nLSDVSODis-UCT showing a possible role of the SOD homolog.

SOD activity assays could not show whether the truncated SOD and full-length SOD homologue exerted their effects in a way that may involve metabolism of the superoxide anion. Initially, it was hypothesised from results of the amino acid alignment that both the truncated and full-length SOD homologues were not functional SOD enzymes. This is because they lacked the catalytic arginine at position 147 and resembled leporipoxvirus SOD homologs (Figure 3.7). This finding was later substantiated by SOD activity assays which did not show any increased SOD activity in cells infected with viruses containing the full-length SOD. Unlike leporipoxviruses' SOD, SOD activity assays did not show a perturbation or inhibition of cellular SOD activity (Figure 3.29). Feedback mechanisms could have contributed to a steady state of the superoxide anion levels. However, the inhibition of camptothecin induced cell death could have been therefore brought about by other mechanisms. *Molluscum Contagiosum* encodes a SOD homologue which binds apoptotic factors in the mitochondria (Coutu et al., 2017, Nichols et al., 2017). Previous studies that have been done to understand the role of the SOD homologue in leporipoxviruses involved generating antibodies to SOD which were then used to purify the protein. This assisted in enzymatic assays and immunoprecipitation assays which showed the involvement of SOD homologues in binding

the copper chaperone for SOD and eventual inhibition of cellular SOD activity (Cao et al., 2002, Teoh et al., 2005, Teoh et al., 2003). Also, having antibodies against SOD will help understand where SOD localises in light of the recent finding by Coutu et al., 2017, that a SOD homolog from *Molluscum Contagiosum* binds apoptotic factors in the mitochondria.

In Chapter 3, it was also shown that the presence of a full-length SOD homologue in SOD knock-in recombinants contributed to resistance to camptothecin induced cell death (possibly via the intrinsic arm of apoptosis). This is an interesting finding in that inhibition of the intrinsic form of apoptosis can result in the propagation of virus and consequential induction of other forms of cell death which may be immunogenic. Apoptosis is not an immunogenic form of death and its inhibition may be associated with induction of other salvage methods of cell death that can contribute to better immunogenicity. Whether this cell death is pyroptosis or the highly desirable necroptosis due to it being an immunogenic form of cell death remains to be tested.

Also, linking the growth curve data with the ability of nLSDVSODis-UCT to inhibit camptothecin induced cell death to a greater extent than the SOD knock-out virus may explain why SOD knock-in viruses grew to higher titres. We hypothesise that the increased titre observed for the SOD knock-in viruses was as a result of the virus inhibiting cell death of the infected cells, which could have given the virus more time to replicate and make infectious virions before the cell died. The presence of a SOD homologue in leporipoxviruses has also been associated with thermal stability and conferring resistance of the virus to protease activity (Zachertowska et al., 2004). This can also be investigated as a plausible explanation why reversion to the full-length SOD observed in Herbivac was favoured. This could have impacted immunogenicity as more stable virus particles could contribute to better immunogenicity.

This thesis has shown a clear difference in phenotype in *in vitro* and *in vivo* studies, helping to understand how the full-length SOD from Herbivac could be contributing to improved immunogenicity. An animal experiment in the natural host of LSDV i.e. cattle, may also help in understanding the role of the full-length SOD in immunogenicity. Using results from this thesis, we hypothesise that that infection of cattle with the SOD knock-in virus will result in greater pathology due to nLSDVSODis inhibiting the intrinsic arm of cell death. This is because of persistence of the virus due to the infected cells not dying. However, this assertion remains to be tested as nLSDVSODis-UCT was associated induction of the extrinsic arm of

apoptosis. This could mean that if there is more virus induced apoptosis following nLSDVSODis-UCT infection, then the infection would be cleared early leading to lesser pathology.

Our CAM histology results, however, would suggest that infection of cattle with the SOD knock-out (nLSDVdSOD-UCT) would result in reduced immune infiltration compared to nLSDVSODis-UCT. The effect of the reduced immune infiltration may be increased pathology as the viral infection is not effectively controlled. Infection of cattle with the SOD knock-in virus will possibly be associated with increased immune infiltration as observed in CAM histology where infection with nLSDVSODis-UCT was associated with greater immune cell infiltration compared to infection with nLSDVdSOD-UCT (Figure 3.28). In the same way, we would speculate that pathology may be reduced following nLSDVSODis-UCT infection. Overall, the recombinant nLSDVSODis-UCT may have greater immune infiltration and therefore better immunogenicity in cows compared to nLSDVdSOD-UCT.

References

1. ABERA, Z., DEGEFU, H., GARI, G. & AYANA, Z. 2015. Review on epidemiology and economic importance of lumpy skin disease. Int. JBA Vir, 4, 8-21.

2. ABUTARBUSH, S., ABABNEH, M., AL ZOUBI, I., AL SHEYAB, O., AL ZOUBI, M., ALEKISH, M. & AL GHARABAT, R. 2015. Lumpy Skin Disease in Jordan: Disease Emergence, Clinical Signs, Complications and Preliminary‐associated Economic Losses. Transboundary and emerging diseases, 62, 549-554.

3. ABUTARBUSH, S., HANANEH, W., RAMADAN, W., AL SHEYAB, O., ALNAJJAR, A., AL ZOUBI, I., KNOWLES, N., BACHANEK‐BANKOWSKA, K. & TUPPURAINEN, E. 2016. Adverse reactions to field vaccination against lumpy skin disease in Jordan. Transboundary and emerging diseases, 63.

4. AGIANNIOTAKI, E. I., CHAINTOUTIS, S. C., HAEGEMAN, A., TASIOUDI, K. E., DE LEEUW, I., KATSOULOS, P.-D., SACHPATZIDIS, A., DE CLERCQ, K., ALEXANDROPOULOS, T. & POLIZOPOULOU, Z. S. 2017. Development and validation of a TaqMan probe-based real-time PCR method for the differentiation of wild type lumpy skin disease virus from vaccine virus strains. Journal of virological methods, 249, 48-57.

5. AKIRA, S., UEMATSU, S. & TAKEUCHI, O. 2006. Pathogen recognition and innate immunity. Cell, 124, 783-801.

6. AKRAM, S., TEONG, H. F., FLIEGEL, L., PERVAIZ, S. & CLEMENT, M. V. 2006. Reactive oxygen species-mediated regulation of the Na+-H+ exchanger 1 gene expression connects intracellular redox status with cells' sensitivity to death triggers. Cell Death Differ, 13, 628-41.

7. AL ALI, S., BALDANTA, S., FERNÁNDEZ-ESCOBAR, M. & GUERRA, S. 2016. Use of Reporter Genes in the Generation of Vaccinia Virus-Derived Vectors. Viruses, 8, 134.

8. ALBAYRAK, H., OZAN, E., KADI, H., CAVUNT, A., TAMER, C. & TUTUNCU, M. 2018. Molecular detection and seasonal distribution of lumpy skin disease virus in cattle

breeds in Turkey. MEDYCYNA WETERYNARYJNA-VETERINARY MEDICINE-SCIENCE AND PRACTICE, 74, 175-178.

9. ALEXANDER, R., PLOWRIGHT, W. & HAIG, D. 1957. Cytopathogenic agents associated with lumpy-skin disease of cattle. Bulletin of epizootic diseases of Africa, 5, 489-492.

10. ALKHAMIS, M. A. & VANDERWAAL, K. 2016. Spatial and Temporal Epidemiology of Lumpy Skin Disease in the Middle East, 2012–2015. Frontiers in Veterinary Science, 3, 19.

11. ALMAZAN, F., TSCHARKE, D. C. & SMITH, G. L. 2001. The vaccinia virus superoxide dismutase-like protein (A45R) is a virion component that is nonessential for virus replication. J Virol, 75, 7018-29.

12. ALTENBURG, A. F., KREIJTZ, J. H. C. M., DE VRIES, R. D., SONG, F., FUX, R., RIMMELZWAAN, G. F., SUTTER, G. & VOLZ, A. 2014. Modified vaccinia virus ankara (MVA) as production platform for vaccines against influenza and other viral respiratory diseases. Viruses, 6, 2735-2761.

13. ANNANDALE, C. H., HOLM, D. E., EBERSOHN, K. & VENTER, E. H. 2014. Seminal transmission of lumpy skin disease virus in heifers. Transboundary and emerging diseases, 61, 443-448.

14. ARANDJELOVIC, S. & RAVICHANDRAN, K. S. 2015. Phagocytosis of apoptotic cells in homeostasis. Nature immunology, 16, 907-917.

15. ARMSON, B., FOWLER, V., TUPPURAINEN, E., HOWSON, E., MADI, M., SALLU, R., KASANGA, C., PEARSON, C., WOOD, J. & MARTIN, P. 2017. Detection of Capripoxvirus DNA Using a Field‐Ready Nucleic Acid Extraction and Real‐Time PCR Platform. Transboundary and emerging diseases, 64, 994-997.

16. ARMSTRONG, J. A. & HART, P. D. 1971. Response of cultured macrophages to Mycobacterium tuberculosis, with observations on fusion of lysosomes with phagosomes. The Journal of experimental medicine, 134, 713-740.

17. ASPDEN, K., VAN DIJK, A. A., BINGHAM, J., COX, D., PASSMORE, J. A. & WILLIAMSON, A. L. 2002. Immunogenicity of a recombinant lumpy skin disease virus (neethling vaccine strain) expressing the rabies virus glycoprotein in cattle. Vaccine, 20, 2693-701.

18. ASSARSSON, E., GREENBAUM, J. A., SUNDSTROM, M., SCHAFFER, L., HAMMOND, J. A., PASQUETTO, V., OSEROFF, C., HENDRICKSON, R. C., LEFKOWITZ, E. J., TSCHARKE, D. C., SIDNEY, J., GREY, H. M., HEAD, S. R., PETERS, B. & SETTE, A. 2008. Kinetic analysis of a complete poxvirus transcriptome reveals an immediate-early class of genes. Proc Natl Acad Sci U S A, 105, 2140-5.

19. AYELET, G., HAFTU, R., JEMBERIE, S., BELAY, A., GELAYE, E., SIBHAT, B., SKJERVE, E. & ASMARE, K. 2014. Lumpy skin disease in cattle in central Ethiopia: Outbreak investigation and isolation and molecular detection of lumpy skin disease virus. Rev Sci Tech Off Int Epiz, 33, 1-23.

20. BABIUK, S. 2018. Taxonomy. Lumpy Skin Disease. Springer.

21. BAHAR, M. W., GRAHAM, S. C., CHEN, R. A. J., COORAY, S., SMITH, G. L., STUART, D. I. & GRIMES, J. M. 2011. How vaccinia virus has evolved to subvert the host immune response. Journal of Structural Biology, 175, 127-134.

22. BALDANTA, S., FERNANDEZ-ESCOBAR, M., ACIN-PEREZ, R., ALBERT, M., CAMAFEITA, E., JORGE, I., VAZQUEZ, J., ENRIQUEZ, J. A. & GUERRA, S. 2017. ISG15 governs mitochondrial function in macrophages following vaccinia virus infection. PLoS Pathog, 13, e1006651.

23. BALINSKY, C., DELHON, G., AFONSO, C., RISATTI, G., BORCA, M., FRENCH, R., TULMAN, E., GEARY, S. & ROCK, D. 2007. Sheeppox virus kelch-like gene SPPV-019 affects virus virulence. Journal of virology, 81, 11392-11401.

24. BARBER, G. N. 2014. STING-dependent cytosolic DNA sensing pathways. Trends in Immunology, 35, 88-93.

25. BEARD, P. M. 2016. Lumpy skin disease: a direct threat to Europe. Veterinary Record, 178, 557-558.

26. BEATTIE, E., KAUFFMAN, E. B., MARTINEZ, H., PERKUS, M. E., JACOBS, B. L., PAOLETTI, E. & TARTAGLIA, J. 1996. Host-range restriction of vaccinia virus E3L-specific deletion mutants. Virus Genes, 12, 89-94.

27. BECKER, M. N., GREENLEAF, W. B., OSTROV, D. A. & MOYER, R. W. 2004. Amsacta moorei Entomopoxvirus Expresses an Active Superoxide Dismutase. Journal of Virology, 78, 10265-10275.

28. BEHREND, L., HENDERSON, G. & ZWACKA, R. M. 2003. Reactive oxygen species in oncogenic transformation. Biochem Soc Trans, 31, 1441-4.

29. BEN-GERA, J., KLEMENT, E., KHINICH, E., STRAM, Y. & SHPIGEL, N. 2015. Comparison of the efficacy of Neethling lumpy skin disease virus and x10RM65 sheep-pox live attenuated vaccines for the prevention of lumpy skin disease–The results of a randomized controlled field study. Vaccine, 33, 4837-4842.

30. BIDGOOD, S. R. & MERCER, J. 2015. Cloak and Dagger: Alternative Immune Evasion and Modulation Strategies of Poxviruses. Viruses, 7, 4800-4825.

31. BLASCO, R., COLE, N. B. & MOSS, B. 1991. Sequence analysis, expression, and deletion of a vaccinia virus gene encoding a homolog of profilin, a eukaryotic actin-binding protein. J Virol, 65, 4598-608.

32. BOSHRA, H., TRUONG, T., NFON, C., GERDTS, V., TIKOO, S., BABIUK, L. A., KARA, P., MATHER, A., WALLACE, D. & BABIUK, S. 2013. Capripoxvirus-vectored vaccines against livestock diseases in Africa. Antiviral Res, 98, 217-27.

33. BOWDEN, T. R., BABIUK, S. L., PARKYN, G. R., COPPS, J. S. & BOYLE, D. B. 2008. Capripoxvirus tissue tropism and shedding: A quantitative study in experimentally infected sheep and goats. Virology, 371, 380-393.

34. BOWIE, A. G. & UNTERHOLZNER, L. 2008. Viral evasion and subversion of pattern-recognition receptor signalling. Nature reviews. Immunology, 8, 911.

35. BOYLE, D. B. & COUPAR, B. E. 1988. A dominant selectable marker for the construction of recombinant poxviruses. Gene, 65, 123-8.

36. BRATKE, K. A., MCLYSAGHT, A. & ROTHENBURG, S. 2013. A survey of host range genes in poxvirus genomes. Infect Genet Evol, 14, 406-25.

37. BRENNER, J., BELLAICHE, M., GROSS, E., ELAD, D., OVED, Z., HAIMOVITZ, M., WASSERMAN, A., FRIEDGUT, O., STRAM, Y. & BUMBAROV, V. 2009. Appearance of skin lesions in cattle populations vaccinated against lumpy skin disease: statutory challenge. Vaccine, 27, 1500-1503.

38. BROYLES, S. S. 2003. Vaccinia virus transcription. Journal of General Virology, 84, 2293-2303.

39. BUONAGURO, L., WANG, E., TORNESELLO, M. L., BUONAGURO, F. M. & MARINCOLA, F. M. 2011. Systems biology applied to vaccine and immunotherapy development. BMC Systems Biology, 5, 146-146.

40. BURDIN, M. L. & PRYDIE, J. 1959. Lumpy Skin Disease of Cattle in Kenya. Nature, 183, 949.

41. BURGESS, HANNAH M. & MOHR, I. 2015. Cellular 5′-3′ mRNA Exonuclease Xrn1 Controls Double-Stranded RNA Accumulation and Anti-Viral Responses. Cell Host & Microbe, 17, 332-344.

42. CAO, J. X., TEOH, M. L. T., MOON, M., MCFADDEN, G. & EVANS, D. H. 2002. Leporipoxvirus Cu-Zn Superoxide Dismutase Homologs Inhibit Cellular Superoxide Dismutase, but Are Not Essential for Virus Replication or Virulence. Virology, 296, 125-135.

43. CARN, V. 1993. Control of capripoxvirus infections. Vaccine, 11, 1275-1279.

44. CARN, V. M. & KITCHING, R. P. 1995a. The clinical response of cattle experimentally infected with lumpy skin disease (Neethling) virus. Archives of Virology, 140, 503-513.

45. CARN, V. M. & KITCHING, R. P. 1995b. An investigation of possible routes of transmission of lumpy skin disease virus (Neethling). Epidemiol Infect, 114, 219-26.

46. CARROLL, K., ELROY-STEIN, O., MOSS, B. & JAGUS, R. 1993. Recombinant vaccinia virus K3L gene product prevents activation of double-stranded RNA-dependent, initiation factor 2 alpha-specific protein kinase. J Biol Chem, 268, 12837-42.

47. CARROLL, M. W. & MOSS, B. 1997. Poxviruses as expression vectors. Current Opinion in Biotechnology, 8, 573-577.

48. CARROLL, M. W., OVERWIJK, W. W., CHAMBERLAIN, R. S., ROSENBERG, S. A., MOSS, B. & RESTIFO, N. P. 1997. Highly attenuated modified vaccinia virus Ankara (MVA) as an effective recombinant vector: a murine tumor model. Vaccine, 15, 387-94.

49. CARTER, G. C., LAW, M., HOLLINSHEAD, M. & SMITH, G. L. 2005. Entry of the vaccinia virus intracellular mature virion and its interactions with glycosaminoglycans. J Gen Virol, 86, 1279-90.

50. CASARENO, R. L. B., WAGGONER, D. & GITLIN, J. D. 1998. The copper chaperone CCS directly interacts with copper/zinc superoxide dismutase. Journal of Biological Chemistry, 273, 23625-23628.

51. CHAN, F. K.-M., LUZ, N. F. & MORIWAKI, K. 2015. Programmed necrosis in the Cross Talk of Cell Death and Inflammation. Annual review of immunology, 33, 79-106.

52. CHAN, F. K.-M., SHISLER, J., BIXBY, J. G., FELICES, M., ZHENG, L., APPEL, M., ORENSTEIN, J., MOSS, B. & LENARDO, M. J. 2003. A role for tumor necrosis factor receptor-2 and receptor-interacting protein in programmed necrosis and antiviral responses. Journal of Biological Chemistry, 278, 51613-51621.

53. CHANG, H. W., WATSON, J. C. & JACOBS, B. L. 1992. The E3L gene of vaccinia virus encodes an inhibitor of the interferon-induced, double-stranded RNA-dependent protein kinase. Proceedings of the National Academy of Sciences of the United States of America, 89, 4825-4829.

54. CHAWLA-SARKAR, M., LINDNER, D., LIU, Y.-F., WILLIAMS, B., SEN, G., SILVERMAN, R. & BORDEN, E. 2003. Apoptosis and interferons: role of interferon-stimulated genes as mediators of apoptosis. Apoptosis, 8, 237-249.

55. CHIHOTA, C. M., RENNIE, L. F., KITCHING, R. P. & MELLOR, P. S. 2001. Mechanical Transmission of Lumpy Skin Disease Virus by Aedes aegypti (Diptera: Culicidae). Epidemiology and Infection, 126, 317-321.

56. CHO, Y., CHALLA, S., MOQUIN, D., GENGA, R., RAY, T. D., GUILDFORD, M. & CHAN, F. K.-M. 2009. Phosphorylation-Driven Assembly of the RIP1-RIP3 Complex Regulates Programmed Necrosis and Virus-Induced Inflammation. Cell, 137, 1112-1123.

57. CLEMENT, M. V. & STAMENKOVIC, I. 1996. Superoxide anion is a natural inhibitor of FAS-mediated cell death. Embo j, 15, 216-25.

58. COETZER, J. 2004. Lumpy skin disease. Infectious diseases of livestock, 2, 1268-1276.

59. COHEN, A., COX, D., VAN DIJK, A., KORBER, A., DUMBELL, K. & WILLIAMSON, A. Lumpy skin disease virus as a recombinant vaccine vector for Rift Valley fever virus and bovine ephemeral fever virus. Proceedings of the 4th Congress of the European Society for Veterinary Virology, Edinburgh, Scotland, 1997. 24-27.

60. CONDIT, R. C. 2007. Vaccinia, Inc.—Probing the Functional Substructure of Poxviral Replication Factories. Cell Host & Microbe, 2, 205-207.

61. CONSORTIUM, G. O. 2004. The Gene Ontology (GO) database and informatics resource. Nucleic Acids Research, 32, D258-D261.

62. COUTU, J., RYERSON, M. R., BUGERT, J. & BRIAN NICHOLS, D. 2017. The Molluscum Contagiosum Virus protein MC163 localizes to the mitochondria and dampens mitochondrial mediated apoptotic responses. Virology, 505, 91-101.

63. COX, W. I., GETTIG, R. R. & PAOLETTI, E. 1995. Poxviruses as Genetic Vectors. In: VOS, J.-M. H. (ed.) Viruses in Human Gene Therapy. Dordrecht: Springer Netherlands.

64. CULOTTA, V. C., KLOMP, L. W., STRAIN, J., CASARENO, R. L. B., KREMS, B. & GITLIN, J. D. 1997. The copper chaperone for superoxide dismutase. Journal of Biological Chemistry, 272, 23469-23472.

65. CULOTTA, V. C., YANG, M. & O'HALLORAN, T. V. 2006. Activation of superoxide dismutases: Putting the metal to the pedal. Biochimica et biophysica acta, 1763, 747-758.

66. CYRKLAFF, M., RISCO, C., FERNÁNDEZ, J. J., JIMÉNEZ, M. V., ESTÉBAN, M., BAUMEISTER, W. & CARRASCOSA, J. L. 2005. Cryo-electron tomography of vaccinia virus. Proceedings of the National Academy of Sciences of the United States of America, 102, 2772-2777.

67. DA FONSECA, F. & MOSS, B. 2003. Poxvirus DNA topoisomerase knockout mutant exhibits decreased infectivity associated with reduced early transcription. Proceedings of the National Academy of Sciences, 100, 11291-11296.

68. DALES, S. 1962. An electron microscope study of the early association between two mammalian viruses and their hosts. The Journal of cell biology, 13, 303-322.

69. DALES, S. 1963. The uptake and development of vaccinia virus in strain L cells followed with labeled viral deoxyribonucleic acid. The Journal of cell biology, 18, 51-72.

70. DANGO, S., MOSAMMAPARAST, N., SOWA, M. E., XIONG, L.-J., WU, F., PARK, K., RUBIN, M., GYGI, S., HARPER, J. W. & SHI, Y. 2011. DNA unwinding by ASCC3 helicase is coupled to ALKBH3-dependent DNA alkylation repair and cancer cell proliferation. Molecular cell, 44, 373-384.

71. DANTHI, P. 2016. Viruses and the Diversity of Cell Death. Annual Review of Virology, 3, 533-553.

72. DAVIES, F. 1981. Sheep and goat pox. Virus diseases of food animals, 2, 733-749.

73. DAVIES, F. G. 1982. Observations on the epidemiology of lumpy skin disease in Kenya. J Hyg (Lond), 88, 95-102.

74. DAVIES, F. G. 1991. Lumpy skin disease of cattle: a growing problem in Africa and the Near East. World Animal Review, 68, 37-42.

75. DAVIES, M. V., CHANG, H. W., JACOBS, B. L. & KAUFMAN, R. J. 1993. The E3L and K3L vaccinia virus gene products stimulate translation through inhibition of the double-stranded RNA-dependent protein kinase by different mechanisms. Journal of Virology, 67, 1688-1692.

76. DE DUVE, C. & WATTIAUX, R. 1966. Functions of lysosomes. Annu Rev Physiol, 28, 435-92.

77. DELALOYE, J., ROGER, T., STEINER-TARDIVEL, Q.-G., LE ROY, D., KNAUP REYMOND, M., AKIRA, S., PETRILLI, V., GOMEZ, C. E., PERDIGUERO, B., TSCHOPP, J., PANTALEO, G., ESTEBAN, M. & CALANDRA, T. 2009. Innate Immune Sensing of Modified Vaccinia Virus Ankara (MVA) Is Mediated by TLR2-TLR6, MDA-5 and the NALP3 Inflammasome. PLOS Pathogens, 5, e1000480.

78. DELANGE, A. M., REDDY, M., SCRABA, D., UPTON, C. & MCFADDEN, G. 1986. Replication and resolution of cloned poxvirus telomeres in vivo generates linear minichromosomes with intact viral hairpin termini. Journal of virology, 59, 249-259.

79. DHIMAN, N., BONILLA, R., O'KANE J, D. & POLAND, G. A. 2001. Gene expression microarrays: a 21st century tool for directed vaccine design. Vaccine, 20, 22-30.

80. DI LISA, F. & ZIEGLER, M. 2001. Pathophysiological relevance of mitochondria in NAD+ metabolism. FEBS letters, 492, 4-8.

81. DIDENKO, V. V., NGO, H. & BASKIN, D. S. 2003. Early Necrotic DNA Degradation : Presence of Blunt-Ended DNA Breaks, 3′ and 5′ Overhangs in Apoptosis, but only 5′ Overhangs in Early Necrosis. The American Journal of Pathology, 162, 1571-1578.

82. DIETZSCHOLD, B., HOOPER, D. C., SCHNELL, M. & RUPPRECHT, C. E. 2006. Genetically engineered rabies recombinant vaccine for immunization of stray dogs and wildlife. Google Patents.

83. DUKE, R. C. & COHEN, J. J. 1986. IL-2 addiction: withdrawal of growth factor activates a suicide program in dependent T cells. Lymphokine Res, 5, 289-99.

84. DUNAI, Z., BAUER, P. I. & MIHALIK, R. 2011. Necroptosis: biochemical, physiological and pathological aspects. Pathol Oncol Res, 17, 791-800.

85. EFSA 2015. Scientific Opinion on lumpy skin disease. EFSA Journal, 13, 3986.

86. EKMEKCIOGLU, S., KURZROCK, R. & GRIMM, E. A. 2008. Chapter 51 - Hematopoietic Growth Factors and Cytokines A2 - Mendelsohn, John. In: HOWLEY, P. M., ISRAEL, M. A., GRAY, J. W. & THOMPSON, C. B. (eds.) The Molecular Basis of Cancer (Third Edition). Philadelphia: W.B. Saunders.

87. EL-KHOLY, A. A., SOLIMAN, H. M. & ABDELRAHMAN, K. A. 2008. Polymerase chain reaction for rapid diagnosis of a recent lumpy skin disease virus incursion to Egypt. Arab J. Biotech, 11, 293-302.

88. ELMORE, S. 2007. Apoptosis: A Review of Programmed Cell Death. Toxicologic pathology, 35, 495-516.

89. EVERETT, H., BARRY, M., LEE, S. F., SUN, X., GRAHAM, K., STONE, J., BLEACKLEY, R. C. & MCFADDEN, G. 2000. M11L: a novel mitochondria-localized protein of myxoma virus that blocks apoptosis of infected leukocytes. J Exp Med, 191, 1487-98.

90. EVERETT, H. & MCFADDEN, G. 1999. Apoptosis: an innate immune response to virus infection. Trends Microbiol, 7, 160-5.

91. FALKNER, F. G. & MOSS, B. 1988. Escherichia coli gpt gene provides dominant selection for vaccinia virus open reading frame expression vectors. Journal of Virology, 62, 1849-1854.

92. FARAH, A. 2017. Review of Lumpy Skin Disease and Its Economic Impacts in Ethiopia.

93. FENNER, F. 1977. The eradication of smallpox. Prog Med Virol, 23, 1-21.

94. FENNER, F. 1980. The global eradication of smallpox. Med J Aust, 1, 455-5.

95. FENNER, F. 1982. A successful eradication campaign. Global eradication of smallpox. Rev Infect Dis, 4, 916-30.

96. FICK, W. C. & VILJOEN, G. J. 1999. Identification and characterisation of an early/late bi-directional promoter of the capripoxvirus, lumpy skin disease virus. Arch Virol, 144, 1229-39.

97. FISCHER, A. H., JACOBSON, K. A., ROSE, J. & ZELLER, R. 2008. Hematoxylin and eosin staining of tissue and cell sections. CSH Protoc, 2008, pdb.prot4986.

98. FOO, C. H., LOU, H., WHITBECK, J. C., PONCE-DE-LEÓN, M., ATANASIU, D., EISENBERG, R. J. & COHEN, G. H. 2009. Vaccinia virus L1 binds to cell surfaces and blocks virus entry independently of glycosaminoglycans. Virology, 385, 368-382.

99. FRIES, L. F., TARTAGLIA, J., TAYLOR, J., KAUFFMAN, E. K., MEIGNIER, B., PAOLETTI, E. & PLOTKIN, S. 1996. Human safety and immunogenicity of a canarypox-rabies glycoprotein recombinant vaccine: an alternative poxvirus vector system. Vaccine, 14, 428-34.

100. FUKAI, T. & USHIO-FUKAI, M. 2011. Superoxide Dismutases: Role in Redox Signaling, Vascular Function, and Diseases. Antioxidants & Redox Signaling, 15, 1583-1606.

101. FURMAN, D. & DAVIS, M. M. 2015. New approaches to understanding the immune response to vaccination and infection. Vaccine, 33, 5271-5281.

102. GAMREKELASHVILI, J., GRETEN, T. F. & KORANGY, F. 2015. Immunogenicity of necrotic cell death. Cellular and Molecular Life Sciences, 72, 273-283.

103. GARI, G., ABIE, G., GIZAW, D., WUBETE, A., KIDANE, M., ASGEDOM, H., BAYISSA, B., AYELET, G., OURA, C. A. L., ROGER, F. & TUPPURAINEN, E. S. M. 2015. Evaluation of the safety, immunogenicity and efficacy of three capripoxvirus vaccine strains against lumpy skin disease virus. Vaccine, 33, 3256-3261.

104. GARI, G., BITEAU-COROLLER, F., LEGOFF, C., CAUFOUR, P. & ROGER, F. 2008. Evaluation of indirect fluorescent antibody test (IFAT) for the diagnosis and screening of lumpy skin disease using Bayesian method. Veterinary microbiology, 129, 269-280.

105. GARI, G., BONNET, P., ROGER, F. & WARET-SZKUTA, A. 2011. Epidemiological aspects and financial impact of lumpy skin disease in Ethiopia. Preventive Veterinary Medicine, 102, 274-283.

106. GARI JIMOLU, G. 2011. Epidemiological Study of Lumpy Skin Disease and Its Economic Impact in Ethiopia.

107. GAUTIER, L., COPE, L., BOLSTAD, B. M. & IRIZARRY, R. A. 2004. affy—analysis of Affymetrix GeneChip data at the probe level. Bioinformatics, 20, 307-315.

108. GENTLEMAN, R., CAREY, V., HUBER, W. & HAHNE, F. 2011. Genefilter: Methods for filtering genes from microarray experiments. R package version, 1.

109. GRIFFITH, THOMAS S. & FERGUSON, THOMAS A. 2011. Cell Death in the Maintenance and Abrogation of Tolerance: The Five Ws of Dying Cells. Immunity, 35, 456-466.

110. GUERRA, S., LÓPEZ-FERNÁNDEZ, L. A., CONDE, R., PASCUAL-MONTANO, A., HARSHMAN, K. & ESTEBAN, M. 2004. Microarray Analysis Reveals Characteristic

Changes of Host Cell Gene Expression in Response to Attenuated Modified Vaccinia Virus Ankara Infection of Human HeLa Cells. Journal of Virology, 78, 5820-5834.

111. GUERRA, S., LOPEZ-FERNANDEZ, L. A., PASCUAL-MONTANO, A., MUNOZ, M., HARSHMAN, K. & ESTEBAN, M. 2003. Cellular gene expression survey of vaccinia virus infection of human HeLa cells. J Virol, 77, 6493-506.

112. GUERRA, S., LÓPEZ-FERNÁNDEZ, L. A., PASCUAL-MONTANO, A., NÁJERA, J. L., ZABALLOS, A. & ESTEBAN, M. 2006. Host response to the attenuated poxvirus vector NYVAC: upregulation of apoptotic genes and NF-κB-responsive genes in infected HeLa cells. Journal of virology, 80, 985-998.

113. GUERRA, S., NÁJERA, J. L., GONZÁLEZ, J. M., LÓPEZ-FERNÁNDEZ, L. A., CLIMENT, N., GATELL, J. M., GALLART, T. & ESTEBAN, M. 2007. Distinct gene expression profiling after infection of immature human monocyte-derived dendritic cells by the attenuated poxvirus vectors MVA and NYVAC. Journal of virology, 81, 8707-8721.

114. GUZMAN, E., CUBILLOS-ZAPATA, C., COTTINGHAM, M. G., GILBERT, S. C., PRENTICE, H., CHARLESTON, B. & HOPE, J. C. 2012. Modified Vaccinia Virus Ankara-Based Vaccine Vectors Induce Apoptosis in Dendritic Cells Draining from the Skin via both the Extrinsic and Intrinsic Caspase Pathways, Preventing Efficient Antigen Presentation. Journal of Virology, 86, 5452-5466.

115. HA, H. C. & SNYDER, S. H. 1999. Poly(ADP-ribose) polymerase is a mediator of necrotic cell death by ATP depletion. Proceedings of the National Academy of Sciences, 96, 13978-13982.

116. HAN, J., ZHONG, C.-Q. & ZHANG, D.-W. 2011. Programmed necrosis: backup to and competitor with apoptosis in the immune system. Nature Immunology, 12, 1143.

117. HEINE, H., STEVENS, M., FOORD, A. & BOYLE, D. 1999. A capripoxvirus detection PCR and antibody ELISA based on the major antigen P32, the homolog of the vaccinia virus H3L gene. Journal of immunological methods, 227, 187-196.

118. HENDRICKSON, R. C., WANG, C., HATCHER, E. L. & LEFKOWITZ, E. J. 2010. Orthopoxvirus genome evolution: the role of gene loss. Viruses, 2, 1933-67.

119. HNATIUK, S., BARRY, M., ZENG, W., LIU, L., LUCAS, A., PERCY, D. & MCFADDEN, G. 1999. Role of the C-terminal RDEL motif of the myxoma virus M-T4 protein in terms of apoptosis regulation and viral pathogenesis. Virology, 263, 290-306.

120. HOLLINSHEAD, M., VANDERPLASSCHEN, A., SMITH, G. L. & VAUX, D. J. 1999. Vaccinia virus intracellular mature virions contain only one lipid membrane. Journal of virology, 73, 1503-1517.

121. HONG, M., YOON, S. I. & WILSON, I. A. 2012. Structure and functional characterization of the RNA-binding element of the NLRX1 innate immune modulator. Immunity, 36, 337-47.

122. HONG, S. J., DAWSON, T. M. & DAWSON, V. L. 2006. PARP and the release of apoptosis-inducing factor from mitochondria. Poly (ADP-Ribosyl) ation. Springer.

123. HORWITZ, S. B., CHANG, C.-K. & GROLLMAN, A. P. 1972. Antiviral action of camptothecin. Antimicrobial agents and chemotherapy, 2, 395-401.

124. HOUSE, J. A., WILSON, T. M., NAKASHLY, S. E., KARIM, I. A., ISMAIL, I., DANAF, N. E., MOUSSA, A. M. & AYOUB, N. N. 1990. The isolation of lumpy skin disease virus and bovine herpesvirus-from cattle in Egypt. Journal of Veterinary Diagnostic Investigation, 2, 111-115.

125. HSIANG, Y.-H., LIHOU, M. G. & LIU, L. F. 1989. Arrest of replication forks by drug-stabilized topoisomerase I-DNA cleavable complexes as a mechanism of cell killing by camptothecin. Cancer research, 49, 5077-5082.

126. HSIAO, J.-C., CHUNG, C.-S. & CHANG, W. 1999. Vaccinia virus envelope D8L protein binds to cell surface chondroitin sulfate and mediates the adsorption of intracellular mature virions to cells. Journal of virology, 73, 8750-8761.

127. HUNTER, P. & WALLACE, D. 2001. Lumpy skin disease in southern Africa: a review of the disease and aspects of control. Journal of the South African Veterinary Association, 72, 68-71.

128. ICTV 2018. Taxonomy. International Committee on Taxonomy of Viruses.

129. IRELAND, D. & BINEPAL, Y. 1998. Improved detection of capripoxvirus in biopsy samples by PCR. Journal of virological methods, 74, 1-7.

130. IRIZARRY, R. A., HOBBS, B., COLLIN, F., BEAZER‐BARCLAY, Y. D., ANTONELLIS, K. J., SCHERF, U. & SPEED, T. P. 2003. Exploration, normalization, and summaries of high density oligonucleotide array probe level data. Biostatistics, 4, 249-264.

131. IYER, L. M., KOONIN, E. V. & ARAVIND, L. 2002. Extensive domain shuffling in transcription regulators of DNA viruses and implications for the origin of fungal APSES transcription factors. Genome Biol, 3, Research0012.

132. JACOBS, S. R. & DAMANIA, B. 2012. NLRs, inflammasomes, and viral infection. Journal of Leukocyte Biology, 92, 469-477.

133. JOHNSTON, J. B., BARRETT, J. W., NAZARIAN, S. H., GOODWIN, M., RICCIUTO, D., WANG, G. & MCFADDEN, G. 2005. A poxvirus-encoded pyrin domain protein interacts with ASC-1 to inhibit host inflammatory and apoptotic responses to infection. Immunity, 23, 587-98.

134. JOHNSTON, R. B., JR., GODZIK, C. A. & COHN, Z. A. 1978. Increased superoxide anion production by immunologically activated and chemically elicited macrophages. J Exp Med, 148, 115-27.

135. KAMINSKYY, V. & ZHIVOTOVSKY, B. 2010. To kill or be killed: how viruses interact with the cell death machinery. J Intern Med, 267, 473-82.

136. KANG, M., DUNCAN, G. A., KUSZYNSKI, C., OYLER, G., ZHENG, J., BECKER, D. F. & VAN ETTEN, J. L. 2014. Chlorovirus PBCV-1 Encodes an Active Copper-Zinc Superoxide Dismutase. Journal of Virology, 88, 12541-12550.

137. KANNEGANTI, T.-D. 2010. Central roles of NLRs and inflammasomes in viral infection. Nature reviews. Immunology, 10, 688-698.

138. KARA, P., AFONSO, C., WALLACE, D., KUTISH, G., ABOLNIK, C., LU, Z., VREEDE, F., TALJAARD, L., ZSAK, A. & VILJOEN, G. 2003. Comparative sequence analysis of the South African vaccine strain and two virulent field isolates of Lumpy skin disease virus. Archives of virology, 148, 1335-1356.

139. KARAJI, N. & SATTENTAU, Q. J. 2017. Efferocytosis of Pathogen-Infected Cells. Frontiers in Immunology, 8.

140. KATSAFANAS, G. C. & MOSS, B. 2007. Colocalization of transcription and translation within cytoplasmic poxvirus factories coordinates viral expression and subjugates host functions. Cell host & microbe, 2, 221-228.

141. KATSOULOS, P. D., CHAINTOUTIS, S., DOVAS, C., POLIZOPOULOU, Z., BRELLOU, G., AGIANNIOTAKI, E., TASIOUDI, K., CHONDROKOUKI, E., PAPADOPOULOS, O. & KARATZIAS, H. 2018. Investigation on the incidence of adverse reactions, viraemia and haematological changes following field immunization of cattle using a live attenuated vaccine against lumpy skin disease. Transboundary and emerging diseases, 65, 174-185.

142. KAWAI, T. & AKIRA, S. 2006. TLR signaling. Cell Death Differ, 13, 816-25.

143. KAWAI, T. & AKIRA, S. 2008. Toll-like receptor and RIG-I-like receptor signaling. Ann N Y Acad Sci, 1143, 1-20.

144. KAWAMATA, H. & MANFREDI, G. 2008. Different regulation of wild-type and mutant Cu,Zn superoxide dismutase localization in mammalian mitochondria. Human Molecular Genetics, 17, 3303-3317.

145. KETTLE, S., BLAKE, N. W., LAW, K. M. & SMITH, G. L. 1995. Vaccinia virus serpins B13R (SPI-2) and B22R (SPI-1) encode M(r) 38.5 and 40K, intracellular polypeptides that do not affect virus virulence in a murine intranasal model. Virology, 206, 136-47.

146. KILCHER, S. & MERCER, J. 2015. DNA virus uncoating. Virology, 479-480, 578-590.

147. KITCHING, R., HAMMOND, J. & BLACK, D. 1986. Studies on the major common precipitating antigen of capripoxvirus. Journal of general virology, 67, 139-148.

148. KLIONSKY, D. J., ESKELINEN, E.-L. & DERETIC, V. 2014. Autophagosomes, phagosomes, autolysosomes, phagolysosomes, autophagolysosomes... wait, I'm confused. Autophagy, 10, 549-551.

149. KOCHAN, G., ESCORS, D., GONZÁLEZ, J. M., CASASNOVAS, J. M. & ESTEBAN, M. 2008. Membrane cell fusion activity of the vaccinia virus A17–A27 protein complex. Cellular microbiology, 10, 149-164.

150. KOCHNEVA, G., KOLOSOVA, I., MAKSYUTOVA, T., RYABCHIKOVA, E. & SHCHELKUNOV, S. 2005. Effects of deletions of kelch-like genes on cowpox virus biological properties. Arch Virol, 150, 1857-70.

151. KRAMMER, P. H. 2000. CD95's deadly mission in the immune system. Nature, 407, 789-95.

152. KREMERS, G.-J., GILBERT, S. G., CRANFILL, P. J., DAVIDSON, M. W. & PISTON, D. W. 2011. Fluorescent proteins at a glance. Journal of Cell Science, 124, 157-160.

153. KRISHNAMOORTHY, T., PAVITT, G. D., ZHANG, F., DEVER, T. E. & HINNEBUSCH, A. G. 2001. Tight binding of the phosphorylated alpha subunit of initiation factor 2 (eIF2alpha) to the regulatory subunits of guanine nucleotide exchange factor eIF2B is required for inhibition of translation initiation. Molecular and cellular biology, 21, 5018-5030.

154. KUMAR, A. P., CHANG, M. K., FLIEGEL, L., PERVAIZ, S. & CLEMENT, M. V. 2007. Oxidative repression of NHE1 gene expression involves iron-mediated caspase activity. Cell Death Differ, 14, 1733-46.

155. KUMAR, S. M. 2011. An outbreak of lumpy skin disease in a Holstein dairy herd in Oman: a clinical report. Asian Journal of Animal and Veterinary Advances, 6, 851-859.

156. KYRIAKIS, C. S., DE VLEESCHAUWER, A., BARBE, F., BUBLOT, M. & VAN REETH, K. 2009. Safety, immunogenicity and efficacy of poxvirus-based vector vaccines expressing the haemagglutinin gene of a highly pathogenic H5N1 avian influenza virus in pigs. Vaccine, 27, 2258-64.

157. LALIBERTE, J. P. & MOSS, B. 2010. Lipid membranes in poxvirus replication. Viruses, 2, 972-986.

158. LAMB, A. L., TORRES, A. S., O'HALLORAN, T. V. & ROSENZWEIG, A. C. 2001. Heterodimeric structure of superoxide dismutase in complex with its metallochaperone. Nat Struct Biol, 8, 751-5.

159. LANGLAND, J. O. & JACOBS, B. L. 2002. The role of the PKR-inhibitory genes, E3L and K3L, in determining vaccinia virus host range. Virology, 299, 133-41.

160. LARTIGUE, A., BURLAT, B., COUTARD, B., CHASPOUL, F., CLAVERIE, J. M. & ABERGEL, C. 2015. The megavirus chilensis Cu,Zn-superoxide dismutase: the first viral structure of a typical cellular copper chaperone-independent hyperstable dimeric enzyme. J Virol, 89, 824-32.

161. LAW, G. L., KORTH, M. J., BENECKE, A. G. & KATZE, M. G. 2013. SYSTEMS VIROLOGY: HOST-DIRECTED APPROACHES TO VIRAL PATHOGENESIS AND DRUG TARGETING. Nature reviews. Microbiology, 11, 455-466.

162. LAW, M., CARTER, G. C., ROBERTS, K. L., HOLLINSHEAD, M. & SMITH, G. L. 2006. Ligand-induced and nonfusogenic dissolution of a viral membrane. Proceedings of the National Academy of Sciences, 103, 5989-5994.

163. LEGRAND, F. A., VERARDI, P. H., JONES, L. A., CHAN, K. S., PENG, Y. & YILMA, T. D. 2004. Induction of potent humoral and cell-mediated immune responses by attenuated vaccinia virus vectors with deleted serpin genes. Journal of virology, 78, 2770-2779.

164. LI, M. & BEG, A. A. 2000. Induction of necrotic-like cell death by tumor necrosis factor alpha and caspase inhibitors: novel mechanism for killing virus-infected cells. J Virol, 74, 7470-7.

165. LIEBERMAN, J. 2010. Granzyme A activates another way to die. Immunological reviews, 235, 93-104.

166. LIEM, J. & LIU, J. 2016. Stress Beyond Translation: Poxviruses and More. Viruses, 8, 169.

167. LIU, F., ZHOU, P., WANG, Q., ZHANG, M. & LI, D. 2018. The Schlafen family: complex roles in different cell types and virus replication. Cell biology international, 42, 2-8.

168. LIU, S.-W., KATSAFANAS, G. C., LIU, R., WYATT, L. S. & MOSS, B. 2015. Poxvirus decapping enzymes enhance virulence by preventing the accumulation of dsRNA and the induction of innate antiviral responses. Cell host & microbe, 17, 320-331.

169. LOCKER, J. K., KUEHN, A., SCHLEICH, S., RUTTER, G., HOHENBERG, H., WEPF, R. & GRIFFITHS, G. 2000. Entry of the Two Infectious Forms of Vaccinia Virus at the Plasma Membane Is Signaling-Dependent for the IMV but Not the EEV. Molecular Biology of the Cell, 11, 2497-2511.

170. LUBINGA, J., TUPPURAINEN, E., STOLTSZ, W., EBERSOHN, K., COETZER, J. & VENTER, E. 2013. Detection of lumpy skin disease virus in saliva of ticks fed on lumpy skin disease virus-infected cattle. Experimental and applied acarology, 61, 129-138.

171. LUBINGA, J. C., TUPPURAINEN, E. S., COETZER, J. A., STOLTSZ, W. H. & VENTER, E. H. 2014. Evidence of lumpy skin disease virus over-wintering by transstadial persistence in Amblyomma hebraeum and transovarial persistence in Rhipicephalus decoloratus ticks. Experimental and applied acarology, 62, 77-90.

172. MA, Z. & DAMANIA, B. 2016. The cGAS-STING defense pathway and its counteraction by viruses. Cell host & microbe, 19, 150-158.

173. MACKETT, M., SMITH, G. L. & MOSS, B. 1982. Vaccinia virus: a selectable eukaryotic cloning and expression vector. Proceedings of the National Academy of Sciences, 79, 7415-7419.

174. MACKETT, M., SMITH, G. L. & MOSS, B. 1984. General method for production and selection of infectious vaccinia virus recombinants expressing foreign genes. J Virol, 49, 857-64.

175. MAGRANÉ, J., HERVIAS, I., HENNING, M. S., DAMIANO, M., KAWAMATA, H. & MANFREDI, G. 2009. Mutant SOD1 in neuronal mitochondria causes toxicity and mitochondrial dynamics abnormalities. Human molecular genetics, 18, 4552-4564.

176. MAK, T. W. & SAUNDERS, M. E. 2006. 17 - Cytokines and Cytokine Receptors. The Immune Response. Burlington: Academic Press.

177. MARTINVALET, D., ZHU, P. & LIEBERMAN, J. 2005. Granzyme A induces caspase-independent mitochondrial damage, a required first step for apoptosis. Immunity, 22, 355-370.

178. MARURI-AVIDAL, L., WEISBERG, A. S. & MOSS, B. 2011. Vaccinia virus L2 protein associates with the endoplasmic reticulum near the growing edge of crescent precursors of immature virions and stabilizes a subset of viral membrane proteins. Journal of virology, JVI. 05573-11.

179. MARZOOK, N. B., PROCTER, D. J., LYNN, H., YAMAMOTO, Y., HORSINGTON, J. & NEWSOME, T. P. 2014. Methodology for the Efficient Generation of Fluorescently Tagged Vaccinia Virus Proteins. Journal of Visualized Experiments : JoVE, 51151.

180. MATHIJS, E., VANDENBUSSCHE, F., HAEGEMAN, A., KING, A., NTHANGENI, B., POTGIETER, C., MAARTENS, L., VAN BORM, S. & DE CLERCQ, K. 2016. Complete Genome Sequences of the Neethling-Like Lumpy Skin Disease Virus Strains Obtained Directly from Three Commercial Live Attenuated Vaccines. Genome Announcements, 4, e01255-16.

181. MATHIJS, E., VANDENBUSSCHE, F., HAEGEMAN, A., KING, A., NTHANGENI, B., POTGIETER, C., MAARTENS, L., VAN BORM, S. & DE CLERCQ, K. 2017. Correction for Mathijs et al., Complete Genome Sequences of the Neethling-Like Lumpy Skin Disease Virus Strains Obtained Directly from Three Commercial Live Attenuated Vaccines. Genome announcements, 5.

182. MAVROMMATIS, E., FISH, E. N. & PLATANIAS, L. C. 2013. The schlafen family of proteins and their regulation by interferons. Journal of interferon & cytokine research : the official journal of the International Society for Interferon and Cytokine Research, 33, 206-210.

183. MAYR, A., HOCHSTEIN-MINTZEL, V. & STICKL, H. 1975. Abstammung, Eigenschaften und Verwendung des attenuierten Vaccinia-Stammes MVA. Infection, 3, 6-14.

184. MAYR, A., STICKL, H., MULLER, H. K., DANNER, K. & SINGER, H. 1978. [The smallpox vaccination strain MVA: marker, genetic structure, experience gained with the parenteral vaccination and behavior in organisms with a debilitated defence mechanism (author's transl)]. Zentralbl Bakteriol B, 167, 375-90.

185. MCCORD, J. M. & FRIDOVICH, I. 1969. Superoxide dismutase. An enzymic function for erythrocuprein (hemocuprein). J Biol Chem, 244, 6049-55.

186. MCFADDEN, G. 2005. Poxvirus tropism. Nat Rev Microbiol, 3, 201-13.

187. MEBRATU, G., KASSA, B., FIKRE, Y. & BERHANU, B. 1984. Observation on the outbreak of lumpy skin disease in Ethiopia. Revue d'élevage et de médecine vétérinaire des pays tropicaux, 37, 395-399.

188. MENASHEROW, S., RUBINSTEIN-GIUNI, M., KOVTUNENKO, A., EYNGOR, Y., FRIDGUT, O., ROTENBERG, D., KHINICH, Y. & STRAM, Y. 2014. Development of an assay to differentiate between virulent and vaccine strains of lumpy skin disease virus (LSDV). J Virol Methods, 199, 95-101.

189. MENG, X., JIANG, C., ARSENIO, J., DICK, K., CAO, J. & XIANG, Y. 2009. Vaccinia Virus K1L and C7L Inhibit Antiviral Activities Induced by Type I Interferons. Journal of Virology, 83, 10627-10636.

190. MENG, X., SCHOGGINS, J., ROSE, L., CAO, J., PLOSS, A., RICE, C. M. & XIANG, Y. 2012. C7L family of poxvirus host range genes inhibits antiviral activities induced by type I interferons and interferon regulatory factor 1. J Virol, 86, 4538-47.

191. MENG, X., WU, X., YAN, B., DENG, J. & XIANG, Y. 2013. Analysis of the role of vaccinia virus H7 in virion membrane biogenesis with a H7-deletion mutant. Journal of virology, JVI. 00845-13.

192. MERCER, A., SCHMIDT, A. & WEBER, O. 2007a. Poxviruses, Springer Science & Business Media.

193. MERCER, A., SCHMIDT, A. & WEBER, O. 2007b. Poxviruses, Springer London, Limited.

194. MERCER, A. A., FLEMING, S. B. & UEDA, N. 2005. F-box-like domains are present in most poxvirus ankyrin repeat proteins. Virus Genes, 31, 127-33.

195. MEYER, H., SUTTER, G. & MAYR, A. 1991. Mapping of deletions in the genome of the highly attenuated vaccinia virus MVA and their influence on virulence. J Gen Virol, 72 (Pt 5), 1031-8.

196. MORROW, W. J. W., SHEIKH, N. A., SCHMIDT, C. S. & DAVIES, D. H. 2012. Vaccinology: principles and practice, John Wiley & Sons.

197. MOSS, B. 1996. Genetically engineered poxviruses for recombinant gene expression, vaccination, and safety. Proc Natl Acad Sci U S A, 93, 11341-8.

198. MOSS, B. 2006. Poxvirus entry and membrane fusion. Virology, 344, 48-54.

199. MOSS, B. 2012. Poxvirus Cell Entry: How Many Proteins Does it Take? Viruses, 4, 688-707.

200. MOSS, B. 2013. Poxvirus DNA Replication. Cold Spring Harbor Perspectives in Biology, 5, a010199.

201. MOSS, B. Membrane fusion during poxvirus entry. Seminars in cell & developmental biology, 2016. Elsevier, 89-96.

202. MULLIGAN, R. C. & BERG, P. 1981. Selection for animal cells that express the Escherichia coli gene coding for xanthine-guanine phosphoribosyltransferase. Proc Natl Acad Sci U S A, 78, 2072-6.

203. NAGATA, S. 2000. Apoptotic DNA Fragmentation. Experimental Cell Research, 256, 12-18.

204. NAGATA, S. 2018. Apoptosis and Clearance of Apoptotic Cells. Annual review of immunology, 36, 489-517.

205. NAGATA, S. & TANAKA, M. 2017. Programmed cell death and the immune system. Nature Reviews Immunology, 17, 333.

206. NÁJERA, J. L., GÓMEZ, C. E., DOMINGO-GIL, E., GHERARDI, M. M. & ESTEBAN, M. 2006. Cellular and biochemical differences between two attenuated poxvirus vaccine candidates (MVA and NYVAC) and role of the C7L gene. Journal of virology, 80, 6033-6047.

207. NAKAYA, H. I., WRAMMERT, J., LEE, E. K., RACIOPPI, L., MARIE-KUNZE, S., HAINING, W. N., MEANS, A. R., KASTURI, S. P., KHAN, N., LI, G. M., MCCAUSLAND, M., KANCHAN, V., KOKKO, K. E., LI, S., ELBEIN, R., MEHTA, A. K., ADEREM, A., SUBBARAO, K., AHMED, R. & PULENDRAN, B. 2011. Systems biology of vaccination for seasonal influenza in humans. Nat Immunol, 12, 786-95.

208. NAWATHE, D., ASAGBA, M., ABEGUNDE, A., AJAYI, S. & DURKWA, L. 1982. Some observations on the occurrence of lumpy skin disease in Nigeria. Zoonoses and Public Health, 29, 31-36.

209. NEAMAT-ALLAH, A. N. 2015. Immunological, hematological, biochemical, and histopathological studies on cows naturally infected with lumpy skin disease. Veterinary world, 8, 1131.

210. NICHOLS, D. B., DE MARTINI, W. & COTTRELL, J. 2017. Poxviruses Utilize Multiple Strategies to Inhibit Apoptosis. Viruses, 9.

211. NIKOLETOPOULOU, V., MARKAKI, M., PALIKARAS, K. & TAVERNARAKIS, N. 2013. Crosstalk between apoptosis, necrosis and autophagy. Biochimica et Biophysica Acta (BBA) - Molecular Cell Research, 1833, 3448-3459.

212. NTOMBIMBINI, Z. M. & KLEIN, K. 2015. Socio-economic impacts of lumpy skin disease and rift valley fever on the South African livestock economy.

213. OFFERMAN, K.-M. 2014. Investigation of local South African avipoxviruses as potential vaccine vectors. University of Cape Town.

214. OFFERMAN, K., CARULEI, O., GOUS, T. A., DOUGLASS, N. & WILLIAMSON, A.-L. 2013. Phylogenetic and histological variation in avipoxviruses isolated in South Africa. The Journal of General Virology, 94, 2338-2351.

215. OFFERMAN, K., DEFFUR, A., CARULEI, O., WILKINSON, R., DOUGLASS, N. & WILLIAMSON, A.-L. 2015. Six host-range restricted poxviruses from three genera induce distinct gene expression profiles in an in vivo mouse model. BMC genomics, 16, 510.

216. OH, Y. K., SHIN, K. S., YUAN, J. & KANG, S. J. 2008. Superoxide dismutase 1 mutants related to amyotrophic lateral sclerosis induce endoplasmic stress in neuro2a cells. Journal of neurochemistry, 104, 993-1005.

217. OIE 2017. Manual of Diagnostic Tests and Vaccines for Terrestrial Animals 2017

218. OIE Terrestial Manual.

219. OLIVEIRA, G. P., RODRIGUES, R. A. L., LIMA, M. T., DRUMOND, B. P. & ABRAHÃO, J. S. 2017. Poxvirus Host Range Genes and Virus–Host Spectrum: A Critical Review. Viruses, 9, 331.

220. OLIVEROS, J. & VENNY, C. 2007. An interactive tool for comparing lists with Venn Diagrams. 2007. Google Scholar.

221. ORZALLI, M. H. & KAGAN, J. C. 2017. Apoptosis and Necroptosis as Host Defense Strategies to Prevent Viral Infection. Trends in Cell Biology, 27, 800-809.

222. PANICALI, D. & PAOLETTI, E. 1982. Construction of poxviruses as cloning vectors: insertion of the thymidine kinase gene from herpes simplex virus into the DNA of infectious vaccinia virus. Proc Natl Acad Sci U S A, 79, 4927-31.

223. PANUS, J. F., SMITH, C. A., RAY, C. A., SMITH, T. D., PATEL, D. D. & PICKUP, D. J. 2002. Cowpox virus encodes a fifth member of the tumor necrosis factor receptor family: a soluble, secreted CD30 homologue. Proceedings of the National Academy of Sciences of the United States of America, 99, 8348-8353.

224. PAOLETTI, E. 1996. Applications of pox virus vectors to vaccination: an update. Proc Natl Acad Sci U S A, 93, 11349-53.

225. PARK, C. & PENG, C. 2018. Species-specific inhibition of the Antiviral Protein Kinase PKR by Capripoxviruses. Taiwan: Dept of Medical Microbiology and Immunology, University of California, Davis, United States.

226. PASARE, C. & MEDZHITOV, R. 2005. Control of B-cell responses by Toll-like receptors. Nature, 438, 364.

227. PASTORET, P. P. & VANDERPLASSCHEN, A. 2003. Poxviruses as vaccine vectors. Comparative Immunology, Microbiology and Infectious Diseases, 26, 343-355.

228. PASZKOWSKI, P., NOYCE, R. S. & EVANS, D. H. 2016. Live-Cell Imaging of Vaccinia Virus Recombination. PLOS Pathogens, 12, e1005824.

229. PAVOT, V., SEBASTIAN, S., TURNER, A. V., MATTHEWS, J. & GILBERT, S. C. 2017. Generation and Production of Modified Vaccinia Virus Ankara (MVA) as a Vaccine Vector. Recombinant Virus Vaccines. Springer.

230. PEPINI, T., PULICHINO, A.-M., CARSILLO, T., CARLSON, A. L., SARI-SARRAF, F., RAMSAUER, K., DEBASITIS, J. C., MARUGGI, G., OTTEN, G. R. & GEALL, A. J. 2017. Induction of an IFN-mediated antiviral response by a self-amplifying RNA vaccine: implications for vaccine design. The Journal of Immunology, 198, 4012-4024.

231. PERRY, J., SHIN, D., GETZOFF, E. & TAINER, J. 2010. The structural biochemistry of the superoxide dismutases. Biochimica et Biophysica Acta (BBA)-Proteins and Proteomics, 1804, 245-262.

232. PERVAIZ, S. & CLEMENT, M. V. 2002a. Hydrogen peroxide-induced apoptosis: oxidative or reductive stress? Methods Enzymol, 352, 150-9.

233. PERVAIZ, S. & CLEMENT, M. V. 2002b. A permissive apoptotic environment: function of a decrease in intracellular superoxide anion and cytosolic acidification. Biochem Biophys Res Commun, 290, 1145-50.

234. PETES, C., ODOARDI, N. & GEE, K. 2017. The Toll for Trafficking: Toll-Like Receptor 7 Delivery to the Endosome. Frontiers in Immunology, 8.

235. PRETORIUS, A., VAN KLEEF, M., COLLINS, N., TSHIKUDO, N., LOUW, E., FABER, F., VAN STRIJP, M. & ALLSOPP, B. 2008. A heterologous prime/boost immunisation strategy protects against virulent E. ruminantium Welgevonden needle challenge but not against tick challenge. Vaccine, 26, 4363-4371.

236. PROZESKY, L. & BARNARD, B. 1982. A study of the pathology of lumpy skin disease in cattle. The Onderstepoort journal of veterinary research, 49, 167-175.

237. QUEMIN, E. R., CORROYER-DULMONT, S. & KRIJNSE-LOCKER, J. 2018. Entry and Disassembly of Large DNA Viruses: Electron Microscopy Leads the Way. Journal of Molecular Biology, 430, 1714-1724.

238. QUEREC, T. D., AKONDY, R. S., LEE, E. K., CAO, W., NAKAYA, H. I., TEUWEN, D., PIRANI, A., GERNERT, K., DENG, J. & MARZOLF, B. 2009. Systems biology approach predicts immunogenicity of the yellow fever vaccine in humans. Nature immunology, 10, 116-125.

239. RAE, T. D., TORRES, A. S., PUFAHL, R. A. & O'HALLORAN, T. V. 2001. Mechanism of Cu,Zn-superoxide dismutase activation by the human metallochaperone hCCS. J Biol Chem, 276, 5166-76.

240. RAMSEY-EWING, A. L. & MOSS, B. 1996. Complementation of a vaccinia virus host-range K1L gene deletion by the nonhomologous CP77 gene. Virology, 222, 75-86.

241. RAY, C. A., BLACK, R. A., KRONHEIM, S. R., GREENSTREET, T. A., SLEATH, P. R., SALVESEN, G. S. & PICKUP, D. J. 1992. Viral inhibition of inflammation: cowpox virus encodes an inhibitor of the interleukin-1 beta converting enzyme. Cell, 69, 597-604.

242. REDKIEWICZ, P., STACHYRA, A., SAWICKA, R. A., BOCIAN, K., GÓRA-SOCHACKA, A., KOSSON, P. & SIRKO, A. 2017. Immunogenicity of DNA Vaccine against H5N1 Containing Extended Kappa B Site: In Vivo Study in Mice and Chickens. Frontiers in Immunology, 8, 1012.

243. REED, L. J. & MUENCH, H. 1938. A simple method of estimating fifty per cent endpoints. American journal of epidemiology, 27, 493-497.

244. REID, R., ROBERTS, F. & MACDUFF, E. 2011. Pathology Illustrated E-Book, Elsevier Health Sciences.

245. RERKS-NGARM, S., PITISUTTITHUM, P., NITAYAPHAN, S., KAEWKUNGWAL, J., CHIU, J., PARIS, R., PREMSRI, N., NAMWAT, C., DE SOUZA, M., ADAMS, E., BENENSON, M., GURUNATHAN, S., TARTAGLIA, J., MCNEIL, J. G., FRANCIS, D. P., STABLEIN, D., BIRX, D. L., CHUNSUTTIWAT, S., KHAMBOONRUANG, C., THONGCHAROEN, P., ROBB, M. L., MICHAEL, N. L., KUNASOL, P. & KIM, J. H. 2009. Vaccination with ALVAC and AIDSVAX to prevent HIV-1 infection in Thailand. N Engl J Med, 361, 2209-20.

246. REYNOLDS, S. E., EARL, P. L., MINAI, M., MOORE, I. & MOSS, B. 2017. A homolog of the variola virus B22 membrane protein contributes to ectromelia virus pathogenicity in the mouse footpad model. Virology, 501, 107-114.

247. RICE, A. D., GRAY, S. A., LI, Y., DAMON, I. & MOYER, R. W. 2011. An efficient method for generating poxvirus recombinants in the absence of selection. Viruses, 3, 217-32.

248. RICHARDSON, J. S. & RICHARDSON, D. C. 2002. Natural β-sheet proteins use negative design to avoid edge-to-edge aggregation. Proceedings of the National Academy of Sciences, 99, 2754-2759.

249. RIEDEL, S. 2005. Edward Jenner and the history of smallpox and vaccination. Proc (Bayl Univ Med Cent), 18, 21-5.

250. ROBERTS, K. L., BREIMAN, A., CARTER, G. C., EWLES, H. A., HOLLINSHEAD, M., LAW, M. & SMITH, G. L. 2009. Acidic residues in the membrane-proximal stalk region of vaccinia virus protein B5 are required for glycosaminoglycan-mediated disruption of the extracellular enveloped virus outer membrane. Journal of General Virology, 90, 1582-1591.

251. ROCK, K. L. & KONO, H. 2008. The inflammatory response to cell death. Annual review of pathology, 3, 99-126.

252. ROJAS-CARABALLO, J., LÓPEZ-ABÁN, J., MORENO-PÉREZ, D. A., VICENTE, B., FERNÁNDEZ-SOTO, P., DEL OLMO, E., PATARROYO, M. A. & MURO, A. 2017. Transcriptome profiling of gene expression during immunisation trial against Fasciola hepatica: identification of genes and pathways involved in conferring immunoprotection in a murine model. BMC Infectious Diseases, 17, 94.

253. ROMERO, C. H., BARRETT, T., EVANS, S. A., KITCHING, R. P., GERSHON, P. D., BOSTOCK, C. & BLACK, D. N. 1993. Single capripoxvirus recombinant vaccine for the protection of cattle against rinderpest and lumpy skin disease. Vaccine, 11, 737-42.

254. ROUBY, S. & ABOULSOUD, E. 2016. Evidence of intrauterine transmission of lumpy skin disease virus. The Veterinary Journal, 209, 193-195.

255. ROVID, S. 2012. Lumpy Skin Disease. The center for food security and public health, Iowa State University. College of Veterinary Medicine.

256. ROYO, S., SAINZ, B., HERNÁNDEZ-JIMÉNEZ, E., REYBURN, H., LÓPEZ-COLLAZO, E. & GUERRA, S. 2014. Differential induction of apoptosis, interferon signaling, and phagocytosis in macrophages infected with a panel of attenuated and nonattenuated poxviruses. Journal of virology, 88, 5511-5523.

257. RYERSON, M. R., RICHARDS, M. M., KVANSAKUL, M., HAWKINS, C. J. & SHISLER, J. L. 2017. Vaccinia virus encodes a novel inhibitor of apoptosis that associates with the apoptosome. Journal of virology, JVI. 01385-17.

258. SADLER, A. J. & WILLIAMS, B. R. 2008. Interferon-inducible antiviral effectors. Nat Rev Immunol, 8, 559-68.

259. SANCHEZ-SAMPEDRO, L., PERDIGUERO, B., MEJIAS-PEREZ, E., GARCIA-ARRIAZA, J., DI PILATO, M. & ESTEBAN, M. 2015. The evolution of poxvirus vaccines. Viruses, 7, 1726-803.

260. SARAIVA, M. & ALCAMI, A. 2001. CrmE, a novel soluble tumor necrosis factor receptor encoded by poxviruses. J Virol, 75, 226-33.

261. SARHAN, M., LAND, W. G., TONNUS, W., HUGO, C. P. & LINKERMANN, A. 2018. Origin and Consequences of Necroinflammation. Physiological reviews, 98, 727-780.

262. SCANDALIOS, J. G. 1993. Oxygen stress and superoxide dismutases. Plant physiology, 101, 7.

263. SCHMIDT, FLORIAN I., BLECK, CHRISTOPHER KARL E., REH, L., NOVY, K., WOLLSCHEID, B., HELENIUS, A., STAHLBERG, H. & MERCER, J. 2013. Vaccinia Virus Entry Is Followed by Core Activation and Proteasome-Mediated Release of the Immunomodulatory Effector VH1 from Lateral Bodies. Cell Reports, 4, 464-476.

264. SCHMIDT, P. J., KUNST, C. & CULOTTA, V. C. 2000. Copper Activation of Superoxide Dismutase 1 (SOD1) in Vivo ROLE FOR PROTEIN-PROTEIN INTERACTIONS WITH THE COPPER CHAPERONE FOR SOD1. Journal of Biological Chemistry, 275, 33771-33776.

265. SCHMIDT, P. J., RAE, T. D., PUFAHL, R. A., HAMMA, T., STRAIN, J., O'HALLORAN, T. V. & CULOTTA, V. C. 1999. Multiple protein domains contribute to the action of the copper chaperone for superoxide dismutase. Journal of Biological Chemistry, 274, 23719-23725.

266. SCHNELL, M. J. 2001. Viral vectors as potential HIV-1 vaccines. FEMS Microbiology Letters, 200, 123-129.

267. SCHOGGINS, J. W. 2014. Interferon-stimulated genes: roles in viral pathogenesis. Current opinion in virology, 0, 40-46.

268. SEDGER, L. M. 2013. microRNA control of interferons and interferon induced anti-viral activity. Molecular Immunology, 56, 781-793.

269. SEET, B. T., JOHNSTON, J., BRUNETTI, C. R., BARRETT, J. W., EVERETT, H., CAMERON, C., SYPULA, J., NAZARIAN, S. H., LUCAS, A. & MCFADDEN, G. 2003. Poxviruses and immune evasion. Annual review of immunology, 21, 377-423.

270. SHANER, N. C., STEINBACH, P. A. & TSIEN, R. Y. 2005. A guide to choosing fluorescent proteins. Nat Methods, 2, 905-9.

271. SHARMA, S., PATNAIK, S. K., THOMAS TAGGART, R., KANNISTO, E. D., ENRIQUEZ, S. M., GOLLNICK, P. & BAYSAL, B. E. 2015. APOBEC3A cytidine deaminase induces RNA editing in monocytes and macrophages. Nature Communications, 6, 6881.

272. SHIMOMURA, O. 2005. The discovery of aequorin and green fluorescent protein. J Microsc, 217, 1-15.

273. SHISLER, J. L. & JIN, X.-L. 2004. The vaccinia virus K1L gene product inhibits host NF-kappaB activation by preventing IkappaBalpha degradation. Journal of virology, 78, 3553-3560.

274. SIHVONEN, L. H. & DEPNER, K. 2016. Urgent advice on lumpy skin disease. EFSA Journal.

275. SILVERMAN, G. A., BIRD, P. I., CARRELL, R. W., CHURCH, F. C., COUGHLIN, P. B., GETTINS, P. G., IRVING, J. A., LOMAS, D. A., LUKE, C. J., MOYER, R. W., PEMBERTON, P. A., REMOLD-O'DONNELL, E., SALVESEN, G. S., TRAVIS, J. & WHISSTOCK, J. C. 2001. The serpins are an expanding superfamily of structurally similar but functionally diverse proteins. Evolution, mechanism of inhibition, novel functions, and a revised nomenclature. J Biol Chem, 276, 33293-6.

276. SILVERMAN, ROBERT H. 2015. Caps Off to Poxviruses. Cell Host & Microbe, 17, 287-289.

277. SIX, A., BELLIER, B., THOMAS‐VASLIN, V. & KLATZMANN, D. 2012. Systems biology in vaccine design. Microbial biotechnology, 5, 295-304.

278. SLAUCH, J. M. 2011. How does the oxidative burst of macrophages kill bacteria? Still an open question. Molecular microbiology, 80, 580-583.

279. SMITH, C. A., DAVIS, T., ANDERSON, D., SOLAM, L., BECKMANN, M. P., JERZY, R., DOWER, S. K., COSMAN, D. & GOODWIN, R. G. 1990. A receptor for tumor necrosis factor defines an unusual family of cellular and viral proteins. Science, 248, 1019-23.

280. SMITH, C. A., DAVIS, T., WIGNALL, J. M., DIN, W. S., FARRAH, T., UPTON, C., MCFADDEN, G. & GOODWIN, R. G. 1991. T2 open reading frame from the Shope fibroma virus encodes a soluble form of the TNF receptor. Biochem Biophys Res Commun, 176, 335-42.

281. SMITH, G. L. & MOSS, B. 1983. Infectious poxvirus vectors have capacity for at least 25 000 base pairs of foreign DNA. Gene, 25, 21-28.

282. SMITH, H. C., GOTT, J. M. & HANSON, M. R. 1997. A guide to RNA editing. RNA (New York, N.Y.), 3, 1105-1123.

283. SMITH, K. A. 2013. Smallpox: can we still learn from the journey to eradication? The Indian journal of medical research, 137, 895-899.

284. SMYTH, G. K. 2005. limma: Linear Models for Microarray Data. In: GENTLEMAN, R., CAREY, V. J., HUBER, W., IRIZARRY, R. A. & DUDOIT, S. (eds.) Bioinformatics and Computational Biology Solutions Using R and Bioconductor. New York, NY: Springer New York.

285. SONNBERG, S., SEET, B. T., PAWSON, T., FLEMING, S. B. & MERCER, A. A. 2008. Poxvirus ankyrin repeat proteins are a unique class of F-box proteins that associate with cellular SCF1 ubiquitin ligase complexes. Proc Natl Acad Sci U S A, 105, 10955-60.

286. SOUZA, A. P., HAUT, L., REYES-SANDOVAL, A. & PINTO, A. R. 2005. Recombinant viruses as vaccines against viral diseases. Braz J Med Biol Res, 38, 509-22.

287. SPARRER, K. M. J. & GACK, M. U. 2015. Intracellular detection of viral nucleic acids. Current opinion in microbiology, 26, 1-9.

288. STURTZ, L. A., DIEKERT, K., JENSEN, L. T., LILL, R. & CULOTTA, V. C. 2001. A fraction of yeast cu, zn-superoxide dismutase and its metallochaperone, ccs, localize to the intermembrane space of mitochondria a physiological role for sod1 in guarding against mitochondrial oxidative damage. Journal of Biological Chemistry, 276, 38084-38089.

289. SUN, P. 2014. Chapter 7 - Structural Recognition of Immunoglobulins by Fcγ Receptors A2 - Ackerman, Margaret E. In: NIMMERJAHN, F. (ed.) Antibody Fc. Boston: Academic Press.

290. SUTTER, G. & MOSS, B. 1992. Nonreplicating vaccinia vector efficiently expresses recombinant genes. Proceedings of the National Academy of Sciences, 89, 10847-10851.

291. SUTTER, G., WYATT, L. S., FOLEY, P. L., BENNINK, J. R. & MOSS, B. 1994. A recombinant vector derived from the host range-restricted and highly attenuated MVA strain of vaccinia virus stimulates protective immunity in mice to influenza virus. Vaccine, 12, 1032-40.

292. SZABO, A., MAGYARICS, Z., PAZMANDI, K., GOPCSA, L., RAJNAVOLGYI, E. & BACSI, A. 2014. TLR ligands upregulate RIG‐I expression in human plasmacytoid

dendritic cells in a type I IFN ‐ independent manner. Immunology and cell biology, 92, 671-678.

293. TAIT, S. W., ICHIM, G. & GREEN, D. R. 2014. Die another way–non-apoptotic mechanisms of cell death. J Cell Sci, 127, 2135-2144.

294. TARTAGLIA, J., COX, W. I., TAYLOR, J., PERKUS, M., RIVIERE, M., MEIGNIER, B. & PAOLETTI, E. 1992a. Highly attenuated poxvirus vectors. AIDS Res Hum Retroviruses, 8, 1445-7.

295. TARTAGLIA, J., PERKUS, M. E., TAYLOR, J., NORTON, E. K., AUDONNET, J.-C., COX, W. I., DAVIS, S. W., VAN DER HOEVEN, J., MEIGNIER, B., RIVIERE, M., LANGUET, B. & PAOLETTI, E. 1992b. NYVAC: A highly attenuated strain of vaccinia virus. Virology, 188, 217-232.

296. TEIGLER, J. E., PHOGAT, S., FRANCHINI, G., HIRSCH, V. M., MICHAEL, N. L. & BAROUCH, D. H. 2014. The canarypox virus vector ALVAC induces distinct cytokine responses compared to the vaccinia virus-based vectors MVA and NYVAC in rhesus monkeys. Journal of virology, 88, 1809-1814.

297. TEOH, M. L., TURNER, P. V. & EVANS, D. H. 2005. Tumorigenic poxviruses up-regulate intracellular superoxide to inhibit apoptosis and promote cell proliferation. J Virol, 79, 5799-811.

298. TEOH, M. L., WALASEK, P. J. & EVANS, D. H. 2003. Leporipoxvirus Cu,Zn-superoxide dismutase (SOD) homologs are catalytically inert decoy proteins that bind copper chaperone for SOD. J Biol Chem, 278, 33175-84.

299. THOMPSON, M. R., KAMINSKI, J. J., KURT-JONES, E. A. & FITZGERALD, K. A. 2011. Pattern Recognition Receptors and the Innate Immune Response to Viral Infection. Viruses, 3, 920-940.

300. TOPLAK, I., PETROVIĆ, T., VIDANOVIĆ, D., LAZIĆ, S., ŠEKLER, M., MANIĆ, M., PETROVIĆ, M. & KUHAR, U. 2017. Complete Genome Sequence of Lumpy Skin

Disease Virus Isolate SERBIA/Bujanovac/2016, Detected during an Outbreak in the Balkan Area. Genome announcements, 5, e00882-17.

301. TORRES, A. S., PETRI, V., RAE, T. D. & O'HALLORAN, T. V. 2001. Copper stabilizes a heterodimer of the yCCS metallochaperone and its target superoxide dismutase. J Biol Chem, 276, 38410-6.

302. TRINCHIERI, G. 2010. Type I interferon: friend or foe? The Journal of Experimental Medicine, 207, 2053-2063.

303. TULMAN, E., AFONSO, C., LU, Z., ZSAK, L., KUTISH, G. & ROCK, D. 2001a. Genome of lumpy skin disease virus. Journal of virology, 75, 7122-7130.

304. TULMAN, E., AFONSO, C., LU, Z., ZSAK, L., SUR, J.-H., SANDYBAEV, N., KEREMBEKOVA, U., ZAITSEV, V., KUTISH, G. & ROCK, D. 2002. The genomes of sheeppox and goatpox viruses. Journal of virology, 76, 6054-6061.

305. TULMAN, E. R., AFONSO, C. L., LU, Z., ZSAK, L., KUTISH, G. F. & ROCK, D. L. 2001b. Genome of Lumpy Skin Disease Virus. Journal of Virology

306. 75, 7122-7130.

307. TUPPURAINEN, E. & GALON, N. 2016. LUMPY SKIN DISEASE: CURRENT SITUATION IN EUROPE AND NEIGHBOURING REGIONS AND NECESSARY CONTROL MEASURES TO HALT THE SPREAD IN SOUTH-EAST EUROPE OIE Regional Commission

308. TUPPURAINEN, E. & OURA, C. A. 2012. lumpy skin disease: an emerging threat to Europe, the Middle East and Asia. Transboundary and Emerging Diseases, 59, 40-48.

309. TUPPURAINEN, E., VENTER, E., SHISLER, J., GARI, G., MEKONNEN, G., JULEFF, N., LYONS, N., DE CLERCQ, K., UPTON, C. & BOWDEN, T. 2017. Capripoxvirus Diseases: Current Status and Opportunities for Control. Transboundary and emerging diseases, 64, 729-745.

310. TUPPURAINEN, E. S., LUBINGA, J. C., STOLTSZ, W. H., TROSKIE, M., CARPENTER, S. T., COETZER, J. A., VENTER, E. H. & OURA, C. A. 2013. Evidence of vertical transmission of lumpy skin disease virus in Rhipicephalus decoloratus ticks. Ticks Tick Borne Dis, 4, 329-33.

311. TUPPURAINEN, E. S., STOLTSZ, W. H., TROSKIE, M., WALLACE, D. B., OURA, C. A., MELLOR, P. S., COETZER, J. A. & VENTER, E. H. 2011. A potential role for ixodid (hard) tick vectors in the transmission of lumpy skin disease virus in cattle. Transbound Emerg Dis, 58, 93-104.

312. TUPPURAINEN, E. S., VENTER, E. & COETZER, J. 2005. The detection of lumpy skin disease virus in samples of experimentally infected cattle using different diagnostic techniques. Onderstepoort Journal of Veterinary Research, 72, 153-164.

313. TUPPURAINEN, E. S. M., PEARSON, C. R., BACHANEK-BANKOWSKA, K., KNOWLES, N. J., AMAREEN, S., FROST, L., HENSTOCK, M. R., LAMIEN, C. E., DIALLO, A. & MERTENS, P. P. C. 2014. Characterization of sheep pox virus vaccine for cattle against lumpy skin disease virus. Antiviral Research, 109, 1-6.

314. UPTON, J. W. & CHAN, F. K.-M. 2014. Staying Alive: Cell Death in Anti-Viral Immunity. Molecular cell, 54, 273-280.

315. VALKENBURG, S. A., LI, O. T., MAK, P. W., MOK, C. K., NICHOLLS, J. M., GUAN, Y., WALDMANN, T. A., PEIRIS, J. M., PERERA, L. P. & POON, L. L. 2014. IL-15 adjuvanted multivalent vaccinia-based universal influenza vaccine requires CD4+ T cells for heterosubtypic protection. Proceedings of the National Academy of Sciences, 111, 5676-5681.

316. VAN GENT, D., SHARP, P., MORGAN, K. & KALSHEKER, N. 2003. Serpins: structure, function and molecular evolution. Int J Biochem Cell Biol, 35, 1536-47.

317. VAN ROOYEN, P. J., MUNZ, E. K. & WEISS, K. E. 1969. The optimal conditions for the multiplication of Neethling-type lumpy skin disease virus in embryonated eggs. Onderstepoort J Vet Res, 36, 165-74.

318. VAN TOL, S., HAGE, A., GIRALDO, M. I., BHARAJ, P. & RAJSBAUM, R. 2017. The TRIMendous Role of TRIMs in Virus-Host Interactions. Vaccines, 5, 23.

319. VAZQUEZ, M. I. & ESTEBAN, M. 1999. Identification of functional domains in the 14-kilodalton envelope protein (A27L) of vaccinia virus. J Virol, 73, 9098-109.

320. VERBIST, K. C., ROSE, D. L., COLE, C. J., FIELD, M. B. & KLONOWSKI, K. D. 2012. IL-15 Participates in the Respiratory Innate Immune Response to Influenza Virus Infection. PLOS ONE, 7, e37539.

321. VERHELST, J., HULPIAU, P. & SAELENS, X. 2013. Mx Proteins: Antiviral Gatekeepers That Restrain the Uninvited. Microbiology and Molecular Biology Reviews : MMBR, 77, 551-566.

322. VEYER, D. L., CARRARA, G., MALUQUER DE MOTES, C. & SMITH, G. L. 2017. Vaccinia virus evasion of regulated cell death. Immunology Letters, 186, 68-80.

323. VIDANOVIĆ, D., ŠEKLER, M., PETROVIĆ, T., DEBELJAK, Z., VASKOVIĆ, N., MATOVIĆ, K. & HOFFMANN, B. 2016. Real-time PCR assays for the specific detection of field Balkan strains of lumpy skin disease virus. Acta Veterinaria, 66, 444-454.

324. VOLZ, A. & SUTTER, G. 2017. Modified vaccinia virus Ankara: history, value in basic research, and current perspectives for vaccine development. Advances in virus research. Elsevier.

325. VON BACKSTROM, U. 1945. Ngamiland cattle disease: preliminary report on a new disease, the etiological agent being probably of an infectious nature. Journal of the South African Veterinary Association, 16, 29-35.

326. WALLACE, D. B. & VILJOEN, G. J. 2005. Immune responses to recombinants of the South African vaccine strain of lumpy skin disease virus generated by using thymidine kinase gene insertion. Vaccine, 23, 3061-7.

327. WALSH, C. M. 2014. Grand challenges in cell death and survival: apoptosis vs. necroptosis. Frontiers in Cell and Developmental Biology, 2, 3.

328. WARNES, G. R., BOLKER, B., BONEBAKKER, L., GENTLEMAN, R., HUBER, W., LIAW, A., LUMLEY, T., MAECHLER, M., MAGNUSSON, A. & MOELLER, S. 2009. gplots: Various R programming tools for plotting data. R package version, 2, 1.

329. WASILENKO, S. T., STEWART, T. L., MEYERS, A. F. & BARRY, M. 2003. Vaccinia virus encodes a previously uncharacterized mitochondrial-associated inhibitor of apoptosis. Proc Natl Acad Sci U S A, 100, 14345-50.

330. WATSON, J. C., CHANG, H. W. & JACOBS, B. L. 1991. Characterization of a vaccinia virus-encoded double-stranded RNA-binding protein that may be involved in inhibition of the double-stranded RNA-dependent protein kinase. Virology, 185, 206-16.

331. WEBER, F., WAGNER, V., RASMUSSEN, S. B., HARTMANN, R. & PALUDAN, S. R. 2006. Double-stranded RNA is produced by positive-strand RNA viruses and DNA viruses but not in detectable amounts by negative-strand RNA viruses. J Virol, 80, 5059-64.

332. WEIR, J. P., BAJSZAR, G. & MOSS, B. 1982. Mapping of the vaccinia virus thymidine kinase gene by marker rescue and by cell-free translation of selected mRNA. Proc Natl Acad Sci U S A, 79, 1210-4.

333. WEISBERG, A. S., MARURI-AVIDAL, L., BISHT, H., HANSEN, B. T., SCHWARTZ, C. L., FISCHER, E. R., MENG, X., XIANG, Y. & MOSS, B. 2017. Enigmatic origin of the poxvirus membrane from the endoplasmic reticulum shown by 3D imaging of vaccinia virus assembly mutants. Proceedings of the National Academy of Sciences.

334. WEISS, K. E. 1968. Lumpy Skin Disease Virus. Cytomegaloviruses. Rinderpest Virus. Lumpy Skin Disease Virus. Berlin, Heidelberg: Springer Berlin Heidelberg.

335. WERDEN, S. J., RAHMAN, M. M. & MCFADDEN, G. 2008. Poxvirus host range genes. Adv Virus Res, 71, 135-71.

336. WOLFFE, E. J., ISAACS, S. N. & MOSS, B. 1993. Deletion of the vaccinia virus B5R gene encoding a 42-kilodalton membrane glycoprotein inhibits extracellular virus envelope formation and dissemination. J Virol, 67, 4732-41.

337. WYATT, L. S., EARL, P. L. & MOSS, B. 2017. Generation of recombinant vaccinia viruses. Current protocols in protein science, 89, 5.13. 1-5.13. 18.

338. XU, Y. & HER, C. 2015. Inhibition of Topoisomerase (DNA) I (TOP1): DNA Damage Repair and Anticancer Therapy. Biomolecules, 5, 1652-1670.

339. YANG, Z., BRUNO, D. P., MARTENS, C. A., PORCELLA, S. F. & MOSS, B. 2010. Simultaneous high-resolution analysis of vaccinia virus and host cell transcriptomes by deep RNA sequencing. Proceedings of the National Academy of Sciences of the United States of America, 107, 11513-11518.

340. YANG, Z., BRUNO, D. P., MARTENS, C. A., PORCELLA, S. F. & MOSS, B. 2011. Genome-wide analysis of the 5' and 3' ends of vaccinia virus early mRNAs delineates regulatory sequences of annotated and anomalous transcripts. J Virol, 85, 5897-909.

341. YÁNGÜEZ, E., GARCÍA-CULEBRAS, A., FRAU, A., LLOMPART, C., KNOBELOCH, K.-P., GUTIERREZ-ERLANDSSON, S., GARCÍA-SASTRE, A., ESTEBAN, M., NIETO, A. & GUERRA, S. 2013. ISG15 regulates peritoneal macrophages functionality against viral infection. PLoS pathogens, 9, e1003632.

342. YAO, X.-D. & EVANS, D. H. 2003. High-frequency genetic recombination and reactivation of orthopoxviruses from DNA fragments transfected into leporipoxvirus-infected cells. Journal of virology, 77, 7281-7290.

343. YAO, X. D. & EVANS, D. H. 2001. Effects of DNA structure and homology length on vaccinia virus recombination. J Virol, 75, 6923-32.

344. YERUHAM, I., NIR, O., BRAVERMAN, Y., DAVIDSON, M., GRINSTEIN, H., HAYMOVITCH, M. & ZAMIR, O. 1995. Spread of lumpy skin disease in Israeli dairy herds. Veterinary Record, 137, 91-91.

345. YOON, S., PARK, S. J., HAN, J. H., KANG, J. H., KIM, J. H., LEE, J., PARK, S., SHIN, H. J., KIM, K., YUN, M. & CHWAE, Y. J. 2014. Caspase-dependent cell death-associated release of nucleosome and damage-associated molecular patterns. Cell Death & Disease, 5, e1494.

346. YUEN, L. & MOSS, B. 1987. Oligonucleotide sequence signaling transcriptional termination of vaccinia virus early genes. Proceedings of the National Academy of Sciences of the United States of America, 84, 6417-6421.

347. ZACHERTOWSKA, A., BREWER, D. & EVANS, D. H. 2004. MALDI-TOF mass spectroscopy detects the capsid structural instabilities created by deleting the myxoma virus cupro-zinc SOD1 homolog M131R. Journal of Virological Methods, 122, 63-72.

348. ZENG, C.-W., ZHANG, X.-J., LIN, K.-Y., YE, H., FENG, S.-Y., ZHANG, H. & CHEN, Y.-Q. 2012. Camptothecin induces apoptosis in cancer cells via miR-125b mediated mitochondrial pathways. Molecular pharmacology, mol. 111.076794.

349. ZHANG, D. & ZHANG, D.-E. 2011. Interferon-Stimulated Gene 15 and the Protein ISGylation System. Journal of Interferon & Cytokine Research, 31, 119-130.

350. ZHANG, G., GURTU, V. & KAIN, S. R. 1996. An enhanced green fluorescent protein allows sensitive detection of gene transfer in mammalian cells. Biochem Biophys Res Commun, 227, 707-11.

351. ZHANG, Z., BAO, M., LU, N., WENG, L., YUAN, B. & LIU, Y. J. 2013. The E3 ubiquitin ligase TRIM21 negatively regulates the innate immune response to intracellular double-stranded DNA. Nat Immunol, 14, 172-8.

352. ZHOU, X., JIANG, W., LIU, Z., LIU, S. & LIANG, X. 2017. Virus infection and death receptor-mediated apoptosis. Viruses, 9, 316.

Appendix 1 – R code used to analyse the mouse transcriptome

```
#set working directory
setwd("c:/R/henry")
#view files in wd
dir("c:/R/henry")

#load packages
library(affy)
library(limma)
library(oligo)
library(annotate)
library(genefilter)
library(Biobase)
library(RColorBrewer)
library(multtest)
library(ArrayTools)
library(pathview)
library(gage)
library(GOstats)
library(ReactomePA)
library(biomaRt)
library(GO.db)
library(mogene20stprobeset.db)
library(mogene20sttranscriptcluster.db)
library(genefilter)
library(gplots)

#load data
RawData <-ReadAffy

#read in .cel files
RawData <- read.celfiles(list.celfiles("C:/R/henry", full.names = T),verbose=TRUE)
```

```
#load phenotype data
pd<-read.AnnotatedDataFrame("phenodata.txt",header=TRUE,row.names=1)
pd.2<-read.table("phenodata.txt",header=T,row.names=1)
x <- varMetadata(pd)
x <- data.frame(x, channel = "_ALL_")
varMetadata(pd) <- x

#RMA normalisation (background correction, normalizing and expression calculation)
OligoEset<-rma(RawData,target="core")
pData(OligoEset)<-pd.2

#boxplots
boxplot(OligoEset, col="red",names=pd$label,las=2,main="Normalized data")

#hist
hist(OligoEset, fig=TRUE)

# Scatterplots
tiff(filename="scatter_OligoEset.tif")
pairs(exprs(OligoEset)[,1:7], pch=".",main="Scatter plots",col=TRUE)
dev.off()

##############################################################################
#############
#annotation
##############################################################################
#############

 # Which platform?
OligoEset@annotation
ls("package:mogene20sttranscriptcluster.db")
ls("package:mogene20stprobeset.db")
```

```
 # Get the transcript cluster IDs from the expressionset
ID <- featureNames(OligoEset)

 # Look up the Gene Symbol, name, and Ensembl Gene ID for each of those IDs
Symbol <- getSYMBOL(ID, "mogene20sttranscriptcluster.db")
Name <- as.character(lookUp(ID, "mogene20sttranscriptcluster.db", "GENENAME"))
Ensembl <- as.character(lookUp(ID, "mogene20sttranscriptcluster.db", "ENSEMBL"))
Entrez <- as.character(lookUp(ID, "mogene20sttranscriptcluster.db", "ENTREZID"))
#GO<-as.character(lookUp(ID, "mogene20sttranscriptcluster.db", "GO"))

# Make a temporary data frame with all those identifiers
tmp <- data.frame(ID=ID, Symbol=Symbol, Name=Name,
Ensembl=Ensembl,Entrez=Entrez, stringsAsFactors=F)

# set the featureData for your expressionset using the data frame you created above.
fData(OligoEset) <- tmp

##########################################################################
##############
#Non-specific filtering (GeneFilter)
##########################################################################
##############

#intensity filter - (intensity of a gene should be >log2(100) in at least 20% of the samples)

f1<-pOverA(0.25, log2(100))

#variance filter - (the interquartile range of log2-intensities should be at least 0.5)
f2<-function(x)(IQR(x) > 0.5)

ff<-filterfun(f1,f2)
selected <- genefilter(OligoEset, ff)
```

```
sum(selected)
esetSub=OligoEset[selected,]

################################################################################
############
#differential expression
################################################################################
############
#limma for linear model of data

# Export all affy expression values to a tab delimited text file
write.exprs(esetSub, file="OligoEset.txt")

#differential expression analysis
# Create appropriate design matrix and assign column names
design <- model.matrix(~-
1+factor(c("PBS","PBS","PBS","iLSDV","iLSDV","iLSDV","MVA","MVA",
"MVA","nLSDV","nLSDV","nLSDV")))
colnames(design)<-c("PBS","iLSDV","MVA","nLSDV")

# Create appropriate contrast matrix for pairwise comparisons
contrast.matrix <- makeContrasts(PBS-iLSDV, PBS-nLSDV, PBS-MVA, levels=design)

# Fit a linear model for each gene based on the given series of arrays
fit <- lmFit(esetSub, design)

# Compute estimated coefficients and standard errors for a given set of
contrasts
fit2 <- contrasts.fit(fit, contrast.matrix)

# Compute moderated t-statistics and log-odds of differential expression by empirical Bayes
shrinkage of the standard errors towards a common value
fit2 <- eBayes(fit2)
```

```
# Generate list of top 10 DEGs for first comparison
topTable(fit2, coef=1, adjust="fdr", sort.by="B",p.value=0.05,number=10)

#Generate heatmap
list=c()
for (i in 1:3){
  genes<-topTable(fit2, coef=i, adjust="fdr", sort.by="B",p.value=0.05,number=600)$ID
  list<-c(list,genes)
}
list2<-unique(list)
length(list2)

gr <- decideTests(fit2 , adjust.method="none")
gr2 <- decideTests(fit2 , adjust.method="fdr")

results<-exprs(OligoEset)[list2,]
colnames(results)<-pd$label

heatmap(results,)
heatmap(results,scale="none")

#heatmap.2 using gplots
heatmap.2(results, col=redgreen(75), scale="none", key=TRUE, symkey=FALSE,
density.info="none", trace="none", cexRow=0.5)

#generate gene lists (dif. expr. genes) for each comparison (1-6)
iLSDV<-topTable(fit2, coef=1, adjust="fdr", sort.by="B",resort.by="logFC",
p.value=0.05,number=Inf)
write.csv(iLSDV, file="iLSDV.csv")

nLSDV<-topTable(fit2, coef=2, adjust="fdr", sort.by="B",resort.by="logFC",
p.value=0.05,number=Inf)
```

```
write.csv(nLSDV, file="nLSDV.csv")

MVA<-topTable(fit2, coef=3, adjust="fdr", sort.by="B",resort.by="logFC",
p.value=0.05,number=Inf)
write.csv(MVA, file="MVA.csv")

#analysis with cluster profiler

library(DOSE)
library(clusterProfiler)
library(ReactomePA)
library(org.Mm.eg.db)
library(GO.db)
library(pathview)



################################################################################
################################
#comparison1 (PBS vs iLSDV)

#data input
iLSDV<-read.csv("c:/R/henry/iLSDV.csv")
head(iLSDV)

# annotate with entrez info
all_genes1 <- iLSDV$Entrez
all_genes1 <- all_genes1[!is.na(all_genes1)]
all_genes1<-all_genes1[!duplicated(all_genes1)]
all_genes1
iLSDV<-as.character(all_genes1)

#GO classification
ggo1 <-groupGO(iLSDV1, organism="mouse", ont = "BP", level=3, readable = TRUE)
```

```
head(summary(ggo1))

#GO enrichment analysis - HYPERGEOMETRIC MODEL (left out universe="")
ego1<-enrichGO(gene=iLSDV1,organism="mouse", ont="BP", pvalueCutoff=0.05,
readable=TRUE)
head(summary(ego1))

#GO enrichment analysis - KEGG pathway enrichment analysis
kk1<-enrichKEGG(gene=iLSDV1,organism="mouse", pvalueCutoff=0.05, readable=TRUE)
head(summary(kk1))

#Reactome pathway enrichment analysis - results in error
rp1<-enrichPathway(gene=iLSDV1,organism="mouse", pvalueCutoff=0.05,
readable=TRUE)

#visualization of results
barplot(ggo1, drop=TRUE, showCategory=12)
barplot(ego1, drop=TRUE, showCategory=10)
barplot(kk1, drop=TRUE, showCategory=10)
barplot(rp1, drop=TRUE, showCategory=10)

##############################################################################
################################
#comparison2 (PBS vs nLSDV)

#data input
nLSDV<-read.csv("c:/R/henry/nLSDV.csv")
head(nLSDV)

# annotate with entrez info
all_genes2 <- nLSDV$Entrez
all_genes2 <- all_genes2[!is.na(all_genes2)]
all_genes2<-all_genes2[!duplicated(all_genes2)]
```

```
all_genes2
nLSDV<-as.character(all_genes2)

#GO classification
ggo2 <-groupGO(nLSDV, organism="mouse", ont = "BP", level=3, readable = TRUE)
head(summary(ggo1))

#GO enrichment analysis - HYPERGEOMETRIC MODEL (left out universe="")
ego2<-enrichGO(gene=nLSDV,organism="mouse", ont="BP", pvalueCutoff=0.05,
readable=TRUE)
head(summary(ego1))

#GO enrichment analysis - KEGG pathway enrichment analysis
kk2<-enrichKEGG(gene=nLSDV,organism="mouse", pvalueCutoff=0.05, readable=TRUE)
head(summary(kk1))

#Reactome pathway enrichment analysis - results in error
rp2<-enrichPathway(gene=nLSDV,organism="mouse", pvalueCutoff=0.05, readable=TRUE)

#visualization of results
barplot(ggo2, drop=TRUE, showCategory=12)
barplot(ego2, drop=TRUE, showCategory=10)
barplot(kk2, drop=TRUE, showCategory=10)
barplot(rp2, drop=TRUE, showCategory=10)

##############################################################################
################################
#comparison3 (PBS vs MVA)

#data input
MVA<-read.csv("c:/R/henry/MVA.csv")
head(MVA)
```

```
# annotate with entrez info
all_genes3 <- MVA$Entrez
all_genes3 <- all_genes3[!is.na(all_genes3)]
all_genes3<-all_genes3[!duplicated(all_genes3)]
all_genes3
MVA<-as.character(all_genes3)

#GO classification
ggo3 <-groupGO(MVA, organism="mouse", ont = "BP", level=3, readable = TRUE)
head(summary(ggo3))

#GO enrichment analysis - HYPERGEOMETRIC MODEL (left out universe="")
ego3<-enrichGO(gene=MVA,organism="mouse", ont="BP", pvalueCutoff=0.05,
readable=TRUE)
head(summary(ego3))

#GO enrichment analysis - KEGG pathway enrichment analysis
kk3<-enrichKEGG(gene=MVA,organism="mouse", pvalueCutoff=0.05, readable=TRUE)
head(summary(kk3))

#Reactome pathway enrichment analysis - results in error
rp3<-enrichPathway(gene=MVA,organism="mouse", pvalueCutoff=0.05, readable=TRUE)

#visualization of results
barplot(ggo3, drop=TRUE, showCategory=12)
barplot(ego3, drop=TRUE, showCategory=10)
barplot(kk3, drop=TRUE, showCategory=10)
barplot(rp3, drop=TRUE, showCategory=10)

##############################################################################
############################
#Biological Theme Comparison
allcomparison<-cbind(iLSDV,nLSDV,MVA)
```

```
allcomparison
write.csv(allcomparison, file="c:/R/henry/allc.csv")

allc<-read.csv("c:/R/henry/allc.csv") #removed first column of numbers 1-.. in excel
names(allc)
allc[1]

ck<-compareCluster(geneCluster=allc, fun="enrichKEGG", organism="mouse",
pvalueCutoff=0.05, readable=TRUE)
head(summary(ck))
cGO<-compareCluster(geneCluster=allc, fun="enrichGO",ont="BP", organism="mouse",
pvalueCutoff=0.05, readable=TRUE)
cGOMF<-compareCluster(geneCluster=allc, fun="enrichGO",ont="MF",
organism="mouse", pvalueCutoff=0.05, readable=TRUE)
cGOCC<-compareCluster(geneCluster=allc, fun="enrichGO",ont="CC", organism="mouse",
pvalueCutoff=0.05, readable=TRUE)

plot(ck, type = "dot", showCategory=NULL, by = "count", title = "KEGG enrichment",
font.size = 12)
plot(ck, type = "bar", showCategory=NULL, by = "count", title = "KEGG enrichment",
font.size = 12)
plot(ck, type = "bar", showCategory=NULL, by = "percentage", title = "KEGG enrichment",
font.size = 12)

plot(cGO, type = "dot", showCategory=30, by = "count", title = "GO enrichment", font.size =
12)
plot(cGO, type = "bar", showCategory=30, by = "count", title = "GO enrichment", font.size =
12)

plot(cGOMF, type = "dot", showCategory=20, by = "count", title = "GO enrichment",
font.size = 12)
plot(cGOCC, type = "dot", showCategory=20, by = "count", title = "GO enrichment",
font.size = 12)
```

```
##############################################################################
#########################

#set working directory
setwd("c:/R/henry/heatmap")

iLSDV<-read.csv("c:/R/henry/heatmap/iLSDV.csv", header=T)
row.names(iLSDV)
iLSDV1<-as.matrix(iLSDV)

nLSDV<-read.csv("c:/R/henry/heatmap/nLSDV.csv", header=T)
row.names(nLSDV)
nLSDV1<-as.matrix(nLSDV)


mva<-read.csv("c:/R/henry/heatmap/MVA.csv", header=T)
row.names(mva)
mva1<-as.matrix(mva)
head(mva1)


library(gplots)

a<-merge(iLSDV1,mva1, by="ID", all = TRUE)
b<-merge(a,nLSDV1, by="ID", all = TRUE)

write.csv(b, "b.csv")

all<-read.csv("c:/R/henry/heatmap/c.csv", header=T, row.names=1)
all[is.na(all)] <- 0
all<-as.matrix(all)
```

```
length(all)

#heatmap.2(all1, cexCol=1, col=redgreen(75),colsep=c(1:4),Colv=NA, scale="none",
key=TRUE, symkey=TRUE, density.info="none", trace="none", cexRow=0.7,
sepwidth=c(0.01), sepcolor="white", lhei = c(0.02,1),lwid = c(1,1),margins=c(5,5) )
heatmap.2(all, col=redgreen(75),scale="row", key=TRUE, symkey=FALSE,symbreaks=F,
density.info="none", trace="none", cexRow=0.5, cexCol=1)

dev.off()
?heatmap.2

##############################################
#Generation of Gene Lists
##############################################

#set working directory
setwd("c:/R/henry/lists")

#annotated UP REGULATED GENES#
iLSDV<-read.csv("c:/R/henry/lists/iLSDVup.csv", header=T)
row.names(iLSDV)
iLSDV1<-as.matrix(iLSDV)

nLSDV<-read.csv("c:/R/henry/lists/nLSDVup.csv", header=T)
row.names(nLSDV)
nLSDV1<-as.matrix(nLSDV)


mva<-read.csv("c:/R/henry/lists/MVAup.csv", header=T)
row.names(mva)
mva1<-as.matrix(mva)
head(mva1)
```

```
a<-merge(iLSDV1,mva1, by="Symbol", all = TRUE)
b<-merge(a,nLSDV1, by="Symbol", all = TRUE)

write.csv(b, "b.csv")

#annotated DOWN REGULATED GENES#
iLSDVd<-read.csv("c:/R/henry/lists/iLSDVdown.csv", header=T)
row.names(iLSDVd)
iLSDV1d<-as.matrix(iLSDVd)

nLSDVd<-read.csv("c:/R/henry/lists/nLSDVdown.csv", header=T)
row.names(nLSDVd)
nLSDV1d<-as.matrix(nLSDVd)


mvad<-read.csv("c:/R/henry/lists/MVAdown.csv", header=T)
row.names(mvad)
mva1d<-as.matrix(mvad)
head(mva1d)

c<-merge(iLSDV1d,mva1d, by="Symbol", all = TRUE)
d<-merge(c,nLSDV1d, by="Symbol", all = TRUE)

write.csv(d, "d.csv")
```

Appendix 2 – pJET map

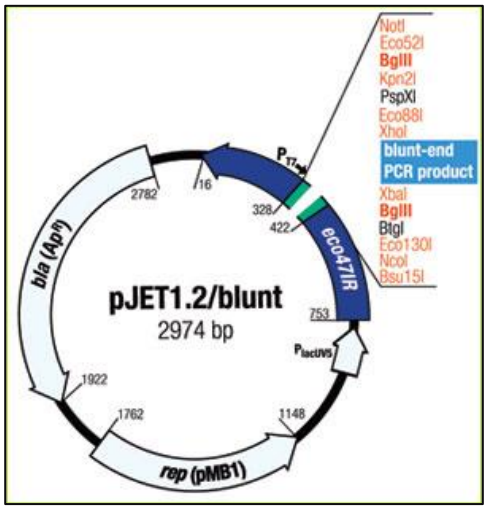

Figure A.34. Plasmid vector map of pJET 1.2 / blunt vector. The vector contains an ampicillin resistance gene, origin of replication and an insertion sited for a blunt end product. The vector contains a lethal gene which if the vector circularises on its own, causes death of bacteria carrying the circularised plasmid. Figure taken from the CloneJet Manual (Thermofisher, USA).

Appendix 3 – Reagent formulations

3.1 McIlvains Buffer pH 7.4

Solution A: 1.8mM citric acid (2.1g citric acid in 100ml dH2O)

Solution B: 0.36mM $Na_2HPO4.12H2O$ (7.2g $Na_2HPO4.12H_2O$ in 100ml dH_2O)

Add 18.17ml Solution A and 1.83ml Solution B and make up to 1L with dH_2O.

3.2 10x Phosphate Buffered solution (PBS)

80g NaCl

2.0g KCl

14.4g Na_2HPO_4

2.4g KH_2PO_4

Dilute in 800ml dH2O. Adjust pH to 7.4 and make up to a volume of 1L with dH_2O.

1x solution made up with 25ml 10X PBS added to 250ml dH_2O

3.3 PBS + Penicillan/Streptomycin and Fungin (PSF)

1x PBS containing the following:

500U/ml penicillin

100µg/ml streptomycin

1µg/ml fungin

3.4 Physiological saline

0.85% w/v NaCl

0.85g NaCl

Made up to a final volume of 100 ml dH_2O

3.5 TE Buffer pH 9.0

10mM Tris-HCL

1mM EDTA

Made up in 400ml dH_2O, adjust pH to 9 and make up to 500ml with dH_2O.

3.6 Complete DMEM (10% FCS in DMEM)

445 ml DMEM

50 ml fetal calf serum (FCS)

5 ml Penicillin and Streptomycin

500 µl